



University of HUDDERSFIELD

University of Huddersfield Repository

Tuccia, Fabiola

A Framework of Morphological and Molecular Methods for the Analysis and Interpretation of Entomological Remains from Archaeological and Forensic Contexts

Original Citation

Tuccia, Fabiola (2020) A Framework of Morphological and Molecular Methods for the Analysis and Interpretation of Entomological Remains from Archaeological and Forensic Contexts. Doctoral thesis, University of Huddersfield.

This version is available at <http://eprints.hud.ac.uk/id/eprint/35384/>

The University Repository is a digital collection of the research output of the University, available on Open Access. Copyright and Moral Rights for the items on this site are retained by the individual author and/or other copyright owners. Users may access full items free of charge; copies of full text items generally can be reproduced, displayed or performed and given to third parties in any format or medium for personal research or study, educational or not-for-profit purposes without prior permission or charge, provided:

- The authors, title and full bibliographic details is credited in any copy;
- A hyperlink and/or URL is included for the original metadata page; and
- The content is not changed in any way.

For more information, including our policy and submission procedure, please contact the Repository Team at: E.mailbox@hud.ac.uk.

<http://eprints.hud.ac.uk/>



**A FRAMEWORK OF MORPHOLOGICAL AND MOLECULAR METHODS
FOR THE ANALYSIS AND INTERPRETATION OF ENTOMOLOGICAL
REMAINS FROM ARCHAEOLOGICAL AND FORENSIC CONTEXTS**

FABIOLA TUCCIA

A thesis submitted to the University of Huddersfield in partial fulfilment of the requirements for the degree of Doctor of Philosophy

Department of Biological and Geographical Sciences
School of Applied Sciences
University of Huddersfield

September 2020

To My Family

COPYRIGHT STATEMENT

- i. The author of this thesis (including any appendices and/ or schedules to this thesis) owns any copyright in it (the “Copyright”) and s/he has given The University of Huddersfield the right to use such Copyright for any administrative, promotional, educational and/or teaching purposes.
- ii. Copies of this thesis, either in full or in extracts, may be made only in accordance with the regulations of the University Library. Details of these regulations may be obtained from the Librarian. This page must form part of any such copies made.
- iii. The ownership of any patents, designs, trademarks and any and all other intellectual property rights except for the Copyright (the “Intellectual Property Rights”) and any reproductions of copyright works, for example graphs and tables (“Reproductions”), which may be described in this thesis, may not be owned by the author and may be owned by third parties. Such Intellectual Property Rights and Reproductions cannot and must not be made available for use without permission of the owner(s) of the relevant Intellectual Property Rights and/or Reproductions.

ACKNOWLEDGEMENTS

My first acknowledgment goes to Leverhulme Trust Doctoral Scholarship programme for funding my doctoral degree.

I would like to express my sincere gratitude to my advisor and my mentor Prof. Stefano Vanin for the support he gave me during my PhD and related research programme. I am so grateful to him because under his guidance I developed a deep appreciation for the academic research and I learnt that there is no better way to succeed in your job than working in a team and doing it with passion and enthusiasm.

Besides my advisor, my sincere acknowledgements go to the members of my thesis committee: Prof Martin B. Richards and Dr Gareth Parkes for accepting the role of supervisor and co-supervisor for the last months of my PhD. I also sincerely thank them, along with Dr Martin Carr, for being my progression viva examiners and for giving me insightful comments and asking me stimulating questions that strongly encouraged me to widen my research.

My sincere thanks go also to Dr Lisa Gillie (Department of Chemical Sciences) for training me in the use of the XRD instrument, essential to my work, and for the time she dedicated to help me with the data interpretation. Thanks also to Dr Paul Bills and Chris Dawson (Department of Engineering and Technology) for giving me the opportunity to perform CT-scan analysis.

I am also very grateful to the team of technicians, with a special acknowledgement to Jim and Felix for being always kind and ready to help me.

In addition, I am thankful to all the people that I met from other academic institutions and whom it has been a pleasure working and established a solid professional network with.

My special acknowledgements are to Dr Jean-Bernard Huchet (Muséum National d'Histoire Naturelle, Paris, France) for being the funder of a fascinating discipline as Funerary Archaeoentomology that made my research unique, and for giving me precious and productive advises.

I am also grateful to Dr Daniel Martín-Vega (Universidad de Alcalá, Madrid, Spain) for providing entomological specimens of his private collection and starting a successful collaboration, and for patiently reviewing one of the chapters.

Thanks to Dr Barbara Wilkens (Università degli Studi di Sassari, Italy), Dr Daniel Withmore (Natural History Museum, London and currently affiliated at Staatliches Museum für Naturkunde, Stuttgart, Germany), and Mirko Traversari (Università di Bologna, Italy) for hosting me in their facilities and providing me essential material for my research.

Last in the list but first in my heart, I want to thank all my loved ones.

My warmest and heartfelt acknowledgements are for my Family, Mum and Dad, my brother Edo and Cinziottide, my little sister Vichi and my special grandma Nonna Sandra. I would have not get to the end of this trip without your lovely support.

I thank my special friends, sisters not in blood but in life, Giorgina, Jennina, and Katha. Together we lived the happiest, the funniest, and the most successful moments in the last four years. Thank you for your incomparable and irreplaceable friendship!

A sincere thanks to my dear friend Nicolò for his exceptional motivational skills! I have been so lucky to have you as my editor-in-chief! Above all, thank you for bringing the beauty of Music back in my life. I will never forget about Piano Concerto No. 2 in F major by Dmitrij Šostakovič as the perfect therapy for the hardest moments.

A special thanks to Rohan for spending days and nights making this thesis sound authentically English! Whether the language or not and whether the distance or not, whatever the place where I'll go, I will be always thankful to you! Your help has been inestimable.

A special thanks goes to Dr Alessandro Sinopoli (Ello), the first person I met when I moved to Huddersfield. Thank you for being a brilliant chemist-friend even in remote-control mood from Qatar! After completing my PhD, I will need to find a new way to call you and tell you "Ale, I have a problem".

A heartfelt thank is to my friends Sara and Ste, Bubi, Giuli and Armi, Ila and Simo for never stopping to be so close to me, despite 4 years of distant friendship, and for always waiting my return home with enthusiasm.

Thanks to my friends and colleagues from JP1/39 Alessandro, George, Gonzalo, Bobby, Rita, Simao, Pierre, Berni, Ines, Marisa, for being an hilarious and supporting company!

As *dulcis in fundo*, thank you Allu for being part of this bitter trip as my sweetest source of motivation.

You all are Family to me.

LIST OF RESEARCH OUTPUTS

In partial fulfilment of the requirements for the degree of Doctor of Philosophy, I contributed either as first author or co-author to publish the following peer-reviewed papers whose outcomes are not included in the PhD thesis here presented:

- 2019 Mukherjee S., Singh P., **Tuccia F.**, Pradelli J., Giordani G., Vanin S. DNA characterization from gut content of larvae of *Megaselia scalaris* (Diptera, Phoridae). *Science and Justice* (in press);
- 2019 Sessa F., Varotto V., Salerno M., Vanin S., Bertozzi G., Galassi F.M., Maglietta F., Salerno M., **Tuccia F.**, Pomara C., Ricci P. First report of Heleomyzidae (Diptera) recovered from the inner cavity of an intact human femur. *Journal of Forensic and Legal Medicine* 66: 4-7
<https://doi.org/10.1016/j.jflm.2019.05.021>;
- 2019 **Tuccia F.**, Zurgani E., Bortolini S., Vanin S. Experimental evaluation on the applicability of necrobiome analysis in forensic veterinary science. *MicrobiologyOpen* e828 <https://doi.org/10.1002/mbo3.828>;
- 2019 Pradelli J., Rossetti C., **Tuccia F.**, Giordani G., Licata M., Birkhoff J.M., Verzeletti A., Vanin S. Environmental necrophagous fauna selection in a funerary hypogeal context: The putridarium of the Franciscan monastery of Azzio (northern Italy). *Journal of Archaeological Science: Reports* 24: 683-692
<https://doi.org/10.1016/j.jasrep.2019.02.028>;
- 2018 Giordani G., **Tuccia F.**, Zoppis S., Vecchiotti C., Vanin S. Record of *Leptometopa latipes* (Diptera: Milichiidae) from a human cadaver in the Mediterranean area. *Forensic Sciences Research* 0:1-7
<https://doi.org/10.1080/20961790.2018.1490473>;
- 2017 Lo Pinto S., Giordani G., **Tuccia F.**, Ventura F., Vanin S. First records of *Synthesiomyia nudiseta* (Diptera: Muscidae) from forensic cases in Italy. *Forensic Science International* 276: e1-e7
<https://doi.org/10.1016/j.forsciint.2017.05.003>.

In addition, I declare that I am the main author responsible for the following publication which has been partially used in Introduction (paragraph 1.3):

- 2018 **Tuccia F.**, Giordani G., Vanin S. Forensic Entomology: an overview. *Crime, Security and Society* 1(1) <https://doi.org/10.5920/css.2018.05>

as well as I contributed to the following publication which has been used to provide historical information about the archaeological site of Castelsardo (paragraph 1.4.4):

- 2018 Giordani G., **Tuccia F.**, Floris I., Vanin S. First record of *Phormia regina* (Meigen, 1826) (Diptera: Calliphoridae) from mummies at the Sant'Antonio Abate Cathedral of Castelsardo, Sardinia, Italy. *PeerJ* 6:e4176
<https://doi.org/10.7717/peerj.4176>

ABSTRACT

Insects and their fragments are often recovered from crime scenes and archaeological deposits as essential evidence in support of forensic and environmental archaeological investigations. Insects colonise the most diverse natural and anthropic environments, however different taxa show different ecological preferences and their development and phenology are species-specific and temperature dependent. Therefore, species identification is of primary importance to make any interpretation of the case. Today, insects identification can be achieved using two different approaches: 1) the morphological analysis of diagnostic features is currently well-established, irreplaceable and traditionally widely used method; 2) on the other hand, the DNA-based identification method has been integrated more recently (second half of 1980s) as a consequence of the rapid advance of molecular biology techniques.

The main objective of this thesis is to provide an accurate framework of how to proceed to analyse entomological remains collected from contexts where conservation status is not optimal. A strong focus is directed on Diptera, using both approaches and providing a pragmatic and critic workflow of analysis for reliable interpretative purposes. In particular, the lack of descriptions of immature stages of poorly studied species is considered and investigated.

To achieve this, three macro-projects concerning either archaeoentomological or forensic entomological investigations are presented through the analysis of two case-studies, respectively.

The outcomes of the whole research include:

- i)* an original contribution to molecular archaeology research, through the *ex novo* design of a DNA-based workflow applied to Diptera puparia;
- ii)* an innovative contribution to the environmental archaeology research belonging to the Italian heritage, through the analysis of mineralised findings recovered from a Sardinian medieval urban well, and found in association to human remains within a Roman grave;
- iii)* an essential contribution to forensic entomology, through the generation of new morphological data of immature stages of *Physiphora alceae* (Diptera: Ulidiidae) and through the comparative descriptions of puparia of ten species of Piophilidae, along with the design of a dichotomy key.

Although the results are overall promising, further research is needed within molecular archaeology field applied on Diptera puparia. An improved workflow which meets all the essential authenticity criteria will be a great achievement and will provide an extra tool of analysis for archaeological records. The great potential of the archaeoentomological investigations in deriving interpretations of the human past and practices has been demonstrated not only through the identification of taxa but also through the analysis of taphonomic processes involved in their preservation. Finally, an integrated taxonomy-DNA based approach is beneficial, whether applicable, to strengthen the accuracy of the identifications; however, a continuous research is necessary to generate new data especially of unexplored and poorly studied taxa of forensic interest.

TABLE OF CONTENTS

1	INTRODUCTION	24
1.1	DIPTERA LIFE-CYCLE AND SYSTEMATICS	25
1.2	INSECTS: WITNESSES OF THE PAST	32
1.3	FORENSIC ENTOMOLOGY	34
1.3.1	Overview of cadaver decomposition	35
1.3.2	Succession of necrophagous insects on cadavers	36
1.3.1	Introduction to Piophilidae of forensic interest	37
1.3.2	Introduction to Ulidiidae, “secondary taxon” of forensic importance	40
1.4	ARCHAEOENTOMOLOGY	43
1.4.1	Archaeoentomology and funerary practices: Archaeology of death	44
1.4.2	Preservation of insects in archaeological contexts	46
1.4.3	Italian archaeoentomological records	48
1.4.4	Description of Italian archaeological sites studied in this thesis	51
1.5	IDENTIFICATION OF ENTOMOLOGICAL SPECIES RETRIEVED FROM FORENSIC AND ARCHAEOLOGICAL CONTEXT	59
1.5.1	Morphology-based approach	59
1.5.2	DNA-based approach	61
1.5.3	Molecular identification in forensic entomology: The other side of the coin	63
1.5.4	Molecular identifications of ancient insects remains	64
1.5.5	Ancient DNA analysis: Features and criteria of authenticity	65
1.6	OBJECTIVES	69
2	MATERIALS AND METHODS	70
2.1	MORPHOLOGICAL ANALYSIS	71
2.1.1	Puparia collection and cleaning	71
2.1.2	Larvae diaphanisation	74
2.1.3	Microscopic techniques	75
2.1.4	Identification keys and external consultants	76
2.2	MICROSTRUCTURE ANALYSIS OF MINERALISED SPECIMENS	77
2.2.1	Computer Tomography Scan (CT-Scan)	77
2.2.2	SEM X-rays microanalysis	78
2.2.3	Fourier Transform Infrared (FTIR) Spectroscopy	78
2.2.4	Powder X-ray Diffraction	78

2.3	ANCIENT DNA ANALYSIS	80
2.3.1	Ancient DNA analysis of Roccapelago samples – Chapter 3	80
2.3.2	Ancient DNA analysis of Castelsardo samples – Chapter 3	82
2.3.3	Ancient DNA analysis of Sassari urban well samples – Chapter 4	84
2.3.4	Downstream analysis of ancient DNA	85
2.3.5	Strategies and protocols to amplify ancient DNA	86
2.3.6	aDNA purification and sequencing	90
2.4	MODERN DNA ANALYSIS	91
2.4.1	Investigations on the impact of cuticular pigments on downstream DNA analysis - Chapter 3	91
2.4.2	DNA barcoding of <i>Physiphora alceae</i> and phylogenetic analysis of Diptera: Ulidiidae - Chapter 5	94
2.4.3	DNA barcoding and phylogenetic analysis of Piophilidae of forensic interest – Chapter 5	95
3	DNA ANALYSIS OF MODERN AND ANCIENT DIPTERA PUPARIA: CHALLENGES, LIMITATIONS, AND POTENTIALITIES	97
3.1	INVESTIGATIONS ON THE IMPACT OF CUTICULAR PIGMENTS ON DOWNSTREAM DNA ANALYSIS	98
3.1.1	Results	98
3.1.2	Discussions	104
3.1.3	Conclusions	107
3.2	MOLECULAR ANALYSIS OF DIPTERA PUPARIA RECOVERED FROM ROCCAPELAGO MUMMIES	108
3.2.1	Results	108
3.3	MOLECULAR ANALYSIS OF DIPTERA PUPARIA RECOVERED FROM CASTELSARDO MUMMIES	116
3.3.1	Results	116
3.4	DISCUSSIONS	125
3.5	CONCLUSIONS	130
4	TAPHONOMIC PROCESSES INVOLVED IN THE PRESERVATION OF ARCHAEOZOOLOGICAL ASSEMBLAGES AND THEIR IMPACT ON DNA ANALYSIS	131
4.1	MINERALISATION OF DIPTERA PUPARIA RECOVERED FROM A MEDIEVAL URBAN WELL IN VIA SEBASTIANO SATTÀ, SASSARI (SARDINIA, ITALY)	132

4.1.1	Results	132
4.1.2	Discussions	160
4.2	MINERALISATION OF ENTOMOLOGICAL REMAINS FROM A HUMAN MASS GRAVE IN MACOMER (SARDINIA, ITALY)	170
4.2.1	Results	170
4.2.2	Discussions	175
4.3	CONCLUSIONS	178
5 MORPHOLOGICAL DESCRIPTIONS AND DNA BARCODING OF DIPTERA OF FORENSIC INTEREST		179
5.1	<i>PHYSYPHORA ALCEAE</i> (PREYSSLER, 1791) (ULIDIIDAE): MORPHOLOGICAL DESCRIPTIONS, DNA BARCODING AND PHYLOGENETIC ANALYSIS	180
5.1.1	Results	180
5.1.2	Discussions	185
5.2	COMPARATIVE STUDY OF “SKIPPER FLIES” (DIPTERA: PIOPHILIDAE) OF FORENSIC INTEREST: DESIGN OF A DICHOTOMY KEY FOR THE IDENTIFICATION OF PUPARIA AND DNA BARCODING	187
5.2.1	Results	187
5.2.2	Discussions	205
5.3	CONCLUSIONS	209
6 FINAL CONCLUSIONS		210
REFERENCES		211
APPENDIX A		230
APPENDIX B		241

LIST OF ACRONYMS AND ABBREVIATIONS

a.s.l.	above sea level
Abs	Absorbance
aDNA	ancient DNA
AIC	Akaike Information Criterion
BC	Before Christ
BIC	Bayesian Information Criterion
BOLD	Barcoding of Life Database
bp	base pair
BP	Before Present
BS	bootstrap
BSA	Bovine Serum Albumin
COI	Cytochrome Oxidase subunit one
CT	Computer Tomography
DNA	Deoxyribonucleic Acid
dNTPs	Deoxyucleotide Triphosphates
dsDNA	double strand Deoxyribonucleic Acid
DTT	Dithiothreitol
EDTA	Ethylenediaminetetraacetic Acid
EDX	Energy Dispersion X-ray
EtOH	ethanol
FLEA	Forensic Laboratory of Entomology and Archaeology
FTIR	Fourier Transform Infra-Red
Fw	Forward
HF	High Fidelity
HW	Hot Water
ICSD	Inorganic Crystal Structure Database
MEGA	Molecular Evolutionary Genetics Analysis
ML	Maximum Likelihood
mPMI	minimum PMI
mt	mitochondrial
NGS	Next Generation Sequencing
NHM	Natural History Museum
PCR	Polymerase Chain Reaction
PVP	Polyvinilpyrrolidone
RNA	Ribonucleic Acid
rRNA	Ribosomal RNA

Rv	Reverse
S.U.	Stratigraphic Unit
SDS	Sodium Dodecyl Sulfate
SEM	Scanning Electron Microscope
SLS	Sodium Lauroyl Sarcosinate
SU	Stratigraphic Unit
T _a	annealing Temperature
<i>Taq</i>	<i>Thermus aquaticus</i>
UV	Ultraviolet
XRD	X-Ray Diffraction

LIST OF FIGURES

Fig. 1.1 Halteres of an adult fly. Distinctive characteristic of the Diptera order, the stick-club-like structures are attached to the mesothorax (white arrow). Scale bars: 1 mm (adult), 500 μ m (detail).	25
Fig. 1.2 Diptera life cycle. A true fly undergoes to four developmental stages. The definition of “pupation”, “pupariation”, “phanerocephalic” and “cryptocephalic” pupa are given in the text...26	26
Fig. 1.3 Head of an adult fly. (A) frontal and (B) lateral view of an adult fly species (Diptera: Ulidiidae).	28
Fig. 1.4 Compound eyes in female and male adult flies.	28
Fig. 1.5 Morphological systematic of Diptera. Relationships at infraorders and superfamilies level are enlightened. Modified picture from Lambkin (Lambkin et al., 2012).	31
Fig. 1.6 Time perception in forensic and archaeological studies. (A) time as perceived by forensic scientist and archaeologists. The boundary between “modern” (red line) and “ancient” (black line) is rather arbitrary and depends upon the phenomena of interest; (B) time line of the entomological specimens studied and presented in this thesis.	33
Fig. 1.7 Schematic representation of the real, maximum, and minimum PMI.	34
Fig. 1.8 Insects succession on cadavers. Necrophagous insects “colonisation waves” on cadavers correlates with the progression of the decomposition. Insects picture images modified from Dr Giorgia Giordani, not in scale.	37
Fig. 1.9 Piophilidae leaping behaviour. Arching, pulling, and releasing phases of the leaping behaviour of Piophilidae larvae is schematically shown. The image has been drawn by the author of this thesis.....	38
Fig. 1.10 Metropolitan area of Milan (Italy). The red spot indicates the place where the cadaver of the woman was found. Picture modified from © 2007–2018 d-maps.com.....	41
Fig. 1.11 Preservation of Diptera remains in archaeological contexts. Puparia collected from diverse contexts may show a different appearance. Scale bars: 1 mm.	47
Fig. 1.12 Palaeoentomological and funerary-archaeoentomological Italian public records. γ BP= years before present; map from © 2007–2018 d-maps.com.....	48
Fig. 1.13 Roccapelago village, Emilia Romagna region (Italy) (44° 12’16”N 10° 35’29”E).	51
Fig. 1.14 Schematically representation of tomb 7. The 64 mummified bodies (S.U. 23) were found piled-up forming a pyramid-like structure.....	52
Fig. 1.15 Pyramid-like structure of mummified corpses found in S.U. 23.	52
Fig. 1.16 Castelsardo village, Sardinia region (Italy) (40° 54’52”N 8° 42’46”E).	54
Fig. 1.17 Sant’Antonio Abate Cathedral in Castelsardo. (A) Promontory overlooking the Asinara gulf where Castelsardo arises; (B) Sant’ Antonio Abate Cathedral view; (C) bone remains nested into one of the walls of the crypts. Photographs shot by the author of this thesis in September 2018.	54
Fig. 1.18 Sassari city, Sardinia region (Italy) (40° 43’36”N 8° 33’33”E)	56

Fig. 1.19 Schematic representation of the Medieval well in Via Sebastiano Satta, Sassari. The division in Stratigraphic Units (S.U.) as defined by the archaeologists and the relative nature of the sediment are reported.	57
Fig. 1.20 Macomer city, Sardinia region (Italy) (40° 15'51"N 8° 46'30.22"E).	58
Fig. 1.21 Diagnostic characters of Diptera puparia. Ventral view and anatomical details of a puparium analysed for the diagnosis of the species are schematically shown. Each element is reliably reproduced from photographs; however, the whole representation is not realistic as the elements are not in scale and have been selected from multiple species.	61
Fig. 2.1 Collection of entomological remains from Roccapelago human remains in Ravenna, 2017. (A-C) Skeletonised human remains partially mummified (D,E) puparia of necrophagous Diptera feeding on the decomposing bodies (white arrows).	71
Fig. 2.2 Larvae preparation workflow. A) Larvae stored in 70% EtOH are subjected to a longitudinal dorsal cut B) to remove the cuticle from the soft tissues C) and D) analyse them through morphological and molecular approach, respectively.	74
Fig. 2.3 Schematic representation of CT-scan data acquisition and processing.	77
Fig. 2.4 DNA extraction and purification workflow of Roccapelago samples. (A) Oshaghi DNA extraction protocol (2006); (B) first strategy, associated homemade purification workflow involving 2 default steps and one extra; (C) second strategy, associated homemade purification workflow involving only one purification step.	81
Fig. 2.5 DNA extraction and purification workflow of Castelsardo samples. Oshaghi protocol (2006) was used to extract DNA from 2 archaeological puparia of <i>H. capensis</i> and modern control of <i>C. vomitoria</i> . Reactions were carried out in triplicates. Two purification steps were applied on the initial lysates using OneStep PCR removal kit (ZymoResearch) and ReliaPrep DNA purification and concentration system (Promega).	83
Fig. 2.6 Mitochondrial barcoding region and primers. A) Universal “barcoding” region and primers (Folmer et al. 1994); B) Dr Bortolini’s newly designed “short-barcoding” primer set (unpublished data). The starting and the ending nucleotides mark the numeration based on <i>Drosophila yakuba</i> mitochondrial genome (Clary and Wolstenholme, 1985).	86
Fig. 2.7 Larval exuviae within a puparium of <i>Calliphora vicina</i>. Black arrow indicates the epithelial tissue of the metamorphosis insect which is left attached to the puparium after the adult emerges. Scale bar: 1 mm.	91
Fig. 2.8 DNA extraction workflow of pigment test. The morphology of the specimens was preserved using a non-destructive submersion method. Left column: “treated samples”, lysate subjected to purification with OneStep PCR Inhibitors Removal kit (ZymoResearch) prior to follow manufacturer’s instruction; right column: “non-treated” samples, lysate processed using QIAquick Investigator Kit (Qiagen). A final purification step of the eluates was performed in both cases on 50 out of 100 µl of DNA eluate.	92
Fig. 3.1 Coloured lysate extracts. <i>T. molitor</i> adult (left) and <i>C. vicina</i> puparia (right) extracts showing a brownish colouration soon after the lysis incubation.	98
Fig. 3.2 Bioanalyzer traces. Electrophoresis on chip results are shown for pigmented non-purified extracts (left column) and transparent purified eluates (right column); *lysates subjected to	

purification with OneStep PCR Inhibitors Removal kit (ZymoResearch) prior to continuing with the extraction; “CTRL” samples, lysate non subjected to purification but processed according to manufacturer’s guidelines.....99

Fig. 3.3. UV absorbance spectra of pigmented post lysis extracts. In all the specimens, an absorbance peak around 290 nm can be observed, higher and well defined in *C. vicina*, way more attenuated in *T. molitor*, suggesting a potential difference in the pigments component of the cuticle. 100

Fig. 3.4 UV absorbance spectra of purified extracts. Peak at 260 nm identify pure DNA solution. Difference in intensities signal was observed in accordance with concentration measurements in Tab. 3.1.; *lysate subjected to purification with OneStep PCR Inhibitors Removal kit (ZymoResearch) prior to continuing with the extraction; CTRL= lysate non-treated, immediately processed using QIAquick Investigator Kit (Qiagen). A final purification step of the eluates was performed in both cases and electrophoresis was performed before (raw DNA eluates, left column) and after (purified DNA eluates, right column). Letters follow Fig. 3.2..... 101

Fig. 3.5 Gel electrophoresis of PCR products from pigment test. Positive amplicons show the expected size (~658 bp). *=lysate treated with One Step purification kit; CTRL=lysate non-treated, directly processed. In both cases, half volumes of the final eluates were purified with a column-based system (purified eluates). Letters were assigned as in Fig. 3.4. DNA Ladder: 100 bp. 102

Fig. 3.6 Pigmentation status of Roccapelago extracts/eluates. Schematic representation of changes in colouration of DNA preparations: the initial brown dark pigmentation of the ROSE extracts was progressively lost through the purification steps. The same phenomenon was observed for archaeological and control samples. 108

Fig. 3.7 NanoDrop Abs spectra. Left column: control samples; right column: Roccapelago samples. One spectrum is reported as representative of each of the conditions for each samples, as data are consistent among samples. 111

Fig. 3.8. Gel electrophoresis from Phusion Blood High Fidelity modified version. Amplification of DNA Op311 short-barcoding fragments is showed for Roccapelago (above) and control (below) samples. Numbers 2,3,5 indicate the number of processed puparia per each condition (raw= non purified lysates, 1st= DNA eluates purified using 1st strategy, and 2nd= DNA eluates purified using the 2nd strategy as per Fig. 2.4. Black arrows indicate the “fire-tails” of high-molecular weight, aspecific UV-signal which do not appear after the second step of purification; DNA ladder: 100 bp. 114

Fig. 3.9 NaOH 10% treatment effect on Castelsardo puparia. Three specimens (CSHYD5 *H. capensis*, CSHYD9 and CSHYD12 *H. aenescens*) are shown as example before and after the NaOH 10% treatment. (A) ventral, (B), dorsal view of the entire puparia; (C) posterior spiracles, (D) anal plate, (E) and ventral spines on the 7th abdominal segment. Scale bars: 1 mm (A,B), 100 µm (C, D, E)..... 117

Fig. 3.10 *Hydrotaea capensis* closed puparia. Column (A) dorsal, column (B) ventral view of the whole specimens; column (C) posterior spiracles, column (D) anal plate, column (E) ventral spines on the 7th abdominal segment. Scale bars: 1 mm (A, B), 100 µm (C, D, E). 118

Fig. 3.11 *Hydrotaea capensis* open puparia. Column (A) dorsal, column (B) ventral view of the whole specimens; column (C) posterior spiracles, column (D) anal plate, column (E) ventral spines on the 7th abdominal segment. Scale bars: 1 mm (A, B), 100 µm (C, D, E)..... 119

Fig. 3.12 Pigmentation status of Castelsardo extracts/eluates. (A) Schematic representation of the progressively discolouration of ROSE extracts; (B) control extracts from <i>C. vicina</i> pupae; (C) Castelsardo extracts from <i>H. capensis</i> pupae.	119
Fig. 3.13 Agilent 2100 Bioanalyzer High Sensitivity Assay of Castelsardo extracts. One out of three replicate only is shown as all the samples share a very similar pattern. The colour blending legend next to the graphs is aimed at helping the reader to associated the fragment assay to the macroscopic “phenotype” of the DNA extract/elution at each step of the workflow.....	122
Fig. 3.14 NanoDrop Abs spectra. One example per sample (control and archaeological) is reported. As in Fig. 3.13, the colour blending legend below the graphs is aimed at facilitating the reader to associate the purity assay to the macroscopic “phenotype” of the DNA extract/elution at each step of the workflow.	123
Fig. 3.15 Gel electrophoresis of PCR products from Platinum™ HotStart protocol. Amplification of DNA Op311 short-barcoding fragments using Platinum™ Hot Start (Invitrogen™, Carlsbad, California, USA) is showed for Castelsardo (above) and control (below) samples. Three reactions (A,B,C) were run in parallel using 2 puparia as initial substratum for DNA extraction; raw= non purified lysates, 1 st = DNA eluates subjected to the first purification step, 2 nd = DNA eluates subjected to the 2 nd purification step. Reaction was positive for double-purified control templates only. DNA ladder: 100 bp.	124
Fig. 3.16 Comparison between double purified Abs spectra. DNA concentration of the eluates is reported to show the correlation with the spectra resolutions.	127
Fig. 4.1 Fanniidae puparia. (A–D) Puparia from this study showing a remarked segmentation and truncated lateral processes; (E–H) examples of Fanniidae larvae described in Dominiguez and Pont (2014): (E) <i>Fannia albitarsis</i> Stein, 1911, (F) <i>Fannia canicularis</i> , Linnaeus, 1758, (G) <i>Fannia mercurialis</i> Dominiguez and Pont, 2014, (H) <i>Zealandofannia mystacina</i> Dominiguez and Pont, 2014.	133
Fig. 4.2 Details of Muscidae puparia. (A) <i>Stomoxys calcitrans</i> puparium dorsal view and (D,G) posterior spiracles; (B) <i>M. domestica</i> puparium dorsal view and (E,H) posterior spiracles; (C) <i>M. prolapsa</i> puparium ventral view and (F,I) posterior spiracles. Scale bars: puparium 1 mm, posterior spiracles 100 µm, single posterior spiracle 50 µm.....	134
Fig. 4.3 Unique specimens of <i>Lispe</i> sp. A,B) puparium dorsal and ventral view; (C,D) anal plate and a spot of spines beneath it; (E,F) posterior spiracles; (G,H) spines belt on the 7 th abdominal ventral segment. Scale bars: 1 mm (A,B), 100 µm (C,E,G), 50 µm (D,F,H).	135
Fig. 4.4 Sphaeroceridae puparia sieved <i>in loco</i>. Hundreds of specimens were collected from each sieved batch of sediment.	136
Fig. 4.5 Form of preservation of Sphaeroceridae puparia. (A) Mineralised, (B) waterlogged specimens collected from S.U. 19335 and S.U.19336, respectively. Scale bar: 5 mm.	137
Fig. 4.6 Morphological comparison between modern and Via Satta Sphaeroceridae puparia. (A–C) <i>T. zosteræ</i> puparia from the collection of Natural History Museum, London; (D–H) Sphaeroceridae puparia from this study. Scale bars: 500 µm for the entire puparium, 100 µm for the forked posterior region, 50 µm for the anal plate, the posterior and anterior spiracle. The latter are missing in open puparia (F,G,H).....	138

- Fig. 4.7 SEM images of Sphaeroceridae puparia details.** (A,B) Posterior spiracles showing a different orientation of the respiratory slits; (C,D) anterior spiracles showing a different numbers of the lateral processes and diverse basal structure. Scale bar: 50 μm 139
- Fig. 4.8 Morphological comparison of ventral abdominal spines.** (A-C) spines belt of modern puparia of *T. zosteriae* from the collection of Natural History Museum, London; (D-H) ventral spines belt of puparia from this study. The schematic model shows the location of the spines analysed. ant= anterior region of the puparium; post= posterior region of the puparium. Letters follow Fig. 4.6. Scale bar: 50 μm 141
- Fig. 4.9 Morphological comparison between pharate-adult and adults specimens.** (A) mineralised pharate adult from this study; (B-E) modern adults specimens of Limosiniinae (Sphaeroceridae) from the London Natural History Museum (NHM) collection. The coloured spotted mark the mutual position of the thoracic bristles. For the comparison, white spots refer to the pharate adult from this study and for the other taxa a colour coded spots have been chosen. Scale bar: 100 μm 142
- Fig. 4.10 Gradient of mineralisation of Diptera puparia.** (A) Sphaeroceridae puparium “normally preserved”; (B) Sphaeroceridae and (D) Fanniidae puparia showing a total replacement of the internal soft tissues; (C) specimens of cast/mold pupa of Muscidae with the organic cuticle conserved and forming a cast in which the internal soft tissues have been replaced by a mineral mould; (E) distribution of the Diptera remains as found within the well. Scale bar: 1 mm..... 144
- Fig. 4.11 Mineralised Diptera fossils.** (A-C) Muscidae; (D-F) Fanniidae; (G-H) Sphaeroceridae. In all the specimens the segmentation typical of larvae and pupae was still observable and the general intact and well preserved morphology allowed to discriminate the families. Scale bars: 1 mm.. 144
- Fig. 4.12 Preserved cephaloskeleton in mineralised pupae.** (A,D) dorsal, and (B,E) lateral view of two total mineralised Sphaeroceridae puparia; (C,F) hard chitinous cephaloskeleton observable intact in the oral region of the developing larva. Scale bars: 1 mm (entire), 500 μm (detail)..... 145
- Fig. 4.13 Mineralised pharate adults.** (A,C,E) dorsal, and (B,D,F) ventral view of mineralised metamorphosis insects. Head and legs are everted and the thorax is well distinguishable by the abdomen also due to the presence of the bristles (E), confirming the final stage of the pupa development prior the adult fly emerged. Scale bars: 500 μm (A-D), 100 μm (E-F)..... 146
- Fig. 4.14 Details of mineralised pharate adults.** (A) bristles head and thoracic pattern; (B) ommatidia; (C) antenna. An exceptional preservation of these details within the mineral matrix can be observed. Scale bars: 100 μm 146
- Fig. 4.15 Internal view of puparia observed via CT scan.** Different degree of mineralisation were spotted. (A) Muscidae specimen showing a well preserved pharate adult within the thick inorganic puparium (*). Head, thorax, and abdomen of the specimen are still recognizable as well as the posterior spiracles (**). (B) Well organized tube-like crystal morphology typical of Sphaeroceridae found in the S.U. 19335..... 147
- Fig. 4.16 Crystals' microstructure visualised at SEM.** (A-F) Different magnifications of spore-like and tube-like structures on a netting matrix typical of totally mineral replaced Sphaeroceridae specimens, recovered from the S.U. 19335; (H,I) spheric, (J-M) and lamellar structures observed in waterlogged Fanniidae, Sphaeroceridae and Muscidae specimens, recovered from S.U. 19336. The scale bar is reported in each figure. 148

- Fig. 4.17 SEM-EDX ID Point microelement analysis.** Consensus spectra are reported per each taxon. In each consensus spectrum, the coloured lines refer to three spectra generated from three points of interest arbitrarily selected on the puparia surface plus the sum spectrum (red line) generated from the whole observed area. Phosphor (P) and Calcium (Ca) were recorded as the most abundant elements. 150
- Fig. 4.18 SEM-EDX mapping microelement analysis.** SEM images and the relative colour-coded bi-dimensional map of the element distribution is shown for puparia of Fanniidae S.U.19336 (A), Sphaeroceridae from S.U.19335 (outer B, inner C), and waterlogged normally preserved Sphaeroceridae puparium (D). Phosphor (P) and Calcium (Ca) were recorded as the most abundant and homogeneously distributed elements. The intensity of the signal for Al, Si, Fe, and Cl was significantly lower. Scale bar is reported in each figure..... 151
- Fig. 4.19 FTIR analysis.** IR analysis has been summarised selecting one representative spectrum per each group of puparia. The spectra showed peaks associated to carbonate ($\sim 1,417, 871, 712 \text{ cm}^{-1}$) and phosphate ions ($1,030, 602, 566 \text{ cm}^{-1}$) as reported in Tab. 4.2, Tab. 4.3. Dashed lines indicate the wavenumber values of the major peaks detected (references in Tab. 4.2 and Tab. 4.3) and their overlapping. 153
- Fig. 4.20 Powder XRD spectra.** XRD spectra of specimens collected from S.U.19336 show an overlapping pattern. Some of the peaks are shared with the specimens collected from S.U.19335 whose profile results more amorphous. Dashed lines help in the visualisation of the shifted signal detected intra spectra and enlighten the overlapping positions of 2θ values. 156
- Fig. 4.21 ICSD-experimental XRD data comparison.** The comparison of the XRD profile of the CaCO_3 -ICSD #37421 (calcite)(A), and of the apatite-(CaOH)(Na, CO_3)-substituted-ICSD #92322 (B) showed a compatibility with the XRD profile obtained from this study..... 157
- Fig. 4.22. Bioanalyzer traces of total DNA extracted from Sphaeroceridae puparia.** The electropherogram and the relative gel-like image are shown as example per each of the DNA extraction methods (A-D) applied on fragmented (left column) or entire (right column) Sphaeroceridae puparia. Letters A-D refer to numbers 1-4 as per Tab. 4.4..... 159
- Fig. 4.23 Via Satta mineralised seeds.** (A,C) unknown origin, (B) grapeseed. Scale bar: 1 mm. . 169
- Fig. 4.24 Diptera puparia nested into human bones from the mass grave in Macomer.** (A,B) The inorganic mineral matrix covering the surface of the bones can be observed along with the nested Diptera puparia (red*). (C) Some specimens were included within the cavity of the bones..... 170
- Fig. 4.25 Mold/cast mineralised puparia extracted from human bones.** Different level of preservation are shown. The organic cuticle was patched and still attached to the mineral component (A-B, I-L), or complete (C-H). Scale bar: 1 mm. 171
- Fig. 4.26 Details of mineralised puparia.** (A) Striped pattern of the dorsal side of the puparium, (B,C) compact and fibrous structure of the mineral casts, (B) microtrichosity of the dorsal surface. (D-F) Calliphoridae posterior spiracles. Scale bars: 500 μm 172
- Fig. 4.27 Calliphoridae posterior spiracles comparison.** (A,D) Specimens of this study; (B) *Lucilia sericata* hand-drawn illustration; (E) *L. sericata* from FLEA modern private collection, pic. by Dr Giorgia Giordani; (C) *Calliphora vicina* hand-drawn illustration; (F) *C. vicina* from FLEA archaeological collection (Giordani et al., 2018b)..... 173

- Fig. 4.28 *Necrobia rufipes*, single elytron.** (A) Dorsal view, (B) ventral view. Scale bar: 1 mm. ... 174
- Fig. 5.1 *Physiphora alceae* adult.** (A) dorsal, (B) lateral, (C) ventral view. The black arrow indicates the foreleg with the creamy-yellow metatarsus. Scale bar: 1 mm. Photos by Dr Giorgia Giordani. 180
- Fig. 5.2 *Physiphora alceae* adult details.** (A) Wing showing the r_{4+5} cell almost closed and (B) frontal view head. The white arrow shows the typical narrow white microtrichose patches. Scale bar: (A) 500 μ m, (B) 100 μ m. Photos by Dr Giorgia Giordani. 180
- Fig. 5.3 *Physiphora alceae* III instar larva morphology.** (A) anterior spiracle, (B) cephaloskeleton (C,D) posterior spiracles. Anatomic details have been observed on III instar specimens stored in EtOH 70%. (A, D) and after diaphanisation of soft tissue in NaOH solution (C, B). Scale bars: 1 mm (full length larva), (B) 200 μ m (B), 100 μ m (A,C,D). 181
- Fig. 5.4 *Physiphora alceae* cephalopharyngeal skeleton morphology of III instar larva.** Mandible is composed of dental sclerite (den scl) and its basal part shows a robust process postero-dorsally oriented (black arrow). The hypopharyngeal sclerite (hyphar) links the mandible to the tentoropharyngeal skeleton composed of parastomal bar (pstm b), dorsal bridge (d bridge), dorsal corn (d corn) and ventral corn (v corn). 182
- Fig. 5.5 *Physiphora alceae* puparium.** (A) dorsal, (B) ventral, (C) lateral view, (D) posterior spiracles, (E) anterior spiracles, (F) ventral spines of abdominal segment 7th. Scale bars: 1 mm (A,B,C), 100 μ m (D,E), 50 μ m (F). Photos by Dr Giorgia Giordani. 183
- Fig. 5.6 Maximum Likelihood phylogenetic tree.** The phylogenetic tree was derived by the alignment of 61 mtCOI barcoding sequences of equal length (520 bp). The displayed topology was obtained upon the selection the best substitution model (Log-likelihood= -6098.9844). The evolutionary distance between Ulidiinae and Otitinae is strongly supported (BS=98). Red arrows point out to the *Homalocephala* sp. 184
- Fig. 5.7 Comparison of ten Piophilidae full puparia.** Dorsal, ventral (‘), and lateral (‘) view of full puparia. (A) *Centrophlebomyia furcata*, (B) *Piophila megastigmata*, (C) *Piophila casei*, (D) *Stearibia nigriceps*, (E) *Prochyliza xanthosoma*, (F) *Prochyliza nigrimana*, (G) *Liopiophila varipes*, (H) *Parapiophila vulgaris*, (I) *Parapiophila flavipes*, (J) *Protopiophila litigata*. Scale bar: 500 μ m. Pictures by Dr Giorgia Giordani. 192
- Fig. 5.8 Piophilidae ventral creeping welts SEM view.** In each picture, the number of rows is counted from the top to the bottom and follow the posterior-anterior orientation. Nomenclature follows Fig. 5.7. (A) *Centrophlebomyia furcata*, (B) *Piophila megastigmata*, (C) *Piophila casei*, (D) *Stearibia nigriceps*, (E) *Prochyliza xanthosoma*, (F) *Prochyliza nigrimana*, (G) *Liopiophila varipes*, (H) *Parapiophila vulgaris*, (I) *Parapiophila flavipes*, (J) *Protopiophila litigata*. Scale bar: 50 μ m. Pictures by Dr Giorgia Giordani. 193
- Fig. 5.9 Piophilidae anterior spiracles.** Keyence digital microscope (left) and SEM images (right) of the anterior spiracles. Nomenclature follows Fig. 5.7. (A) *Centrophlebomyia furcata*, (B) *Piophila megastigmata*, (C) *Piophila casei*, (D) *Stearibia nigriceps*, (E) *Prochyliza xanthosoma*, (F) *Prochyliza nigrimana*, (G) *Liopiophila varipes*, (H) *Parapiophila vulgaris*, (I) *Parapiophila flavipes*, (J) *Protopiophila litigata*. Scale bars: 50 μ m. Pictures by Dr Giorgia Giordani. 194
- Fig. 5.10 Anal region of Piophilidae puparia.** Ventral (left) and lateral (right) view of the anal division showing the extension of the ventral anal tubercles (red*) elongated in (C,D,E,H).

Nomenclature follows Fig. 5.7. (A) *Centrophlebomyia furcata*, (B) *Piophila megastigmata*, (C) *Piophila casei*, (D) *Stearibia nigriceps*, (E) *Prochyliza xanthosoma*, (F) *Prochyliza nigrimana*, (G) *Liopiophila varipes*, (H) *Parapiophila vulgaris*, (I) *Parapiophila flavipes*, (J) *Protopiophila litigata*. Scale bar: 200 µm. Pictures by Dr Giorgia Giordani.195

Fig. 5.11 Posterior spiracles of Piophilidae puparia. Keyence digital microscope and SEM images of the anterior spiracles. Nomenclature follows Fig. 5.7. (A) *Centrophlebomyia furcata*, (B) *Piophila megastigmata*, (C) *Piophila casei*, (D) *Stearibia nigriceps*, (E) *Prochyliza xanthosoma*, (F) *Prochyliza nigrimana*, (G) *Liopiophila varipes*, (H) *Parapiophila vulgaris*, (I) *Parapiophila flavipes*, (J) *Protopiophila litigata*. Scale bars: 500 µm. Pictures by Dr Giorgia Giordani.....196

Fig. 5.12 Maximum Likelihood consensus tree. Log Likelihood= -3745.76. The colours of the branches are clarified in Fig. 5.13. Yellow boxes= species out of the expected clusters. Black arrow and line= German *Parapiophila vulgaris* sequences out of the expected clusters.203

Fig. 5.13 Taxonomic and molecular phylogenetic resolutions of Piophilidae. (A) summary of the Piophilidae taxonomy listing genera used in the phylogenetic analysis of this study; (B) schematic representation of the mtCOI barcoding phylogenetic reconstruction of the Maximum Likelihood tree showed in Fig. 5.12. Grey dashed lines= two main clusters (BS 75). The controversial resolution of the genera *Centrophlebomyia* and *Parapiophila* is also underlined in grey.204

LIST OF TABLES

Tab. 1.1 World-wide records of Ulidiidae sampled during experiments	40
Tab. 1.2 Italian palaeontomological and funerary-archaeontomological published records.....	50
Tab. 1.3 Key references for morphological identification of Diptera of forensic interest.	60
Tab. 2.1 List of ancient puparia studied in this thesis. d =delivered samples; i.s. = <i>in situ</i> collection; *by archaeologists in charge of the site; **Laboratorio di Antropologia Fisica e DNA Antico - Dipartimento di Beni Culturali in Ravenna, Università di Bologna, Italy; ***Centre for Renovation and Conservation of the Cultural Heritage in Li Punti, Sassari, Italy.....	72
Tab. 2.2 List of modern puparia studied in this thesis. d =delivered samples; i.s. = <i>in situ</i> collection; *School of Applied Science, University of Huddersfield, United Kingdom; **by forensic archaeologist, Università degli Studi di Milano, Italy; ***by Dr Daniel Martín-Vega, Universidad de Alcalá, Madrid, Spain; ^a species for comparative study listed in Tab. 2.3.	72
Tab. 2.3 List of Piophilidae species analysed for comparative study.....	73
Tab. 2.4 List of chemicals used to clean puparia surface. 0= no corrosive, 1=low level of corrosiveness, 2= medium level of corrosiveness, 3=high level of corrosiveness.....	73
Tab. 2.5 Identification keys used in this thesis.	76
Tab. 2.6 XRD analysis methods tested in this thesis.	79
Tab. 2.7 Oshaghi buffer composition.	80
Tab. 2.8 DNA isolation methods applied on Sassari ancient samples. Method 1: procedure followed manufacturer's instructions; methods 2-4: original digestion buffer within the kit was replaced with a non-commercial buffer; *composition reported in Tab. 2.9.....	84
Tab. 2.9 Home-made digestion buffers compositions.	84
Tab. 2.10 Op311 primer specifications.	87
Tab. 2.11 PCR specifications listed per archaeological site. *as per Tab. 2.12; ** as per Tab. 2.13.	87
Tab. 2.12 aDNA PCR protocols. HF*= High Fidelity.	88
Tab. 2.13 Amplification programmes. ^a modified version; ^b used for templates derived from 8 puparia only;	89
Tab. 2.14 Additional Piophilidae specimens subjected to DNA analysis.....	95
Tab. 3.1 Qubit® 3.0 Fluorometer DNA quantification. *=lysate treated with One Step purification kit; CTRL=lysate non treated, directly processed. In both cases, half volumes of the final eluates were purified with a column-based system (purified eluates). The percentage of DNA lost is calculated as ratio of concentration of purified eluates over concentration of raw DNA eluates.	98
Tab. 3.2 NanoDrop™ Abs ratios.....	102
Tab. 3.3 BLAST species identification. Letters were assigned as in Fig. 3.4.....	103
Tab. 3.4 First strategy Qubit® 3.0 Fluorometer DNA quantification. Concentration values are expressed in ng/μl ± standard deviation (s.dv) calculated on three measurements of the same template. Percentages of DNA lost are calculated as ratio of concentration of purified eluates (2 nd)	

over concentration of ROSE buffer extracts; b.l.t.= below lowest threshold of the instrument (0.01 ng/μl).	109
Tab. 3.5 Second strategy Qubit® 3.0 Fluorometer DNA quantification. Concentration values are expressed in ng/μl ± standard deviation (s.dv) as in Tab. 3.4. b.l.t.= below lowest threshold of the instrument (0.01 ng/μl). Percentage of DNA lost calculated as in Tab. 3.4.	110
Tab. 3.6 PCR results summary. Red= failure; green= success; *=UV signal of higher intensity in contrast to other positive counterparts; grey= not performed.	113
Tab. 3.7 BLAST results of Roccapelago aDNA Op311 short-barcoding fragments.	115
Tab. 3.8 Qubit® 3.0 Fluorometer DNA quantification extracted from puparia pre-treated with NaOH 10%. Concentration values are expressed in ng/μl ± standard deviation (s.dv) calculated on three Qubit reads; A,B,C = triplicates; b.l.t.= below lowest threshold of the instrument (0.01 ng/μl); percentages of DNA lost are calculated as ratio of concentration of purified eluates (2 nd) over concentration of ROSE buffer extracts; *values calculated assuming concentrations equal to 0.099 ng/μl after the second purification step.....	120
Tab. 4.1 Identified taxa. *number are reported as an estimation.	132
Tab. 4.2 Carbonate ions wavenumbers assignment. The range of observed wavenumbers per each group has been compared to literature data and specifically assigned to asymmetric C-O stretch, O-C-O out of plane bend vibrations mode and to calcium carbonate molecule.	154
Tab. 4.3 Phosphate ions wavenumbers assignment. The range of observed wavenumbers per each group has been compared to literature data and specifically assigned to asymmetric O-P-O phosphate bend vibration mode and to Tribasic calcium phosphate molecule.....	154
Tab. 4.4. Qubit® 3.0 Fluorometer DNA quantification extracted from Sphaeroceridae puparia. Concentration values are expressed in ng/μl ± standard deviation (s.dv) calculated on triplicate reactions.	158
Tab. 5.1 Summary of morphological characters of Piophilidae puparia in this study.	197
Tab. 5.2 Qubit® 3.0 Fluorometer DNA quantification extracted from Piophilidae pupae. Concentration values are expressed in ng/μl ± standard deviation (s.dv) calculated on triplicate reads on Qubit.	200
Tab. 5.3 BLAST species identification. *=the same score was obtained for the listed species.	201

1 INTRODUCTION



1.1 DIPTERA LIFE-CYCLE AND SYSTEMATICS

The majority of specimens collected, analysed and interpreted in this thesis belong to Diptera, also known as “true flies”, one of the largest orders within the class Insecta. So far, 160,000 species of flies have been discovered and described, though current estimates suggest there could be as many as 400,000 and 800,000 species of flies (Marshall, 2012), making up the ~15% of known animal species. The name *Diptera* was coined by Aristotle and comes from the union of the words “dis” (δύς) = two and “pteron” (πτερόν) = wing (Marshall, 2012), denoting the presence of a single pair of membranous wings. This is the most important and distinctive diagnostic character as the majority of winged insects have two pair of wings, except for Strepsiptera. In the true flies, the original second pair of wings is reduced to a pair of stick-club-like structures called *halters* and attached to the mesothorax (Fig. 1.1). Each halter is supported by a base full of sense organs and is used to maintain stability during the flight (Marshall, 2012).

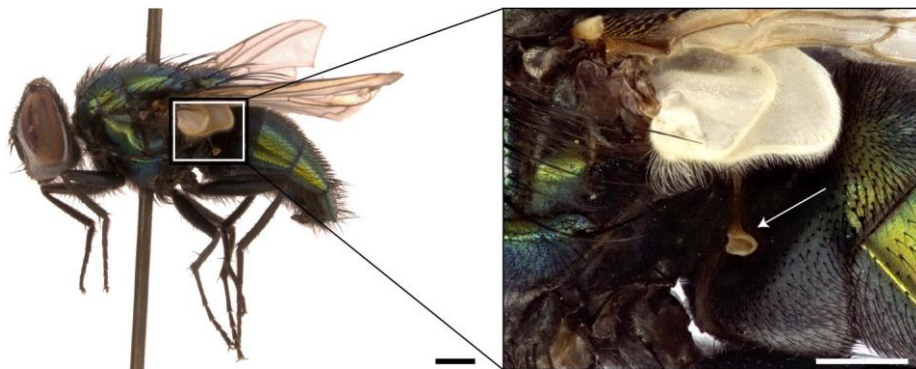


Fig. 1.1 Halteres of an adult fly. Distinctive characteristic of the Diptera order, the stick-club-like structures are attached to the mesothorax (white arrow). Scale bars: 1 mm (adult), 500 μm (detail).

Thousands of species are of significant economic and ecological importance to humans, as they have an important role in providing ecosystem services such as pollination of plants, biological control of pest insects, recycling of dung, carrion and any other organic matter (Marshall, 2012). In addition, a few dozen species are responsible for transmitting several diseases, and damaging forests, crops and store products, thus being of medical and agricultural importance.

Introduction

Diptera are holometabolous insects going through four distinct developmental stages: eggs, larva (I,II,III instars), pupa, and adult or imago¹ (Fig. 1.2).

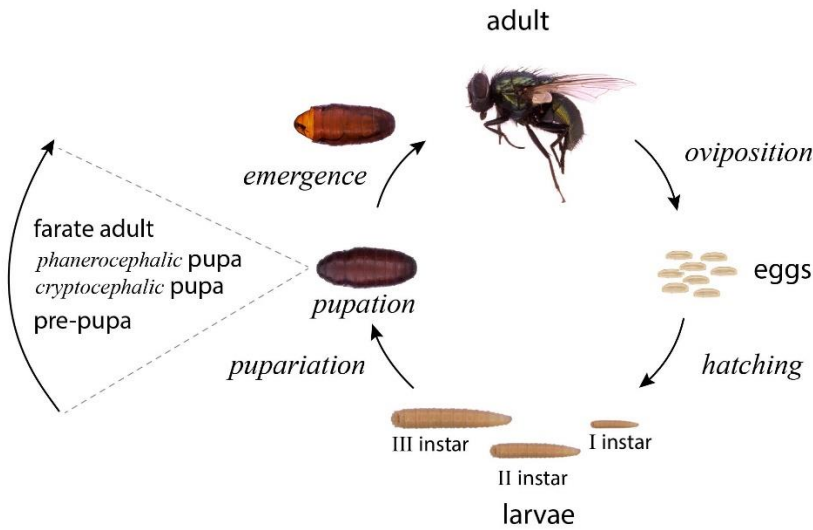


Fig. 1.2 Diptera life cycle. A true fly undergoes to four developmental stages. The definition of “pupation”, “pupariation”, “phanerocephalic” and “cryptocephalic” pupa are given in the text.

Eggs. The majority of flies are oviparous, i.e. they lay eggs fertilised when still in the oviducts of the female. Oviposition generally occurs on or near the pabulum required by the offspring, after hatching, where the presence of high moisture is guaranteed. The eggs, measuring a few hundreds of μm , have a grain of rice shape and are covered by a protective coat form of the vitelline membrane and the chorion. The whole design is aimed to allow fertilisation, facilitate the oviposition, and guarantee the right level of selectivity for the optimal developmental conditions. In many species the dorsal side of the chorion has a polygonal pattern, while the ventral side is rich in microscopic peduncles and appendices involved in the adhesion to the substratum and the exchange of gas and substances with the external environment.

Larva. After a period of time which is species-specific and temperature dependent, the eggs hatch. Usually there are three larval stages or instars differing mainly in size and in the presence of anatomic features which appear only during the late instars. Commonly known as maggots, fly larvae have segmented bodies whose pointed end reveals the

¹ For the purposes of this thesis, the *Ciclorrhapta* life cycle is illustrated.

presence of hardened dark structures forming the mouth parts; they are composed of an internal part called *cephaloskeleton*, and an external visible part called mouthhooks used to literally tear the *pabulum* apart. The intake of food occurs upon selective-filter system and proceeds until larva enters the “post-feeding state”, defining the transition to next stage of the life cycle.

Pupa. The life cycle continues with a “resting pupal stage” (Gullan and Cranston, 2014) occurring inside a hard, opaque, barrel shape puparium formed from the cuticle of the third instar larva (Martín-Vega et al., 2016). The formation of this structure is called *pupariation* and it is the first event after the contraction of the post-feeding larva (Martín-Vega et al., 2016). Within the puparium, the metamorphosis from larval to adult takes place through a series of events involving the rearrangement of the internal organs of the immatures, and the progressive development of new features typical of a mature fly. During this hormone controlled and complex process called *pupation*, the insect undertaking the metamorphosis is generally named *pupa*. However, due to the confusion generated in the literature, Martín-Vega and co-authors (2016) recently re-defined the nomenclature by observing the transformation of flies within the puparium:

- *Prepupa*. Insect still attached to the puparium, prior to the first apolytic event
- *Pupa*. Insect physically separated from the puparium
- *Cryptocephalic pupa*. Pupa with legs and wings partially everted, but not the head
- *Phanerocephalic pupa*. Pupa with legs, wings, and head completely everted; head, thorax, and abdomen visible
- *Pharate adult*. Phanerocephalic pupa which is completely separated from the pupal cuticle

An exceptional resolution of each metamorphosis stage has been also provided through micro CT scan analysis (Hall and Martín-Vega, 2019).

Adult. At the completion of pharate adult development, the fly emerges from the puparium in different ways which are taxon specific. The head of an adult fly and its main anatomical features is shown in Fig. 1.3. The two large compound eyes are composed of thousands of small units called *ommatidia* each of which produce a partial fraction of an image, and only all the ommatidia together allow the visualisation of the whole image.

Introduction

In many species the distance between eyes is used for the diagnosis of the sex, as in females (Fig. 1.4A) the distance is larger than in males (Fig. 1.4B,C). Additionally, the orientation of the bristles can be used as a discriminant characters (Ball, 2015).

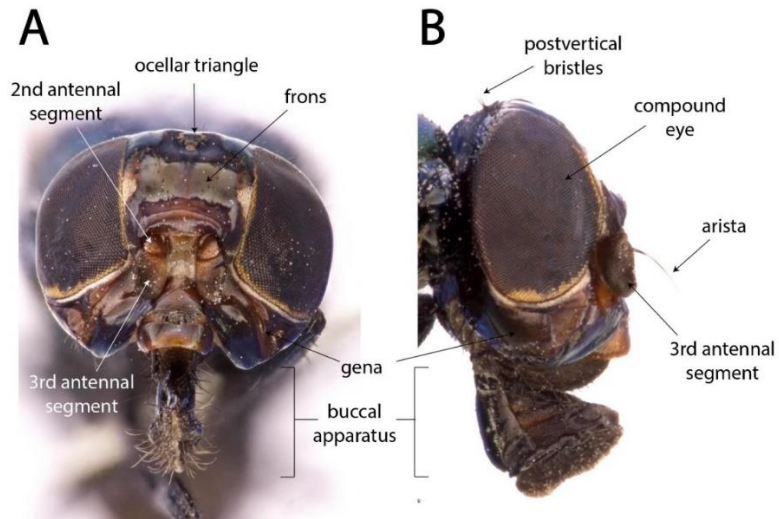


Fig. 1.3 Head of an adult fly. (A) frontal and (B) lateral view of an adult fly species (Diptera: Ulidiidae).

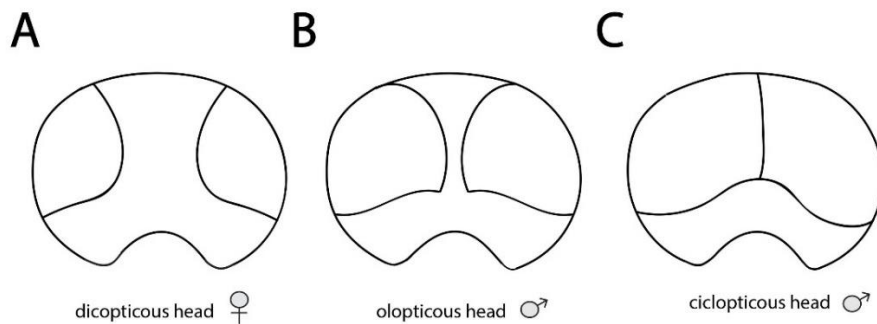


Fig. 1.4 Compound eyes in female and male adult flies.

Thorax is composed mainly of meso-thorax that is a segment more developed than the other two segments (proto- and meta-) as it bears the pair of wings and the midlegs. The legs are equipped with appendixes which allow them to adhere to smooth surfaces (Masutti and Zangheri, 2001). The genital organs are located in the caudal segments of the abdomen. In females, the urites extend till forming the ovipositor with a telescopic structure, while in the males the last caudal urites are organised to form a protective structure for the external genitals (Masutti and Zangheri, 2001), which are essential to the

species determinations in some species (e.g. Sarcophagidae (Giroux et al., 2010), Calliphoridae, Phoridae, etc).

Diptera have been classified into approximately 10,000 genera, 150 families, 8-10 infraorders, and 2 suborders (Yeates et al., 2007). Elucidating the phylogenetic relationships of such a large component of the global biodiversity is challenging but is essential to understand their evolutionary history. In comparison to the first systematic classification of the order by German entomologist Willi Hennig (1913-1976), significant advances have been made in the last few decades (Yeates et al., 2007). Recent research has been characterised by the use of methods analysing morphological characters along with the inclusion of large volumes of molecular sequence data, as well as a high number of well-preserved fossils from the Triassic (250-200 million years BP) (Yeates et al., 2007). In addition, the novelty of the past decades is the attempt to summarise phylogenetic data cross-checking large components of it by using rigorous numerical approaches producing the so-called *supertree* (Yeates et al., 2007). The last update of the phylogenetic relationships among infraorders and superfamilies of Diptera is presented in Fig. 1.5 (Lambkin et al., 2012). The analysis was based on evaluation of 371 morphological characters of larvae, pupae and 42 species of adults and the results are partially consistent with molecular studies (Lambkin et al., 2012)

As previously mentioned, Diptera monophyly is well-established on the basis of the presence of modified hind-wings into halteres, as well as the specialisation of adult mouthparts, and locomotory organs of the larvae (Lambkin et al., 2012).

Lower Diptera. This group of flies was historically known as the suborder “Nematocera”, distinguishable by long antennae with more than 6 articulate segments. Within the lower Diptera, two main infraorder form monophyletic groups that are highly supported, Culicomorpha and Bibionomorpha, including mosquitos and other flies, vectors of pathogenic microorganisms (Giangaspero, 1997).

Brachycera (or higher Diptera). Brachycera are one of the best supported lineages of the order and are undoubtedly monophyletic. Among the characters that allow to distinguish them from the lower Diptera, there are short antennae composed of 6 antennomeres and compound eyes (Giangaspero, 1997).

Introduction

The *lower Brachycera* are paraphyletic in relation to the other Brachycera and the two groups are distinguishable as the lower Brachycera do not undergo pupariation involving the formation of the hardened puparium (Lambkin et al., 2012). Tabanomorpha (horse flies) and Stratiomorpha are the major infraorders, including families with medical and veterinary implications.

Eremoneura. It is a species-rich group comprising of Empidoidea and Cyclorrapha. The latter is a well-supported clade whose members undergo pupation within the puparium and include the major family-level diversity group under the name of *Schizophora*. Their identification as monophyletic group arose from the presence of the *ptilinum*, a sort of bag placed on the head of the flies serving to force off the end of the puparium allowing the adult to emerge. The structure collapses soon after, leaving a marked ptilinal suture (Giangaspero, 1997).

A further division within Schizophora concerns the calypters, membranes located close to the wings junction which are absent in Acalyptrate flies and present in the Calyptrate flies (Fig. 1.1).

As far as this thesis concerns, families belonging to Muscoidea and Oestroidea (Calyptratae) superfamilies have been analysed (Fig. 1.5).

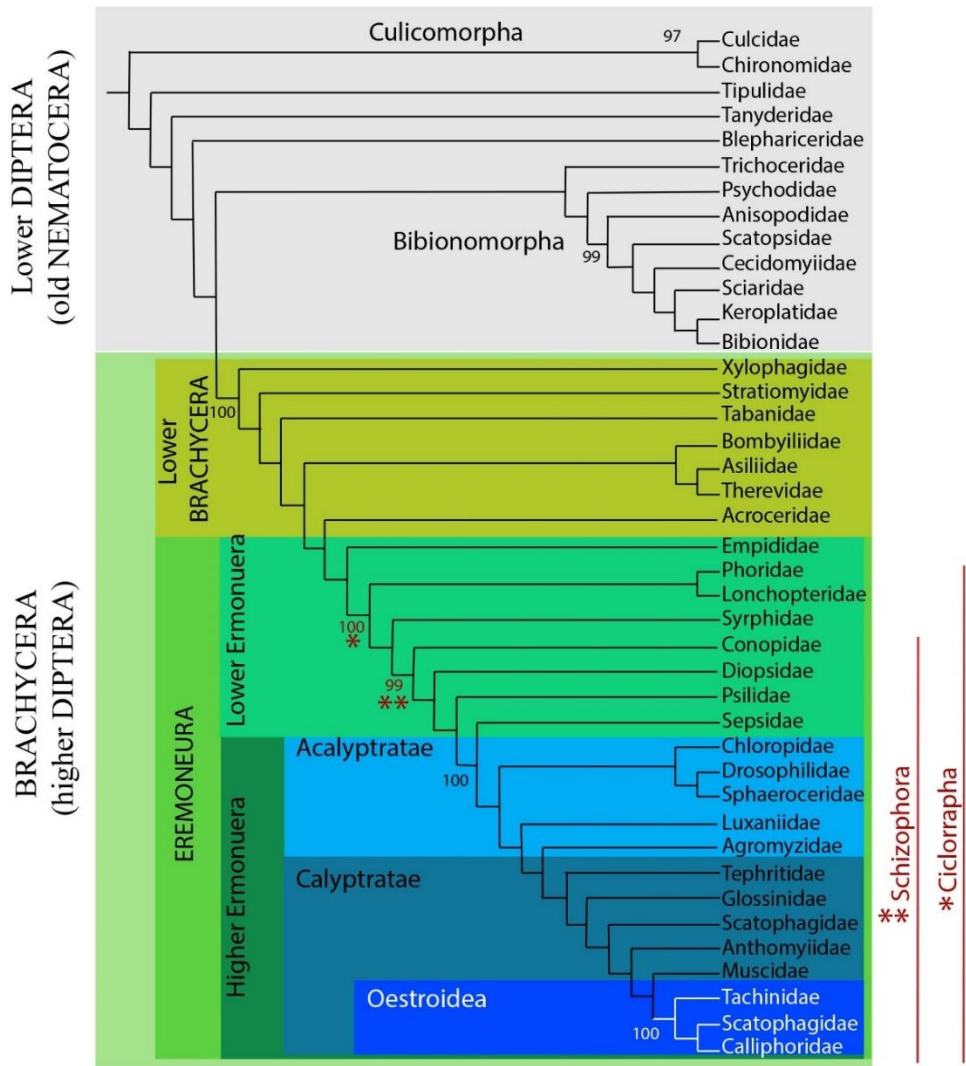


Fig. 1.5 Morphological systematic of Diptera. Relationships at infraorders and superfamilies level are enlightened. Modified picture from Lambkin (Lambkin et al., 2012).

1.2 INSECTS: WITNESSES OF THE PAST

The interest for insects by men is rooted in prehistoric times, as supported by the finding of a rock-painted bee from 13,000 BC. However, the acknowledge of entomology as scientific discipline is relatively recent, dating back in the late 16th century (Saltini, 1984). Nowadays, entomology is widely applied to other scientific fields, including but not limited to agriculture and pest control, animal and human health, and other present topics related to a major eco-compatibility, such as the waste biodegradation (Sarpong et al., 2019, Setti et al., 2019) and eco-sustainability. In addition, in the last decades, the study of insects has been applied to forensic and archaeological investigations focussing on their role as “witnesses of past events”, the key concept of this thesis.

Forensic entomology has been acknowledged among forensic sciences, as it is based upon the observation, identification and interpretation of insects as physical evidence during legal investigations (Amendt et al., 2007). Despite the ancient origin of the term “forensic”, its current use lacks of a precise definition on a temporal scale to define whether a context, or a finding, is forensic or not. Conventionally, the scientific community uses “forensic” as synonymous of “modern”, *i.e.* belonging to the “present time” and implicitly extends it and establishes its limit to the Second World (Fig. 1.6A). Indeed, it is part of our conventional understanding of the world that the present is what we observe around us and can know about through direct experience (Bailey, 2007). It is worth mentioning that, in case of homicide, the crime is no longer investigated after the death of the perpetrator, so human lifespan can be used as the temporal frame for the appropriate usage of the word “forensic”.

On the contrary, there are defined temporal borders in archaeology which, however, are subjected to enormous variations. For example, the social anthropologists consider the “present” the past 100 years, whereas for some historians the “present era” extends to about 300 years. Palaeolithic archaeologists, however, refer to anything after 10,000 years ago as “modern” (Bailey, 2007). Overall, appears the boundary between present and past is rather arbitrary and depends on the phenomena of interest that are being investigated (Fig. 1.6A). Bailey refers to a “durational present” explaining that, in all cases mentioned

above, the “present” has a fixed duration, which is quite different depending on the observers. In other words, the time scale is largely flexible (Bailey, 2007). An event occurred in a far past, thus “archaeological” on the time scale, may have had forensic implications at the time when the event occurred. Vice versa, a forensic, modern, case cannot have any conceptual relation with the archaeology.

In this thesis, in compliance with what has been established by the scientific community, the adjectives “modern” and “forensic” will refer to entomological specimens being of forensic importance and either collected from experimental trials, crime scenes, reared in laboratory under controlled conditions, or belonging to museum collections. The term is specifically used in opposition to “archaeological” samples which, instead, do not have any legal implication, and highlights the “chronological age” of the samples (Fig. 1.6B).

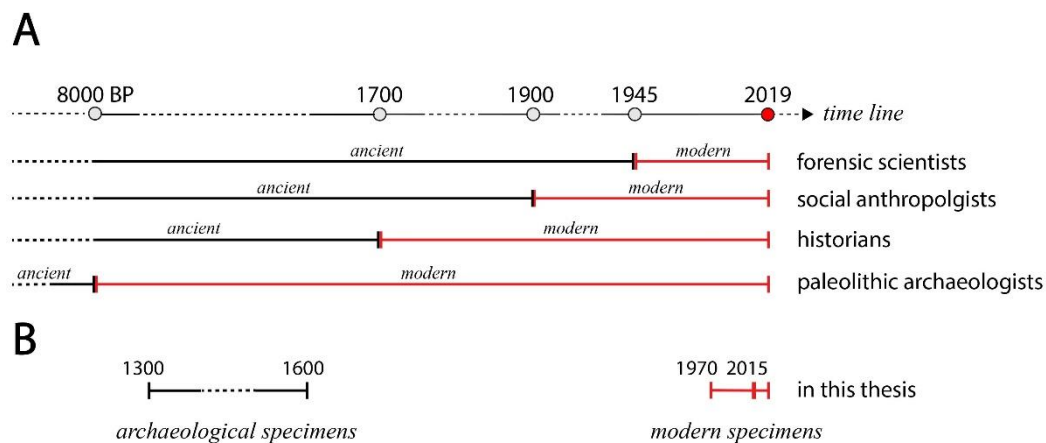


Fig. 1.6 Time perception in forensic and archaeological studies. (A) time as perceived by forensic scientist and archaeologists. The boundary between “modern” (red line) and “ancient” (black line) is rather arbitrary and depends upon the phenomena of interest; (B) time line of the entomological specimens studied and presented in this thesis.

1.3 FORENSIC ENTOMOLOGY

For the purposes of this thesis, “forensic entomology” addresses the medico-legal aspect of the discipline, focusing on necrophagous insects that feed on cadavers and actively take part to the decomposition process.

The analysis of the cadaveric entomofauna leads to the interpretation of *peri mortem* circumstances of an individual and allows the following:

- to determine if a cadaver has been moved from a primary to a secondary crime scene;
- to determine if a cadaver has been left exposed, how long for, or if has been concealed (Amendt et al., 2011, Hall et al., 2012);
- to identify sites of trauma on the body (Campobasso et al., 2005);
- to evaluate the involvement of drug consumption (entomotoxicology) (de Carvalho, 2010);
- to link a person to a location, or identify the victim in the absence of the cadaver through DNA extraction from larvae gut content and human STR genotyping (Wells et al., 2001, Campobasso et al., 2005, Di Luise et al., 2008);
- to estimate the minimum *post mortem* interval (PMI), *i.e.* the time elapsed between the oviposition of flies on the cadaver and the discovery of the cadaver, also known as *time of colonisation* (TOC) or *period of insects activity* (PIA) (Fig. 1.7) ((Byrd and Castner, 2001, Amendt et al., 2011, Hall et al., 2012).

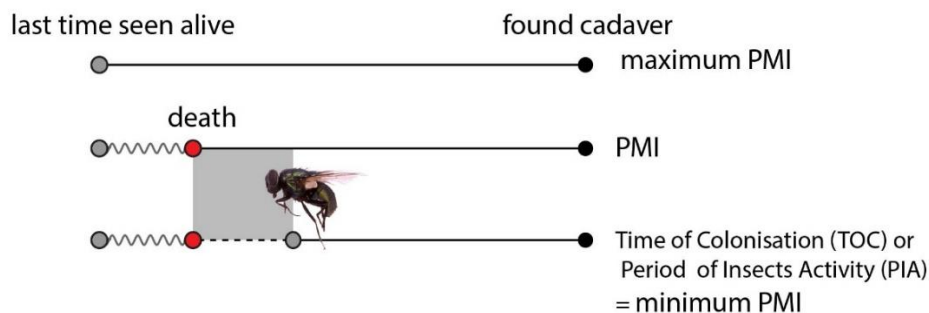


Fig. 1.7 Schematic representation of the real, maximum, and minimum PMI.
Twisted lines indicate unknown time range; dashed lines indicate variable time range.

The role of forensic entomology in the time since death estimation is irreplaceable in case of concealment, body dismemberment, explosion, and burning of the corpse when the morphological features of the cadaver are so damaged that there is no standardised methods based on experimental studies for deriving time since death in an accurate way (Vanin et al., 2013). The minPMI hardly overlaps to the real PMI, instead it is usually shorter and this explains the reason why only an estimation of this time can be given.

1.3.1 Overview of cadaver decomposition

From an ecological perspective, the decomposition of a corpse is a dynamic and complex process involving the combined action of abiotic and biotic factors (Benbow et al., 2015). Humidity and temperature act as physical modulators of the activity of microbial communities, necrophagous insects, and animal scavengers which find in the cadaver/carrion their preferred *pabulum* and their coordinate action result in the breakdown of the cadaver/carrion (Carter et al., 2007). Although decomposition is a constant and continuing process, three main phases and five sub-stages (Payne, 1965) can be distinguished:

1) *autolysis or self-digestion*. It's the natural breakdown of the cells following the death of a living organism. (Smith, 1986, Campobasso et al., 2001). This phase corresponds to the "fresh" stage;

2) *putrefaction* is the breakdown of soft tissues by bacteria releasing gases (VOCs) (Davis et al., 2013) that attract the first flies. In this phase, fly activity on the corpse will reach the highest peak (Smith, 1986, Amendt et al., 2004a). This phase includes "bloat", "active decay" and "advance decay" stages;

3) skeletal bones *decomposition* attracts mainly insects within Coleoptera order. This phase corresponds to the "dry" stage;

It is worth mentioning that environmental conditions can module the rate of decomposition until the point to inhibit or stop the process as in the case of mummified bodies. Dry climates (whether very hot or very cold) cause high level of dehydration (Brenner, 2004) preventing the breakdown at the roots of the process and making the *pabulum* non-attractive to insects and scavengers (Smith, 1986, Byrd and Castner, 2001).

Introduction

In these circumstances, the mPMI estimation can not be provided, however, entomological investigations are still helpful to derive information about seasonality of death, exposition of the body or concealment.

1.3.2 Succession of necrophagous insects on cadavers

The entomofauna found on a corpse include several taxa that have been grouped by Smith in four ecological categories (Smith, 1986):

- necrophagous species feeding on cadavers/carcasses and fundamental in mPMI estimation (Diptera and Coleoptera);
- predators and parasites/parasitoids of necrophagous species (Diptera, Coleoptera, Hymenoptera);
- omnivorous species feeding both on cadavers as well as on their inhabitants, necrophagous and predators of necrophagous species (Hymenoptera, Coleoptera);
- adventive species inhabiting the environment where the cadaver is found but not feeding on it, only using it as part of their natural habitat and accidentally collected along with other species.

From a forensic point of view, species belonging to the first and second groups are the most important. Specifically, it is well accepted, although recently debated, that necrophagous species do not occur simultaneously on a cadaver, rather their pattern arrival occurs sequentially. In 1894, Mégnin coined the expression *travailleurs de la mort* organised in *escadrons*, describing a continuous but predictable flow of flies and other arthropods (Mégnin, 1894) that participate to the depletion of a cadaver. This faunal succession include eight so called “colonisation waves” and is shown in Fig. 1.8 in order to provide a complete scenario of the entomological perspective of decomposition. As the decomposition of a corpse progresses, necrophagous Diptera predominant in the initial phases are progressively replaced by Coleoptera, well known to feed on drier tissue. It is also worth to mention that other than major families including Calliphoridae, Sarcophagidae, Fanniidae, Muscidae, Piophilidae, Spaheroceridae, and Phoridae (Fig. 1.8) which are well known body colonisers, less common taxa, renamed “secondary taxa”,

might be occasionally collected from a corpse. These groups include species within the families Trichoceridae, Psychodidae, Drosophilidae, and Milichiidae (Giordani et al., 2018c). Acknowledging their appearance on cadavers is important to avoid species misidentification and contribute to accurately interpret *peri mortem* events.

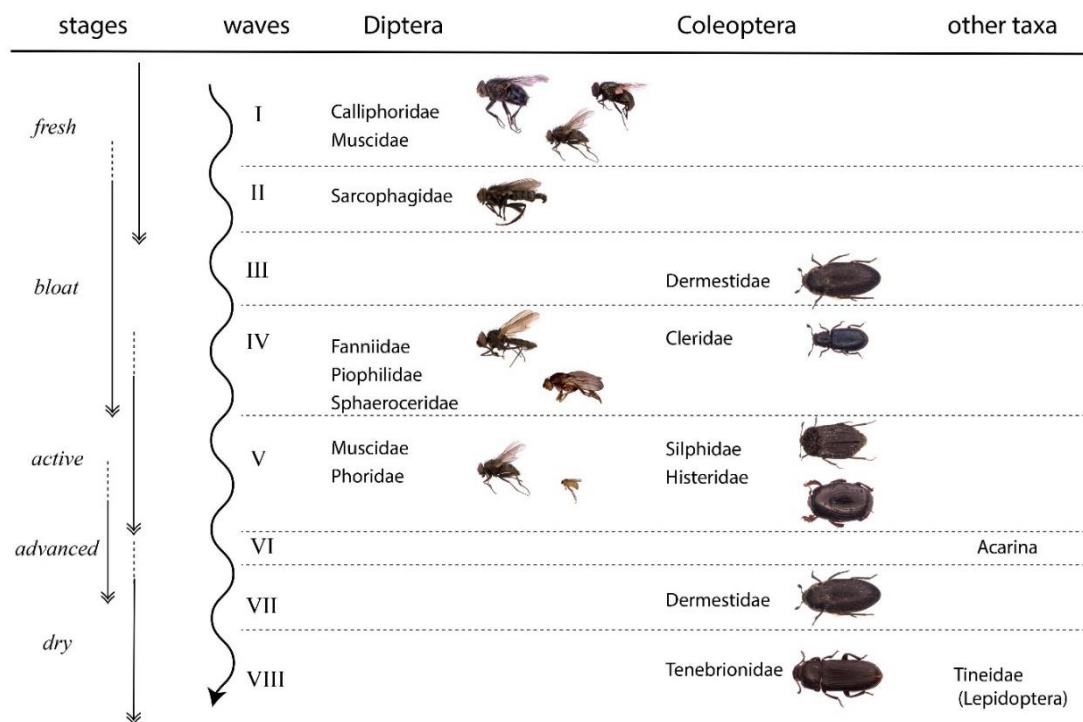


Fig. 1.8 Insects succession on cadavers. Necrophagous insects “colonisation waves” on cadavers correlates with the progression of the decomposition. Insects picture images modified from Dr Giorgia Giordani, not in scale.

1.3.1 Introduction to Piophilidae of forensic interest

Piophilidae is a small family of Diptera numbering about 70 species with a worldwide distribution and historically associated to human activities (McAlpine, 1977, Marshall, 2012). They are commonly called “skipper flies” due to the leaping behaviour shown by their post-feeding larvae which consists on arching the body until the anterior mouth hooks contact with the posterior anal tubercles, pulling and suddenly releasing them (Bonduriansky, 2002) (Fig. 1.9). It has been suggested that this behaviour is aimed to avoid parasitism and predators, especially when the larvae leave their feeding substratum and move to pupation site (Bonduriansky, 2002).

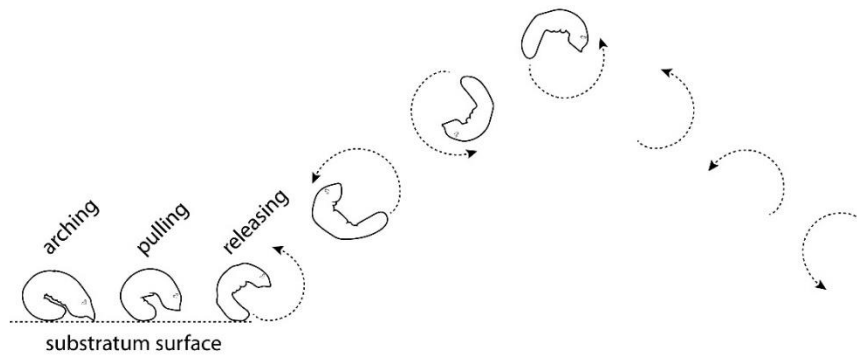


Fig. 1.9 Piophilidae leaping behaviour. Arching, pulling, and releasing phases of the leaping behaviour of Piophilidae larvae is schematically shown. The image has been drawn by the author of this thesis.

For centuries, Piophilids have been well-known as food pests, mainly infesting protein-rich animal products (Simmons, 1927, Zuska and Laštovka, 1969) especially the so-called “cheese skippers”, reported to cause significant economic losses to the food industry in Europe and North America until the first half of the 20th century. Today, the improvement of the hygienic and storage conditions effectively reduced their economic impact and, on the other hand, in some European countries the larvae are used to produce traditional cheeses such as the Italian “casu martzu” (Miokovic et al., 1997, Mazzette et al., 2010). The majority of the members of this family have necrophagous habits and, in particular, they feed on cadavers in advanced stages of the decomposition when fatty acid and caseic metabolites are produced (Smith, 1986). Some species are also known to parasitise living tissues in humans, especially the intestinal and urino-genital tract, causing myiasis (Saleh and el Sibae, 1993). Therefore, they have an important impact in forensic entomology and overall in medico-legal investigations (Martín-Vega, 2011, Martín-Vega et al., 2012, Martín-Vega, 2017). *Piophilidae casei* (Linnaeus, 1758) is certainly the most frequently recorded species reported in forensic entomology studies (Rocheffort et al., 2015), often as a consequence of misidentification due to the high similarity of certain morphological characters shared with other species. For example, the species *Piophilidae megastigmata* McAlpine, 1978 coexists with *P. casei* in the Afrotropical and Palaearctic regions; the two species also share a similar ecological niche and feeding habits (Panos et al., 2013), but they may show different seasonal and successional patterns on carrion (Martín-Vega et al., 2011). Both species can easily be misidentified (Prado e Castro et al.,

2012) also due to the fact that *P. megastigmata* was known to be a typical inhabitant of South Africa and only recently has been reported in various areas of the Iberian Peninsula (Panos et al., 2013). This is explicative of how is important the constant monitoring of the geographical distribution of the species which might change over time, due climatic changes or the abundant commercial trades worldwide (Lo Pinto et al. 2017).

So far, the identification of Piophilidae flies at all the developmental stages represents indeed one of the biggest challenge for forensic entomologists. McAlpine's work (1977) is the most complete work for the adult identifications, however is not ideal to identify species of forensic interest as it mainly describes other species. Moreover, McAlpine's descriptions are based on colour differences which can be a misleading characters due to the intraspecific variation as in the case of *Parapiophila atrifrons*, *Parapiophila vulgaris* and *Prochyliza nigrimana* (Rochefort and Wheeler, 2015). Rochefort provided identification keys of adult of the Nearctic species of forensic importance some of which are present also in Europe (Rochefort et al., 2015). The information available for the immature stages are limited to a small number of species (Smith, 1986, Freidberg, 1981, Ebejer, 2012, Martín-Vega et al., 2012, Martìn-Vega et al., 2014, Martín-Vega, 2017, Panos et al., 2013, Sukontason et al., 2001), and the knowledge on the topic certainly requires further research. In order to fill this gap a collaboration was established with Dr Daniel Martín-Vega, Senior Lecturer at the Universidad de Alcalà in Madrid and actively Researcher at the Natural History Museum in London, with the aim to describe the morphology of the puparium of those Piophilidae species which are more frequently found in association with human cadavers in Europe and North America. Dr Martín-Vega provided part of the specimens on which the analysis here reported are based.

1.3.2 Introduction to Ulidiidae, “secondary taxon” of forensic importance

Ulidiidae, known as “picture-winged” flies, are a small family of Diptera found on animal carcasses and other decomposing biological remains (Marshall, 2012) (Tab. 1.1). One of the species most frequently recorded is *Physiphora alceae* (Preyssler, 1791) belonging to the subfamily Ulidiinae. Larvae of this species develop in dung, decaying vegetable matter and compost heaps (Ebejer, 2015). *Physiphora alceae* is distributed in all the biogeographical regions (Kameneva and Korneyev, 2010a) and in Europe, based on the Fauna Europaea data (<https://fauna-eu.org/>), it is widespread in the majority of the countries with the exception of the Northern countries such as Iceland, Ireland, Norway, Baltic region, and the west coast of the Balcanic region.

Tab. 1.1 World-wide records of Ulidiidae sampled during experiments conducted for forensic purposes.

species	country	source	references
<i>Physiphora alceae</i>	Malaysia	monkeys carcasses	(Rumiza et al., 2010)
	Egypt/Kuwait	rabbits carcasses	(Sawaby et al., 2018) (Al-Mesbah et al., 2012)
	Spain	squat-baited traps	(Martín-Vega and Baz, 2013, Baz et al., 2015)
<i>Physiphora</i> sp.	Malaysia	composting piles	(Morales and Wolff, 2010)
		horse dung	(Heo et al., 2015)
<i>Pseudexesta prima</i>	Island of Guam	traps carrion baited human faeces	(Bohart and Gressitt, 1951)
Ulidiidae	Portugal	decomposing rats	(Monteiro and Penereiro, 1987)
		swines	(Prado e Castro et al., 2012)

In addition to the published records (Tab. 1.1) specimens of *P. alceae* were recently identified within the entomological assemblage collected from the cadaver of a woman, reported missing two months prior to being found in a small town in September within the metropolitan area of Milan (Italy)² (Fig. 1.10). The description of such a context is intended to provide the background for the analysis described in Chapter 5 of this thesis.

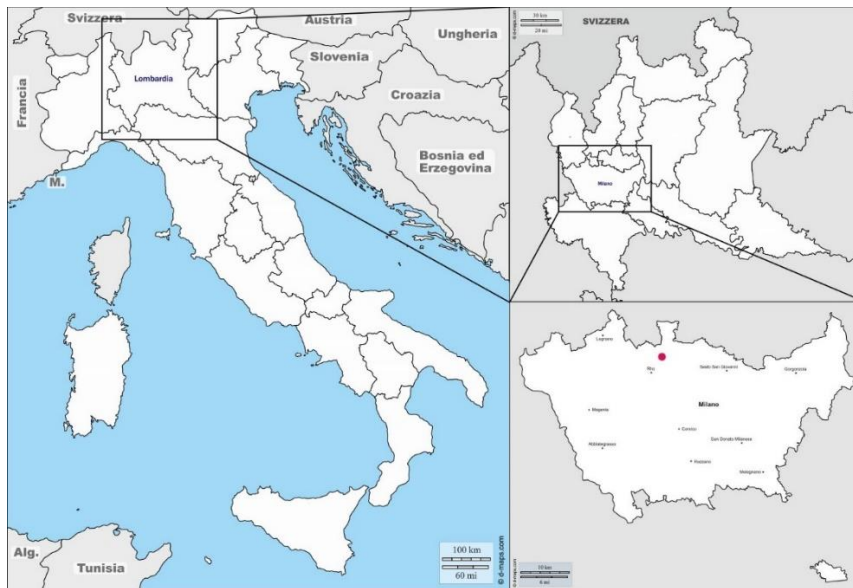


Fig. 1.10 Metropolitan area of Milan (Italy). The red spot indicates the place where the cadaver of the woman was found. Picture modified from © 2007–2018 d-maps.com.

The remains laid in an urban region surrounded by forest and agricultural areas. The body was beheaded, buried in an artificial grave and covered with plastic clothes. A few days after the discovery of the cadaver, the missing skull was found in a plastic bag a few kilometers away from the place where the body was recovered. Both parts of the body were found in advance decay and partially skeletonised. The analysis of the insect community assemblage revealed two different colonization patterns, one for the head composed by species in the families Calliphoridae, Muscidae, Fanniidae and Phoridae whereas the body was colonised by Muscidae, Stratiomyidae, Phoridae and Ulidiidae, including *P. alceae*. Based on the absence of Calliphorids as first colonisers of exposed cadavers, the forensic entomologist in charge hypothesised the cadaver was concealed soon after the death of the woman.

² For legal reasons, no additional data are provided about the case

Introduction

This is the most recent finding of *P.alceae* and the first record of the species on a human cadaver, as well as a further evidence of the role that this “secondary taxon” may play in forensic entomology (Giordani et al., 2018c) in helping to provide further indications about the history of a cadaver. However, still little information is known about the biology of the species, as well as about the morphology. Adults are difficult to be identified as the flies share some morphological characters with other close-related species (e.g. *Physiphora longicornis* (Hendel, 1909) (Chen and Kameneva, 2007)). Furthermore, there are no available descriptions of the immature stages which are routinely found on a crime scene. Overall, only a few descriptions of larvae and puparia of Ulidiidae were provided in the past (Bohart and Gressitt, 1951), but none concerns any species of potential forensic interest.

1.4 ARCHAEOENTOMOLOGY

Archaeoentomology is defined as the study of invertebrates, *i.e.* insects and other arthropods, recovered during archaeological excavations, with the aim to understand environmental, climatic, and/or cultural conditions of the past. It is worth mentioning that archaeoentomology deals with anthropic settlements where insects are found in microhabitats very similar to their natural environments and benefit from their facultative or obligate association with humans (King, 2014). The use of insects in the interpretation of past environments likely had its beginnings in Egypt, as documented in a paper by the Oxford entomologist Reverend F. W. Hope on insect remains found in the gut of a mummified ibis (*Threskiornis aethiopicus* Latham, 1790). Despite the skepticism of the ornithologists, Hope was able to identify beetle remains in the ibis' gut content and helped in clarifying the bird's diet habits (Panagiotakopulu, 2001).

Indeed, archaeoentomology is a branch of environmental archaeology which is a large interdisciplinary subject involving specialists in geology, geography, climatology, biology, history, and anthropology (Kenward, 2009), all collaborating and providing field-specific information in order to draw a scenario as accurate and complete as possible about human past. As stated by Kenward, "*No archaeological project involving excavation can now be regarded as having been properly executed unless the full range of evidence has been properly examined...*" (2009).

What makes insects an exceptional, although often underestimated, evidence to study is that they are the most ecologically diverse group of animals, capable of surviving in a large variety of habitats characterised by the most diverse environmental conditions (Buckland et al., 2014). Therefore, archaeoentomological investigations are essentially based on habitat preferences of species recovered from ancient deposits to infer past scenarios, considering that the majority of them did not evolve in the last 2 million years and still exist nowadays, allowing the data comparison (Buckland et al., 2014, Forbes et al., 2013). Through identification of taxa found within an archaeological assemblage, information about the following topics can be derived:

Introduction

- past climate and environments, both inland and marine (estuarine and coastal) (Elias, 2014, Buckland et al., 2016, Ashworth et al., 1997, Smith, 2017);
- human diet (Panagiotakopulu, 2001);
- agricultural practices, even through the study of stable isotopes accumulated in the insects exoskeleton (King, 2012);
- commercial trades, as in the case of the finding of the khapra beetle (*Trogoderma granarium* Everts, 1898), recovered from grain seeds within the Egyptian Museum of Turin's collection, which may indicate an early contact with the Indian subcontinent (Panagiotakopulu, 2003);
- human living conditions and attitudes to hygiene (Chapter 5 of this thesis), (Panagiotakopulu, 2004, McCobb et al., 2004, Kenward and Hall, 1997). For example, ectoparasites living on hosts' body such as lice (*Pediculus humanus* Linnaeus, 1758), fleas (*Pulex irritans* Linnaeus, 1758), and bedbugs (*Cimex lectularius* Latreille, 1802) were found in archaeological sites in Europe, North and South America, and Near East. Although they are generally indicators of poor sanitary conditions (Raoult et al., 2006, Bain, 2004, Forbes et al., 2013, Forbes et al., 2015), Bain (2004) points out that in making these assumptions we are imposing modern Western standards of hygiene on those living in the past;
- permanence of settlements (Ponel et al., 2000, Panagiotakopulu et al., 2007, Panagiotakopulu and Buchan, 2015);
- funerary practices (Huchet, 1996)

1.4.1 Archaeoentomology and funerary practices: Archaeology of death

While studying the entomofauna assemblage discovered during the archaeological investigation of a 10th century sarcophagus attributed to one of the members of the family of the Counts of Toulouse, the well-known entomologist Jean-Bernard Huchet coined the expression *archéoentomologie funéraire*, or funerary archaeoentomology (1996). Huchet announced the birth of a new line of research where knowledge about medico-legal entomology, archaeology, as well as history found themselves weaved together in a very original way that nobody before thought about, and that can be summarised as the

“application of the medico-legal forensic entomology to the study and interpretation of insect remains associated with graves in archaeological contexts” (Huchet, 1996). As previously mentioned, medico-legal forensic entomology mainly deals with the estimation of mPMI. However, if, obviously mPMI cannot be traced in any archaeological context, the study of the arthropods remains collected from a grave, combined with their biology, can provide relevant information about the “history” of the cadaver, including *peri* and *post mortem* events such as seasonality of death, estimation of the corpse exposure duration, delayed burial, grave reopening, identification of secondary burials and other aspects concerning the reconstruction of the taphonomic process³ (Huchet and Greenberg, 2010, Huchet et al., 2013b, Huchet, 2014b).

When analysing insects assemblages collected from archaeological burials, four categories of taxa can be distinguished (Huchet, 2014b):

- 1) taxa associated to corpses (skeletonised or mummified) and strictly associated to the decomposition process, as members of one of the “successional waves” described in paragraph 1.3.2 of this chapter. In regard of the “colonisation mode”, it is worth reminding that two kind of taxa can be identified (Huchet, 2014b):
 - *pre-depositional phase taxa*, including necrophagous insects colonising corpses or carcasses shortly after death in a time period prior burial;
 - *post-depositional phase taxa*, specialised in colonising underground corpses only (Diptera: Muscidae and Phoridae).

This distinction is essential to reconstruct the taphocenosis (*i.e.* the assemblage of cadaveric organisms) *post facto*, as the biodiversity of the entomofauna of buried corpses is less diverse than the one of exposed corpses;

³ As defined by Efremov (1940) taphonomy was originally defined as the study of the transition of animal remains from the biosphere to the lithosphere as the result of geological and biological processes. In the text, the term is used in its derived meaning, adapted and extended to forensic field, and defined as the study of the *post mortem* changes of human remains, discriminating the products of human behaviour from those created by the Earth’s biological, physical, chemical, and geological subsystems (Haglund and Sorg, 1997).

Introduction

- 2) taxa associated with offerings such as clothes, ornaments, personal artefacts, or vegetal matter as in the recovery of the cutting leaves ant *Acromyrmex versicolor* Pergande, 1894 from a Mexican funerary bundle (Huchet et al., 2013b);
- 3) taxa resulting from subsequent contaminations (Huchet, 2010);
- 4) taxa identified as vectors of pathogens as in the case of Napoleon's soldiers corpses carrying lice from which the DNA of the gram-negative bacteria *Bartonella quintana* (Schmincke 1917) Brenner et al. 1993, the agent of trench fever, was retrieved (Raoult et al., 2006).

1.4.2 Preservation of insects in archaeological contexts

The entomofauna preserved in archaeological contexts include fragments or remains of two major order of insects, Coleoptera (beetles) and Diptera (true flies), often acknowledged as the only preserved organic remains (Ponel, 1993). Isolated parts of Coleoptera body such as elytra, legs, head, abdomen, or thorax, and puparia of Diptera are the typical remains emerging from excavations. In fact, it is well-established that the exoskeleton of adult beetles and the puparium of flies is mainly composed of chitin, a linear polysaccharide consisting of β -(1,4)- linked-2-acetamido-2-deoxy-Dglucose, made more resistant by the presence of internal cross-links between the monomers of sugars and other molecules (Minke et al. 1978). The term originates from the ancient Greek "kitón" (κίτων)= tunic, coating and its chemical composition is a determining factor in the *post mortem* survival of insects remains (Vanin and Huchet, 2017). Although the exoskeleton is chemically stable, bacteria and fungi may play a role in its decay, therefore dry and very cold or very hot environments or waterlogging conditions (Buckland et al., 2014) are more conducive to preservation, for the same principles previously described for mummification of a corpse. In addition, the pressure of sediments can contribute to the physical degradation of the exoskeleton, hence intact specimens are barely found. Whether full or empty puparia are found on a site is highly informative to reconstruct the events linked to that site: empty puparia indicate that the life cycle has been completed before burial or secondary events occurred, while full puparia indicate that the burial mode or the environmental conditions interrupted the development of the

flies (Huchet, 2014b). Different environmental conditions can contribute to differently preserve puparia specimens and, ultimately, lead to severely diverse phenotypes at the moment of their discovery (Fig. 1.11).



Fig. 1.11 Preservation of Diptera remains in archaeological contexts. Puparia collected from diverse contexts may show a different appearance. Scale bars: 1 mm.

In addition, mites (Arachnida: Acarina), can be remarkably well-preserved in sediments even aged on the geological time scale (e.g. 400 million years ago (Norton et al., 1988). In archaeological contexts, mites have been found in association to human mummies including those of a Capuchin monk in Palermo (Sicily, Italy), whose examination proved it was infested by *Sarcoptes scabiei* (Linnaeus, 1758), a parasitic mite and aetiological agent of scabies. Their study results in the birth of a quite recent branch of archaeozoology, known as “archaeo-acarology” (Huchet, 2014b).

It is also worth mentioning that when environmental conditions are not conducive enough to guarantee the preservation of organic matter, insect’s activity can still be revealed by imprints or traces on objects left as offerings in the burials such as textile, metal, ceramics, as well as bones. In archaeology, the science studying the interaction between living organisms and the substratum they were attached to leaving their traces is known as “ichnoarchaeology” (Huchet, 2014b). When the reference substratum consists of bones, the investigated process is called osteophagy and it can be the result of subterranean termites (Backwell et al., 2012) and Dermestidae beetles (Huchet et al., 2013a). The latter either feed on or literally dig the so-called “pupariation chambers”, cavities dig into bone tissues used as sheltered places where either the insect undertakes the metamorphosis or avoids predation or cannibalism by other larvae (Huchet et al., 2011). The identification and the correct interpretation of these imprints as insects traces

are crucial in order to avoid their misinterpretation with pathological marks of the individual.

1.4.3 Italian archaeoentomological records

Compared to the rest of Europe, the archaeoentomology field has received little attention in Italy (Fig. 1.12, Tab. 1.2). Only a small number of studies report palaeoentomological records either from high altitudes (Ponel and Richoux, 1997, Foddai and Minelli, 1994) or at sea level (Sacchi and Petti, 2008) (Tab. 1.2).

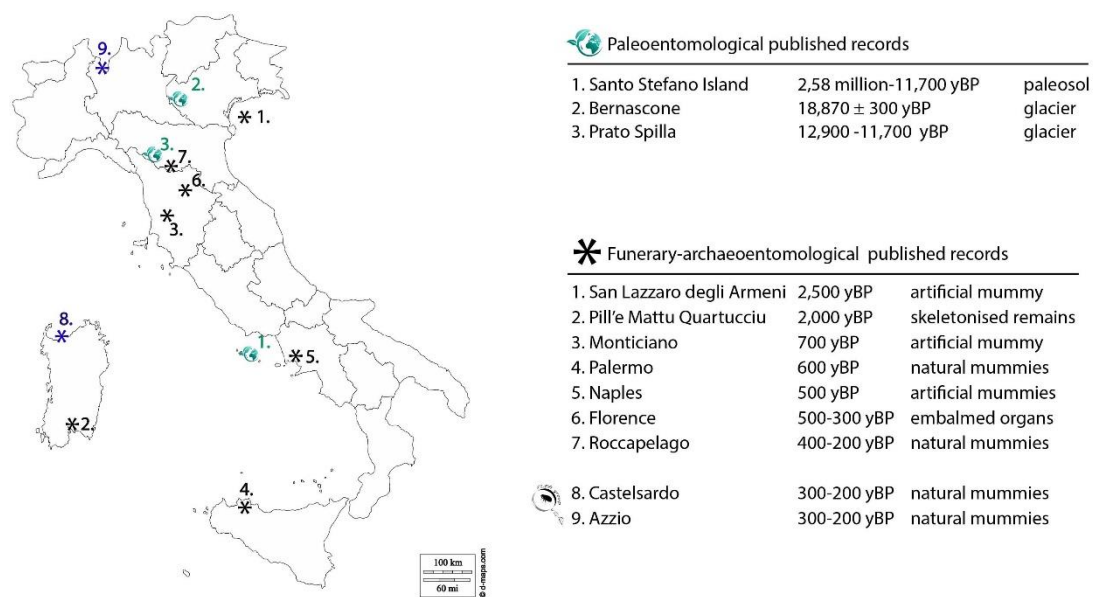


Fig. 1.12 Palaeoentomological and funerary-archaeoentomological Italian public records. yBP= years before present; map from © 2007-2018 d-maps.com.

The published records concerning funerary-archaeoentomological research are more abundant, show a quite wide distribution on the Italian peninsula, and, on the time scale, cover a range approximately between 2,500 and 200 years ago (Fig. 1.12, Tab. 1.2).

The most ancient record is the Egyptian mummy *Namenkhet Amun* conserved at San Lazzaro degli Armeni Monastery, a small island in the Venice lagoon (Northern Italy). The studies conducted by Huchet (2010) reveal insects taxa in accordance with the hypothesis of a short exposition of the body prior the evisceration was completed and the body treated for the mummification (Huchet, 2010).

The Sardinian case of Pill'e Mattu Quartucciu necropolis, numbering more than 270 burials of the Roman time period, is a unique study conducted on skeleton remains and proved that the osteolytic lesions were caused by wild bees and solitary wasps (Pittoni, 2009).

The other records concern natural or artificial mummies, often discovered in places of Christian Catholic worship such as underground crypts.

Two of the current published records are outcomes of the research conducted in the Forensic Laboratory of Archaeology and Entomology (FLEA) at the University of Huddersfield which is where the author of this thesis worked, developing her PhD programme. In particular, the hypogeal taxa found in association with natural mummies of Franciscan friars in Azzio suggests that the corpses were prevented from external exposition and that the decomposition occurred completely in the *putridarium*, an underground room of Catholic Churches used in some Italian monasteries as typical burial from the 16th until the early 20th century (Pradelli et al., 2019). On the other hand, studies conducted on Castelsardo mummies, source of investigation also for this thesis, confirmed the burial practices and have been matter of reflection of the distribution of *Phormia regina* (Meigen, 1826) (Diptera: Phoridae) which is no longer present in Sardinia.

Tab. 1.2 Italian palaeontomological and funerary–archaeoentomological published records.

location	deposit	age (years BP)	taxa	reference
Santo Stefano Island	palaeosols	2.58 million–11,700	Coleoptera ichnofossils	(Sacchi and Petti, 2008)
Bernascone	peat in glacial site	18,870 ± 300	Coleoptera, Hemiptera, Acarina (Arachnida)	(Foddai and Minelli, 1994)
Prato Spilla	glacial site	12,900–11,700	Coleoptera	(Ponel and Richoux, 1997)

location	source of findings	age (years BP)	taxa	reference
San Lazzaro degli Armeni	Egyptian mummy	~2,500	Diptera, Coleoptera	(Huchet, 2010)
Pill'e Matta Quartucciu	necropolis	~2,000	Hymenoptera	(Pittoni, 2009)
Monticiano	Blessed Antonio Patrizi	~700	Diptera, Lepidoptera	(Morrow et al., 2015)
Plaermo	Chapucin monks	~600	Anoplura (lice)	(Gutierrez, 1990)
Naples	Ferdinand II of Aragon	~500	Anoplura (lice)	(Fornaciari et al., 2009)
Naples	Isabella of Aragon	~500	Diptera	(Benelli et al., 2014)
Florence	Medici family embalming jars	~500–300	Diptera, Acarina (Arachnida)	(Morrow et al., 2016)
Roccapelago	local community	~400–200	Diptera, Coleoptera	(Vanin, 2012)
Castelsardo	local community	~300–200	Diptera, Coleoptera, Lepidoptera	(Giordani et al., 2018b)
Azzio	Franciscan community	~300–200	Diptera, Coleoptera, Acarina (Arachnida)	(Pradelli et al., 2019)

1.4.4 Description of Italian archaeological sites studied in this thesis

Crypts of Roccapelago, Emilia Romagna.

Roccapelago is a small village located in the Apennines (1,095 m a.s.l.) in the province of Modena in Emilia-Romagna region ($44^{\circ}12'16''\text{N}$ $10^{\circ}35'29''\text{E}$) (Fig. 1.13). Stabilisation works performed to the “Conversion of San Paolo” church between 2009 and 2011 revealed the medieval village remains (13th-14th century) on which a pre-existing church and its underground crypts, used between the early 15th and the late 18th century, were built (Labate et al., 2011, Traversari et al., 2014). The archaeological excavations brought to light seven tombs containing 281 human remains including infants and adults of which 217 completely skeletonised and 64 partially mummified. Historical investigations revealed that the bodies belonged to an entire population inhabiting Roccapelago between the 16th and the 18th century (Traversari et al., 2014). Two aspects are particularly interesting. The first concerns the fact that, contrary to the usual findings on the national territory, the tombs contained only low-social class people, mainly hard workers, as documented by their clothes and by the anthropological/osteological investigations, and neither monks nor aristocrats were buried there (Gruppioni et al., 2010, Traversari et al., 2014). The second interesting aspect is that it is a case of bodies naturally mummified still showing skin, tendons and hair, found fully dressed, wrapped in gunny bags or *sudaria* and set down one onto the other (Gruppioni et al., 2010, Traversari et al., 2014).



Fig. 1.13 Roccapelago village, Emilia Romagna region (Italy) ($44^{\circ}12'16''\text{N}$ $10^{\circ}35'29''\text{E}$).
(© 2007-2018 d-maps.com).

Introduction

The corpses were piled up forming a pyramid-like structure in the tomb number 7 to which the access was allowed through the presence of stairs (Fig. 1.14, Fig. 1.15).

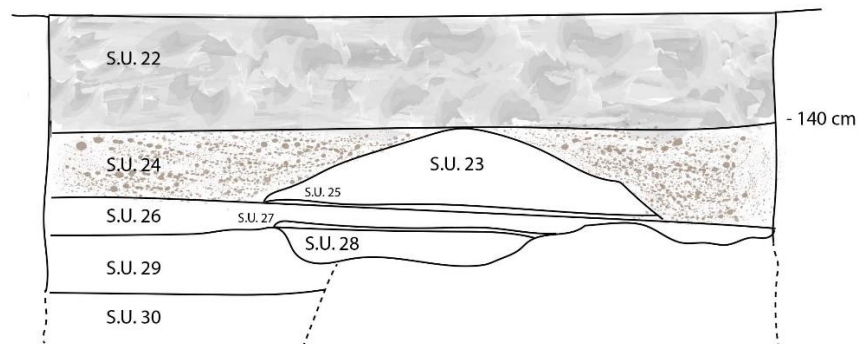


Fig. 1.14 Schematically representation of tomb 7. The 64 mummified bodies (S.U. 23) were found piled-up forming a pyramid-like structure.



Fig. 1.15 Pyramid-like structure of mummified corpses found in S.U. 23.
Picture from Gruppioni et al. (2010).

The first 140 cm underground (S.U. 22) were filled of large bedrocks, likely placed long after the last deposition of the corpses pile, renamed as S.U. 23. The bodies on top, in fact, were found without any evident damage possibly caused by the compression (Gruppioni et al., 2010, Traversari et al., 2014). According to the nature of the tomb illustrated in 1.14, the first burials, therefore the oldest, took advantage of the natural structure of the cliff (S.U. 28) and the skeletons found at that level were badly preserved likely due to the

weight of the following depositions. On the contrary, the remains of the S.U. 23 showed a better state of preservation (Fig. 1.15). As previously described, the natural process of mummification requires particular environmental conditions including very high or very low temperature and a constant ventilation (Byrd and Castner, 2001). In this particular case, a continuous flow air was provided by the presence of two openings excavated within the wall of the rectangular underground room, and the absorption of the decomposition fluids was accelerated by clothes and *sudaria* which were in fact found glued together and still showing visible coloured spots. Some of the Roccapelago mummies today are conserved and exposed at the Museo of Roccapelago (www.museomummieroccapelago.com), while others are still under investigation in Ravenna (Laboratorio di Antropologia Fisica e DNA Antico- Dipartimento di Beni Culturali, Università di Bologna) where a multidisciplinary team is working to provide better insights of the habits and tradition of the population of Roccapelago from the 16th to the 18th century. The FLEA was consulted by Prof Gruppioni (Università di Bologna, Dipartimento di Beni Culturali) to investigate the cadaveric entomofauna found in association to the human remains.

Introduction

Crypts of Castelsardo, Sardinia.

Castelsardo is a small village in the Sassari province located on a promontory overlooking the Asinara gulf in the Northern coast, 114 m a.s.l. ($40^{\circ}54'52''\text{N}$ $8^{\circ}42'46''\text{E}$) (Fig. 1.16, Fig. 1.17A).



Fig. 1.16 Castelsardo village, Sardinia region (Italy) ($40^{\circ}54'52''\text{N}$ $8^{\circ}42'46''\text{E}$).
(© 2007–2018 d-maps.com).



Fig. 1.17 Sant'Antonio Abate Cathedral in Castelsardo. (A) Promontory overlooking the Asinara gulf where Castelsardo arises; (B) Sant' Antonio Abate Cathedral view; (C) bone remains nested into one of the walls of the crypts. Photographs shot by the author of this thesis in September 2018.

The funerary scenario on the background of this study is a group of sepulchral crypts located under the Sant'Antonio Abate Cathedral, an ancient Romanic Church in the old part of the city (Fig. 1.17B). Modern renovation works conducted in 2011 to expand the area of the Diocesan museum revealed a burial site, with a great number of individuals organised in several layers piled up at the bottom of the crypt dated from the 18th to the 19th century (Mazzarello et al., 2014). Eighteen individuals were identified including 16 partially mummified and two almost entirely well-preserved mummified, along with bones remains. Some of them are still visible nested into the rocks walls of the excavated crypts (Fig. 1.17C) which, nowadays, are part of the Museum of the Cathedral.

The site represents a priceless treasure for Sardinian cultural heritage and for the small community of Castelsardo which recruited a multidisciplinary team involving archaeologists and anthropologists who reconstructed the chronology of the depositions and provided new insights to the health conditions and the state of preservation of the individuals there buried. In this context, the FLEA performed the entomological investigations suggesting that the corpses were left exposed, likely in a warm season, as demonstrated by a conspicuous finding of Calliphoridae puparia along with puparia belonging to the muscid *H. capensis* known to be a secondary coloniser of buried corpses (Giordani et al., 2018b). Among Calliphoridae, the record of *Phormia regina* (Meigen, 1826) offered an interesting object of investigations as this species does not appear in any modern record on the Island, suggesting that either climate change or anthropic activity may have played an important role in the presumed extinction of this fly. A detailed description and discussion of the necrophagous fauna found in association to the mummies of Castelsardo is documented in the PhD thesis of Dr Giordani (2018) and published in Giordani and co-workers (2018). It is therefore worth mentioning how the archaeoentomological investigations conducted in funerary contexts can provide information not only related to the funerary practices, but as well as related to the phenology of the species allowing to draw palaeo-environmental reconstruction.

Introduction

Urban well in Via Sebastiano Satta, Sassari, Sardinia.

The city of Sassari is located in the North-West of Sardinia (Italy), 17 km from the coast ($40^{\circ}43'36''\text{N } 8^{\circ}33'33''\text{E}$, 225 m a.s.l.) (Fig. 1.18).



Fig. 1.18 Sassari city, Sardinia region (Italy) ($40^{\circ}43'36''\text{N } 8^{\circ}33'33''\text{E}$).
(© 2007–2018 d-maps.com).

Although the first records of human settings date back to the Ancient Neolithic period (5,000 BC), the city probably developed during the 12th century (Rovina and Fiori, 2010). From 1998, the city has been involved in many archaeological excavations coordinated by “Comune di Sassari” and the High Commission of the Authority of the Cultural Heritage of Sassari and Nuoro provinces (http://sabap_ssnu.beniculturali.it/). The project aimed to restore the old part of the city providing new insights to the archaeological knowledge. As part of the urban archaeological restoration, the remains of a well came to light during renovation works of the road surface in 2011. The well, located in Via Sebastiano Satta and dated to the first quarter of the 14th century, was part of a private courtyard on the property of a medieval wealthy family, as confirmed by pottery findings and food remains (Wilkins, 2016). The well measured 13.55 m in depth and the diameter of the circular opening measured 0.9 m. From the road surface level, different layers of sediments were identified and technically defined as Stratigraphic Units (S.U.): the first 3.6 meters underground were unfilled; dry sediment (from -3.6 m to -7 m); wet sediment (from -7 m to -9 m); waterlogged deposit (from -9 m to -13.55 m) (Fig. 1.19).

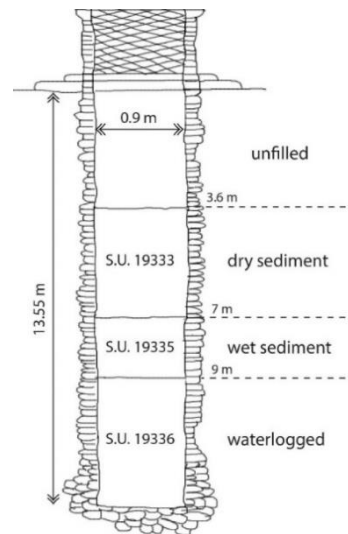


Fig. 1.19 Schematic representation of the Medieval well in Via Sebastiano Satta, Sassari. The division in Stratigraphic Units (S.U.) as defined by the archaeologists and the relative nature of the sediment are reported.

Since the beginning of the excavations, a multidisciplinary team was involved in the collection, analysis and interpretation of the findings in order to draw a more complete scenario of the habits of Sassari population during the Middle Ages. Based on the up-to-date findings, archaeologists derived the following hypothesis. The well, excavated in correspondence with a groundwater source, was built for the collection of water for domestic use; as confirmed by the recovery of pottery, vertebrate bones including farm animals, domestic animals and fish, plants and fruits remains (Wilkens, 2016), was then used as a dump settlement for waste. This change in function can be read as a violation of the “*Statuti Sassaresi*”, established in 1316 AD with the purpose of regulating the wastes disposal and the hygienic conditions of the city of Sassari (Wilkens, personal communications): urban wastes had to be discarded out of the walls of the city. Furthermore, carpological analysis carried out on seeds of fruits by the Laboratory of Palinology and Archaeobotany of Università di Modena e Reggio Emilia (Italy) demonstrated the hypothesis of a short-term usage of the well as dump, likely lasted over only one warm season. In fact, archaeobotanists found seeds of *Ficus carica* Linnaeus 1753 (fig), *Cucumis melo* Linnaeus 1753 (melon), *Cucumis citrullus* Seringe 1828 (watermelon), *Rubus fruticosus* Linnaeus 1753 (blackberry), which are typical of the summer season (Bosi

Introduction

and Mazzanti, 2013). After a short phase used as cesspit, the well was finally infilled and abandoned.

Mass grave of Macomer, Sardinia.

The town of Macomer, situated in the mid-west of Sardinia, ~30 kilometres from the coast ($40^{\circ}15'51''\text{N } 8^{\circ}46'30.22''\text{E}$, 563 m a.s.l.) (Fig. 1.20), has Punic origin. During the 3rd century BC, it was conquered by Romans who took advantage of its strategic position in the centre of the Island. During archaeological excavations started in 1965, a mass grave containing several skeletonised human remains was discovered. Fifteen was the minimum number of individuals estimated by the anthropologists and the remains were dated to the Iron Age, between the 2,900- and 2,700-years BP (C^{14} data by Rodriguez (Universitat Autònoma de Barcelona), personal communication). As reported by the experts working on the field, the burial context appeared intact and the bones were submerged in a water-mud sediment. These human remains preserved in waterlogged conditions were covered by a inorganic mineral matrix, likely as a consequence of multiple depositional events, and appeared dark in colour and with bluish spots. The presence of non-human evidence nestled within bone materials required the involvement of an entomologist.



Fig. 1.20 Macomer city, Sardinia region (Italy) ($40^{\circ}15'51''\text{N } 8^{\circ}46'30.22''\text{E}$).
(© 2007–2018 d-maps.com).

1.5 IDENTIFICATION OF ENTOMOLOGICAL SPECIES RETRIEVED FROM FORENSIC AND ARCHAEOLOGICAL CONTEXT

Forensic entomology and archaeoentomology share the same approach of collection, analysis, and preservation of the samples as well as they provide a similar approach for the interpretation of the entomological remains (Huchet, 1996). Whether a specimen will be used as evidence to support legal investigations or archaeological hypothesis, species identification is the keypoint (Amendt et al., 2004a, Amendt et al., 2007, Amendt et al., 2011) (Kenward, 2009, Buckland et al., 2014) and can be carried out with two main approaches described in the following paragraphs.

1.5.1 Morphology-based approach

The study of the morphology is an established, traditional, straightforward method of identification. The method includes the observation of diagnostic anatomical traits of interest, the use of identification keys, and the comparison with published morphological descriptions. As far as Diptera of forensic interest concern, available data focused on certain groups of flies for which lot of information are available for adult specimens, while immature stages often lack of exhaustively descriptions (Tab. 1.3). Difficulties are mainly due to the few diagnostic characters that eggs, larvae, and puparia show (*e.g.* Fig. 1.21), and to the fact that the same features may not be equally useful to distinguish different species (Giordani et al., 2018a). Additionally, although it is rather frequent that puparia retain the same characters from the larval stage (Szpila, 2010, Martín-Vega et al., 2012), due to the pupariation event (Martín-Vega et al., 2016) physical modifications (*e.g.* contraction) may occur, resulting in a partial loss of definition of the details. Therefore, studying the morphology of the immatures not only requires an exceptional effort by taxonomists, but it also requires researchers to have a high knowledge of taxonomy.

Tab. 1.3 Key references for morphological identification of Diptera of forensic interest.

geographical distribution	taxonomic group	descriptions for	keys for	reference
British and Europe	Diptera	all	larvae adults	(Smith, 1986)
Nearctic region	Diptera	adults	n/a	(McAlpine et al., 1981)
Nearctic region	Diptera	all	puparia adults (genera)	(McAlpine et al., 1987)
Europe	Calliphoridae	larvae	✓	(Szpila, 2010)
Europe	Calliphoridae	adults	✓	(Szpila, 2012)
World	Muscidae	immatures	larvae	(Skidmore, 1985)
Western Palearctic region	Muscidae	larvae	✓	(Grzywacz et al., 2017a)
Europe-South America	<i>Hydrotaea</i> sp. (Muscidae)	puparia	✓	(Giordani et al., 2018a)
World	Sarcophagidae	adults	n/a	(Pape, 1996)
Europe	Sarcophagidae	larvae	✓	(Szpila et al., 2015)
Nearctic region	Piophilidae	adults	✓	(Rocheffort et al., 2015)
Europe	Piophilidae	immatures	n/a	(Martín-Vega, 2017, Martín-Vega et al., 2012, Martín-Vega et al., 2014)
New Zeland	Fanniidae	all	larvae adults	(Domínguez and Pont, 2014)
British	Sphaeroceridae	all	adults	(Pitkin, 1988)
British	Phoridae	adults	✓	(Disney, 1994)

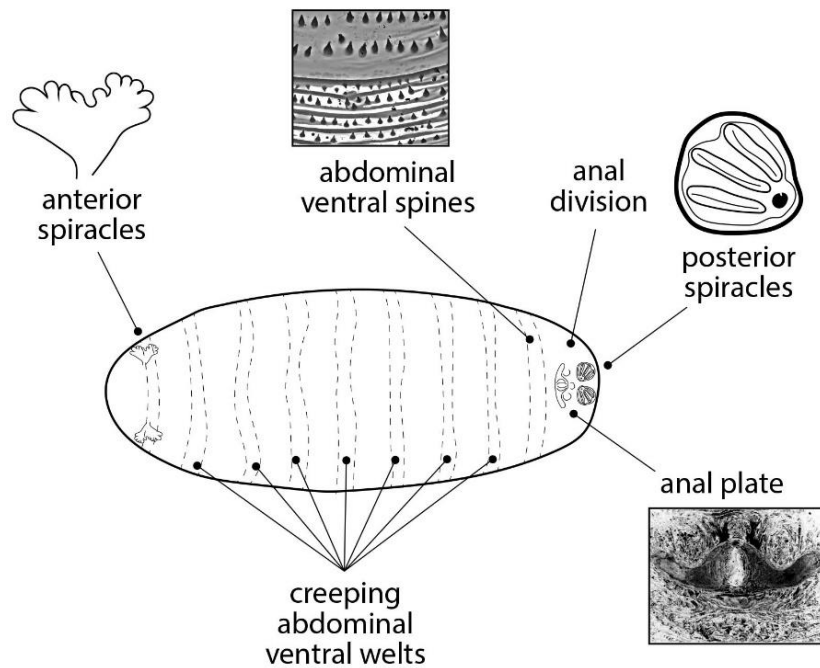


Fig. 1.21 Diagnostic characters of Diptera puparia. Ventral view and anatomical details of a puparium analysed for the diagnosis of the species are schematically shown. Each element is reliably reproduced from photographs; however, the whole representation is not realistic as the elements are not in scale and have been selected from multiple species.

With specific regard to forensic and archaeological investigations, further limitations are encountered: laboratory rearings of the immature can fail (Amendt et al., 2007), storage conditions, and environmental factors strictly linked to decomposition of organic matter, can have an impact on the accuracy of the identification. In these circumstances, comparing insects remains to private or natural history museum collections and cooperating with experts in taxonomy can be crucial to successfully identify a certain species (Kenward, 2009, Buckland et al., 2014, King et al., 2009). Alternatively, a DNA-based approach is undertaken.

1.5.2 DNA-based approach

Molecular identification has become a widely used tool to corroborate the identification of the species in support to traditional morphological studies (Tuccia et al., 2016b, Tuccia et al., 2016a). Insect species can be univocally identified by sequencing a distinctive DNA region known as “barcode” (Hebert et al., 2003). As outcome of the Barcoding of Life Project, the mitochondrial COI has been selected as molecular target to distinguish

Introduction

several metazoan species (Hebert et al., 2003), as it provides the highest pairwise inter-specific divergence, and the lowest pairwise intra-specific divergence, defined as the frequency of mutations given two DNA sequences (GilArriortua et al., 2014). It is well-established that mitochondrial targets are present in high copy number in the cells and show higher mutational rate compared to nuclear targets. COI (1,535 bp in its whole length) codifies for subunit I of Cytochrome Oxidase, a protein involved in the electron-transport chain of the cellular respiration process. However, only 658 bp in 5' end of the gene have been renamed as “barcoding region” which can be amplified through the use of “universal primers” (Folmer et al., 1994). Furthermore, new sets of primers annealing within or between the barcoding region have been designed and recently reviewed (Tuccia et al., 2016b). However, if the use of shorter barcode sequences is successful when applied to Fanniidae of forensic interest (Grzywacz et al., 2017b), DNA fragments shorter than ~200 bp are not recommended to be used to identify Sarcophagidae species (Jordaens et al., 2013). The use of multiple primer pairs renamed “mini-barcoding” allows to amplify overlapping fragments which can be aligned through *in silico* analysis, generating a longer nucleotide sequence. This approach is advantageous to increase the success of the amplification when DNA is highly degraded, as well as in the case of ancient samples (paragraph 1.5.5).

Whether the use of COI shows a low inter-specific divergence impacting the reliability of the discrimination, as in the case of closely related species such as *Lucilia caesar* (Linnaeus, 1758) and *Lucilia illustris* Meigen, 1826 (Diptera: Calliphoridae) (GilArriortua et al., 2015), other targets can be used. Alternatives include either mitochondrial targets such as COII (Boheme et al., 2011), Cytb (GilArriortua et al., 2013, GilArriortua et al., 2014, Giraldo et al., 2011), ND5 (Zehner et al., 2004, Bortolini et al., 2018), 28S rDNA (McDonagh and Stevens, 2011), or nuclear, such as EF-1a (Bortolini et al., 2018), ITS1 (GilArriortua et al., 2014, GilArriortua et al., 2015), ITS2 (Yusseff-Vanegas and Agnarsson, 2017), and PER (Guo et al., 2014, Bortolini et al., 2018). The combined use of these targets, known as “concatenation” (Bortolini et al., 2018), is a further option to improve the resolution of closely related species.

The main advantage of using genotyping for identification purposes is that it can be applied to any specimens, regardless the developmental stages. The approach is well-established for adults and larvae of all instars, whereas still needs to be validate when applied on puparia. The reason is related to the amount of DNA extractable wither from one or the other source: in fact, the epithelial tissue (larval exuviae) which separates the metamorphic fly from the puparium until the transformation is complete is the only available source of DNA. In this regards, Mazzanti and co-workers reported to have successfully identified 42 Diptera puparia collected from crime scenes (Mazzanti et al., 2010), however the topic needs further investigations as only a little information is known.

1.5.3 Molecular identification in forensic entomology: The other side of the coin

Although the laboratory procedures to identify insects species are well-established, there are several pitfalls related to data interpretation (Wells and Stevens, 2008) which is the crucial step in every scientific investigation. World-wide researchers generate nucleotide sequences which populate reference DNA databases: GenBank maintained at the National Center for Biotechnology Information (NCBI) the European Bioinformatics Institute (EBI) include information for over 100,000 Eukaryotic species. However, the submission of DNA sequences to the database is open to all users and is not subjected to any request of prove of the identification of the specimens, meaning that the systems are not in compliance with standard guidelines established by taxnomically-oriented databases, therefore resulting inaccurate (Tautz et al., 2003). Ensuring that only high-quality sequences contamination-free populate the databases is also another aspect that the users are implicitly expected to follow. On these bases, in 2003 Tautz launched the idea of a taxonomically-oriented database where data could have been subjected to a innovative management to ensure their authenticity and traceability, which was later realised with the Barcode of Life Data System (BOLD) (Ratnasingham and Hebert, 2007), repository of mtCOI barcoding sequences only.

As far as the species of forensic interest concerns, it is worth mentioning that much research has been dedicated to the most common taxa of forensic interest, especially in

Introduction

the families Calliphoridae, Sarcophagidae and Muscidae, whose DNA sequences largely populate DNA databases; on the contrary, little effort has been directed towards less common taxa including Muscidae, Phoridae, Piophilidae for which only limited datasets of sequences are available. For these reasons, molecular phylogenetic analysis should be carefully considered and interpreted. Wells and Stevens (2008) accurately reviewed all these aspects falling under the “other side of the coin” of molecular analysis applied on species identification in forensic entomology.

1.5.4 Molecular identifications of ancient insects remains

Zooarchaeological studies have been deeply revolutionized since the invention of DNA amplification via PCR, giving birth to the “molecular archaeology” era (Paabo et al., 1989). As summarised by King and co-workers (2009), three main reasons drive researchers to perform ancient DNA analysis on insects: *i*) testing the hypothesis that the genetic information of fossil specimens is well preserved as their morphology can be; *ii*) identifying distinctive genetic variation and using them to track the dispersal of the species; *iii*) identifying the species based on their genetic features rather than their morphology, thus providing a convenient tool which, although firmly anchored within traditional taxonomy, permits to overcome the weaknesses of the traditional method (Tautz et al., 2003). Up to date data mainly originate from insects encased in amber, including Coleoptera and Hymenoptera, and involved the use of nuclear-multi copy targets as 18S rDNA and ITS (Cano et al., 1992, Cano et al., 1993, Desalle et al., 1992). However, research in this field is still poorly understood and controversial: in fact, if certainly the preservation of the morphological structure is unquestionable, the way DNA can survive intact has always been a source of debate within the scientific community (Poinar, 1994, Austin et al., 1997b). Some experiments alleging successful DNA retrieval from remains aged hundred millions of years ago were debated for long, as they are in conflict with the evidence that ancient DNA can possibly survive as long as 100,000 years (Austin et al., 1997b). Considering closer geological time scales, ancient DNA has been successfully extracted from Coleoptera remains of 5,900–560,000 years ago conserved in permafrost (Heintzman et al., 2013), as well as from Coleoptera (Reiss, 2006, King et al.,

2009) and Orthoptera (grasshoppers and crickets) (Chapco and Litzenberger, 2004) recovered from glaciers, or natural deposits in very arid climate favourable to long-term conservation (Reiss, 2006) and dated between 20,000 and 400 years old; in these more recent case, COI and other mitochondrial targets were amplified. With respect of Diptera, only one record is about an adult specimens of the genus *Orfelia* Costa 1857 (Mycetophilidae) (Poinar, 1994); certainly, no attempt has ever been made to characterise aDNA from Diptera puparia.

1.5.5 Ancient DNA analysis: Features and criteria of authenticity

From the extensive research conducted on ancient human DNA (Hagelberg et al., 2014) and ancient DNA of environmental origin, including plants, soil, vertebrate and invertebrate animals, it is well-established that aDNA has distinctive characteristics.

Fragmentation and chemical modifications. DNA retrieved from ancient substrata is highly fragmented (Glocke and Meyer, 2017, Reiss, 2006, Austin et al., 1997b, Fulton and Stiller, 2012, Hofreiter et al., 2001, King et al., 2009, Smith et al., 2003, Handt et al., 1994, Pedersen et al., 2015, Yang and Watt, 2005). Several factors occur in causing the “natural” or induced breakdown of the double helix. After an organism dies, all the molecular mechanisms involved in DNA repair cease, and at the same time endogenous DNA nucleases may be activated, thus causing degradation of the nucleic acid polymer (Hofreiter et al., 2001, Reiss, 2006). Moreover, the collapse of the cellular structures causes the exposition of the nuclear contents to attack of biotic and abiotic environmental factors, including exogenous nucleases (Wilson, 1997, Pedersen et al., 2015) released by the microbial communities which in the meantime are spreading and feeding on dead tissues (Benbow et al., 2015). Additionally, exposure to UV light further induce double-strand breaks in DNA molecules. Under specific circumstances, including rapid desiccation and low temperatures, the fragmentation might be reduced, however chemical modifications may occur and further destabilise the DNA backbone. Oxidation of the nitrogenous bases, hydrolytic processes of deamination or depurination, cross-links formation with other molecules are the most common damages contributing to DNA decay (Hofreiter et al., 2001) and can lead either to the rupture of the DNA molecules, or

Introduction

make them inaccessible to DNA polymerase during the PCR (Reiss, 2006). Evaluating the survival of aDNA is highly recommended in order to enable researchers to focus on material characterised by a greater chances of amplification success, thus avoiding the loss of precious and often unique archaeological material (Smith et al., 2003). Different methods have been successfully developed to address this issue, including the evaluation of the amino acids racemisation via HPLC (Poinar et al., 1996) or the “thermal age” calculation of fossils which require to know the palaeo-temperature data (Smith et al., 2003). However, these methods are time consuming and rather complex, and no one of them has been validated for insects. On the contrary, the Agilent 2100 Bioanalyzer (Agilent Technologies) which is commonly used to assess the size of NGS PCR libraries, provide useful information also on the fragmentation status of genomic DNA preparations and it has been applied on insects museum species (Tin et al., 2014).

PCR inhibition. DNA modifications prevent polymerase bypass, thus creating real blocking lesions that inhibit amplification and sequencing (Heyn et al., 2010). In order to reduce this inhibitory effect, the use of high-performing *high-fidelity* Taq DNA polymerases such as Phusion or Platinum (Thermo Fisher, Waltham, Massachusetts, USA) is highly recommended as they have been engineered in order to be able to interact with damaged bases, and couple low misincorporation rates with proofreading activity to give faithful replication of the target DNA of interest (Fulton and Stiller, 2012, Heyn et al., 2010).

The highly fragmentation status of aDNA is another cause of PCR inhibition, as it prevents the annealing of the primers; the initial copy number can also affect the amplification success (Handt et al., 1994). A routinely applied strategy is therefore using species-specific primer pairs to amplify short (~ 200 bp) and overlapping sequences (Paabo et al., 1989, Fulton and Stiller, 2012) targeting multi copy genes within the whole cellular genome (Handt et al., 1994). As previously mentioned for modern species, mitochondrial genes such as COI, COII, 16S rDNA present in thousands of copies per cell and 18S rDNA or ITS2 genes, organised as tandem-repeat sequences within the nuclear genome, are the preferred targets (Reiss, 2006). However, even assuming that the

planned strategy has high probability of success, other exogenous mechanisms of inhibition may occur at any point of the molecular interaction during the amplification. The most obvious origin of PCR inhibitors is due to compounds co-extracted with DNA often resulting in impure DNA samples if not sufficiently purified (Wilson, 1997). The exact molecular mechanism behind it is poorly understood, however, it has been speculated that these compounds can either form high-molecular weight complexes with the template, or with DNA polymerases, thus sequestering the substratum to the enzyme or vice versa (Wilson, 1997). Furthermore, some compounds can chelate Mg^{2+} which is the essential co-factor of DNA polymerases. Although it is difficult to predict the nature of the inhibitors affecting environmental samples, a list of compounds that can be co-extracted with the host DNA is acknowledged and includes: polysaccharides, humic and humic-like compounds, other polyphenolic compounds, fulvic acids, and heavy metals (Wilson, 1997). Interestingly, Pedersen and co-workers (2015) point out that humic acids binds to DNA molecules due to their negative surface charge allowing the formation of molecular complexes of inhibition, but it is indeed due to the formation of such complexes that aDNA can effectively survive for prolonged times. In order to overcome this issue when working with environmental samples, the addition to the PCR of compounds such as PVP or PVPP and BSA has been proposed as a solution: in fact these compounds show an affinity for the inhibitors higher than the affinity showed by the inhibitors for the reaction component effectively inhibited (DNA template or DNA polymerases) (McGregor et al., 1996, Kemp et al., 2006, Fulton and Stiller, 2012).

Contamination. In ancient DNA studies, “contaminant DNA” specifically refers to DNA which is identical or similar to the target ancient template and therefore could be indiscriminately amplified, generating false positive results (Yang and Watt, 2005). Therefore, human DNA should not be considered as a source of contamination when working with entomological remains, and the use of species-specific primer sets intrinsically avoids this issue. For the same reason, the “pre-laboratory contamination controls” that are expected to be followed by on-field operators (*e.g.* archaeologists) are not essential when dealing with entomological samples, as much as they are when human

Introduction

remains are recovered and intended to be subjected to genetic analysis (Yang and Watt, 2005). On the contrary, contamination can occur by modern reference insect DNA used in previous reactions or used as positive controls during PCR (Yang and Watt, 2005, Handt et al., 1994). Some researchers recommend to not use positive control and possibly use ancient positive controls (Kemp et al., 2006). However, ancient positive controls from insects remains rarely exist. Furthermore, as the starting concentration is so low in ancient samples, the probability of having any amplifiable DNA from another ancient sample drastically reduces. To minimise any risk, extraction procedures should be performed in a place physically separated by where PCRs are carried out, as well as wearing PPE (personal protection equipment, *e.g.* sterile gloves, lab-coats, lab glasses) at all times, and carefully clean the working bench at the beginning and at the end of the procedure using bleach, ethanol and, if possible, through UV-irradiations (Austin et al., 1997b, Reiss, 2006, Yang and Watt, 2005, Handt et al., 1994).

Criteria of authenticity. Ancient DNA sequences, to be so named, must meet some criteria of authenticity (Paabo et al., 1989, Austin et al., 1997b, Handt et al., 1994, Hofreiter et al., 2001): *i)* a correct use of the reaction controls and their expected results which exclude that any contamination occurred at any of the steps while the process was undertaken has to be proven; *ii)* extracted DNA should show an inverse relationship between amplification success and amplicon length; *iii)* reactions should be carried out in replicates with each replicate giving the same result; *iv)* extraction and amplification have to be successfully repeated from the same sample in another facility and, possibly, from another research group and *v)* the sequence should be phylogenetically meaningful. Many of the successful records previously mentioned lack of one or more criterion, and were therefore severely criticised (Austin et al., 1997).

1.6 OBJECTIVES

Insects represent an important source of information in archaeological and forensic contexts, with Diptera puparia representing the main fraction of the entomological assemblage. A dedicated literature research on the topic reveals the lack of a standardised protocol to study this entomological evidence, from a morphological and molecular point of view. The final goal of this thesis is to provide a pragmatic and critical approach to investigate dipteran immatures, recovered from archaeological and forensic contexts, with particular regards of puparia. In order to achieve the general aims the following objectives were intended to be pursued:

- to evaluate the extractability of DNA from the cuticle of modern puparia and the feasibility of genotyping the immatures in forensic entomology, investigating the impact of cuticular pigments on molecular analysis (Chapter 3);
- to verify the possibility to identify empty puparia recovered from archaeological contexts through ancient DNA genotyping, designing an *ex novo* workflow (Chapter 3);
- to demonstrate the potentialities of archaeoentomological investigations in reconstituting human activities and funerary practices, through species identification and state of preservation of the specimens (Chapter 4);
- to investigate how taphonomic processes *stricto sensu*⁴ and/or *lato sensu*⁵ are involved in the preservation of Diptera remains and their impact on *post mortem* DNA survival (Chapter 4);
- to generate new morphological data for the immatures of the “picture-winged fly” *Physiphora alceae* (Preysslér, 1791) (Diptera: Ulidiidae) and for puparia of 10 species of “skipper flies” (Diptera: Piophilidae), acknowledged as poorly studied and taxonomically unresolved taxa in forensic entomology investigations (Chapter 5);
- to evaluate the quality of genetic data in non-taxonomy-based DNA databases through the phylogenetic approach, demonstrating how a critical and combined approach of analysis is key in forensic entomology (Chapter 5).

⁴ Taphonomic processes of the insect itself contributing to its preservation (*e.g.* mineralisation);

⁵ “Allo-taphonomic” processes occurring at the expense of the organic matter (*e.g.* human remains) surrounding insects impacting insects themselves.

2 MATERIALS AND METHODS



2.1 MORPHOLOGICAL ANALYSIS

2.1.1 Puparia collection and cleaning

Puparia specimens analysed in this thesis were collected from archaeological and forensic contexts described in the Introduction chapter. In the majority of the cases, samples were delivered to the University of Huddersfield by collaborators; occasionally, in situ collection was performed by the writer of this thesis (Fig. 2.1). In the latter case, entomological sieves with a mesh size between 1.7-0.6 mm, and entomological tweezers were used. Source of collection, number of analysed specimens and the applied cleaning methods are reported in

Tab. 2.1 and

Tab. 2.2, respectively. Tab. 2.3 lists the species analysed to conducted comparative taxonomic study.

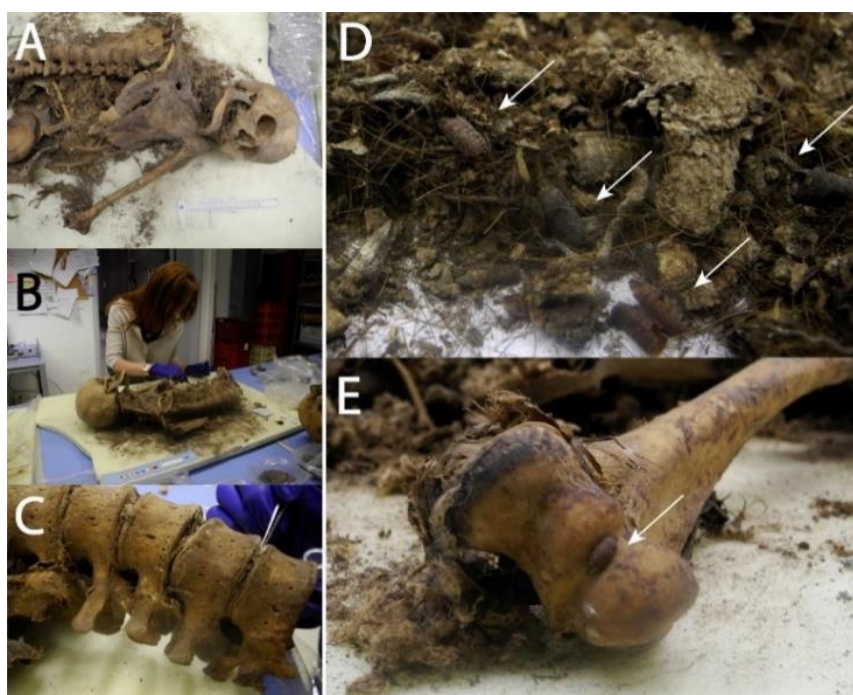


Fig. 2.1 Collection of entomological remains from Roccapelago human remains in Ravenna, 2017. (A-C) Skeletonised human remains partially mummified (D,E) puparia of necrophagous Diptera feeding on the decomposing bodies (white arrows).

Tab. 2.1 List of ancient puparia studied in this thesis. d =delivered samples; i.s. = *in situ* collection; *by archaeologists in charge of the site; **Laboratorio di Antropologia Fisica e DNA Antico - Dipartimento di Beni Culturali in Ravenna, Università di Bologna, Italy; ***Centre for Renovation and Conservation of the Cultural Heritage in Li Punti, Sassari, Italy.

archaeological site	source of collection	chapter	number of specimens analysed/type	cleaning method
• crypts of Roccapelago	mummified human remains (d*, i.s.**)	3	19/empty	H ₂ O 40° C
• crypts of Castelsardo	mummified human remains (d*)	3	10/full, 4/empty	NaOH 10% + H ₂ O 60° C
• urban well in Sassari	soil deposits (d*, i.s.***)	4	n/a full/empty/mineralised	C ₂ H ₄ O ₂ + H ₂ O 40° C, H ₂ O 80° C, NaClO 0.5%
• mass grave in Macomer	skeletonised human remains (d*)	4	n/a /mineralised	EtOH 70%

Tab. 2.2 List of modern puparia studied in this thesis. d =delivered samples; i.s. = *in situ* collection; *School of Applied Science, University of Huddersfield, United Kingdom; **by forensic archaeologist, Università degli Studi di Milano, Italy; ***by Dr Daniel Martín-Vega, Universidad de Alcalá, Madrid, Spain; ^{a)} species for comparative study listed in Tab. 2.3.

forensic context	source of collection	chapter	number of specimens analysed/type	cleaning method
• in-house decomposition experiment	rabbit carcasses (i.s.*)	3	14/empty	H ₂ O 40° C, NaClO 0.5%
• crime scene-North Italy	human remains (d**)	5	2/empty, 1/full	C ₂ H ₄ O ₂ + H ₂ O 40° C
• <i>ex loco</i> decomposition experiment/crime scene/laboratory collection	animal (d***) carcasses/human remains	5	85 ^{a)} /full, empty	H ₂ O 40° C

Tab. 2.3 List of Piophilidae species analysed for comparative study

species	number of puparia
<i>Piophila casei</i> (Linnaeus, 1758)	16
<i>Stearibia nigriceps</i> (Meigen, 1826)	1
<i>Piophila megastigmata</i> McAlpine, 1978	11
<i>Parapiophila flavipes</i> (Zetterstedt, 1847),	10
<i>Parapiophila vulgaris</i> (Fallen, 1820),	1
<i>Protopiophila litigata</i> Bonduriansky, 1995	10
<i>Liopiophila varipes</i> (Meigen, 1830),	13
<i>Prochyliza nigrimana</i> (Meigen, 1826)	10
<i>Prochyliza xanthosoma</i> (Walker, 1849)	10
<i>Centrophlebomyia furcata</i> (Fabricius, 1794)	3

The cleaning method was chosen in accordance to the state of preservation of puparia. The level of corrosiveness of the reagents established by manufacturer's Safe Data Sheets was arbitrarily converted in a range between 0 (not at all corrosive) and 3 (extremely corrosive) (Tab. 2.4). In all cases, tiny brushes were used to clean the specimens under a stereomicroscope, rolled into laboratory paper and dried at room temperature.

Tab. 2.4 List of chemicals used to clean puparia surface. 0= no corrosive, 1=low level of corrosiveness, 2= medium level of corrosiveness, 3=high level of corrosiveness.

reagent	concentration	corrosiveness
H ₂ O (40,60,80 °C)	/	0
EtOH	70%	0
NaClO (sodium hypochlorite)	0.5%	1
NaOH (sodium hydroxide)	10%	2
C ₃ COOH (acetic acid)	glacial	3

2.1.2 Larvae diaphanisation

The process of diaphanisation makes the larval cuticle transparent, so that the anatomical features impressed on its surface are highlighted, including intersegmental spines pattern, posterior and anterior spiracles, and other sclerotised elements such as oral sclerites. Larvae of *P. alceae* studied in Chapter 5 (n=2) were prepared in accordance to the protocol developed by Tuccia and co-workers (2016). An entomological pin was used to perform a longitudinal cut on the dorsal surface of the specimens and entomological tweezers were used to separate the cuticle from soft tissues; the latter were used as substratum to perform DNA analysis (paragraph 2.4.2) while the cuticle was incubated in a saturated NaOH solution to digest the remaining residual soft tissues and morphological features were observed using an optical microscope.

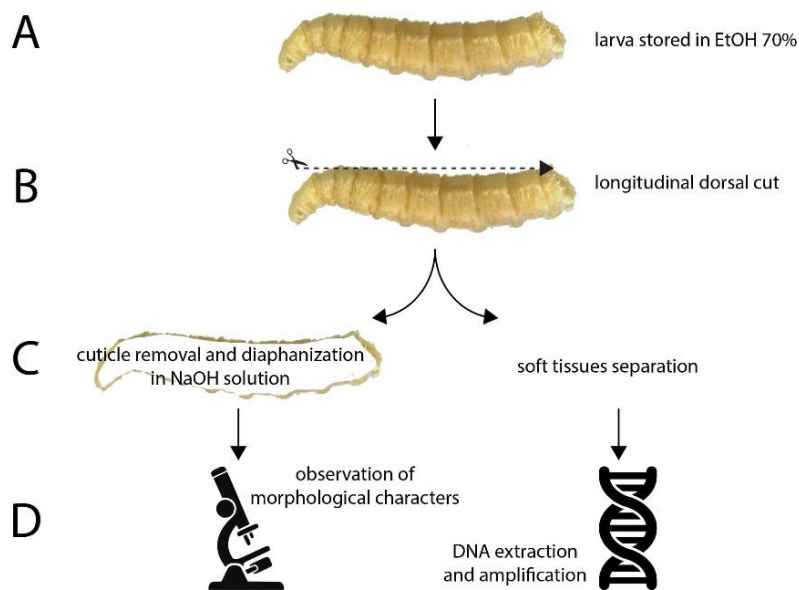


Fig. 2.2 Larvae preparation workflow. A) Larvae stored in 70% EtOH are subjected to a longitudinal dorsal cut B) to remove the cuticle from the soft tissues C) and D) analyse them through morphological and molecular approach, respectively.

2.1.3 Microscopic techniques

Stereomicroscopy. The operation of a stereomicroscope is based on the reflected light of the observed object enabling its stereo-resolution (three dimensional) which makes it largely used for entomological dissection applications. In this thesis, the following stereomicroscopes were used: Leica EZ4 and Leica M60 equipped with a CCD camera (Weitzlar, Germany); Keyence VHX-S90BE (VHX 2000 series) digital stereomicroscope equipped with VH-Z20R and VH-Z250R lenses, and VHX-2000 v.2.2.3.2 software (Japan).

Scanning Electron Microscopy. In contrast to light microscopy, electron microscopy is based on the use of electron beam as source of “illumination”. In the scanning electron microscope (SEM), the object is scanned by incident electrons generating its image and revealing its topography, e.g. texture and roughness of the surface (Zhou et al., 2006). In this thesis the instrument FEI Quanta 650 FEG (Oregon, USA) was used to analyse puparia specimens. Samples were pre-treated with Au-Pd (gold-palladium) coating (1 nm). Analyses were conducted in high vacuum mode (9.64×10^{-4} Pa), setting the acceleration voltage at 20 keV and with an emission current of $140 \mu\text{A}$.

The use of digital stereomicroscope and SEM allowed to create a morphological pictorial archive used as internal laboratory database to track the encountered species and enable morphological comparisons.

2.1.4 Identification keys and external consultants

The identification of the species was carried out using morphological identification keys reported in Tab. 2.5. The nomenclature of the morphology for adult specimens and immature stages of flies of forensic interest follows McAlpine (1981); descriptions of Piophilidae puparia follows the nomenclature used in the most updated literature of the family (Martín-Vega, 2017).

Tab. 2.5 Identification keys used in this thesis.

Taxon	Reference
Calliphoridae	(Smith, 1986, McAlpine et al., 1987) (Szpila, 2010)
Fanniidae	(Domínguez and Pont, 2014)
Muscidae	(Grzywacz et al., 2015, Skidmore, 1985, Giordani et al., 2018a, Grzywacz et al., 2017a)
Piophilidae	(McAlpine et al., 1987) Rochefort (2015)
Sphaeroceridae	(Okely, 1974, Pitkin, 1988) (Skidmore, 1996)
Ulidiidae	(McAlpine et al., 1987, Kameneva and Korneyev, 2010b)

Additionally, collaborations with external consultants were established aimed at enabling the facilitation of species identification for poorly studied species. Dr Daniel Withmore, senior curator of Diptera and Siphonaptera collections of London Natural History Museum, provided specimens of Sphaeroceridae property of the NHM collection which were used to investigate puparia retrieved from Sassari archaeological deposits (Chapter 4).

2.2 MICROSTRUCTURE ANALYSIS OF MINERALISED SPECIMENS

Mineralised Diptera specimens from Sassari archaeological deposits were investigated using CT-scan, SEM energy dispersion X-ray analysis, the FTIR spectroscopy and the X-ray diffraction (Marshall et al., 2008). With the exception for the CT scan, the other analyses were performed in replicates per each of the identified taxon recovered from the S.U. 19335 and S.U. 19336 (Fig. 1.19) in order to detect any potential difference linked to the conditions of the surrounding environment (*e.g.* depth and type of sediment composing the stratigraphic units).

2.2.1 Computer Tomography Scan (CT-Scan)

CT scan analysis were performed on selected puparia samples in collaboration with the research team led by Dr Paul Bills from the School of Computing and Engineering at the University of Huddersfield, using the XT H 225 ST – Industrial CT scanning (Nikon®). Without any pre-treatment, puparia were placed on a rotatory plate and the stationary X-ray beam was generated and directed against the objects (Hermanek et al., 2018). The resulting attenuated energy electromagnetic waves were detected and acquired as two-dimensional (2D) projections from different angles and finally converted to three-dimensional (3D) representations of the object, generating volumetric reconstruction of cross-sectional (tomographic) images (Fig. 2.3).

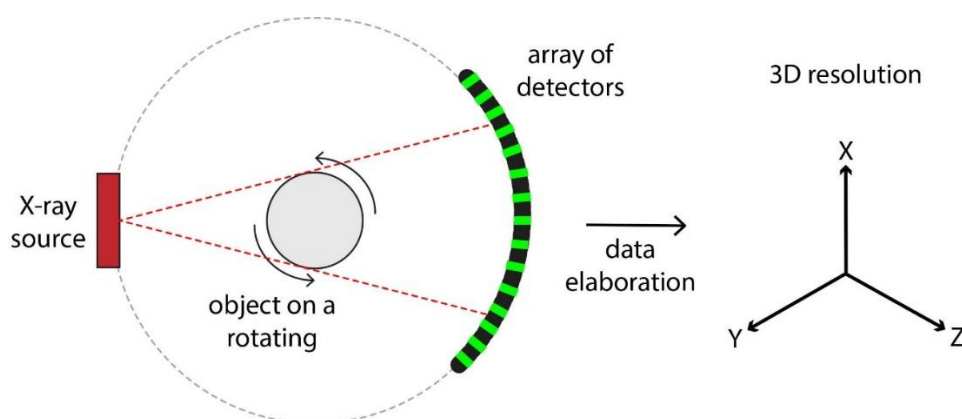


Fig. 2.3 Schematic representation of CT-scan data acquisition and processing.

2.2.2 SEM X-rays microanalysis

X-ray microanalysis, also known as EDX (energy-dispersion X-Ray), was applied to investigate the elemental chemical composition of puparia specimens through the generation of characteristic X-rays by incident beam electrons. Analysis on puparia were conducted with FEI Quanta™ 650 FEG scanning electron microscope without any pre-treatment coating. Three mineralised specimens were chosen per taxon and three individual points of interest on their surface were arbitrarily selected to perform a qualitative analysis setting the default parameters (life time: 60 s, process time: 5, acceleration voltage 20 KeV). An additional measurement was taken extending the selection to the full area of the analysed samples, *i.e.* the full image transmitted by the electron microscope. Furthermore, a mapping analysis was carried out in order to evaluate the distribution of the detected chemical elements, summarised as a colour-coded bi-dimensional image. Both the inner and outer surface of the puparia were investigated. INCA software (Oxford Instruments) was used for the collection and analysis of data. Literature data were used for comparison enabling the identification of the generated spectra.

2.2.3 Fourier Transform Infrared (FTIR) Spectroscopy

The chemical structure and bonding of minerals were analysed by FTIR, known as a variant of the traditional infra-red spectroscopy due to the application of the mathematical algorithm known as Fourier Transform for data elaboration (Smith, 2011). Three puparia per each taxon were placed on a plate diamond, ground and scanned through the IR wavelengths range between 4,000 and 400 cm^{-1} using a Nicolet 380 FT-IR Spectrometer (Thermo Fisher Scientific, Waltham, Massachusetts, USA). Literature data were used to identify the “vibrational spectra” including peaks of a given energy referring to the vibrational frequency of functional groups of the molecule within the sample (Che Man et al., 2010).

2.2.4 Powder X-ray Diffraction

Powder X-ray diffraction was used to evaluate the crystallinity and phases of the mineral component of puparia using a D2 Phaser top-bench diffractometer (Bruker) equipped

with a source of Cu ($\lambda=1.5406 \text{ \AA}$). The selected specimens were pulverised using a plastic pestle. Five different analysis methods were assessed (Tab. 2.6) in order to evaluate which input could generate the best output resolution, as no standard guidelines for this kind of analyses were available in the published literature at the time of the analysis.

Tab. 2.6 XRD analysis methods tested in this thesis.

diffraction angle (2θ)	run time (min)	type of holder
5-100	4	low background
5-100	4	flat
5-100	8	low background
5-100	8	flat
15-80	60	low background

Per each of the five combinations, a number of specimens between 10 and 30, based on the size of the specimens, were selected in order to obtain a sufficient volume of ground samples (until fill up the holder) to run the analysis. The raw data (*.raw*) were converted in *.uxd*, and visualised in Excel. The reference data collected by petrologists and available on the Inorganic Crystal Structure Database (ICSD) (<http://icsd.cds.rsc.org>) were used for data interpretation.

2.3 ANCIENT DNA ANALYSIS

The following instructions refer to ancient DNA analysis carried out on puparia specimens collected from archaeological sites described in paragraph 1.4.4. DNA isolation methods are described per each site, while downstream analyses are described once as they were applied to all the extracts. During the analysis, protective clothing and equipment was worn; the working surfaces, tweezers and pins were cleaned with bleach 5% (Handt et al., 1994) and EtOH 70%; pipettes with filtered tips were used; PCRs were performed under laminar flow cabinet model PURAIR PCR-36 (AirScience®, Florida, USA) and UV irradiation was applied after setting each PCR.

2.3.1 Ancient DNA analysis of Roccapelago samples – Chapter 3

Nineteen puparia morphologically identified *C. vicina* were selected from human remains found in Roccapelago Crypts. Only specimens showing visible internal *exuviae* were selected and the external surface was cleaned up using warm water (40 °C). In parallel, 19 modern *C. vicina* puparia four years old were selected from a batch of flies remains of an experiment carried out in 2015, processed as previously described, and used as control samples. The screening of the archaeological material did not provide replicates samples. Five parallel DNA extractions were undertaken on 1, 2, 3, 5, and 8 puparia using a slightly modified protocol from Oshaghi et al. (2006). Samples were grounded by using a plastic pestle and incubated with three-hundred µl Rapid One Step Extraction (ROSE) buffer (Tab. 2.7) until complete submersion in a 1.5 ml centrifuge tube.

Tab. 2.7 Oshaghi buffer composition.

Sodium Lauroyl Sarcosinate (sarkosyl); **Polyvinylpyrrolidone-40, water soluble.

reagent	concentration
Tris buffer	10 mM
SLS*	1%
PVP-40**	1%
EDTA	312.5 mM

Protocol steps are illustrated in Fig. 2.4A; supernatants were transferred to a new tube avoiding the remaining chitinous matrix and purified applying two strategies: a) the OneStep PCR removal kit (Zymo Research, Irvine, California, USA) was used followed by the ReliaPrep DNA purification and concentration system (Promega, Madison, Wisconsin, USA). If necessary, a further purification step was undertaken after adding 20 μ l of sterile deionised water in order to dilute any potential PCR contaminants still present Fig. 2.4B; b) ReliaPrep DNA purification and concentration system (Promega, Madison, Wisconsin, USA) was applied as single purification step on 50 μ l of the lysis extract (Fig. 2.4C).

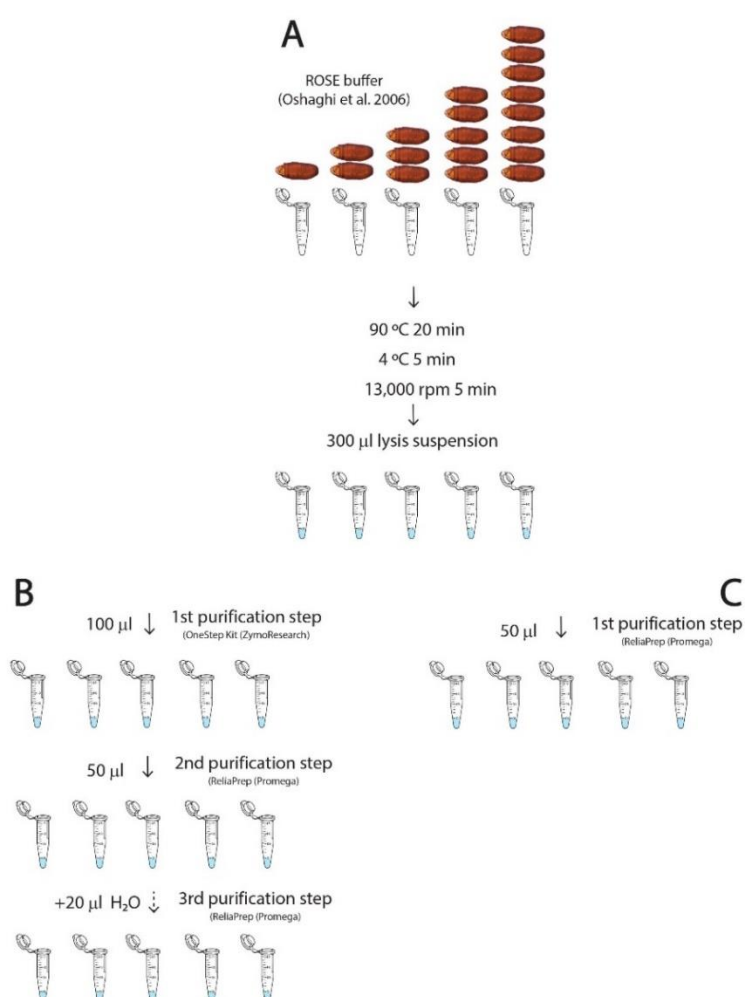


Fig. 2.4 DNA extraction and purification workflow of Roccapelago samples. (A) Oshaghi DNA extraction protocol (2006); (B) first strategy, associated homemade purification workflow involving 2 default steps and one extra; (C) second strategy, associated homemade purification workflow involving only one purification step.

Manufacturer's specifications of the clean up kits were double checked to ensure their use was suitable and compatible with ancient DNA samples:

- OneStep™ PCR Inhibitor Removal Kit (Zymo Research). The spin-columns are designed to efficiently retain polyphenolic compounds, humic/fulvic acids, tannins, melanin and others from impure DNA mixture. The resin within the column is not designed to bind nucleic acids which therefore are not retained on the membrane, rather flow through it;
- ReliaPrep™ DNA Clean-Up and Concentration System (Promega) is designed to purify DNA solutions, extract and purify DNA fragments of 100 bp–10 kb. Additionally, the membrane-based protocol allows to concentrate the DNA preparations, therefore suitable for low DNA concentration.

2.3.2 Ancient DNA analysis of Castelsardo samples – Chapter 3

Ten full and four empty puparia belonging to the genus *Hydrotaea* sp. were selected within the pool of entomological remains found in association to mummified human remains. Puparia surface was treated as reported in paragraph 2.1.1, Tab. 2.1.

A circular cut was performed along the transversal section of nine specimens using a surgical scalpel previously decontaminated using NaClO 0.5% and EtOH 70%. The cut was carefully applied in the middle of the pupal cage avoiding any damage to the content and preserving the anterior and the anal regions containing the morphological diagnostic characters. Insects, pupae at a non-definable stage of development (Martín-Vega et al., 2016), were extracted using entomological tweezers carefully sterilised. After ensuring they belonged to the same species, three groups of two pupae were isolated and transferred to a clean micro centrifuge tube. In parallel, two pupae of *C. vomitoria* purchased from a local fishing shop in Huddersfield were used as modern controls, pre-treated with NaOH 10% and processed in triplicates. DNA was isolated and purified as illustrated in Fig. 2.5.

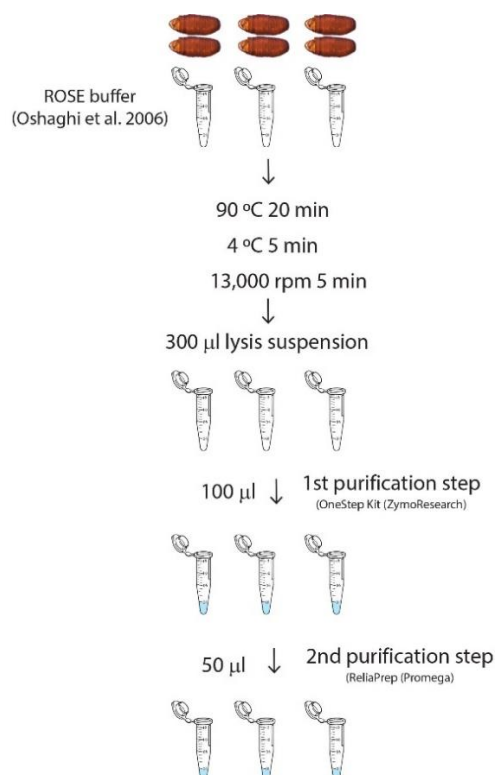


Fig. 2.5 DNA extraction and purification workflow of Castelsardo samples. Oshaghi protocol (2006) was used to extract DNA from 2 archaeological puparia of *H. capensis* and modern control of *C. vomitoria*. Reactions were carried out in triplicates. Two purification steps were applied on the initial lysates using OneStep PCR removal kit (ZymoResearch) and ReliaPrep DNA purification and concentration system (Promega).

2.3.3 Ancient DNA analysis of Sassari urban well samples – Chapter 4

Fifty mg of puparia of *Thoracochaeta zosteræ* Haliday, 1833 were selected from a batch collected *in situ* in 2018 and treated with hot water or diluted bleach (Tab. 2.1). Puparia were either mechanically fragmented with a plastic pestle or left intact. Total DNA was isolated using methods listed in (Tab. 2.8). All the reactions were performed in triplicates.

Tab. 2.8 DNA isolation methods applied on Sassari ancient samples. Method 1: procedure followed manufacturer’s instructions; methods 2-4: original digestion buffer within the kit was replaced with a non-commercial buffer; *composition reported in Tab. 2.9.

method	home-made digestion buffer	Proteinase K working concentration	commercial kit (Qiagen)
1	n/a	n/a	DNeasy® PowerSoil® Kit
2	Gilbert (2007)*	250 µg/ml (Promega)	QIAamp® DNA investigator Kit
3	Campos (2012)*	0.1 mg/ml (Promega)	QIAquick PCR Purification Kit
4	incubation in NaClO 0.5% + four washing steps in deionised H2O combined to method N°3		

Tab. 2.9 Home-made digestion buffers compositions.

references	(Gilbert et al., 2007)	(Campos and Gilbert, 2012)
Tris buffer	100 mM	10 mM
NaCl	100 mM	10 mM
CaCl ₂	3 mM	5 mM
SDS	2X	2X
DTT	40 mM	40 mM
EDTA	-	2.5 mM

The use of QIAquick PCR Purification Kit (Qiagen), designed to purify amplicons within the range 100 bp – 10 Kb, was compatible with downstream DNA amplification strategy targeting DNA sequences over 200 bp.

2.3.4 Downstream analysis of ancient DNA

Further analyses were performed on all ancient DNA preparations in order to test purity level, to measure the concentration, and to assess the size of DNA fragments.

Ancient DNA purity assessment.

Absorbance within the wavelength range of 220–340 nm was measured using a NanoDrop™ 2000c (Thermo Fisher, Waltham, Massachusetts, USA) in accordance to manufacturer's instructions. Spectral resolution and A260/A280 -A260/A230 ratios were obtained. Pre-purification and post-purification assays were run on raw extracts and purified DNA solutions, in order to evaluate the effect of the applied purification method in removing endogenous and exogenous contaminants co-extracted in aDNA preparations.

Ancient DNA quantification

Qubit® 3.0 Fluorometer (Invitrogen™, Carlsbad, California, USA) was used to measure the concentration of DNA preparations prior and after each purification. Qubit® dsDNA High Sensitivity Assay, designed to detect DNA concentrations within the range 10 pg/μl to 100 ng/μl, was performed following manufacturer's instructions.

Statistical analysis

PAST v.3.25 free software (Hammer et al., 2001) was used to performed two-ways ANOVA test carried out on DNA concentration data in order to investigate whether the archaeological origin of samples and the applied purification steps had a significant impact on the observed data.

Ancient DNA fragment analysis

Agilent 2100 Bionalyzer System and the High Sensitivity dsDNA Assay (Agilent Technologies, California, USA) were used to evaluate the size of aDNA molecules within the extracts, in order to plan the amplification strategy and optimise the success of PCR. Following the manufacturer's instruction, 1 μl of aDNA extracts was pipetted on a micro-chip and subjected to capillary electrophoresis applying voltage within the range 100–240 V±10%. The size of DNA fragments within a pool was evaluated through

electropherograms reporting the intensity of the signal as Fluorescent Units plotted with the length of the fragments. DNA ladder ranged between 35 and 10,380 bp. The associated gel-like images helped with the graphical visualisation and interpretation of the results.

2.3.5 Strategies and protocols to amplify ancient DNA

Due to the expected high fragmentation level of aDNA molecules, all PCRs were carried out on BioRad C1000 Thermal Cycler (Bio-Rad Laboratories, Inc.) using “short-barcoding” primers, targeting the “universal” barcoding region (658 bp) (Hebert et al., 2003) within the mitochondrial gene COI. Specifically, degenerated Op111, Op211, and Op311 primer pairs were used to amplify DNA fragments of 236 bp, 210 bp, and 179 bp, respectively. These primers belong to a non-published newly designed set provided by Dr Sara Bortolini (Fig. 2.6). The optimal annealing temperature (T_a) (47 °C) was assessed by gradient PCR. Other specifications are reported in Tab. 2.10. Raw DNA extracts and purified solutions as per protocol in Fig. 2.4, Fig. 2.5 were used as template.

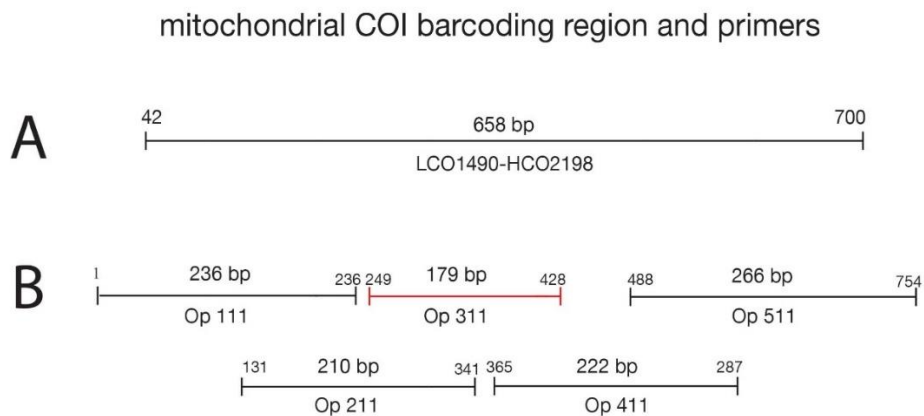


Fig. 2.6 Mitochondrial barcoding region and primers. A) Universal “barcoding” region and primers (Folmer et al. 1994); B) Dr Bortolini’s newly designed “short-barcoding” primer set (unpublished data). The starting and the ending nucleotides mark the numeration based on *Drosophila yakuba* mitochondrial genome (Clary and Wolstenholme, 1985).

Tab. 2.10 Op311 primer specifications.
5', 3' positions refer to *Drosophila yakuba* mitochondrial genome.

primer	sequence	5' position	3' position	amplicon length (bp)
Op111 fw	TCGCAACAATGGTTATTCTCT (21 bp)	1	22	236
Op111 rv	TCAATTACCRAATCCTCCAAT (21 bp)	215	236	
Op211 fw	GTAATTGTAACAGCTCATGC (20 bp)	131	151	210
Op211 rv	AACCAGTACCAGCTCCGTTT (20 bp)	322	342	
Op311 fw	CWCGAATAAATAATATAAGTTTTYTG (25 bp)	249	274	179
Op311 rv	ATTCCWGCTAARTGWARAGA (20 bp)	418	428	

Primers and protocols used are reported for each archaeological site in Tab. 2.11, while additional information about reagents included in each protocols and amplification programmes are reported in Tab. 2.12 and Tab. 2.13, respectively; as far as Sassari samples concern, primers targeting environmental DNA including bacterial 16S rRNA (V1-3 region) (Pechal et al., 2013) and eukaryotic 18S rRNA (Soares et al., 2013) were also used, setting a T_a of 52.3 °C and 54 °C, respectively.

Tab. 2.11 PCR specifications listed per archaeological site. *as per Tab. 2.12; ** as per Tab. 2.13.

samples from	primers used	PCR protocols*	amplification programmes**
crypts of Roccapelago	Op311	all five protocols listed in Tab. 2.12	all six protocols listed in Tab. 2.13
crypts of Castelsardo	Op311	Platinum™ HotStart	Platinum
urban well in Sassari	Op111 Op211 Op311 16S rRNA (v1-v3) 18S rRNA	archaeological standard	archaeological standard

Tab. 2.12 aDNA PCR protocols. HF*= High Fidelity.

reagents			archaeological standard	archaeological HF*	Phusion Blood HotStart HF*	Phusion HotStart HF*	Platinum™ HotStart
Buffer	GoTaq Buffer	Promega	1X	1X	-	-	-
	Blood Buffer	Thermo Fisher	-	-	1X	-	-
	Buffer HF*	Thermo Fisher	-	-	-	1X	-
	Platinum HotStart	Thermo Fisher	-	-	-	-	1X
MgCl₂	MgCl ₂	Promega	5 mM	5 mM	3 mM	0.5-1 mM	1.5 mM
Extra	BSA	Promega	1 mg/ml	1 mg/ml	-	-	-
	PVP	Sigma Aldrich	1%	-	-	-	-
Primers	Primer1	IDT	0.25 pmol/μl	0.25 pmol/μl	0.5 μM	0.5 μM	0.2 μM
	Primer2	IDT	0.25 pmol/μl	0.25 pmol/μl	0.5 μM	0.5 μM	0.2 μM
dNTPS	dNTPS	Promega	0.25 mM	0.25 mM	-	0.2 mM	-
DNA Taq Polymerase	GoTaq Flexi	Promega	0.06 U/μl	-	-	-	-
	HotStart II HF*	Thermo Fisher	-	0.02 U/μl	0.04 U/μl	0.02 U/μl	-
	PlatinumII HotStart	Thermo Fisher	-	-	-	-	0.04 U/μl

Tab. 2.13 Amplification programmes. ^{a)} modified version; ^{b)} used for templates derived from 8 puparia only;
 **www.thermofisher.com/tmcalculator

protocol	initial denaturation	denaturation	annealing	extension	final extension	cycles
archaeological standard	10 min 95 °C	1 min 95 °C	1 min 47 °C	1 min 72 °C	10 min 72 °C	35
archaeological HF	10 min 95 °C	1 min 95 °C	1 min 47 °C	1 min 72 °C	10 min 72 °C	35
Phusion Blood HF	30 s 98 °C	10 s 98 °C	30 s 52.1 °C**	15 s 72 °C	5 min 72 °C	30
Phusion Blood HF ^{a)}	30 s 98 °C	10 s 98 °C	30 s 50 °C	15 s 72 °C	5 min 72 °C	33
Phusion HF ^{b)}	30 s 98 °C	10 s 98 °C	30 s 52.1 °C**	15 s 72 °C	5 min 72 °C	30
Platinum Hot Start	2 min 94 °C	30 s 94 °C	30 s 52 °C	30 s 68 °C	-	28

Bovine Serum Albumin (BSA) and polyvinylpyrrolidone (PVP-40 kDa, water soluble) were added in order to minimise the inhibition effect by contaminants (Fulton and Stiller, 2012). Standard and high-fidelity DNA polymerases with enhanced 3'-5' proofreading activity were used. Due to the lack of positive archaeological controls, in all the reactions DNA template extracted from a modern specimen of *H. capensis* was used as positive control (Lo Pinto et al. 2017), to ensure the proper functioning of the used reagents and, most of all, to evaluate the efficiency of the designed DNA purification. Reactions were assembled under a PCR laminar flow cabinet model PURAIR PCR-36 (AirScience®, Florida, USA) which was physically separated from the bench dedicated to the manipulation and DNA extraction of the samples, in order to prevent cross contaminations between archaeological samples and modern reference controls.

PCR products were separated on 1.5% w/v agarose gel at 100 V and UV-visualised using Midori Green Advanced DNA Stain (Geneflow, Elmhurst, UK). DNA ladder 100 bp (Promega, Madison, Wisconsin, USA) was used to verify the size of the amplicons.

2.3.6 aDNA purification and sequencing

Positive amplicons were purified using QIAquick PCR Purification kit (Qiagen, Hilden, Germany), designed for amplicons within the range 100 bp – 10 Kb. The purified products were sequenced by the external company Eurofins Operon MWG (Ebersberg, Germany). Bi-directional sequencing using both the forward and reverse primers was applied in order to minimise the loss of the fragment extremities and improve the final output data subjected to alignment. The quality of aDNA sequences was evaluated through visualisation of the electropherograms using the free alignment editor and package analysis software BioEdit v.7.1.10 (Hall, 1999). Conserved central portions were identified and flanking low quality regions were trimmed prior to align the forward and reverse sequences of the same fragments using Molecular Evolutionary Genetics Analysis (MEGA) package v7.0 (Kumar et al., 2016). Sequences were used as queries in nucleotide-BLAST® (Altschul et al., 1990).

2.4 MODERN DNA ANALYSIS

The following instructions refer to modern entomological specimens studied in chapters 3 and 5, either collected from laboratory breeding or forensic contexts.

2.4.1 Investigations on the impact of cuticular pigments on downstream DNA analysis - Chapter 3

This experiment was designed to evaluate whether the pigments released by the exoskeleton of Diptera puparia have an impact on downstream applications (PCR); additionally, obtained data will be used as reference for aDNA analysis. Adult Coleoptera were also included in the experiment as alternative source to investigate the effect of cuticular pigments, as well as they were used as internal positive control since the buffer applied within DNA isolation method was specifically designed for museum beetles (Gilbert et al. 2007).

Two adults of the mealworm beetle *Tenebrio molitor* Linnaeus, 1758 (Coleoptera: Tenebrionidae) were selected from the population reared in the FLEA. In addition, two and five puparia (in duplicate) of *Calliphora vicina* Robineau-Desvoidy, 1830 (Diptera: Calliphoridae) were selected from a pool of puparia collected over the summer 2015 during a decomposition experiment involving rabbit carcasses (Tuccia et al. 2019). Puparia showing larvae exuviae internally attached were carefully selected, as unique source of epithelial cells usable as substratum for the host DNA extraction (Fig. 2.7).



Fig. 2.7 Larval exuviae within a puparium of *Calliphora vicina*. Black arrow indicates the epithelial tissue of the metamorphosis insect which is left attached to the puparium after the adult emerges. Scale bar: 1 mm.

All the specimens were pre-washed in warm water (40° C) and let air-dried at room temperature; a sterile entomological pin was used to perforate the ventral abdominal region of *T.molitor* in order to allow the lysis buffer to easily penetrate and reach the

Materials and Methods

internal soft tissues during DNA extraction. Overall, the integrity of the specimens was preserved.

DNA extraction. Total DNA was isolated as described in paragraph 0, Tab. 2.8, method 2. The protocol was modified when applied on one of the two batches of duplicitaes by purifying the lysates prior to proceed with manufacturer's instructions (treated batch). A final purification step was applied (Fig. 2.8).

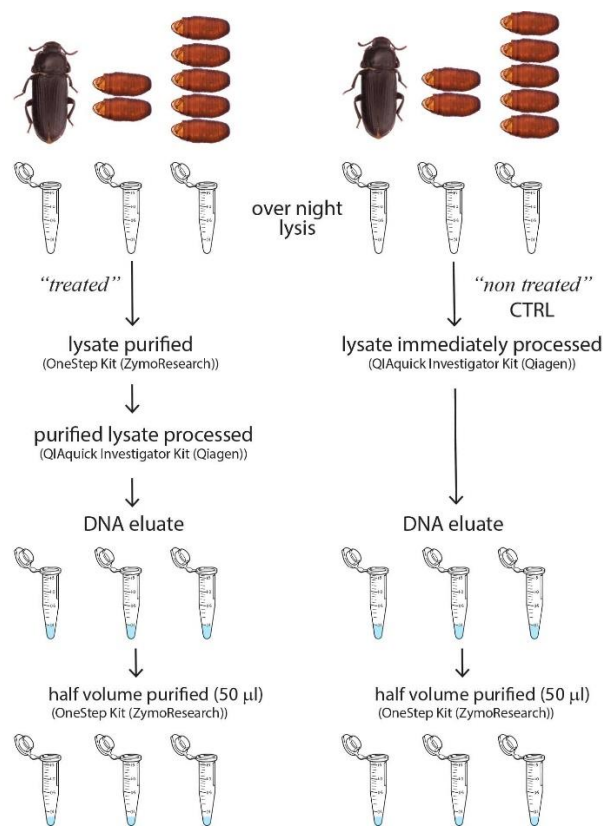


Fig. 2.8 DNA extraction workflow of pigment test. The morphology of the specimens was preserved using a non-destructive submersion method. Left column: "treated samples", lysate subjected to purification with OneStep PCR Inhibitors Removal kit (ZymoResearch) prior to follow manufacturer's instruction; right column: "non-treated" samples, lysate processed using QIAquick Investigator Kit (Qiagen). A final purification step of the eluates was performed in both cases on 50 out of 100 µl of DNA eluate.

DNA quantification. Qubit[®] 3.0 Fluorometer (Thermo Fisher, Waltham, Massachusetts, USA) was used to quantify the total concentration of DNA extracted before and after the final purification following instructions as in paragraph 2.3.4.

DNA size assessment. Agilent 2100 Bionalyzer System and the High Sensitivity dsDNA Assay (Agilent Technologies, California, USA) were used to evaluate the size genomic DNA following manufacturer's instructions as explained in paragraph 2.3.4.

DNA amplification and sequencing. Universal mtCOI barcoding primers (Folmer et al., 1994) were used in the PCRs to amplify a fragment of 658 bp. Promega GoTaq® Flexi Polymerase protocol was followed to prepare a 20 µl reaction: 4 µl of Colourless GoTaq Flexi Buffer (5×), 2 µl of MgCl₂ (25 mM), 0.5 µl of each primer (10 pmol/µl), 0.5 µl of dNTPs Mix (10 mM), 0.25 µl GoTaq DNA Polymerase (5 u/µl) and 2 µl of DNA template (5-10 ng/ µl initial concentration). The amplification program was set on the thermal cycler BioRad C1000 (Bio-Rad Laboratories, Inc., Hercules, California, USA). The initial heat activation step at 95 °C for 10 min was followed by 35 cycles of 95 °C for 1 min, 49.8 °C for 1 min, 72 °C for 1 min and a final extension step at 72 °C for 10 min. Positive and negative control samples were added to the reactions as established procedure. A PCR laminar flow cabinet model PURAIR PCR-36 (AirScience®, Florida, USA) was used to assemble all the reactions and prevent cross contaminations between samples. Electrophoresis in agarose gel 1.5% (w/v) stained with Midori Green Advanced DNA Stain (Geneflow Ltd., Lichfield, UK) was performed to evaluate the quality of the reactions.

Positive amplicons were purified using QIAquick PCR Purification Kit® (Qiagen, Hilden, Germany) following the manufacturer's instructions, eluted in 40 µl of EB and sequenced by Eurofins Genomics (Ebersberg, Germany). The identity of the sequences was searched by BLAST® (Altschul et al., 1990).

2.4.2 DNA barcoding of *Physiphora alceae* and phylogenetic analysis of Diptera: Ulidiidae - Chapter 5

Two larvae of *Physiphora alceae* were diaphanized as described in paragraph 2.1.2 and soft tissues were pooled together; one adult was selected as well. All the specimens were ground using a sterile plastic pestle. QIAamp DNA Investigator Kit (Qiagen) was used to extract total DNA following manufacturer's instruction but using Promega Proteinase K at 0.1 mg/ml. DNA quantification, amplification, purification and sequencing were carried out as in paragraph 2.4.1.

Sequence dataset for phylogenetic analysis. Fifty-four mtCOI barcoding sequences of Ulidiidae (Diptera) with a length over 580 bp were downloaded from GenBank and BOLD database. A final dataset of 61 sequences including 59 public record and 2 domestic sequences was generated. The same species analysed by Galinskaya and collaborators (2014) were chosen. The complete list is reported in Appendix A, Supplementary Table A1.

Multiple sequences alignment and phylogenetic reconstruction. DNA sequences were aligned using ClustalW within MEGA v7.0. obtaining blunt ends sequences blocks. ModelFinder tool on online Cypres Gateway IQ-Tree v.1.6.10 (Kalyaanamoorthy et al., 2017) was herein used to evaluate the best nucleotide substitution model for the given dataset. The best-fit model was chosen based on the highest w-AIC_c (second order Akaike Information Criterion) and on the lowest BIC (Bayesian Information Criterion) parameters values (Fabozzi et al., 2014). The same software was used to implement the construction of Maximum Likelihood phylogenetic tree (Felsenstein, 1981), providing a topology that best reflects the observed data. The reliability of the topology was tested inferring 1000 bootstrap replicates using the ultrafast bootstrap parameter (Hoang et al., 2018). The bootstrap values were expressed as percentage.

2.4.3 DNA barcoding and phylogenetic analysis of Piophilidae of forensic interest – Chapter 5

Other than single pupae of Piophilidae species listed in Tab. 2.3, specimens listed in Tab. 2.14 were used as source for molecular analysis, for a total of 13 specimens grouped in 11 species.

Tab. 2.14 Additional Piophilidae specimens subjected to DNA analysis.

Developmental stages are identified as second instar larva= II-L, pupa= P, puparium= Pu, adult=A

species	geographical origin	number of specimens/ developmental stage	source
<i>Parapiophila atrifrons</i> (Melander and Spuler, 1917)	Spain	1/P	laboratory collection (Dr Martín-Vega)
<i>Parapiophila vulgaris</i> (Fallen, 1820)	United Kingdom	2/A	rabbit carcasses
<i>Stearibia nigriceps</i> (Meigen, 1826)	Italy	1/II-L , 1/A	human remains

DNA extraction. Larvae were prepared as described in paragraph 2.1.2. Pupae were prepared applying a variant of the method by Tuccia et al. (2016). A sterile entomological pin was used to perform a cut along the major width of the pupal cage which was then removed carefully in order to ensure the integrity of the anal region and the oral sclerites of the specimen. The pupal cage was then stored in EtOH 70%. Soft tissues were ground using a sterile plastic pestle. Adult specimens were pierced on the abdomen using a sterile entomological pin and submerged into the extraction buffer. Total genomic DNA was extracted using QIAamp DNA Investigator Kit (Qiagen) as described in paragraph 2.4.2. DNA quantification, amplification, sequencing and identity confirmation followed paragraph 2.4.1.

Sequence dataset for phylogenetic analysis. Ninety-three mtCOI barcoding sequences were downloaded from GenBank and BOLD, and 13 in-house mt COI sequences (non-published) of Piophilidae were included in the dataset. Two sequences of *O. formosa* (Diptera: Ulidiidae) were used as outgroups (Appendix A, Supplementary Table A2).

Materials and Methods

Multiple sequences alignment and phylogenetic reconstruction. Analysis were carried out as described in paragraph 2.4.2. Additionally, a subset including all *Parapiophila vulgaris* and *Allopiophila vulgaris* sequences was subjected to pairwise distance analysis on MEGA v7.0.

3

DNA ANALYSIS OF MODERN AND ANCIENT
DIPTERA PUPARIA: CHALLENGES, LIMITATIONS, AND
POTENTIALITIES

3.1 INVESTIGATIONS ON THE IMPACT OF CUTICULAR PIGMENTS ON DOWNSTREAM DNA ANALYSIS

3.1.1 Results

After the overnight incubation at 56 °C, lysates' aliquots appeared turbid and coloured, varying from light to dark brown, more intense for *Tenebrio molitor* adult rather than *C. vicina* puparia. Although lessened, this colouration was kept after the first treatment with the purification kit, and gradually the aliquots turned into transparent (Fig. 3.1).

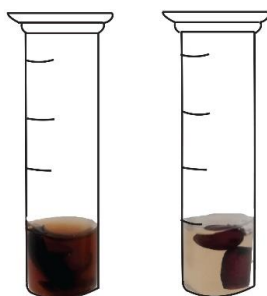


Fig. 3.1 Coloured lysate extracts. *T. molitor* adult (left) and *C. vicina* puparia (right) extracts showing a brownish colouration soon after the lysis incubation.

All DNA extractions succeeded providing concentrations in accordance to the initial amount of soft tissue as usable source (Tab. 3.1.). Overall, neither the intermediate purification treatment nor the purification of the eluates significantly affected the concentrations (2 ways ANOVA p value = 0.83, p value = 0.85, respectively).

Tab. 3.1 Qubit® 3.0 Fluorometer DNA quantification. *=lysate treated with One Step purification kit; CTRL=lysate non-treated, directly processed. In both cases, half volumes of the final eluates were purified with a column-based system (purified eluates). The percentage of DNA lost is calculated as ratio of concentration of purified eluates over concentration of raw DNA eluates.

specimen	raw DNA eluates (ng/μl)	purified DNA eluates (ng/μl)	lost (%)
<i>T. molitor</i> *	139.67	114.33	18.14
<i>T. molitor</i> CTRL	165.33	140.67	14.92
2 <i>C. vicina</i> *	1.16	1.06	8.60
2 <i>C. vicina</i> CTRL	4.37	3.93	9.92
5 <i>C. vicina</i> *	2.37	1.61	32.02
5 <i>C. vicina</i> CTRL	3.62	3.25	10.31

Bioanalyzer traces show that the raw treated eluates have less fragmented DNA within the range of 100 bp to 600 bp (Fig. 3.2A). The same results derived from the clean eluates (Fig. 3.2B,D). On the other hand, the non-treated eluted DNA of *C. vicina* (Fig. 3.2) shows a lower level of fragmentation in comparison to the counterpart subjected to the intermediate purification step (Fig. 3.2E). Instead, a similar pattern was observed between the purified DNA eluates, treated and non-treated (Fig. 3.2F,H). Five puparia of *C. vicina* showed the same pattern of two puparia, therefore, the shown data are representative of both.

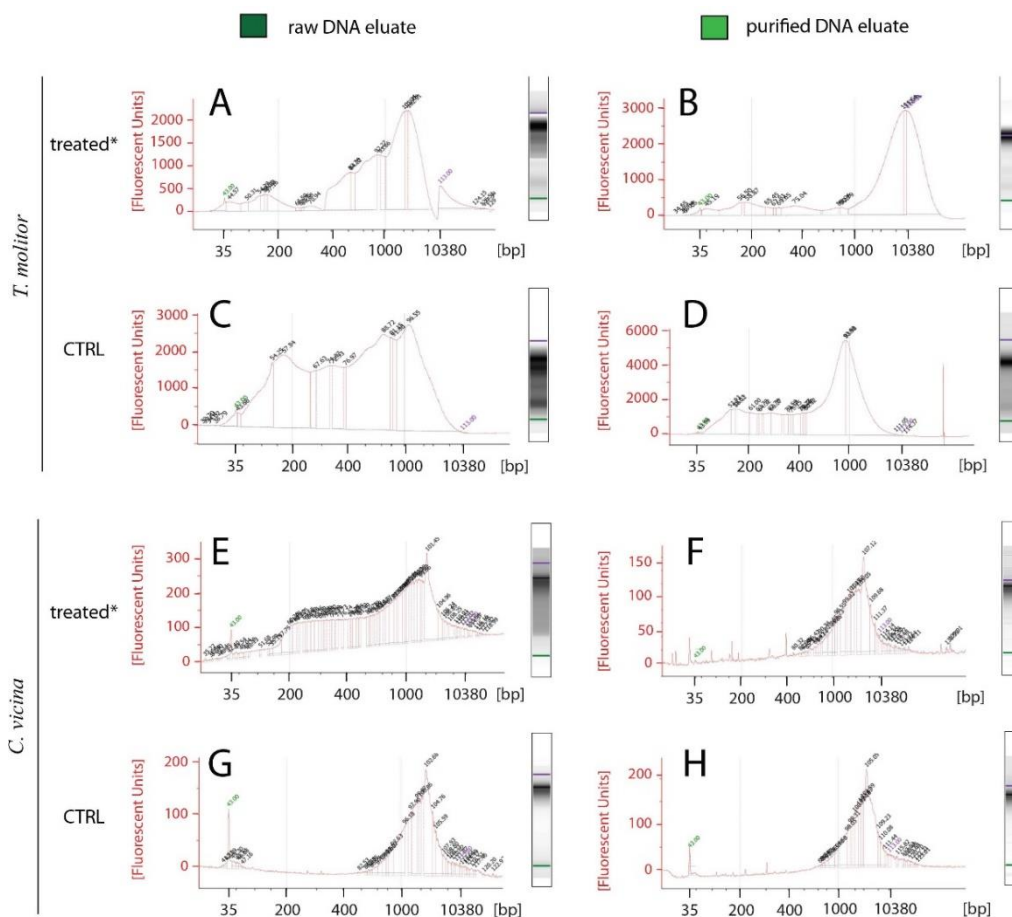


Fig. 3.2 Bioanalyzer traces. Electrophoresis on chip results are shown for pigmented non-purified extracts (left column) and transparent purified eluates (right column); *lysates subjected to purification with OneStep PCR Inhibitors Removal kit (ZymoResearch) prior to continuing with the extraction; “CTRL” samples, lysate non-subjected to purification but processed according to manufacturer’s guidelines.

The absorbance measured soon after the lysis step of all the specimens revealed a strong peak at ~230 nm along with a peak at ~290 nm well defined for puparia of *C. vicina* and more attenuated for *T. molitor* (Fig. 3.3).

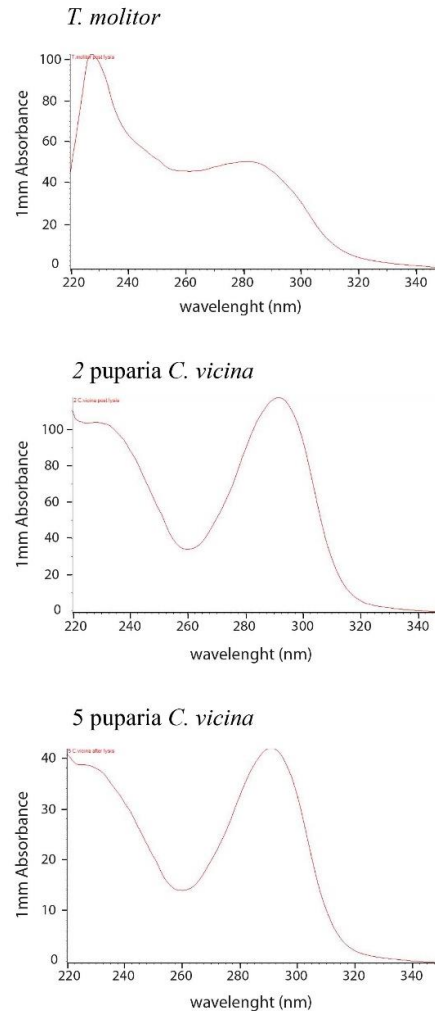


Fig. 3.3. UV absorbance spectra of pigmented post lysis extracts. In all the specimens, an absorbance peak around 290 nm can be observed, higher and well defined in *C. vicina*, way more attenuated in *T. molitor*, suggesting a potential difference in the pigmentation of the cuticle.

The profile of the spectra, significantly changed at the end of the isolation process, showing pure DNA solutions both for raw pigmented DNA and purified samples, and no difference was observed between treated and non-treated samples (Fig. 3.4). Absorbance ratios values are reported in Tab. 3.2

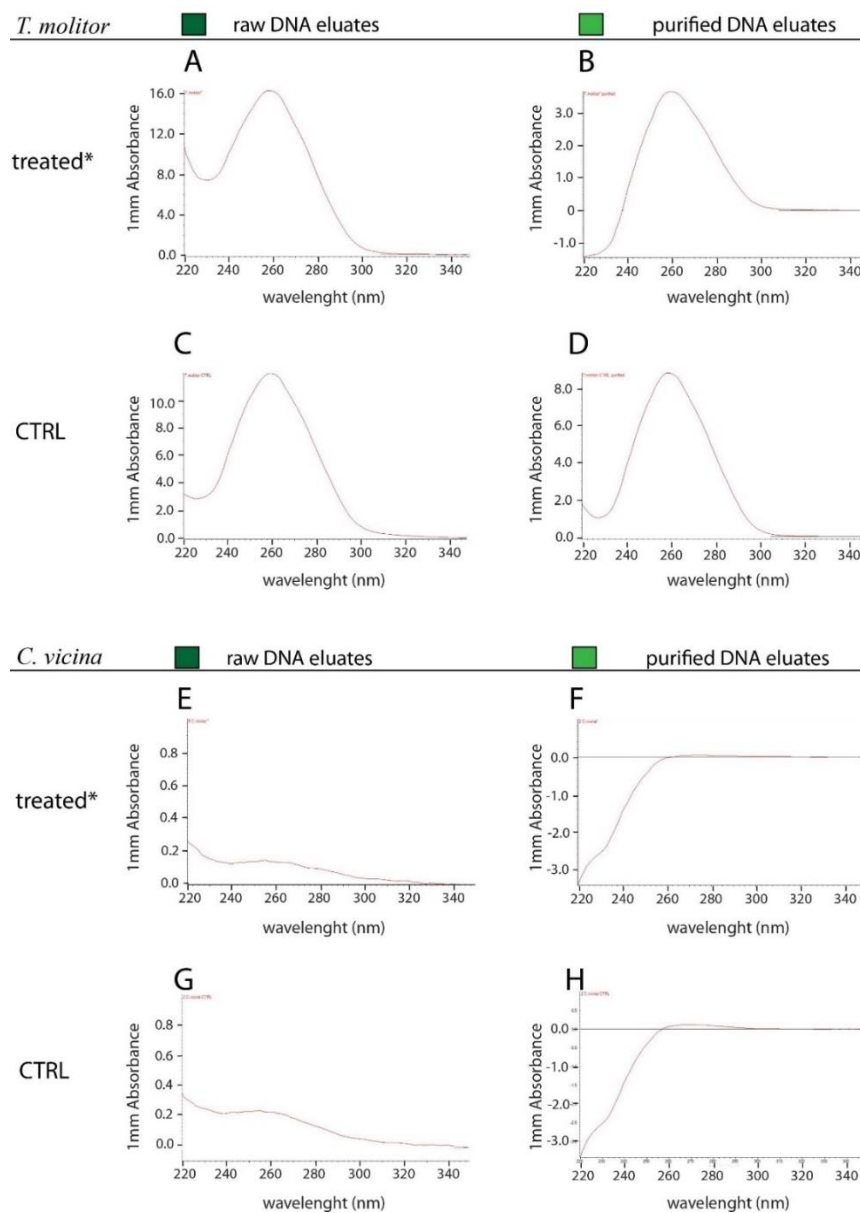


Fig. 3.4 UV absorbance spectra of purified extracts. Peak at 260 nm identify pure DNA solution. Difference in intensities signal was observed in accordance with concentration measurements in Tab. 3.1.; *lysate subjected to purification with OneStep PCR Inhibitors Removal kit (ZymoResearch) prior to continuing with the extraction; CTRL= lysate non-treated, immediately processed using QIAquick Investigator Kit (Qiagen). A final purification step of the eluates was performed in both cases and electrophoresis was performed before (raw DNA eluates, left column) and after (purified DNA eluates, right column). Letters follow Fig. 3.2.

Tab. 3.2 NanoDrop™ Abs ratios.

*=lysate treated with One Step purification kit; CTRL=lysate non-treated, directly processed.

SOURCE	raw eluates		purified eluates	
	260/280	260/230	260/280	260/230
<i>T. molitor</i> *	2.05	2.19	2.04	3.97
<i>T. molitor</i> CTRL	1.94	2.00	1.93	6.30
2 <i>C. vicina</i> *	1.86	0.85	0.87	0.01
2 <i>C. vicina</i> CTRL	1.72	0.91	0.73	0.02
5 <i>C. vicina</i> *	1.46	0.88	0.08	0.01
5 <i>C. vicina</i> CTRL	0.58	0.45	0.64	0.03

The amplification of the mtCOI barcoding region was successful for all the templates treated and non treated with the exception for 2 puparia of *C. vicina*, with an increased UV signal showed by the purified eluates in comparison to the raw DNA (Fig. 3.5). DNA amplicons showed the expected size (~658 bp) and sequencing successfully confirmed the morphological identification of the species (Tab. 3.3). Sequences are reported in Appendix B, Supplementary Table B1.

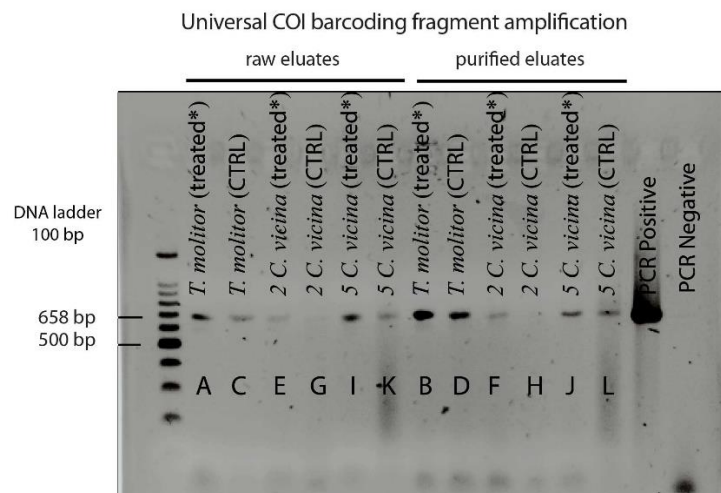


Fig. 3.5 Gel electrophoresis of PCR products from pigment test. Positive amplicons show the expected size (~658 bp). *=lysate treated with One Step purification kit; CTRL=lysate non-treated, directly processed. In both cases, half volumes of the final eluates were purified with a column-based system (purified eluates). Letters were assigned as in Fig. 3.4. DNA Ladder: 100 bp.

Tab. 3.3 BLAST species identification. Letters were assigned as in Fig. 3.4

source	size bp	BLAST query cover	BLAST E-value	BLAST max ID value	morphological ID confirmed
A <i>T. molitor</i>	627	99%	0.0	99.84%	✓
B <i>T. molitor</i>	607	94%	0.0	91.16%	✓
C <i>T. molitor</i>	638	94%	2e-53	76.57%	✓
D <i>T. molitor</i>	624	96%	0.0	90.40%	✓
E <i>C.vicina</i>	448	92%	0.0	95.26%	✓
F <i>C.vicina</i>	653	96%	0.0	87.48%	✓
I <i>C.vicina</i>	653	96%	0.0	95.25%	✓
J <i>C.vicina</i>	644	99%	0.0	97.82%	✓
K <i>C.vicina</i>	648	99%	0.0	99.84%	✓
L <i>C.vicina</i>	650	98%	0.0	99.84%	✓

3.1.2 Discussions

Species identification through genotyping is a well-established method in forensic entomology as it can be applied to all the specimens regardless their stage of development. Puparia and adult Coleoptera are more frequently found in forensic scenarios in those cases where a long-time frame elapsed between the death of the individual and its discovery. If molecular analysis is commonly applied to identify Coleoptera, just a scarce number report the use of genotyping to address the identification of the species in puparia (Malgorn and Coquoz, 1999, Mazzanti et al., 2010, Meiklejohn et al., 2013). The amount of tissue suitable to extract DNA in one or the other specimens significantly differ (Tab. 3.1), and can explain the unbalanced literature data. Additionally, the two pieces of evidence have a pigmented chitinous exoskeleton but little information is known about the impact that the pigmentation has on molecular analysis. As no *ad hoc* commercial kit are currently available to isolate DNA from insects, in this work the combination of a home-made lysis buffer and a commercial kit has been used: Gilbert's digestion buffer was specifically design to extract DNA from dry museum beetle species aged up to 92 years (Gilbert et al., 2007), and QIAamp® DNA investigator Kit by Qiagen has been developed specifically to extract DNA from forensic trace samples, *i.e.* containing low quantity of genetic material. The extent of the colour loss showed by the analysed specimens during the incubation with the digestion buffer certainly correlates with the size of the specimens and their cuticular pigmentation, which is given by melanin and other compounds. Insect cuticle supports and protects the soft body parts against parasites and pathogens (immunological defence reaction) (Sugumaran, 2002), as well as prevents the dehydration of the organism and allows gaseous exchange with the external environment (Sugumaran, 2009). The colour patterns are the manifestation of pheomelanin, eumelanin (form of melanin with different structure) and other derivatives whose production is driven by a complex set of enzymes and control elements. The genetics behind these biochemical complexities is not completely understood yet. However, some progress has been made and it seems that the pathways involved in the pigmentation are linked to the ones involved in the hardening of the cuticle (sclerotisation) (Sugumaran, 2009). Specifically, it has been proven that there is a

correlation between a brown cuticle with the N- β -alanyldopamine (NBAD) (Barek et al., 2017), one of the major precursors of the cuticle sclerotisation (Sugumaran, 2009), as in the case of *C. vicina* puparia and *T. molitor* used in this study. Interestingly, Diptera puparia undergo to a colour change from light yellow to dark brown as the metamorphosis of the insect progresses. Such a change correlates with the hardening of the pupal cage and in *Sarcophaga bullata* (Parker, 1916) (Diptera: Sarcophagidae) the turning into dark brown of the cuticle pigmentation is due to a progressive accumulation of pheomelanin rather than eumelanin (Barek et al., 2017). Likely, the observed discolouration of the specimens was due to the removal of cuticular pigments by the action of detergents included in the formulation of lysis buffers. A similar post lysis phenomenon was observed for mosquitos (Giantsis et al., 2015). Spectra in Fig. 3.3 show the detection of contaminants in the post-lysis extracts, likely salts for abs= 230 nm, and unknown compounds absorbing at 290 nm; while it is well-established that the human skin melanin absorbs UV light at 335 nm, and that the melanins inside the insect exoskeleton vary from those of mammalian epidermal melanin due to different precursors involved in the biosynthesis (Barek et al., 2017), there is a lack of experimental data concerning this topic which did not allow to compare the obtained UV spectra in Fig. 3.3. However, the fact that observed absorption peaks do not correspond to melanin and its derivatives (in addition to proteins or other contaminants) cannot be excluded *a priori*; certainly the topic requires deeper research to characterise the compounds through techniques of analytical chemistry that were not be applied in this context.

The hydrosoluble melanin-derived pigments were efficiently removed during the washing steps of the protocol which, moreover, includes an extra washing step with EtOH 99% compared to the other Qiagen kit silica- column based. As a result, the total DNA was successfully extracted (Tab. 3.1.) providing, as expected, considerably diverse concentrations for a single adult beetle and a few empty fly puparia. The few works focussing on the DNA extraction from empty puparia don't report the concentration values (Mazzanti et al., 2010, Meiklejohn et al., 2013), and allege that the applied method of quantification did not allow to detect any reliable concentration measurement (Malgorn and Coquoz, 1999). In this study, on average, after the purification of the

Chapter 3

eluates, a depletion of the 16.53%, 9.26%, and 21.16% was observed for *T. molitor*, two and five puparia of *C. vicina*, respectively. This datum suggests that the synthetic resin partially retains DNA molecules and, likely, these molecules are the shortest fragments within the whole extraction solution. In fact, Bioanalyzer traces (Fig. 3.2) show a reduction of the amount of fragmented DNA represented by the decreased intensity of the curve between the range 35-700 bp. Overall, the PCR were successful on all the templates except for *C. vicina* (2 puparia-CTRL), for which a potential explanation follows below.

All the considerations made so far reflect on the downstream application of DNA analysis as follows. First, the initial concentration is key for a successful PCR, as per visible different UV signal obtained from *T. molitor* adult and *C. vicina* puparia; cuticular pigments and other contaminants are efficiently removed with the used DNA isolation protocols, however, we are led to think that an additional purification of the samples soon after the lysis contributes to improve the yield of the reactions, as per Fig. 3.5; moreover, the purification of the final eluates leads to an increased UV signal, and therefore recommended.

3.1.3 Conclusions

From what has been here proposed as “reference experiment”, the following conclusions can be drawn:

- DNA can be efficiently isolated from “modern” empty puparia of Diptera, using QIAamp® DNA investigator Kit by Qiagen in combination with Gilbert’s digestion buffer;
- during the lysis step, insect hydro soluble cuticular pigments are released with an extent which correlates with the size of the specimen, and are efficiently removed during DNA isolation based on the use of silica columns as per manufacturer’s instructions;
- treating the lysis preparation and the final DNA eluates with a purification step is highly recommended to improve the downstream amplification, despite the synthetic resins tend to retain short DNA molecules (< 100 bp) and therefore causing a decrease of the final concentration;
- the application of this protocol allows to successfully identify puparia species through genotyping, demonstrating the role of the molecular biology as a powerful tool for the species identification in forensic entomology in support of morphological analysis.

3.2 MOLECULAR ANALYSIS OF DIPTERA PUPARIA RECOVERED FROM ROCCAPELAGO MUMMIES

3.2.1 Results

Ancient DNA analysis

After the incubation with the ROSE buffer, the lysis volumes of both archaeological and control samples showed a brown dark-pigmented colouration with the intensity proportional to the number of processed puparia (Fig. 3.6). The colouration diminished progressively as two consecutive steps of purification were applied and it finally turned into transparent (Fig. 3.6). Fifty μl of the lysis extract directly processed using the second strategy (Fig. 2.4C) appeared immediately transparent.

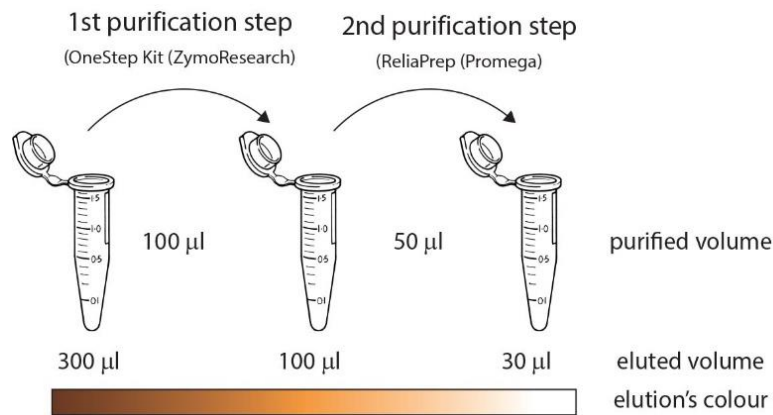


Fig. 3.6 Pigmentation status of Roccapelago extracts/eluates. Schematic representation of changes in colouration of DNA preparations: the initial brown dark pigmentation of the ROSE extracts was progressively lost through the purification steps. The same phenomenon was observed for archaeological and control samples.

According to the first Qubit[®] measures performed on the “raw extracts”, DNA was successfully extracted from the puparia showing concentrations proportional to the number of puparia processed as initial substratum, with the exception for the group of eight archaeological puparia (Tab. 3.4).

Tab. 3.4 First strategy Qubit® 3.0 Fluorometer DNA quantification. Concentration values are expressed in ng/μl ± standard deviation (s.dv) calculated on three measurements of the same template. Percentages of DNA lost are calculated as ratio of concentration of purified eluates (2nd) over concentration of ROSE buffer extracts; b.l.t.= below lowest threshold of the instrument (0.01 ng/μl).

number of puparia	raw DNA eluates		purified DNA eluates (1 st)		purified DNA eluates (2 nd)		Lost (%)
	ROSE buffer		(OneStep kit (ZymoResearch))		(ReliaPrep (Promega))		
	[DNA] (ng/μl)	s.dv	[DNA] (ng/μl)	s.dv	[DNA] (ng/μl)	s.dv	
CTRL 1	0.51	0.01	0.2	0.01	0.27	0.02	90.83
CTRL 2	1.83	0.02	0.66	0.01	0.18	0.04	99.90
CTRL 3	2.78	0.01	0.77	0.01	0.14	0.01	98.29
CTRL 5	3.46	0.03	1.43	0.01	0.4	0.02	95.66
CTRL 8	7.42	0.03	2.00	0.03	b.l.t	n/a	89.74
Roccapelago 1	1.09	0.02	0.35	0.01	0.001	0.00	47.06
Roccapelago 2	5.1	0.05	1.26	0.01	0.01	0.01	90.2
Roccapelago 3	7.6	0.15	2.45	0.04	0.13	0.02	95.0
Roccapelago 5	7.37	0.04	2.61	0.03	0.32	0.07	88.4
Roccapelago 8	3.51	0.01	1.28	0.01	0.36	0.02	99.99

The results of the first strategy show that after performing the first purification on the raw extracts using the OneStep PCR Inhibitor removal kit (Zymo Research, Irvine, California, USA), a lost in the concentration equal to $65.7\pm 5.9\%$ and $67.8\pm 4.12\%$ was calculated on average for the control and the Roccapelago samples, respectively. Similarly, after the second purification using the ReliaPrep DNA purification and concentration system (Promega, Madison, Wisconsin, USA), a further loss of $81.6\pm 11.26\%$ and $90.7\pm 10.39\%$ was calculated on average for the control and the Roccapelago samples, respectively. Only the single control puparium showed an increasing of 35% between the first and the second purification step.

On the other hand, the results of the second strategy show that, after applying a single purification step using the ReliaPrep DNA purification and concentration system (Promega, Madison, Wisconsin, USA), the concentration decreased of $87.8\pm 6.3\%$ and $89.6\pm 14\%$ for the control and Roccapelago samples, respectively (Tab. 3.5).

Tab. 3.5 Second strategy Qubit® 3.0 Fluorometer DNA quantification. Concentration values are expressed in $\text{ng}/\mu\text{l} \pm$ standard deviation (s.dv) as in Tab. 3.4. b.l.t.= below lowest threshold of the instrument ($0.01 \text{ ng}/\mu\text{l}$). Percentage of DNA lost calculated as in Tab. 3.4.

# puparia	raw DNA eluates		purified DNA eluates (1 st)		Lost (%)
	ROSE buffer		(ReliaPrep (Promega))		
	[DNA] ($\text{ng}/\mu\text{l}$)	s.dv	[DNA] ($\text{ng}/\mu\text{l}$)	s.dv	
CTRL 1	0.51	0.01	0.12	0.01	76.47
CTRL 2	1.83	0.02	0.24	0.01	86.89
CTRL 3	2.78	0.01	0.24	0.02	91.37
CTRL 5	3.46	0.03	0.16	0.01	95.38
CTRL 8	7.42	0.03	0.83	0.04	88.81
Roccapelago 1	1.09	0.02	0.14	0.05	87.16
Roccapelago 2	5.1	0.05	0.03	0.06	99.41
Roccapelago 3	7.6	0.15	b.l.t.	b.l.t.	99.9
Roccapelago 5	7.37	0.04	0.14	0.01	98.10
Roccapelago 8	3.51	0.01	1.29	0.05	63.25

No significant difference was found in the concentrations between control and archaeological samples (2 ways ANOVA p -value: 0.212), whereas the purifications step had a significant impact on the concentrations (2 ways ANOVA p -value: 0.0001). Fig. 3.7 show absorbance spectra of non-purified lysis suspensions and purified DNA eluates; peaks absorbing at ~230–240 and ~250 nm were observed in non-purified suspensions, of both control and the archaeological samples, respectively. Additionally, a peak of minor intensity ~270–280 nm was observed in the control sample. However, the recorded high intensities are over the expected range of absorbance (~3).

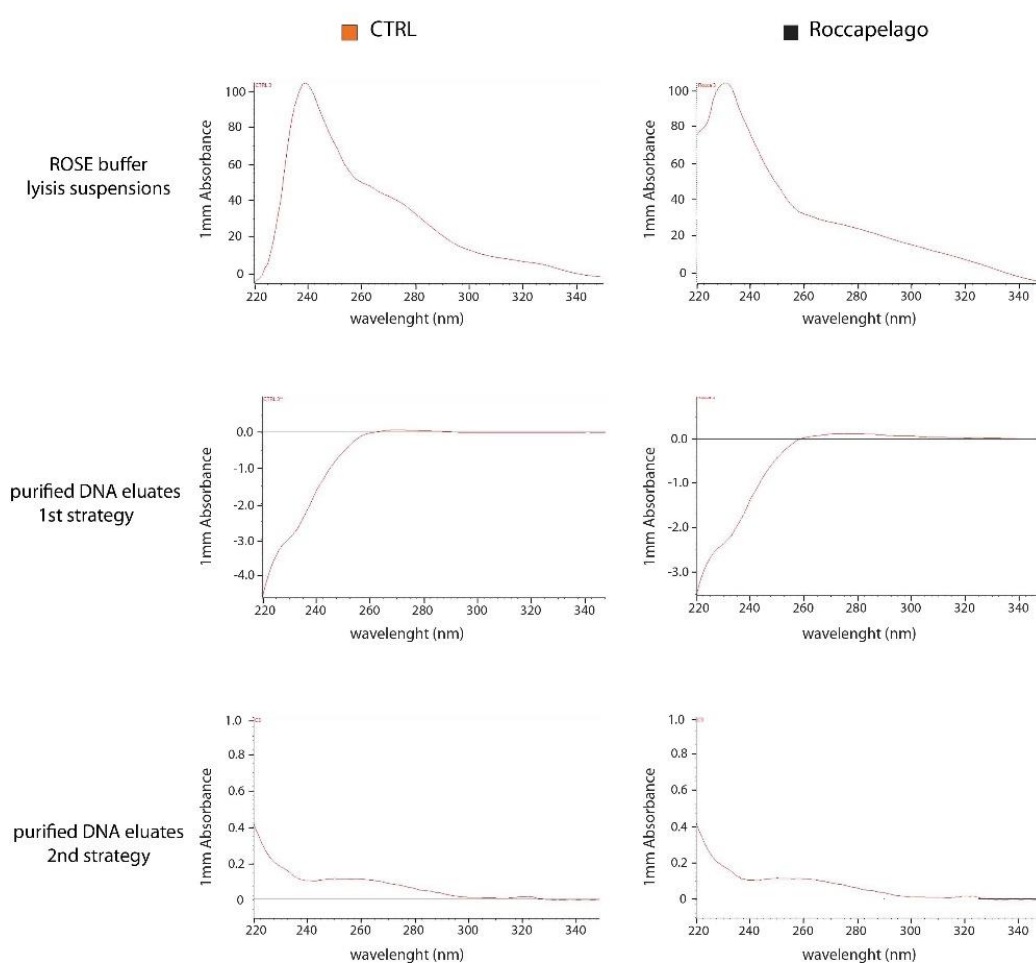


Fig. 3.7 NanoDrop Abs spectra. Left column: control samples; right column: Roccapelago samples. One spectrum is reported as representative of each of the conditions for each sample, as data are consistent among samples.

The absorbance ratios revealed A260/280 values between 1.3–1.7 and 1.2–1.5, and A260/230 values between 1.1–2.4 and 1.1–1.9 for control and Roccapelago samples, respectively (Appendix A, Supplementary Table A3). The eluates purified using the second strategy, overall showed increase A260/280 absorbance values compared to the raw extracts, but still lower than the expected values for pure nucleic acid solution (1.8–2), whereas the A260/230 did not vary consistently. The relative spectra show a decreased intensity in accordance to the low concentration of these templates (Tab. 3.5) and a shifted peak towards 260 nm, indicating purified DNA.

The results of the amplification reactions using the primer pairs Op311 are summarised in Tab. 3.6. PCRs failed in all the cases (controls and archaeological) when the amplification protocols “Archaeological High Fidelity” and “Phusion Blood High Fidelity” (Tab. 2.13) were applied. On the contrary, positive results were obtained both for double-purified control and Roccapelago samples, with the exception of one single control puparium and two archaeological samples (single and eight puparia), when using “archaeological standard” protocol and the modified version of “Phusion Blood High Fidelity” protocol (Tab. 2.13, Tab. 3.6). The use of “Phusion High Fidelity” protocol resulted in a successful PCR only when the “ultra-purified” CTRL template was used in the reaction. The use of the “Platinum Hot Start” protocol did not provide any positive results (Tab. 3.6). In the majority of the cases, when the electrophoresis gels were UV-visualised, the presence of conspicuous “fire-tails” of high-molecular weight signals were observed especially in correspondence with the raw or single-purified templates (*e.g.* in Fig. 3.8).

Tab. 3.6 PCR results summary. Red= failure; green= success; *=UV signal of higher intensity in contrast to other positive counterparts; grey= not performed.

		CTRL																		
		raw					1st step					2nd step					u.c.		2 nd strategy	
number of puparia		1	2	3	5	8	1	2	3	5	8	1	2	3	5	8	8		all samples	
protocol																				
1	archaeological		2	3	5			2	3	5			2	3	5					
2	archaeological modified		2	3	5			2	3	5			2	3	5					
	with High-Fidelity (HF) DNA Polymerase		2	3	5			2	3	5			2	3	5					
3	Phusion Blood HotStart High-Fidelity (HF)		2	3	5			2	3	5			2	3	5					
4	Phusion Blood HotStart High-Fidelity (HF), modified version	1	2	3	5	8	1	2	3	5	8	1	2*	3*	5*	8*		8		
5	Phusion HotStart HF																	8		
6	Platinum HotStart																			
		Roccapelago																		
		raw					1st step					2nd step					u.c.		2 nd strategy	
number of puparia		1	2	3	5	8	1	2	3	5	8	1	2	3	5	8	8		all samples	
protocol																				
1	archaeological		2	3	5			2	3	5			2	3	5					
2	archaeological modified		2	3	5			2	3	5			2	3	5					
	with High-Fidelity (HF) DNA Polymerase		2	3	5			2	3	5			2	3	5					
3	Phusion Blood HotStart High-Fidelity (HF)		2	3	5			2	3	5			2	3	5					
4	Phusion Blood HotStart High-Fidelity (HF), modified version	1	2	3	5	8	1	2	3	5	8	1	2*	3*	5*	8		8		
5	Phusion HotStart HF																	8		
6	Platinum HotStart																			

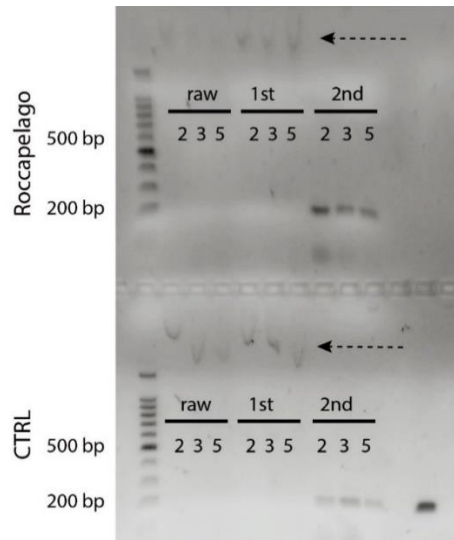


Fig. 3.8. Gel electrophoresis from Phusion Blood High Fidelity modified version. Amplification of DNA Op311 short-barcoding fragments is showed for Roccapelago (above) and control (below) samples. Numbers 2,3,5 indicate the number of processed puparia per each condition (raw= non-purified lysates, 1st= DNA eluates purified using 1st strategy, and 2nd= DNA eluates purified using the 2nd strategy as per Fig. 2.4. Black arrows indicate the “fire-tails” of high-molecular weight, aspecific UV-signal which do not appear after the second step of purification; DNA ladder: 100 bp.

Forward and reverse sequencing of positive fragments (Appendix B, Supplementary Table B2) provided on average fragments of 144 ± 15 bp (Archaeological Standard protocol) and 137 ± 3 bp (Phusion Blood High-Fidelity protocol); however, no one of the fragments provided a reliable match in BLAST for identification purposes.

Due to succesfull amplifications only limited to Op311 fragment, it was not possible to reconstitute a longer barcoding region.

Tab. 3.7 BLAST results of Roccapelago aDNA Op311 short-barcoding fragments.

number of puparia	DNA amplified with	fw/rv strand	size bp	BLAST query cover	BLAST E-value	BLAST max ID value	identified species
2	Archaeological standard protocol	fw	136	97%	3e-53	98.39%	<i>Paradelia</i> sp.
2		rv	127	97%	2e-50	95.49%	<i>Hyelemya</i> sp.
3		fw	159	98%	1e-52	98.39%	<i>Paradelia</i> sp.
3		rv	126	95%	2e-56	94.16%	<i>Hyelemya</i> sp.
5		fw	158	88%	4e-53	95.04%	<i>Hyelemya</i> sp.
5		rv	160	79%	3e-50	96.83%	<i>Paradelia</i> sp.
2	Phusion Blood High Fidelity	fw	140	97%	2e-46	93.38%	<i>Hyelemya</i> sp.
2		rv	134	93%	7e-55	99.20%	<i>Lasiomma</i> sp.
3		fw	139	94%	5e-52	96.21%	<i>Caisua testacea</i>
3		rv	141	93%	2e-51	96.24%	<i>Pegomya winthemi</i>
5		fw	132	97%	5e-56	98.45%	<i>Calliphora vomitoria</i>
5		rv	140	93%	2e-55	97.73%	<i>Calliphora vomitoria</i>
8		fw	133	97%	2e-56	98.46%	<i>Sarcophaga argyrostoma</i>
8		rv	134	96%	6e-56	98.46%	<i>Sarcophaga argyrostoma</i>

3.3 MOLECULAR ANALYSIS OF DIPTERA PUPARIA RECOVERED FROM CASTELSARDO MUMMIES

3.3.1 Results

NaOH treatment and morphological identification

The impurities forming an encrusted layer wrapping puparia surface were efficiently removed using a brush soaked in NaOH 10% solution. The mix of faint sand and other non-identifiable matter composing the environmental sediment was easily dissolved allowing to show the diagnostic characters used to identify the species. In Fig. 3.9 the comparison of whole puparia, posterior spiracles and anal plate of three specimens pre-treatment and after NaOH 10% treatment is shown.

The majority of the analysed specimens were identified as *Hydrotaea capensis*, while two specimens were identified as *Hydrotaea aenescens* (Wiedemann, 1830). Although these two species show a close similarity, the combination of the anal plate and the ventral spines on the 7th abdominal segment allows an accurate discrimination (Giordani et al., 2018a). In fact, the anal plate of *H. capensis* shows narrow and thin wings which reach the external border of the subanal papillae. The intersegmental spines are large and smoothly rounded and they are disposed in several packed lines. The external rows are smaller than the central (CSHYD 5 in Fig. 3.9, pupae in Fig. 3.10, and puparia in Fig. 3.11). *Hydrotaea aenescens* shows a spiculation pattern quite similar to *H. capensis*, however its anal plate has well-defined wings thicker than *H. capensis* but narrower than the median area and broadly rounded apically (CSHYD 9 and CSHYD 12 in Fig. 3.9).

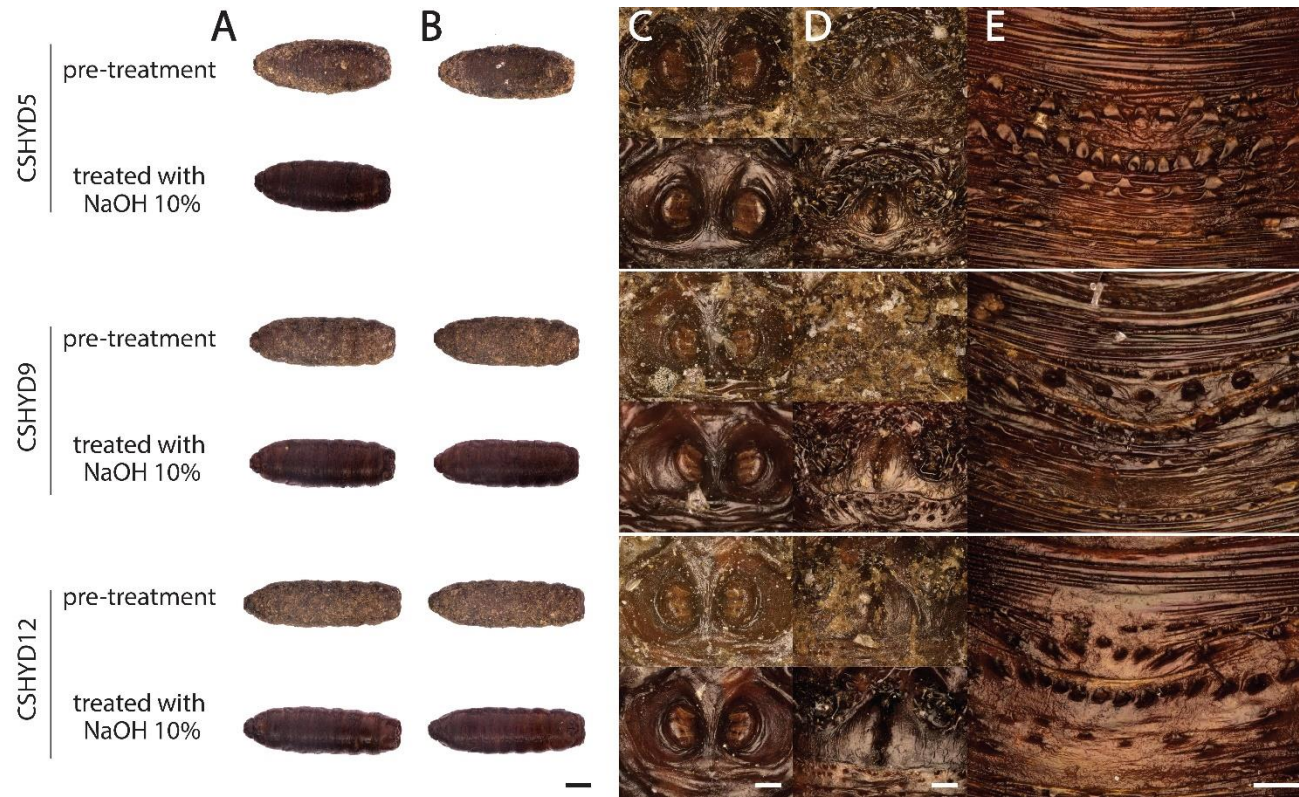


Fig. 3.9 NaOH 10% treatment effect on Castelsardo puparia. Three specimens (CSHYD5 *H. capensis*, CSHYD9 and CSHYD12 *H. aenescens*) are shown as example before and after the NaOH 10% treatment. (A) ventral, (B), dorsal view of the entire puparia; (C) posterior spiracles, (D) anal plate, (E) and ventral spines on the 7th abdominal segment. Scale bars: 1 mm (A,B), 100 μ m (C, D, E).

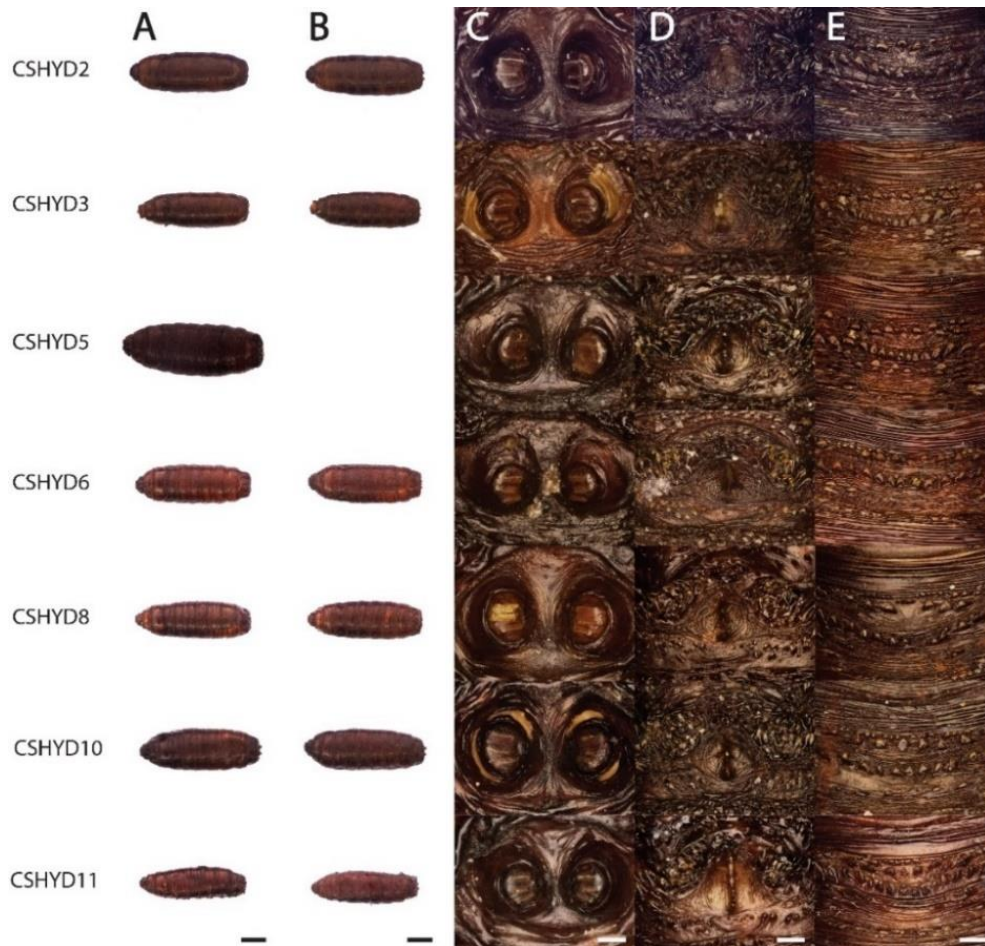


Fig. 3.10 *Hydrotaea capensis* closed puparia. Column (A) dorsal, column (B) ventral view of the whole specimens; column (C) posterior spiracles, column (D) anal plate, column (E) ventral spines on the 7th abdominal segment. Scale bars: 1 mm (A, B), 100 μ m (C, D, E).

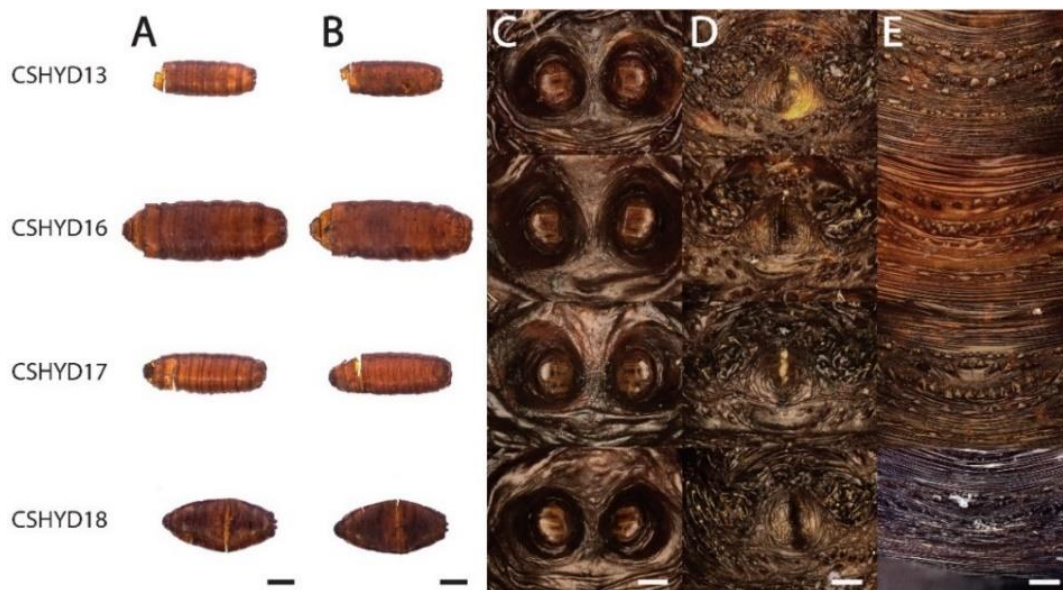


Fig. 3.11 *Hydrotaea capensis* open puparia. Column (A) dorsal, column (B) ventral view of the whole specimens; column (C) posterior spiracles, column (D) anal plate, column (E) ventral spines on the 7th abdominal segment. Scale bars: 1 mm (A, B), 100 µm (C, D, E).

Ancient DNA analysis

ROSE buffer extracts from Castelsardo puparia content appeared dark to light brown/yellow in colour, in both the control and archaeological samples, with a major intensity observed in the archaeological samples. The coloured phenotype of the extracts progressively decreased during the purification steps (Fig. 3.12).

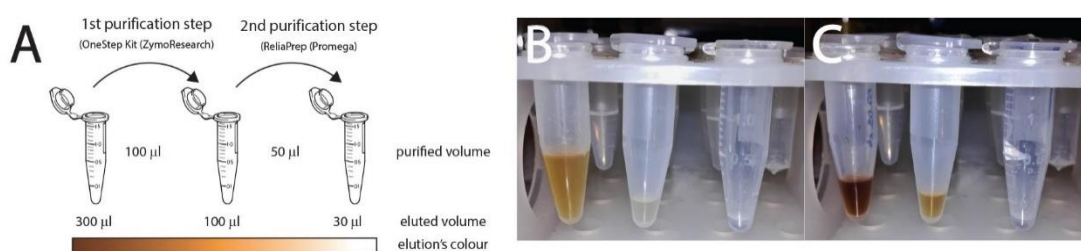


Fig. 3.12 Pigmentation status of Castelsardo extracts/eluates. (A) Schematic representation of the progressively discolouration of ROSE extracts; (B) control extracts from *C. vicina* pupae; (C) Castelsardo extracts from *H. capensis* pupae.

Total DNA was successfully extracted from both modern and archaeological samples previously treated with NaOH 10% solution. A progressive reduction in the total dsDNA concentration through the double-steps purification was observed (Tab. 3.8). Overall,

between the raw extracts and the double-purified eluates, an average DNA loss of the 60.27 ± 4.6 % and $>99.960 \pm 0.004$ % was calculated for control and archaeological samples, respectively.

Tab. 3.8 Qubit® 3.0 Fluorometer DNA quantification extracted from puparia pre-treated with NaOH 10%. Concentration values are expressed in $\text{ng}/\mu\text{l} \pm$ standard deviation (s.dv) calculated on three Qubit reads; A,B,C = triplicates; b.l.t.= below lowest threshold of the instrument ($0.01 \text{ ng}/\mu\text{l}$); percentages of DNA lost are calculated as ratio of concentration of purified eluates (2^{nd}) over concentration of ROSE buffer extracts; *values calculated assuming concentrations equal to $0.099 \text{ ng}/\mu\text{l}$ after the second purification step.

source	workflow step		[DNA] ($\text{ng}/\mu\text{l}$)	s.dv	average \pm s.dv
CTRL <i>C. vicina</i>	raw DNA extracts	A	27.06	0.25	22.52 \pm 3.60
		B	22.20	0.30	
		C	18.30	0.16	
	purified eluates (1^{st}) OneStep (ZymoResearch)	A	15.4	0.20	12.81 \pm 2.40
		B	13.4	0.30	
		C	9.65	0.16	
	purified eluates (2^{nd}) ReliaPrep (Promega)	A	10.6	0.12	9.0 \pm 1.90
		B	10.12	0.14	
		C	6.30	0.07	
	Lost (%)	A	60.83	4.57	60.27 \pm 4.60
		B	54.41	5.58	
		C	65.57	0.00	
Castelsardo <i>H. capensis</i>	raw DNA extracts	A	2.75	0.009	2.95 \pm 0.30
		B	2.71	0.07	
		C	3.40	0.12	
	purified eluates (1^{st}) OneStep (ZymoResearch)	A	0.83	0.04	1.05 \pm 0.20
		B	1.04	0.03	
		C	1.29	0.06	
	purified eluates (2^{nd}) ReliaPrep (Promega)	A	b.l.t.	n/a	< 0.01
		B	b.l.t.	n/a	
		C	b.l.t.	n/a	
	Lost (%)	A	99.96*	0.00	99.960 \pm 0.004
		B	99.96*	0.01	
		C	99.97*	0.00	

Differences observed in the concentrations between control and archaeological samples were statistically significant (2 ways ANOVA p -value $\ll 0.0001$), as well as values measured after the lysis and the purification steps ((2 ways ANOVA p -value: 0.0002).

Bioanalyzer traces shows a wide distribution of DNA sizes within the raw ROSE extracts, as indicated by the belt-shape of the fluorescent profiles which cover the full size range defined by the lower (35 bp) and the upper marker (10,380 bp) (Fig. 3.13). After the first step of purification, a similar pattern was observed and in two case out of three a slight increase in the fluorescent signal was detected. On the contrary, the double-purified eluates showed a drastic reduction in the fluorescent signal on the edge of null value, which is in accordance to the almost total depletion of dsDNA molecules measured with Qubit[®] (Tab. 3.8). The gel lane also illustrates the initial wide fragmentation of total DNA, as well as it confirms the depletion of dsDNA fragments at the final step of the workflow) (Fig. 3.13).

Absorbance spectra of the raw extracts and of the eluates obtained after the first purification step showed a remarked peak slightly shifted to 240 nm for all the samples, control and archaeological. In addition, a less defined peak at ~280/290 nm was observed in the control extracts. Fig. 3.14 reports only selected examples as in all the cases a very similar profile was obtained, demonstrating consistency among the replicates. The second purification step provided a pure acid nucleic curve in the control sample, whereas a null absorbance profile was observed for the archaeological sample.

Non-purified DNA preparations showed absorbance ratios $A_{260}/_{230}$ and $A_{260}/_{280}$ values between 1.8-1.0 and 1.5-1.6 for control and archaeological samples, respectively (Appendix A, Supplementary Table A4). These values progressively increased over the purification procedures until reaching optimal values very close to 2.0 in the double-treated control eluates, in accordance with the spectrum showed in Fig. 3.14. Similar values were also recorded for the archaeological double-treated eluates. On the contrary, $A_{260}/_{230}$ ratios are constant and far from the optimal value established by the manufacturers (2.0-2.2), denoting a persisting presence of compounds absorbing at 230 nm (Appendix A, Supplementary Table A4).

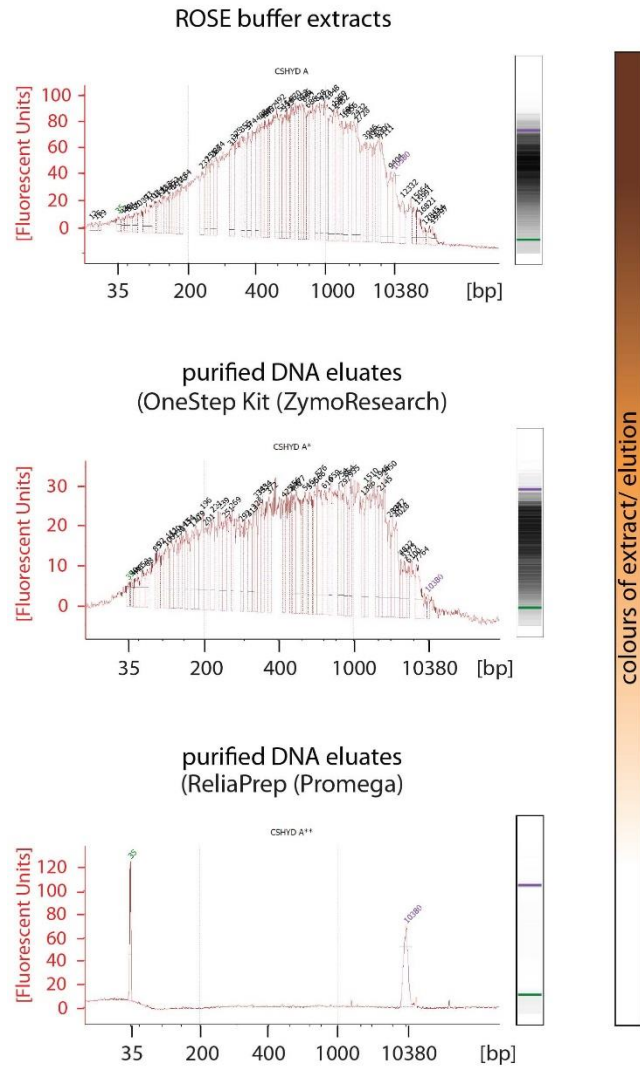


Fig. 3.13 Agilent 2100 Bioanalyzer High Sensitivity Assay of Castelsardo extracts. One out of three replicate only is shown as all the samples share a very similar pattern. The colour blending legend next to the graphs is aimed at helping the reader to associated the fragment assay to the macroscopic “phenotype” of the DNA extract/elution at each step of the workflow

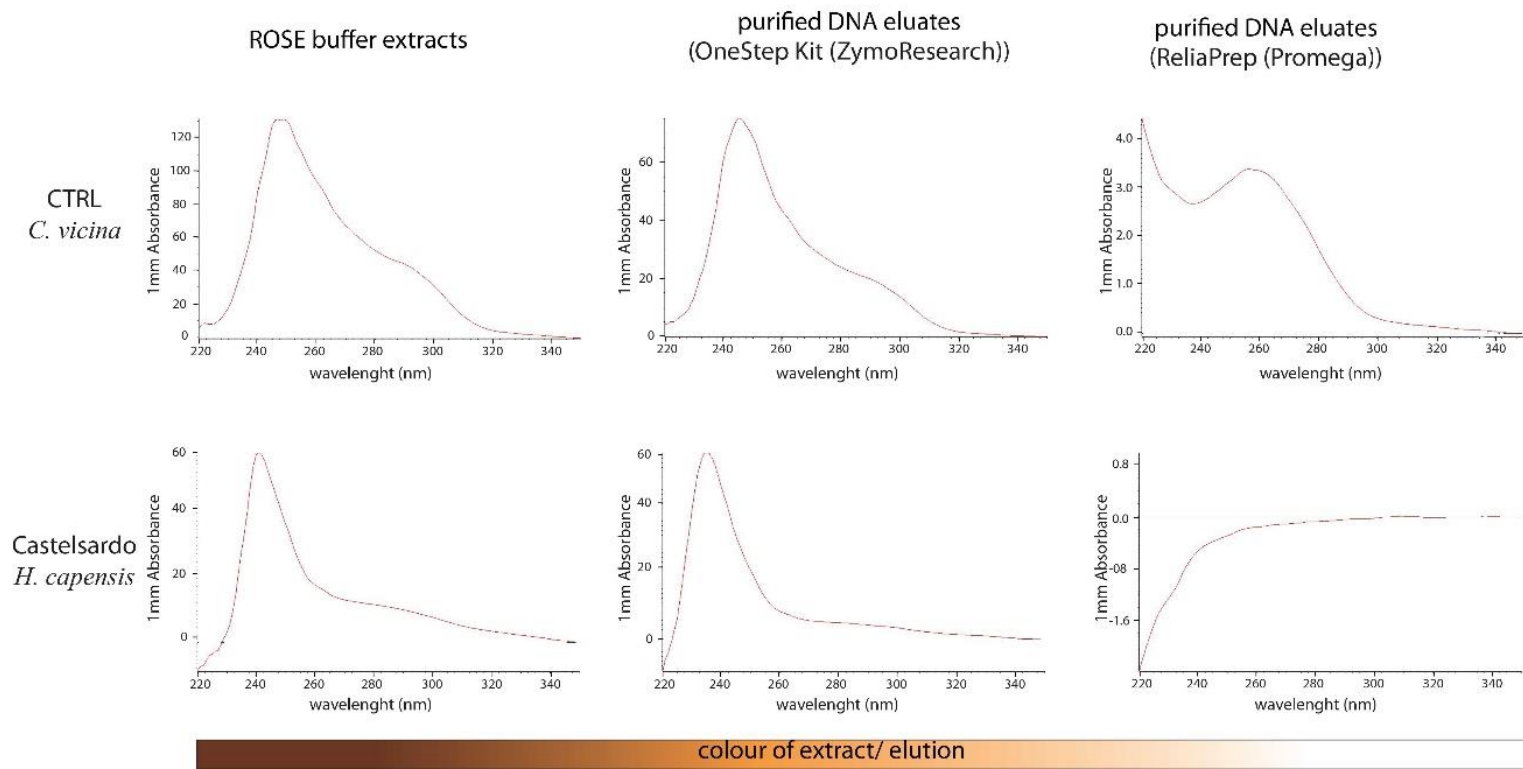


Fig. 3.14 NanoDrop Abs spectra. One example per sample (control and archaeological) is reported. As in Fig. 3.13, the colour blending legend below the graphs is aimed at facilitating the reader to associate the purity assay to the macroscopic “phenotype” of the DNA extract/elution at each step of the workflow.

PCRs targeting short-barcoding fragments using primer pair Op311 failed in all the cases except when double-purified DNA extracted from the modern control samples was used as template in the reaction (Fig. 3.15).

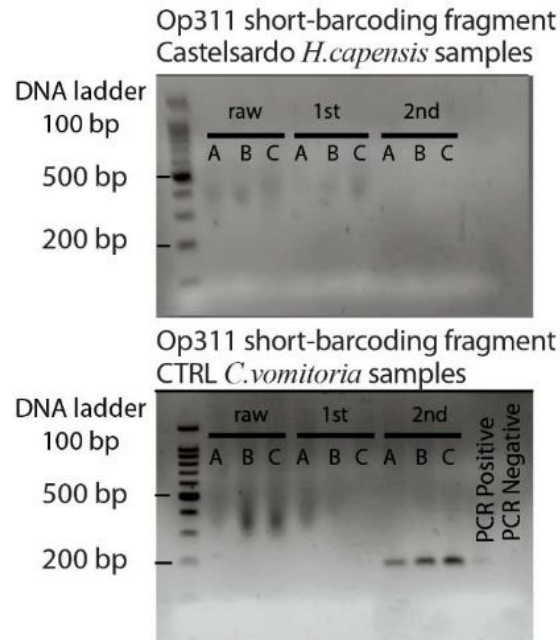


Fig. 3.15 Gel electrophoresis of PCR products from Platinum™ HotStart protocol. Amplification of DNA Op311 short-barcoding fragments using Platinum™ Hot Start (Invitrogen™, Carlsbad, California, USA) is shown for Castelsardo (above) and control (below) samples. Three reactions (A,B,C) were run in parallel using 2 puparia as initial substratum for DNA extraction; raw= non purified lysates, 1st= DNA eluates subjected to the first purification step, 2nd= DNA eluates subjected to the 2nd purification step. Reaction was positive for double-purified control templates only. DNA ladder: 100 bp.

3.4 DISCUSSIONS

Up to date, there is a lack of knowledge about molecular investigations applied on Diptera puparia recovered from archaeological contexts, as well as there are no information on the topic concerning Diptera remains retrieved from human remains in funerary contexts found (Huchet, 1996). Likely, the relative recent development of funerary archaeoentomological studies (Huchet, 1996) and a common recalcitrance in applying genetic analysis on archaeoentomological remains can explain the lack of research in this field. Rather, the evaluation of diagnostic features to identify the species is still the most applied method which, however, requires the treatment of the specimens to restore their original appearance and expertise in taxonomy. In this study, the use of NaOH 10% solution was key to remove depositional impurities from puparia surface collected from Castelsardo crypts, keeping the integrity of the specimens, and allowing an accurate species of identification of the specimens as *H.capensis/H.aenescens*. In order to explore the feasibility of genetic analysis in archaeoentomological studies as a tool to rapidly identify the species regardless their state of conservation (King et al., 2009), an *ex-novo* workflow was applied on ancient puparia, as no guidelines were available.

The applied workflow including the use of homemade buffer (Oshaghi et al. 2006) in combination with a column-based purification procedure showed to be suitable to retrieve DNA from archaeological puparia, although Qubit concentrations were as little as shown in (Tab. 3.4 and Tab. 3.8), and often showed undetectable value (< 0.01 ng/ μ l), which is in accordance with the low amount of tissues used as source of extraction. DNA preparations contained highly fragmented dsDNA (Fig. 3.13), in line with the expectations when working with aDNA (Hofreiter et al., 2001). The phenotype of the extracts clearly indicate that during the initial lysis performed at high temperature causes the release of hydro soluble cuticular pigments which gave the extracts a brownish-yellowish dark colouration (Sugumaran, 2009). As in all the cases the specimens were subjected to a washing step using warm-hot water (40–60 °C) or NaOH 10% solution, we can exclude that these pigments derive from the external environment, rather we are led to think that are endogenous organic compound likely identifiable as melanin. This phenomenon, first described in paragraph 3.1 on modern

specimens, was observed on archaeological puparia, either open (Roccapelago) or closed (Castelsardo), demonstrating that both the pupal cage and the metamorphic flies are source of such melanin molecules responsible for the pigmentation. As the extracts of specimens used as modern controls had the same phenotype, we are led to think that pigmentation is strictly linked to an innate feature of the flies, regardless the chronological age. As stated in paragraph 3.1.2, melanin is a well-known polyphenolic compound and a tinted DNA extract was suggested to be a potential source of PCR inhibitors (Kemp et al., 2006) which are often co-extracted with aDNA (Fulton and Stiller, 2012). Due to the lack of data about cuticular pigments, it was not possible to fully characterize these compounds, which, however, have been detected as impurities by NandoDrop measurements. The double purification procedure overall shows the following changes in DNA preparations: its application led to transparent DNA solutions (Fig. 3.6, Fig. 3.12), contaminants-free elution volumes at least based on A260/280 ratios (Fig. 3.7, Fig. 3.14, Appendix A, Supplementary Table A3, A4), a drastic reduction of dsDNA content as shown by the loss % values in Tab. 3.4 and Tab. 3.8; the latter is likely associated to the depletion of dsDNA short fragments within ancient DNA extracts (Fig. 3.13) kept by filtered columns used during the purification procedures, as per results obtained with modern specimens in paragraph 3.1. Overall, the appreciation of the efficiency of the purification system correlates with the initial DNA concentrations, as evident by differences outlined between modern and control samples as well as between empty puparia and puparia content (Fig. 3.16). The choice of applying purification systems was obliged as the original use of the ROSE buffer includes serial dilutions with DNA-free water, as common technique to circumvent inhibitors (Kemp et al., 2006). Considering the relative low DNA concentrations obtained from archaeological puparia (Tab. 3.1, Tab. 3.8) the “dilution technique” was avoided and replaced by the use of filtering columns developed for efficiently removing polyphenolic compounds, humic/fulvic acids, tannins, and melanins from most impure DNA preparations as in the case of Roccapelago and Castelsardo samples.

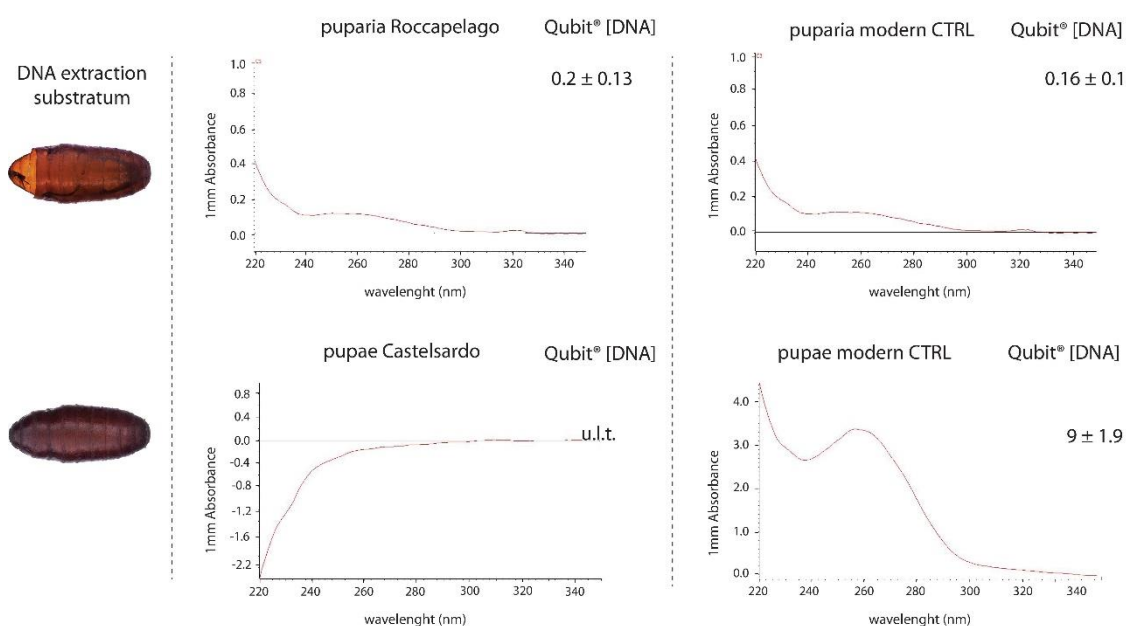


Fig. 3.16 Comparison between double purified Abs spectra. DNA concentration of the eluates is reported to show the correlation with the spectra resolutions.

Obtaining purified aDNA solutions, although in very little amount, was key to successful PCRs (Tab. 3.6), at least as far as Roccapelago samples concern. As the templates used were the same in all protocols, and the same amount of puparia was processed, differences in the components of the PCR protocols likely played a crucial role in the success or failure of the amplifications. The use of 1% PVP in the standard archaeological protocol could have played a role in forming complexes with polyphenolic compounds often co-extracted with the nucleic acids and that are well known inhibitors of DNA amplification (Rogers and Bendich, 1985); PVP contained in the extraction buffer contains could have strengthened to this beneficial role. Moreover, increasing the number of units of *Taq* polymerase ($0.06 \text{ U}/\mu\text{l}$) may have counterbalanced the effect of inhibitors which normally inactivate the polymerase (Kemp et al., 2006). For similar reasons, a lower concentration of *Taq* ($0.02 \text{ U}/\mu\text{l}$), as well as the manual addition of dNTPS and a lower $[\text{Mg}^{2+}]$, could have been the cause of the failure of the Phusion Hot Start. On the other hand, doubling the initial DNA quantity and increasing the number of cycles could have been crucial to the success of the Phusion Blood Hot Start High-Fidelity (HF) in comparison to its standard counterpart Finally, it is worth to mentioning that the dilution-concentration strategy (Kemp et al., 2006) adopted for double-

purified extracts deriving from eight puparia improved the success of the amplification (Tab. 3.6). Other considerations can be made to explain the failure of the other amplification reactions, both concerning Roccapelago and Castelsardo samples. First of all, it is worth to remind that each substratum was unique, although the same number of puparia was used and specimens were from the same environment. Furthermore, the use of a fluorometric method to quantify dsDNA within archaeological extracts doesn't allow to distinguish whether the detected DNA is from the host or exogenous, and, in case of mixtures, it's not possible to know the relative proportions, therefore resulting in an a-specific method (Handt et al., 1994). Additionally, either the selected primer pair (Op311) might have failed to anneal to the designated region due to breaks in the double strand, or DNA was undetectable during the PCR due to biochemical modifications including cross-linkage to itself or other molecules, modifications of nitrogenous bases (e.g. oxidation, deamination, depurination) which ultimately could have contributed to destabilise the backbone of DNA molecules (Hofreiter et al., 2001, Reiss, 2006, Handt et al., 1994) and further caused breaks in it. The degradative effect caused by the use of NaOH 10% as cleaning solution for Castelsardo specimens is excluded as, unlike RNA, DNA is not prone to alkaline hydrolysis due to the missing hydroxylic group in 2' of the ribose if not at higher concentration of NaOH (1 N) at 100 °C (Hurst, 1956). Overall, PCR negative controls lacking of any amplification product demonstrated that reactions were undertaken in a clean environment and contamination didn't occur, in compliance with one of the authenticity criteria of aDNA sequences (Austin et al., 1997a, Austin et al., 1997b, Hofreiter et al., 2001, Reiss, 2006). The use of positive controls, although modern, was key to interpret the effect of PCR inhibitors in the non-purified extracts, as evident in Castelsardo samples. Unfortunately, since the success of PCR and sequencing was limited to fragments amplified with Op311 primers only, the reconstitution of a longer barcoding sequences long enough to allow to use the molecular data for identification purposes was not possible, and no one of the single fragments resulted in a reliable identification (Tab. 3.7).

Further considerations about ancient DNA survival can be made in light of the environment where Diptera remains have been found, as it has been speculated that it is a key parameter

with a greater impact than the age of the specimen (Austin et al., 1997b). All the specimens studied in this work were collected in association to partially mummified human remains that, *illo tempore*, were actively decomposing. As described in Chapter 1, paragraph 1.3.1, decomposition process is started by the microbial communities residing in/on the corpses as well as in the surrounding environment (Benbow et al., 2015). The microbial activity, in turn, is strictly associated to the water content which is initially released upon the cellular autolysis. The higher the water content, the faster the microorganism growth is, and the higher the degradation of macromolecules by microbial enzymes, including the digestion nucleic acids by exogenous nucleases activity (Hofreiter et al., 2001, Reiss, 2006). In the burial sites of Roccapelago and Castelsardo, multiple depositions have been documented, and the finding of mummified bodies proved that the microbial growth was slow down and arrested. These circumstances therefore suggest that the same environmental conditions that provided the preservation of the human tissues, contributed as well to the preservation of Diptera remains and to the survival of their genetic material.

It is worth considering that the limited number of puparia showing specific features of integrity and preservation represented a big limit to the research. As far as Roccapelago analysis concern, it was hard to find replicates of 2-3-5-8 puparia of the same species (*C. vicina*), morphologically well-preserved to verify the belonging to the same species, and still containing the *exuviae* essential to improve the success of the DNA characterisation. Rather, a unique batch was selected to improve the success of the molecular analysis based on the number of analysed specimens. On the other hand, as far as Castelsardo analysis concern, it was even harder finding higher number of replicates of puparia still containing the insect in metamorphosis as, *per se*, it is already a rare finding within an archaeological insect remain assemblage. Therefore, analysis conducted on these two archaeological sites well address the issue of reproducibility, defined as the most important authentication criterion to be in compliance with in molecular archaeology (Paabo et al., 1989): “*amplified sequences should be consistently and reproducibly obtained from the same extracts from any one specimen and from different specimens of the same species*” (Austin et al. 1997). This criterion was not met as specimens from which nucleic acids were isolated were unique, and therefore the experiment

could not be repeated neither by the first investigator, nor by other research groups (Handt et al., 1994).

3.5 CONCLUSIONS

The molecular analyses conducted on Diptera puparia found in association to human remains retrieved from the Italian archaeological sites of Roccapelago and Castelsardo provide new insights of DNA characterisation from ancient puparia and paint the first framework around this extremely challenging field of research:

- The combination of Rapid One Step Extraction (ROSE) DNA buffer by Oshaghi (2006) combined with two consecutive purification systems including OneStep PCR removal kit (Zymo Research, Irvine, California, USA), and ReliaPrep DNA purification and concentration system (Promega, Madison, Wisconsin, USA) revealed to be an efficient *ex-novo* workflow to isolate pure DNA from ancient Diptera remains.
- Due to the low quantities and the highly fragmented nature of aDNA, whether possible, increasing the amount of the initial substratum of the extraction is recommended to improve the final yield and the use of primers targeting short DNA sequences (<200 bp) is encouraged.
- Environmental storage conditions of ancient remains has to be carefully considered as they play a key role in the survival of genetic material
- PVP 1%, *Taq* polymerase concentration >0.02 U/ μ l, and Mg^{2+} concentration > 3 mM revealed to play a crucial role in the optimisation of PCR protocol, however, further investigations are needed as template, quality and level of inhibition are unique to each extract.

The single DNA fragment successfully sequenced is certainly a piece of new in this field of research; however, the chance to define a standard procedure of the analysis is still very far to be concrete, mainly due to the impossibility to predict with enough rigour the nature and the number of factors affecting DNA extractability and its downstream characterisation. Further research needs to be done prior to allege that genotyping can be a reliable tool of species identification in archaeoentomology.

4

TAPHONOMIC PROCESSES INVOLVED IN THE
PRESERVATION OF ARCHAEOZOOLOGICAL
ASSEMBLAGES AND THEIR IMPACT ON DNA
ANALYSIS

4.1 MINERALISATION OF DIPTERA PUPARIA RECOVERED FROM A MEDIEVAL URBAN WELL IN VIA SEBASTIANO SATTA, SASSARI (SARDINIA, ITALY)

4.1.1 Results

Taxa description

Morphological analysis of the entomological remains revealed the presence of three main Diptera families identified as Fanniidae, Muscidae and Sphaeroceridae. Identified species and genera are reported in Tab. 4.1.

Tab. 4.1 Identified taxa. *number are reported as an estimation.

family	fragments counts*	identified species/genera
Fanniidae	~ 300	<i>Fannia</i> Robineau-Desvoidy 1830 <i>Musca domestica</i> Linnaeus, 1758
Muscidae	> 500	<i>Stomoxys calcitrans</i> Linnaeus, 1758 <i>Muscina prolapsa</i> (Harris, 1780) <i>Muscina stabulans</i> (Fallén, 1817) <i>Lispe</i> Latreille, 1796
Sphaeroceridae	> 10,000	<i>Thoracochaeta zosteræ</i> Haliday, 1833 <i>Thoracochaeta</i> Kuznetzova, 1986

Fanniidae

Fanniidae, a small family in the superfamily Muscoidea with over 360 described species, are found predominantly in temperate areas, with the majority of the species occurring in the Holarctic, although there are a considerable number of Neotropical species. However, the family overall, has a worldwide distribution (Domínguez and Pont, 2014). Larvae of Fanniidae flies are the most easily recognisable of any family of the so-called higher Diptera (Chapter 1, paragraph 1.1), and their main morphological features are conserved in puparia, *e.g.*: body with an evident segmentation and elongated dorso-lateral processes (Fig. 4.1). Within the whole Diptera assemblage excavated from the well, Fanniidae represent the least abundant taxon counting more than 300 specimens and were exclusively collected from the S.U.19336. Despite the peculiar state of preservation, the residuals of conspicuous feathery, forked, tufted, or button-like segmental processes which characterise most of the dorsal body surface were still recognisable (Domínguez

and Pont, 2014) (Fig. 4.1). Based on this morphological datum, the genus *Fannia* was identified, however, no reliable species identification could be asserted due to the loss of the other fundamental features such as anterior and posterior spiracles.

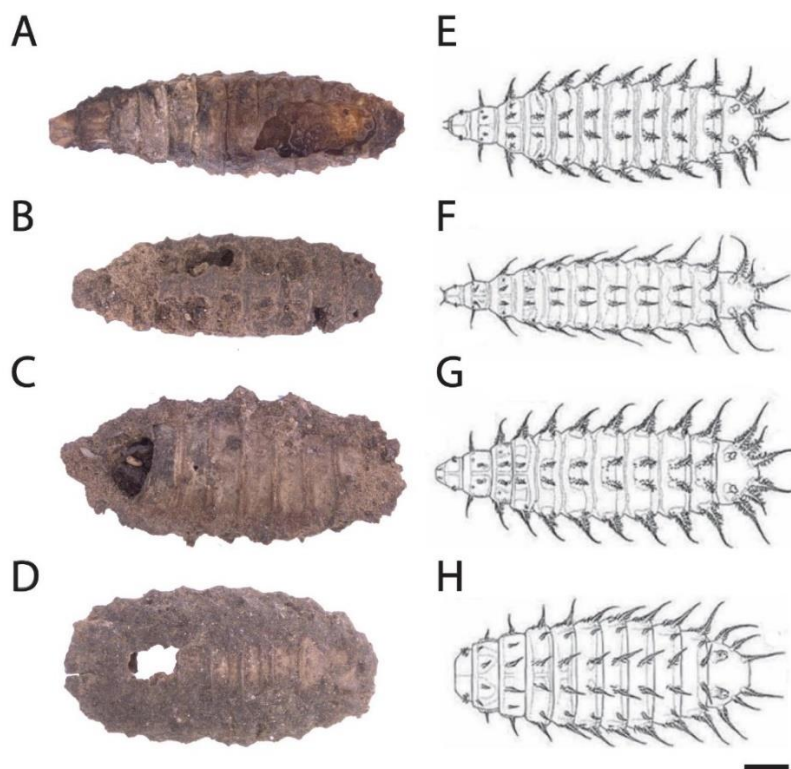


Fig. 4.1 Fanniidae puparia. (A-D) Puparia from this study showing a remarked segmentation and truncated lateral processes; (E-H) examples of Fanniidae larvae described in Dominiguez and Pont (2014): (E) *Fannia albitarsis* Stein, 1911, (F) *Fannia canicularis*, Linnaeus, 1758, (G) *Fannia mercurialis* Dominiguez and Pont, 2014, (H) *Zealandofannia mystacina* Dominiguez and Pont, 2014.

Muscidae

Muscidae is a large worldwide family of calyptrate Diptera numbering 5,200 known species (Marshall, 2012). The majority of the species are sarcophagus or facultative predators, and only a few are phytophagous or parasitic of other invertebrates. The puparia of these flies are easily recognisable by their “barrel-shape” and the posterior spiracles are a discriminating character for many species (Skidmore, 1985). Within the assemblage collected from S.U. 19336, the smallest fraction was represented by the “stable fly” *S. calcitrans* (Fig. 4.2 A,D,G) and the “house-fly” *M. domestica* (Fig. 4.2 B,E,H) counting approximately a few tens of specimens. The largest fraction was composed of

species within the genus *Muscina*, either the “false-stable fly” *M. prolapsa* or the “stable fly” *M. stabulans* (Fig. 4.2 C,F,I). Scarce information is available on the morphology of the puparium of these two species which appear very similar (Skidmore, 1985), preventing to accurately discriminate them.

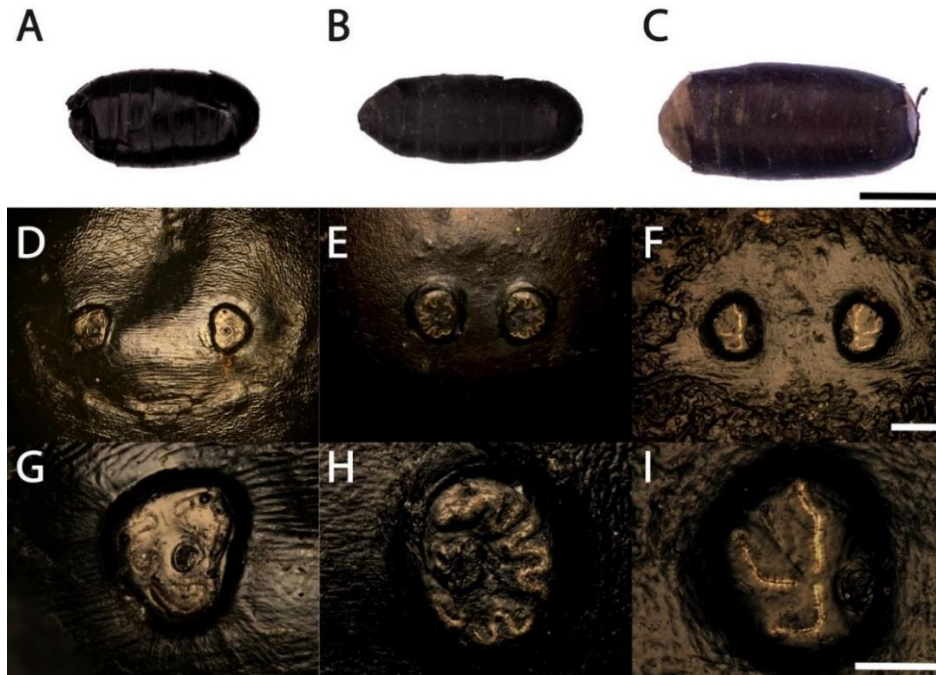


Fig. 4.2 Details of Muscidae puparia. (A) *Stomoxys calcitrans* puparium dorsal view and (D,G) posterior spiracles; (B) *M. domestica* puparium dorsal view and (E,H) posterior spiracles; (C) *M. prolapsa* puparium ventral view and (F,I) posterior spiracles. Scale bars: puparium 1 mm, posterior spiracles 100 μm , single posterior spiracle 50 μm .

In addition, a unique specimen shown in Fig. 4.3 was found. The shape and the size of the puparium (Fig. 4.3 A,B) and the shape of the anal plate with the basal tapered arms (Fig. 4.3 C) led to identify it as belonging to *Hydrotaea* genus (Giordani et al., 2018a). However, the orientation of the posterior spiracle slits (Fig. 4.3 F) does not match with any of the described *Hydrotaea* species, rather they show a close similarity with the genus *Lispe* (Skidmore, 1985). Due to the poor state of preservation of the posterior spiracles which also collapsed during the preparation of the specimen, and due to the lack of intact anterior spiracles, the identification of this specimen cannot be confirmed.

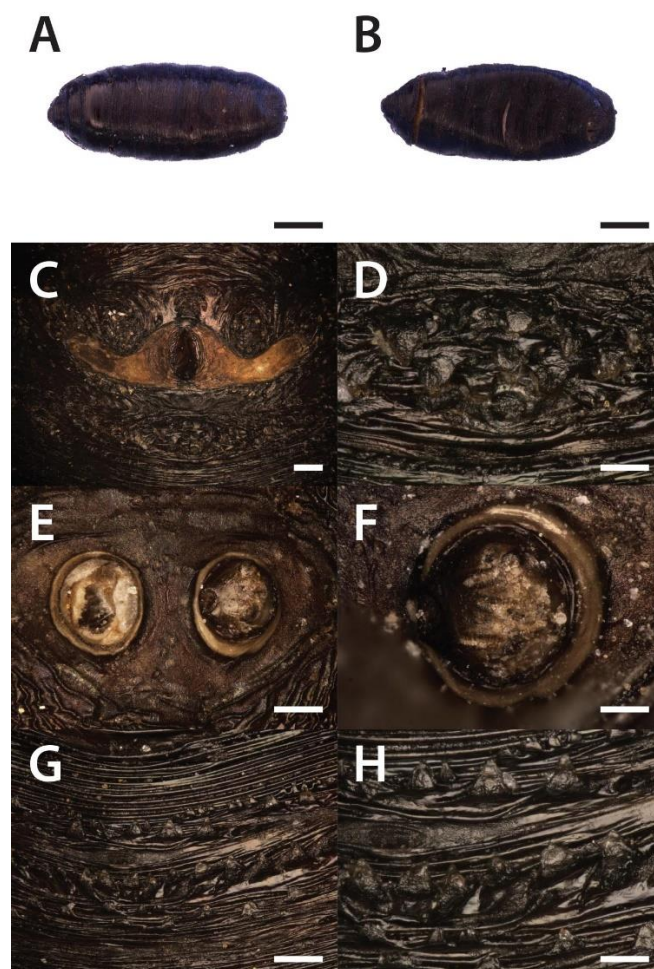


Fig. 4.3 Unique specimens of *Lispe* sp. A,B) puparium dorsal and ventral view; (C,D) anal plate and a spot of spines beneath it; (E,F) posterior spiracles; (G,H) spines belt on the 7th abdominal ventral segment. Scale bars: 1 mm (A,B), 100 μ m (C,E,G), 50 μ m (D,F,H).

Sphaeroceridae

Sphaeroceridae are small acalyptrate flies with 1,550 known species, distributed worldwide (Marshall et al., 2011). Marshall points out that these little, dull-coloured flies are deserving the term “ubiquitous” as they literally can be found “in all reasonably humid terrestrial environments” (Marshall, 2012). The adults of many species are frequently found in association with the excrement of various mammals especially cattle, horses and sheep that have earned for this family the common name of “dung flies” (Tenorio, 1968). However, different species have diverse habitat preferences and breed on different kinds of decaying organic matter (Pitkin, 1988). As estimation, more than 10,000 of Sphaeroceridae puparia were recovered from the S.U. 19335 and S.U.19336 representing

Chapter 4

87% of the entire dipterological assemblage. The proportion of the abundance of this taxon remarkably increased following the collection performed *in loco* by the author of this thesis at the end of 2018. The presence of thousands of Sphaeroceridae puparia could be macroscopically observed as a dark-brown spots fluctuating within the sand sediments while the material was sieved (Fig. 4.4). Their light weight allowed an easy recovery as the assemblage tended to be deposited on the surface of the sediment. Sphaeroceridae puparia usually have an elongated cylindrical structure, tapering at either end and flattened at the anterior end (Pitkin, 1988). In some species, as in the one recorded from the Sardinian cesspit, the posterior spiracles protrude in a fork shape. Two pools of puparia were collected at different depth from the pit and found differently preserved: the mineralised fraction was recovered from the S.U.19335 composed of dry sediment (Fig. 4.5A), while the waterlogged fraction, representing the most abundant, was recovered from S.U.19336, 9 m underground (Fig. 4.5B).



Fig. 4.4 Sphaeroceridae puparia sieved *in loco*. Hundreds of specimens were collected from each sieved batch of sediment.

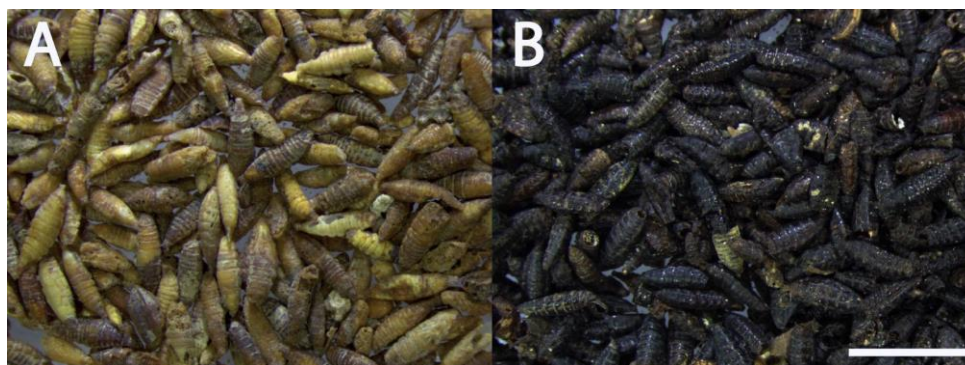


Fig. 4.5 Form of preservation of Sphaeroceridae puparia. (A) Mineralised, (B) waterlogged specimens collected from S.U. 19335 and S.U.19336, respectively. Scale bar: 5 mm.

Detailed morphological studies were only conducted on the waterlogged puparia as the morphological features used for the identification were lost in the others due the transformation into mineral fossils. The comparison with the few available literature information (Okely, 1974, Pitkin, 1988) and with modern *T. zosteriae* puparia collected by Adrian Pont in 1978 on seashore in Whitesand Bay, South West Cornwall (50.082° N 5.699° W), now part of the Natural History Museum collection, allowed to identify the majority of the puparia as belonging to this species. The pictorial archive shows the compared study conducted by observing the anal plate, the posterior spiracles, the anterior spiracles (Fig. 4.6) of modern museum specimens (Fig. 4.6 A-C) and archaeological ones (Fig. 4.6D-H).

Unlike other species (*e.g. Hydrotaea* sp.), the anal plate of the studied Sphaeroceridae did not provide any useful discriminatory feature. In fact, this character was damaged in the archaeological puparia as well as the anterior spiracles which, also, in many cases were missing (Fig. 4.6F-H). On the contrary, the analysis of posterior spiracles revealed a clear orientation of the respiratory slits: in the majority of the cases, the median slit is perpendicular to the superior and inferior, while in one case all the slits show a parallel/semi-radial orientation (Fig. 4.6H). A better resolution of anterior and posterior spiracles of archaeological specimens was enlightened by SEM which allowed to identify at least two species within the Sphaeroceridae assemblage (Fig. 4.7). However, due to the scarce information of puparia belonging to this poorly studied family, the identification of the second morphotype was not confirmed.

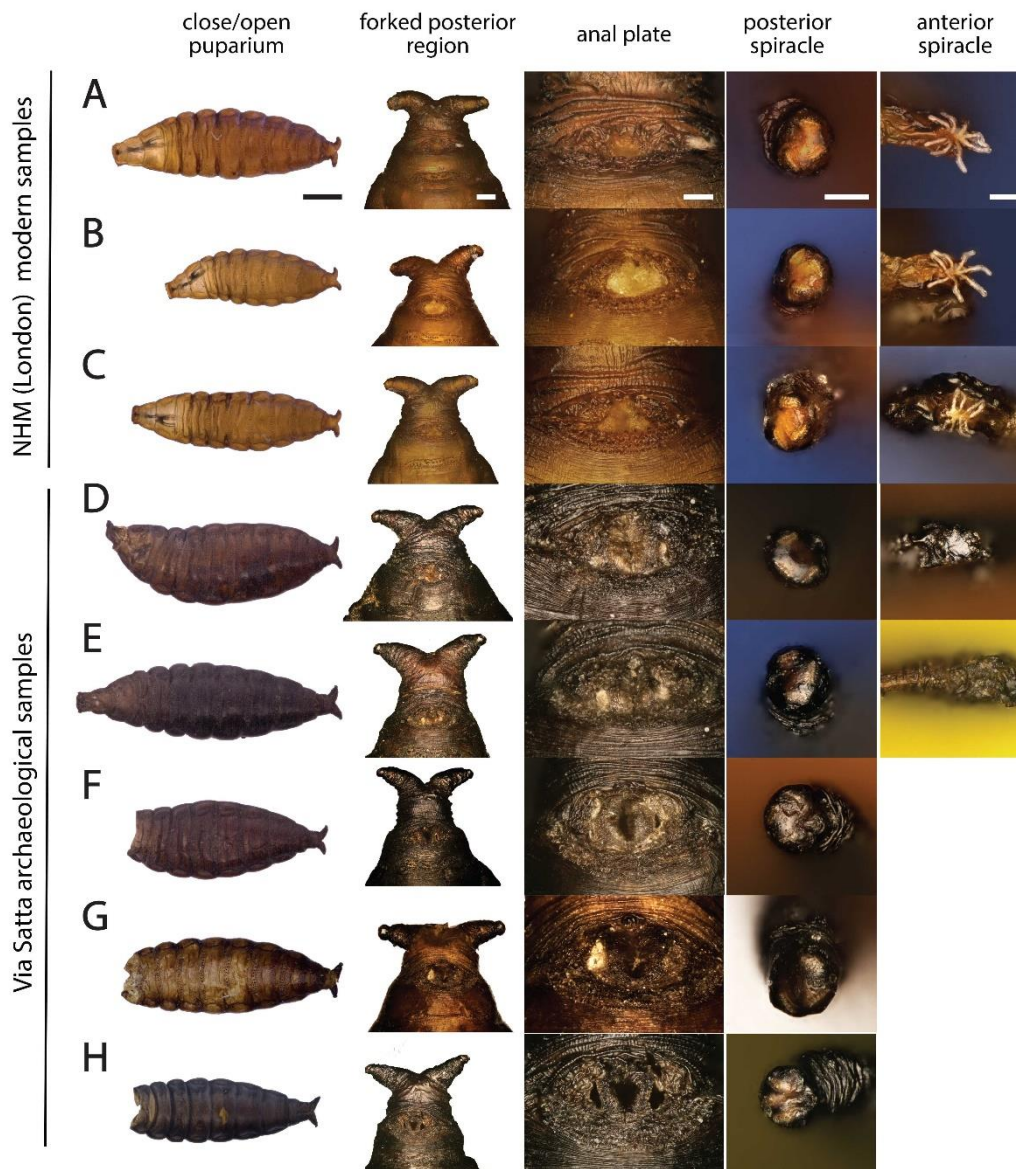


Fig. 4.6 Morphological comparison between modern and Via Satta Sphaeroceridae puparia. (A-C) *T. zosteræ* puparia from the collection of Natural History Museum, London; (D-H) Sphaeroceridae puparia from this study. Scale bars: 500 μm for the entire puparium, 100 μm for the forked posterior region, 50 μm for the anal plate, the posterior and anterior spiracle. The latter are missing in open puparia (F,G,H).

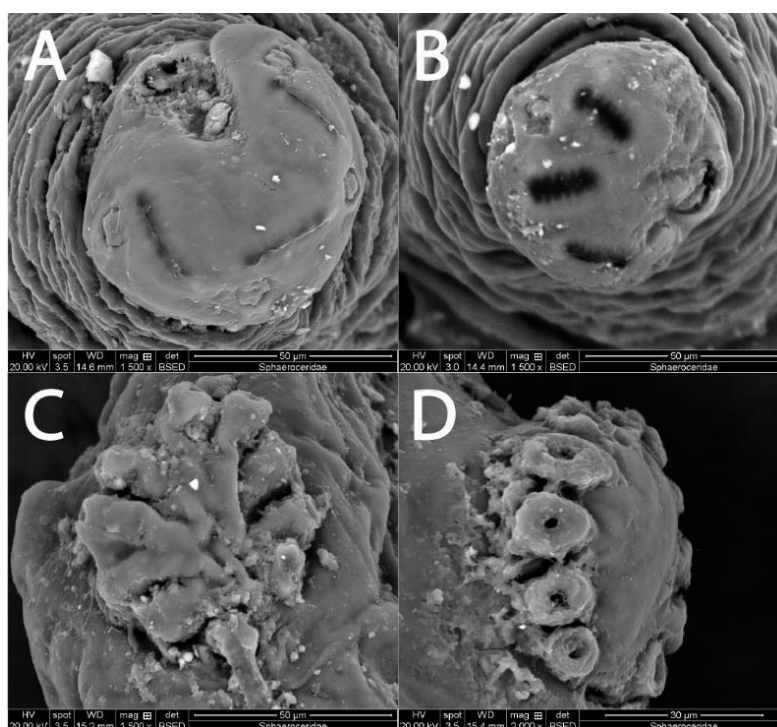


Fig. 4.7 SEM images of Sphaeroceridae puparia details. (A,B) Posterior spiracles showing a different orientation of the respiratory slits; (C,D) anterior spiracles showing a different numbers of the lateral processes and diverse basal structure. Scale bar: 50 μ m.

The morphology of the spines belt on the 7th, 6th, and 5th abdominal ventral segments (Fig. 4.8) were also analysed. On the 6th segment, a high level of similarity was observed among the specimens showing a pattern composed of big bottom-like spines in a central row framed by two smaller thick rows. One single row or multiple continuous rows (up to three) of narrow spines form the edge of the frame on the superior (towards the anal region) and on the inferior side, respectively. The same arrangement was observed for the spines on the 5th abdominal segment with the only difference that in addition to the three continuous rows of narrow spines, a shorter central row is present below (Fig. 4.8). On the contrary, the 7th abdominal segment showed a more peculiar arrangement of loop-like of tapered spines. In some specimens, two larger round shape spines were present, close to the edge (Fig. 4.8D-F) or at the centre of each buttonhole of the loop (Fig. 4.8H). In addition, a central row of smaller spines forming a sort of bridge between the two buttonholes of the loop can be present (Fig. 4.8E,F), or the loop can appear flattened (Fig. 4.8D,H). The described differences noticed at the level of the spines are in

accordance with the other differences observed in terms of size and posterior spiracles of the specimens (Fig. 4.7) indicating, overall, a co-presence of at least two species of Sphaeroceridae.

Pharate adults showing a great conservation of the thoracic dorsal spines (Fig. 4.9A) were compared with the following modern adult specimens belonging to the subfamily Limosiniinae provided by the collection of the Natural History Museum in London: *Thoracochaeta zosterae*, *Thoracochaeta brachystoma* (Stenhammar, 1855), *Thoracochaeta seticosta* (Spuler, 1925), and *Leptocera caeonsa* (Róndani, 1880) (Fig. 4.9B-E). Five pairs of thoracic bristles, of which two pairs closest to the edge of the *scutellum*, were identified to investigate any potential conserved pattern at least genus specific. Each bristle was marked as a spot colour-coded per species. The same number of bristles were identified also on the thoracic surface of the mineralised pharate adult (Fig. 4.9A). The results of the inter-specific overlapping allowed to exclude a match with *L. caeonsa* as this is the species having the most different pattern and also showing one extra pair of bristles (Fig. 4.9E). The other three *Thoracochaeta* species show a very similar pattern (Fig. 4.9B-D) which did not allow to propose any reliable identification further than at genus level.

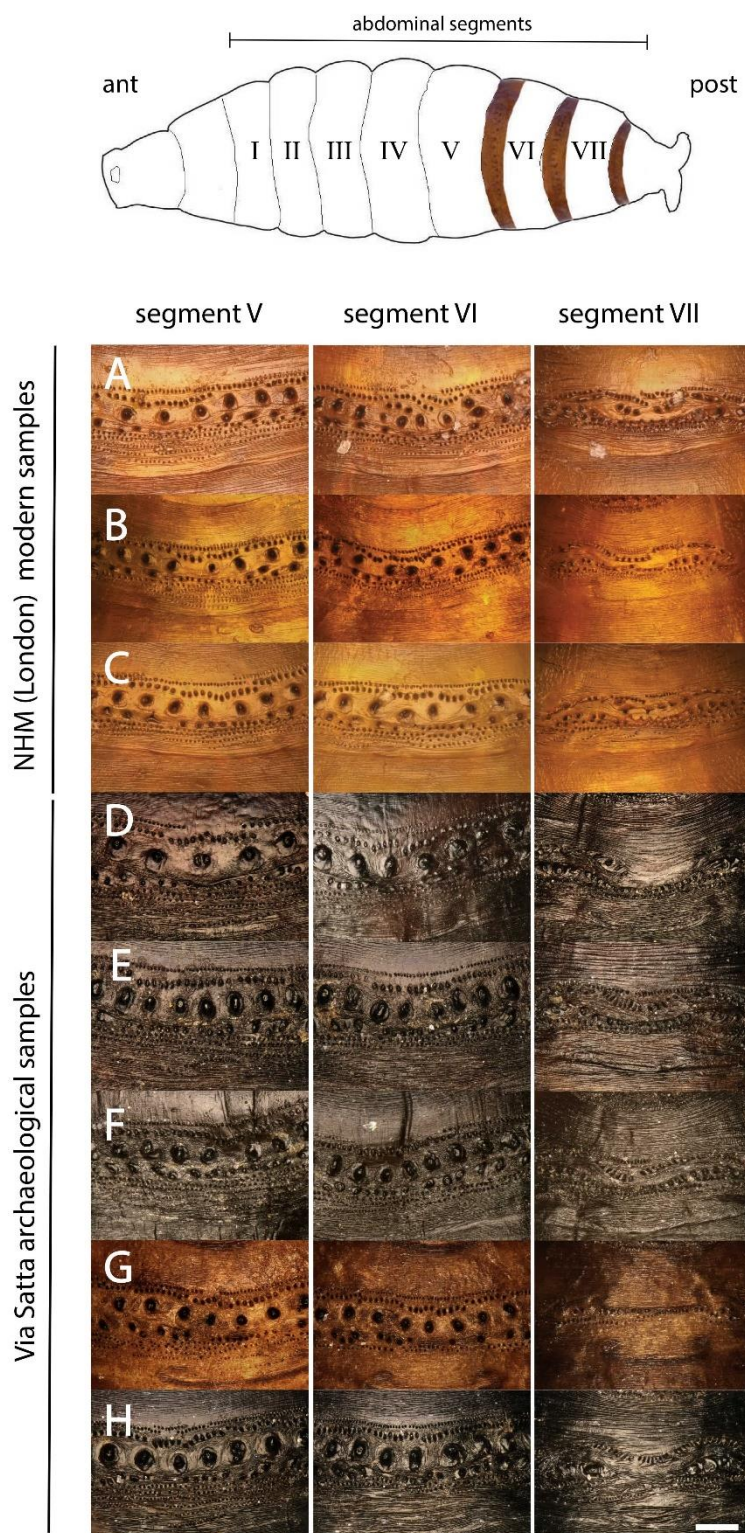


Fig. 4.8 Morphological comparison of ventral abdominal spines. (A-C) spines belt of modern puparia of *T. zosteræ* from the collection of Natural History Museum, London; (D-H) ventral spines belt of puparia from this study. The schematic model shows the location of the spines analysed. ant= anterior region of the puparium; post= posterior region of the puparium. Letters follow Fig. 4.6. Scale bar: 50 μ m.

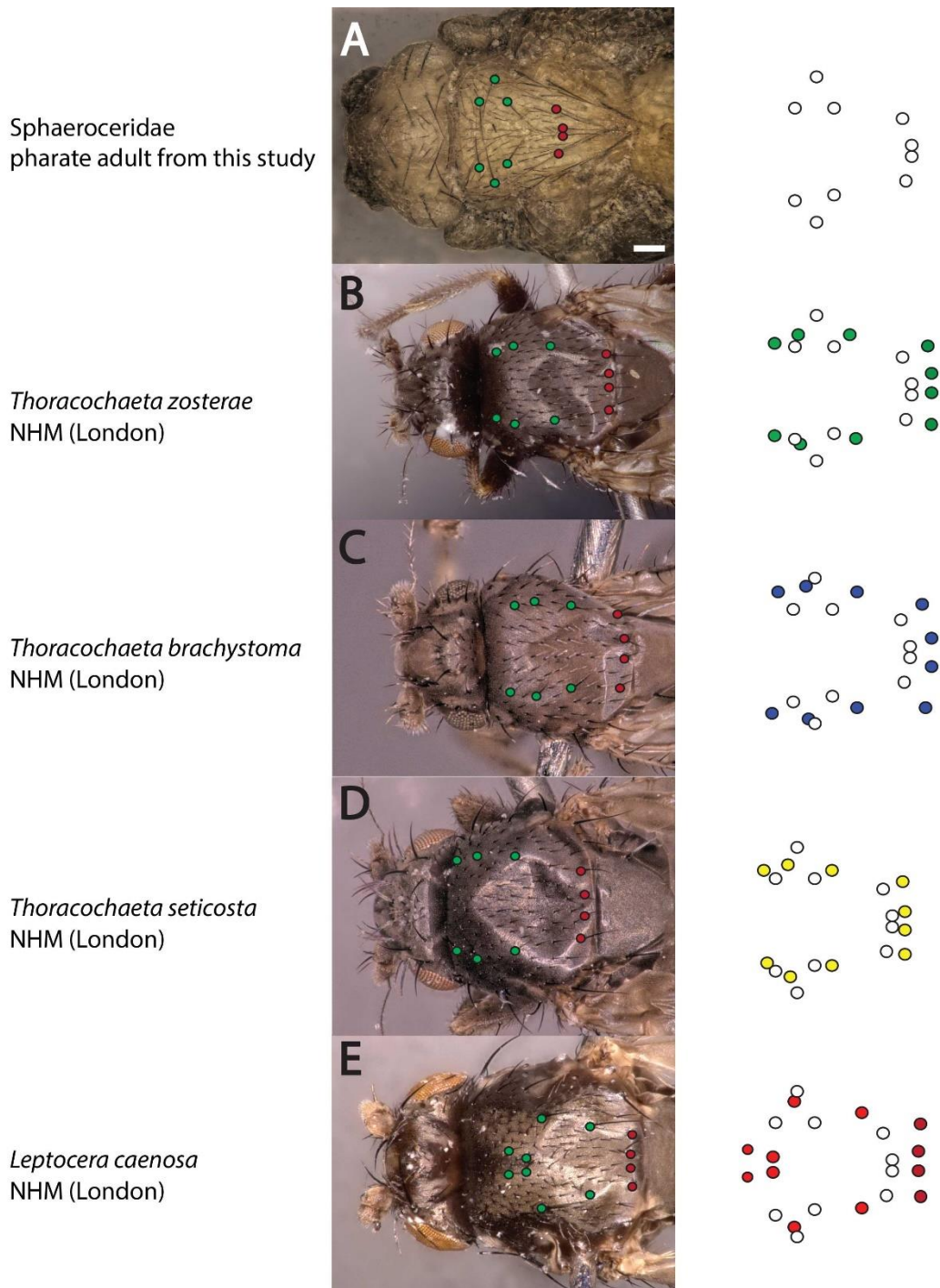


Fig. 4.9 Morphological comparison between pharate-adult and adults specimens. (A) mineralised pharate adult from this study; (B-E) modern adults specimens of Limosiniinae (Sphaeroceridae) from the London Natural History Museum (NHM) collection. The coloured spotted mark the mutual position of the thoracic bristles. For the comparison, white spots refer to the pharate adult from this study and for the other taxa a colour coded spots have been chosen. Scale bar: 100 μm .

Mineralogical studies

Within Dipteran assemblage, three groups of puparia were identified based on their state of preservation:

- i)* puparia showing the expected “normal preservation” as commonly found in archaeological excavations or modern crime scenes, with the organic puparia structure perfectly intact and recognisable morphological features. The majority of specimens falling within this category belong to Sphaeroceridae (Fig. 4.10A);
- ii)* closed puparia preserving an intact organic cuticle forming a mould in which the internal soft tissues have been replaced by inorganic salts copying the original anatomy of the organism. The majority of specimens presenting this type of preservation belong to Sphaeroceridae and Muscidae (Fig. 4.10C, Fig. 4.10A-C). To simplify the reading of the results, the term “cast/mold” will be used throughout the text to refer to this group;
- iii)* closed puparia showing a total replacement of the internal soft tissues by a mineral matrix and the organic pupal cage included or absent. Specimens belonging to Sphaeroceridae and Fanniidae showed this kind of preservation more than the others (Fig. 4.10B,D). The surface of Fanniidae puparia appeared opaque, friable, and porous (Fig. 4.10D, Fig. 4.11D-F); while the surface of puparia Sphaeroceridae appeared smooth and showed a kind of translucent and white-yellow colour surface (Fig. 4.10B, Fig. 4.11G-I). To simplify the reading of the results, the term “mineral replaced” will be used throughout the text to refer to this group.

It is also worth mentioning that the majority of the totally mineral replaced specimens were found in the upper stratigraphic unit S.U. 19335 unlike those described in the groups *i)* and *ii)* which were mainly recovered from the waterlogged deposit in the lower stratigraphic unit S.U. 19336 of the well (Fig. 4.10E).

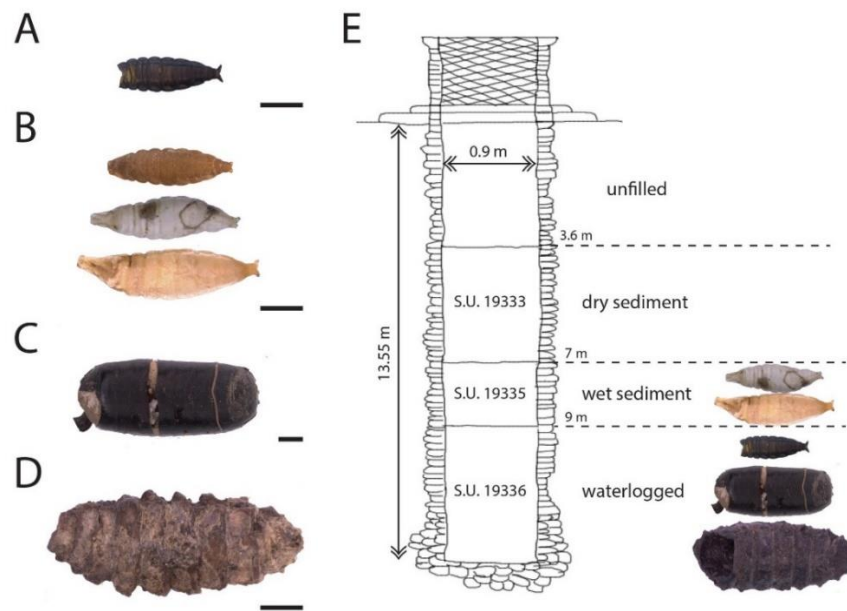


Fig. 4.10 Gradient of mineralisation of Diptera puparia. (A) Spaheroceridae puparium “normally preserved”; (B) Sphaeroceridae and (D) Fanniidae puparia showing a total replacement of the internal soft tissues; (C) specimens of cast/mold pupa of Muscidae with the organic cuticle conserved and forming a cast in which the internal soft tissues have been replaced by a mineral mould; (E) distribution of the Diptera remains as found within the well. Scale bar: 1 mm.

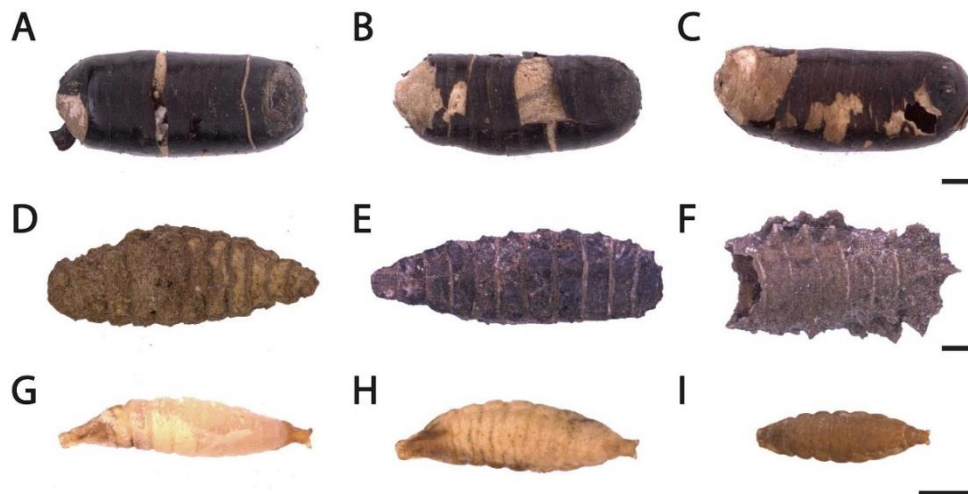


Fig. 4.11 Mineralised Diptera fossils. (A-C) Muscidae; (D-F) Fanniidae; (G-H) Sphaeroceridae. In all the specimens the segmentation typical of larvae and pupae was still observable and the general intact and well-preserved morphology allowed to discriminate the families. Scale bars: 1 mm.

The “translucent mineral replaced” specimens lack of the external morphological characters preventing an accurate identification of taxa at species level. However, in a few cases some anatomical details of the mineralised specimens appeared gratefully preserved. Fig. 4.12 shows two specimens with the hard chitinous cephaloskeleton which is still easily distinguishable. This is an example of how the fossilisation through inclusion in mineral matrix exceptionally preserved the endoskeleton of the developing immature stage (Fig. 4.12C,F).

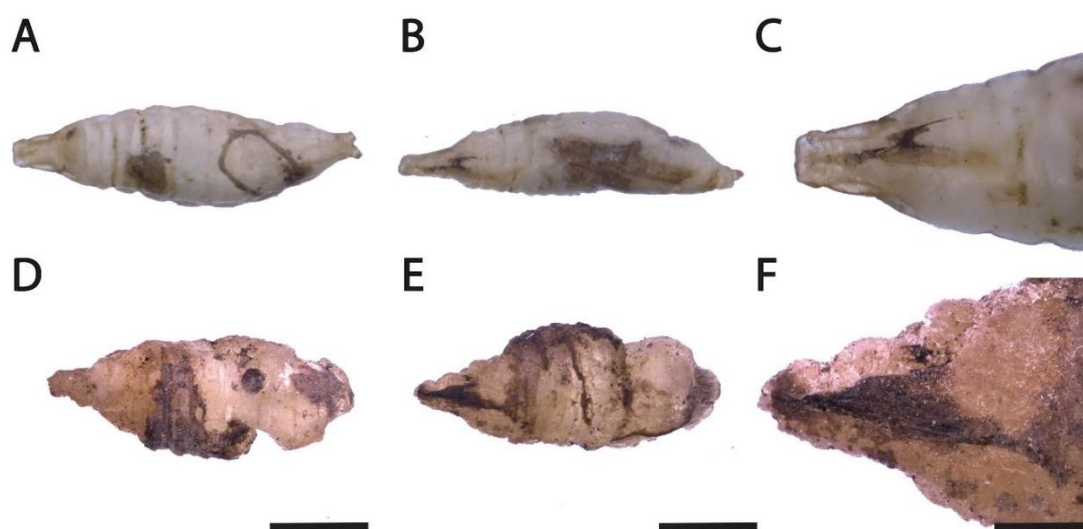


Fig. 4.12 Preserved cephaloskeleton in mineralised pupae. (A,D) dorsal, and (B,E) lateral view of two total mineralised Sphaeroceridae puparia; (C,F) hard chitinous cephaloskeleton observable intact in the oral region of the developing larva. Scale bars: 1 mm (entire), 500 µm (detail).

Within the total mineral replaced Sphaeroceridae group, a few pharate adults specimens as by definition of Dr Martín-Vega (Martín-Vega et al., 2016) were observed as another magnificent example of integrity preservation. The term pharate adult refers to the last stage of development of a pupa just prior the emergence of the adult and, therefore, shows head, legs and wings completely everted and the thorax distinguishable by the abdomen. All these details, except for the wings, were identified in some of the mineralised fossils recovered from the well (Fig. 4.13). In some cases, the head and the thoracic bristles were also already developed when the flies died and the pattern, still recognisable, allowed to determine the genus *Thoracochaeta*. Moreover, anatomical details such as ommatidia, the

smallest units of the flies' compound eyes, and an antenna also showed an exceptional *post mortem* preservation (Fig. 4.14B,C).

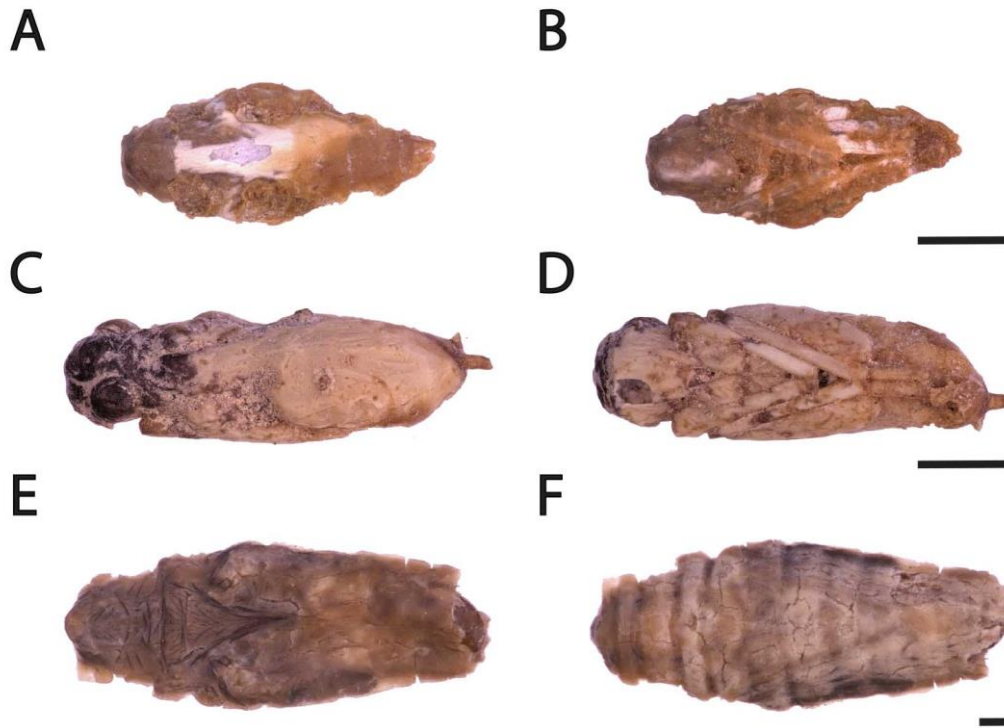


Fig. 4.13 Mineralised pharate adults. (A,C,E) dorsal, and (B,D,F) ventral view of mineralised metamorphosis insects. Head and legs are everted and the thorax is well distinguishable by the abdomen also due to the presence of the bristles (E), confirming the final stage of the pupa development prior the adult fly emerged. Scale bars: 500 μm (A-D), 100 μm (E-F).



Fig. 4.14 Details of mineralised pharate adults. (A) bristles head and thoracic pattern; (B) ommatidia; (C) antenna. An exceptional preservation of these details within the mineral matrix can be observed. Scale bars: 100 μm .

Microstructure analysis

Microscopic analysis conducted via CT scan and SEM revealed a different degree of mineralisation of puparia which played an important role in the extent of the morphological preservation of the specimens (Fig. 4.15). Through the X-rays data elaboration, the presence of an intact pharate of Muscidae adult within its mineralised thick pupal cage was observed. The head, the thorax, and the segmented abdomen were accurately distinguishable (Fig. 4.15A). This example has been documented as unique among the small batch of CT-scanned specimens, however it does not exclude *a priori* the presence of other specimens showing a similar preservation of the internal morphology. On the contrary, in the majority of the analysed cases, the degree of mineralisation was higher and differently extended (Fig. 4.15B). Results came both from CT scan and SEM revealing multiple well-structured morphotype of crystals (Fig. 4.16). A spore-like microstructure (Fig. 4.16A-D) and a tube-like structure on a netting matrix (Fig. 4.15B, Fig. 4.16E,F) was observed in the majority of the cases in totally mineral replaced Sphaeroceridae specimens, recovered from the S.U. 19335. On the contrary, spheric (Fig. 4.16H) and lamellar structures (Fig. 4.16J-M) were more typical of waterlogged Fanniidae, Sphaeroceridae and Muscidae specimens, recovered from S.U. 19336.

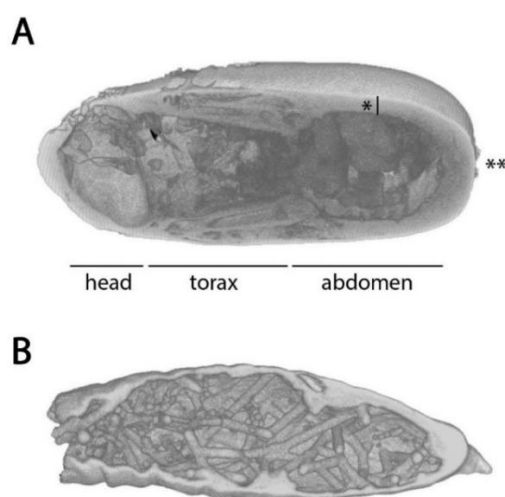


Fig. 4.15 Internal view of puparia observed via CT scan. Different degree of mineralisation were spotted. (A) Muscidae specimen showing a well preserved pharate adult within the thick inorganic puparium (*). Head, thorax, and abdomen of the specimen are still recognizable as well as the posterior spiracles (**). (B) Well organized tube-like crystal morphology typical of Sphaeroceridae found in the S.U. 19335.

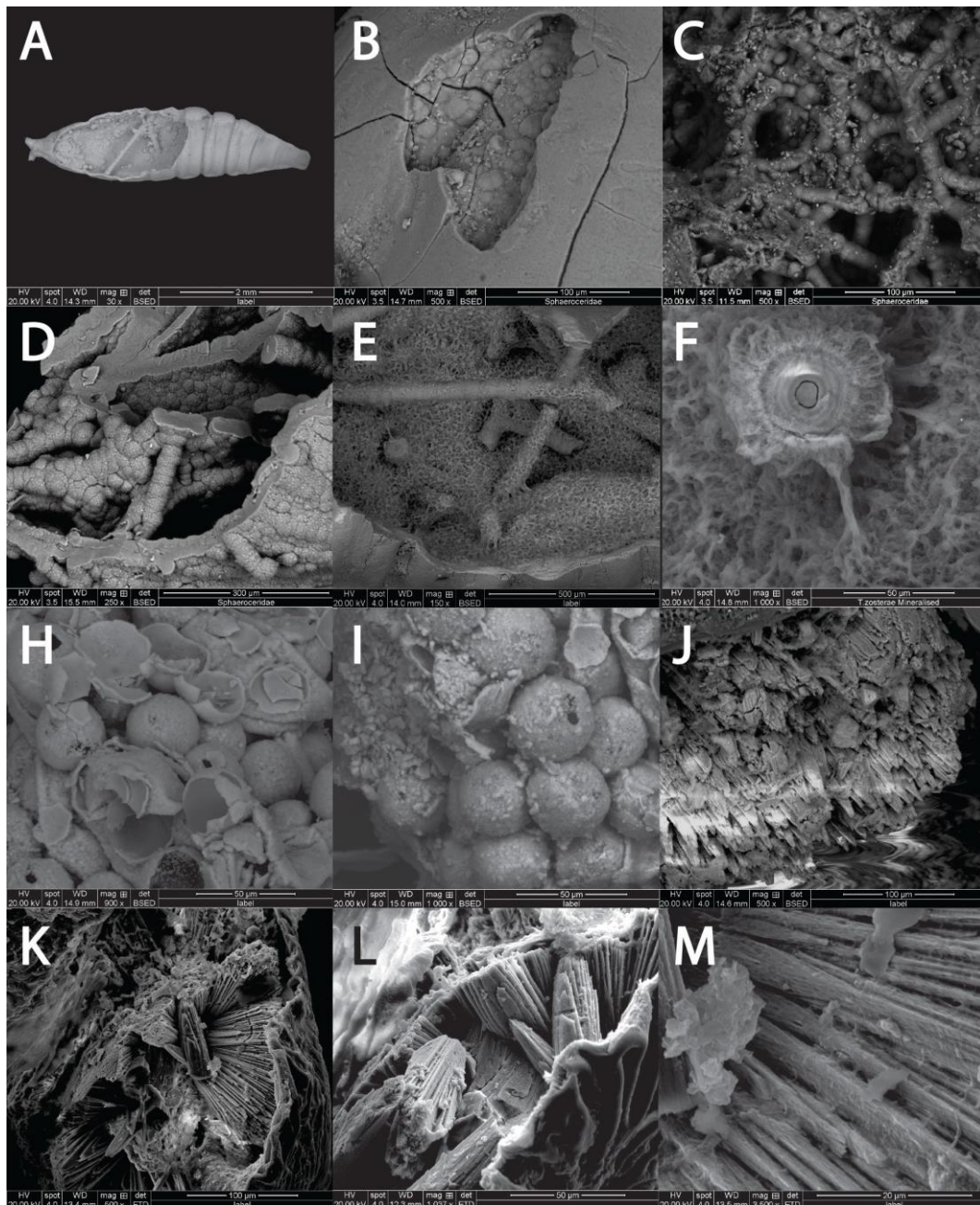
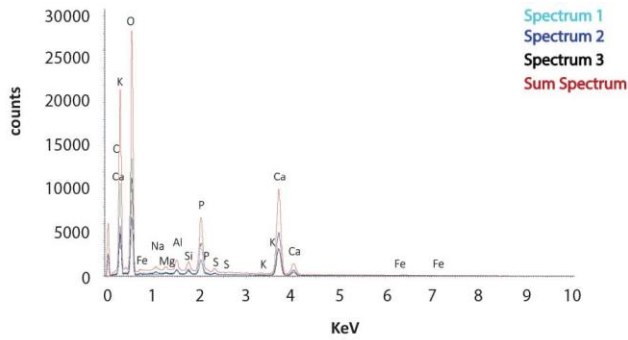


Fig. 4.16 Crystals' microstructure visualised at SEM. (A-F) Different magnifications of spore-like and tube-like structures on a netting matrix typical of totally mineral replaced Sphaeroceridae specimens, recovered from the S.U. 19335; (H,I) spheric, (J-M) and lamellar structures observed in waterlogged Fanniidae, Sphaeroceridae and Muscidae specimens, recovered from S.U. 19336. The scale bar is reported in each figure.

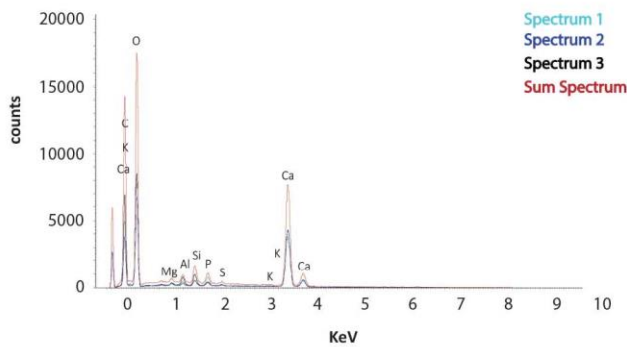
Microelement analysis

As a result of the SEM-EDX element analysis performed on specimens belonging to the three families, three spectra were generated including, in turn, the overlapping spectra derived by the three selected point of interest and the additional sum spectrum covering the whole area of the investigated surface. In Fig. 4.17 only a consensus spectrum is reported for each taxon: Fanniidae S.U. 19336, Muscidae S.U. 19336, Sphaeroceridae S.U. 19336, Sphaeroceridae S.U.19335. In all the cases, the highest significant counts were recorded for Phosphorous (P) and Calcium (Ca) which were revealed to be the major elements forming the inorganic salt matrix. Compared to the waterlogged specimens recovered from the S.U. 19336, the spectra of the total mineralised Sphaeroceridae specimens recovered from the S.U. 19335 showed higher peaks of P and Ca (Fig. 4.17). In addition, Magnesium (Mg), Aluminium (Al), Silicon (Si), Iron (Fe), and Chlorine (Cl) were also detected as minor components in the output spectra. The overlapping of the spectra for each taxon demonstrated that the chemical profile is homogeneous on the whole surface. The same results were graphically derived by mapping analysis (Fig. 4.18) which, in accordance to the ID-point analysis, showed that P and Ca were the chemical elements with the highest intensity, as reported in the colour-coded bi-dimensional image, thus corresponding to the most abundant ones. Moreover, both the elements showed and homogeneous distribution on the whole analysed area (Fig. 4.18A-C). A slight difference in intensity between samples recovered from different S.U. was observed, (Fig. 4.18A,B), while no difference at intra-specific level in terms of outer and inner surface (Fig. 4.18B,C) was observed. In the latter case, other elements such as Fe and Cl were detected, but not Al and Si (Fig. 4.18C). On the contrary, the surface of a waterlogged non-mineralised Sphaeroceridae puparium used as a control showed a significantly reduced presence of Ca and P, and an equal weak presence and distribution of minor elements compared to mineralised specimens (Fig. 4.18D). The comparison with published data led to identify a close similarity with the apatite $\text{Ca}_5(\text{PO}_4)_3$ SEM-EDX profile (Welton, 2003).

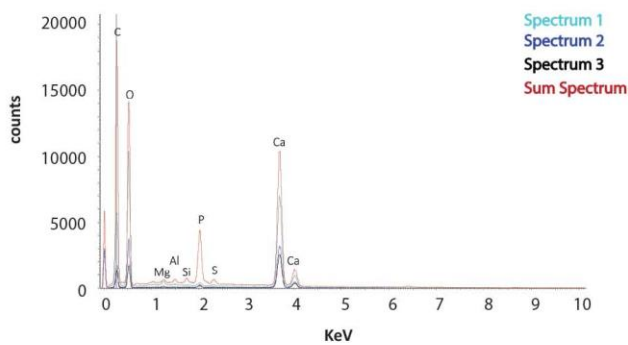
Chapter 4



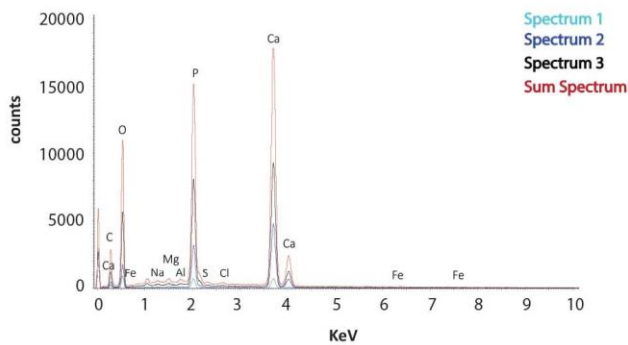
mineral replaced Fanniidae
S.U.19336



mold/cast Muscidae
S.U.19336



mold/cast Sphaeroceridae
S.U.19336



mineral replaced Sphaeroceridae
S.U.19335

Fig. 4.17 SEM-EDX ID Point microelement analysis. Consensus spectra are reported per each taxon. In each consensus spectrum, the coloured lines refer to three spectra generated from three points of interest arbitrarily selected on the puparia surface plus the sum spectrum (red line) generated from the whole observed area. Phosphor (P) and Calcium (Ca) were recorded as the most abundant elements.

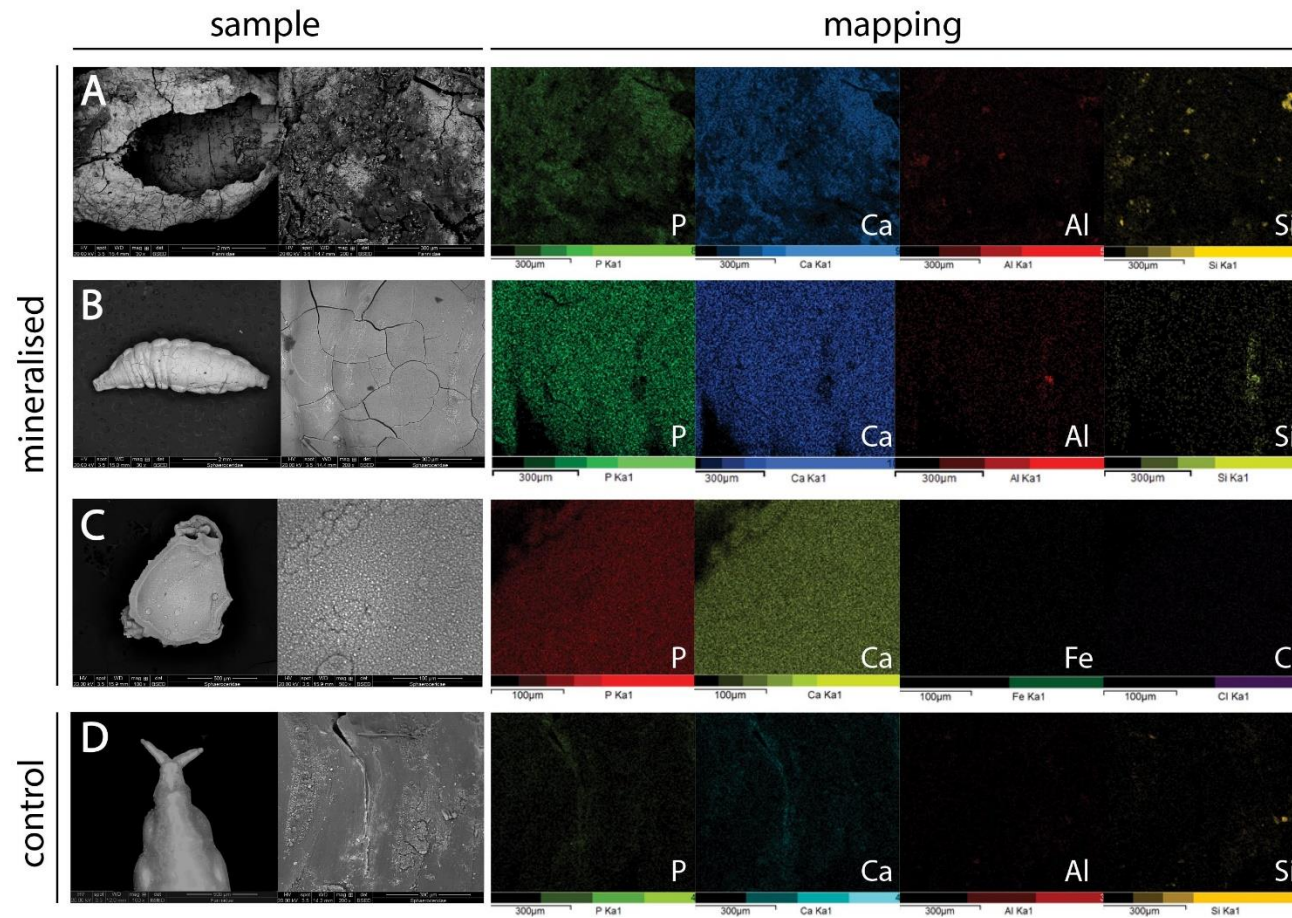


Fig. 4.18 SEM-EDX mapping microelement analysis. SEM images and the relative colour-coded bi-dimensional map of the element distribution is shown for puparia of Fanniidae S.U.19336 (A), Sphaeroceridae from S.U.19335 (outer B, inner C), and waterlogged normally preserved Sphaeroceridae puparium (D). Phosphor (P) and Calcium (Ca) were recorded as the most abundant and homogeneously distributed elements. The intensity of the signal for Al, Si, Fe, and Cl was significantly lower. Scale bar is reported in each figure.

Chapter 4

A total of twenty FTIR spectra were produced revealing a pattern of peaks consistent among the majority of the analysed samples with no evident difference but in the intensity of the signal (Fig. 4.19). One spectrum has been chosen as representative of each group of puparia. The recorded wavenumbers (cm^{-1}), reported in Tab. 4.2 and Tab. 4.3, were assigned to two distinctive functional groups: carbonate and phosphate. Some shifts in the referring frequency were detected, however, a general consistency in all the mineralised samples was found and carbonate-apatite is suggested to be the major component. It is worth mentioning that in mineral replaced Fanniidae group a typical calcium carbonate (CaCO_3) spectrum showing a weaker $\sim 1,030 \text{ cm}^{-1}$ peak and stronger peaks at 871 and 712 cm^{-1} was recorded, indicating a mixed composition among the specimens belonging to the same family.

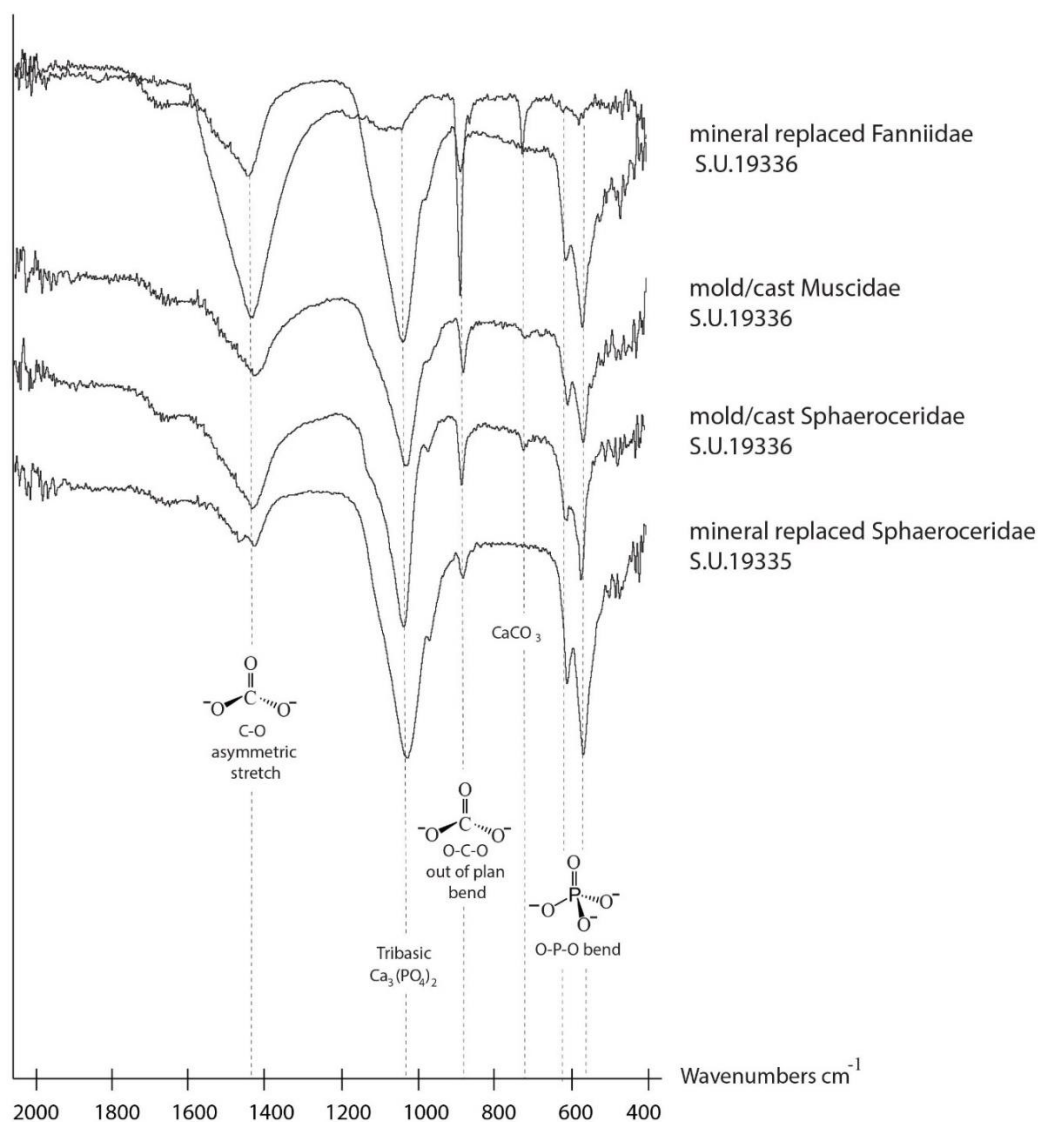


Fig. 4.19 FTIR analysis. IR analysis has been summarised selecting one representative spectrum per each group of puparia. The spectra showed peaks associated to carbonate ($\sim 1,417, 871, 712 \text{ cm}^{-1}$) and phosphate ions ($1,030, 602, 566 \text{ cm}^{-1}$) as reported in Tab. 4.2, Tab. 4.3. Dashed lines indicate the wavenumber values of the major peaks detected (references in Tab. 4.2 and Tab. 4.3) and their overlapping.

Tab. 4.2 Carbonate ions wavenumbers assignment. The range of observed wavenumbers per each group has been compared to literature data and specifically assigned to asymmetric C-O stretch, O-C-O out of plane bend vibrations mode and to calcium carbonate molecule.

sample	wavenumbers (cm^{-1}) range	assigned to
mineral replaced Fanniidae S.U.19336	1,401-1,419	
mold/cast Muscidae S.U.19336	1,395.7 -1,417	asymmetric
mold/cast Sphaeroceridae S.U.19336	1,413 – 1,418	C-O stretch (Calcite)
mineral replaced Sphaeroceridae S.U.19335	1,395 – 1,416	
mineral replaced Fanniidae S.U.19336	871.2 – 871.5	
mold/cast Muscidae S.U.19336	871 – 871.7	O-C-O
mold/cast Sphaeroceridae S.U.19336	871.3 – 871.7	out of plane
mineral replaced Sphaeroceridae S.U.19335	871.4 – 871.9	bend (Calcite)
mineral replaced Fanniidae S.U.19336	702 – 712	
mold/cast Muscidae S.U.19336	710 – 713	CaCO ₃
mold/cast Sphaeroceridae S.U.19336	n/a	
mineral replaced Sphaeroceridae S.U.19335	711 – 712	

Tab. 4.3 Phosphate ions wavenumbers assignment. The range of observed wavenumbers per each group has been compared to literature data and specifically assigned to asymmetric O-P-O phosphate bend vibration mode and to Tribasic calcium phosphate molecule.

sample	wavenumbers (cm^{-1}) range	assigned to
mineral replaced Fanniidae S.U.19336	1,017 – 1,059	
mold/cast Muscidae S.U.19336	1,020 – 1,028	Tribasic
mold/cast Sphaeroceridae S.U.19336	1,016 – 1,027	Ca ₃ (PO ₄) ₂ (Calcite)
mineral replaced Sphaeroceridae S.U.19335	1,022 – 1,069	
mineral replaced Fanniidae S.U.19336	598 – 602	
mold/cast Muscidae S.U.19336	598 – 610	O-P-O bend
mold/cast Sphaeroceridae S.U.19336	599 – 601	Phosphate (Calcite)
mineral replaced Sphaeroceridae S.U.19335	565 – 611	
mineral replaced Fanniidae S.U.19336	555 – 568	
mold/cast Muscidae S.U.19336	560– 566	CaCO ₃
mold/cast Sphaeroceridae S.U.19336	554 – 561	
mineral replaced Sphaeroceridae S.U.19335	559 – 565	

XRD profiles with the best resolution were obtained when the X-rays were scanned through 2θ range between 15 and 80 selecting a step size of 0.02° . The analysis enlightened an overlapping profile observed for all the analysed waterlogged specimens collected from the S.U.19336 (Fig. 4.20). The distinct and well resolved peaks, indicating a high level of crystallization, were observed at 2θ values as per Fig. 4.20. On the contrary, the XRD profile of mineral replaced Sphaeroceridae pupae collected from S.U.19335 revealed a more amorphous nature of the crystal, as indicated by the lack of well resolved peaks, showing a partial match with the above mentioned (Fig. 4.20). In addition, in this analysis one extra sample labelled as “mineral replaced Sphaeroceridae S.U.19336” was included. These pupal cages, representing only a small fraction within the whole assemblage, were sieved from a sediment fraction collected from the lower stratigraphic unit (19336) but appeared as their counterpart collected from the S.U.19335. Their relative XRD profile matched with the taxa from S.U.19336, showing that the detected differences between the two patterns of spectra can eventually be related to the nature of the layer rather than to the taxon *per se*. As per comparison of results with data from the Inorganic Crystal Structure Database (ICSD) (<http://icsd.cds.rsc.org>), the profile of waterlogged specimens fitted into the CaCO_3 -ICSD #37421 (calcite) with high probability (Fig. 4.21A); while the apatite-(CaOH)(Na(CO₃))-substituted-ICSD #92322 seemed to have the closest profile to specimens preserved in the wet sediment S.U. 19335 (Fig. 4.21B). However, the co-presence of more than one mineral form cannot be excluded (Fig. 4.21C).

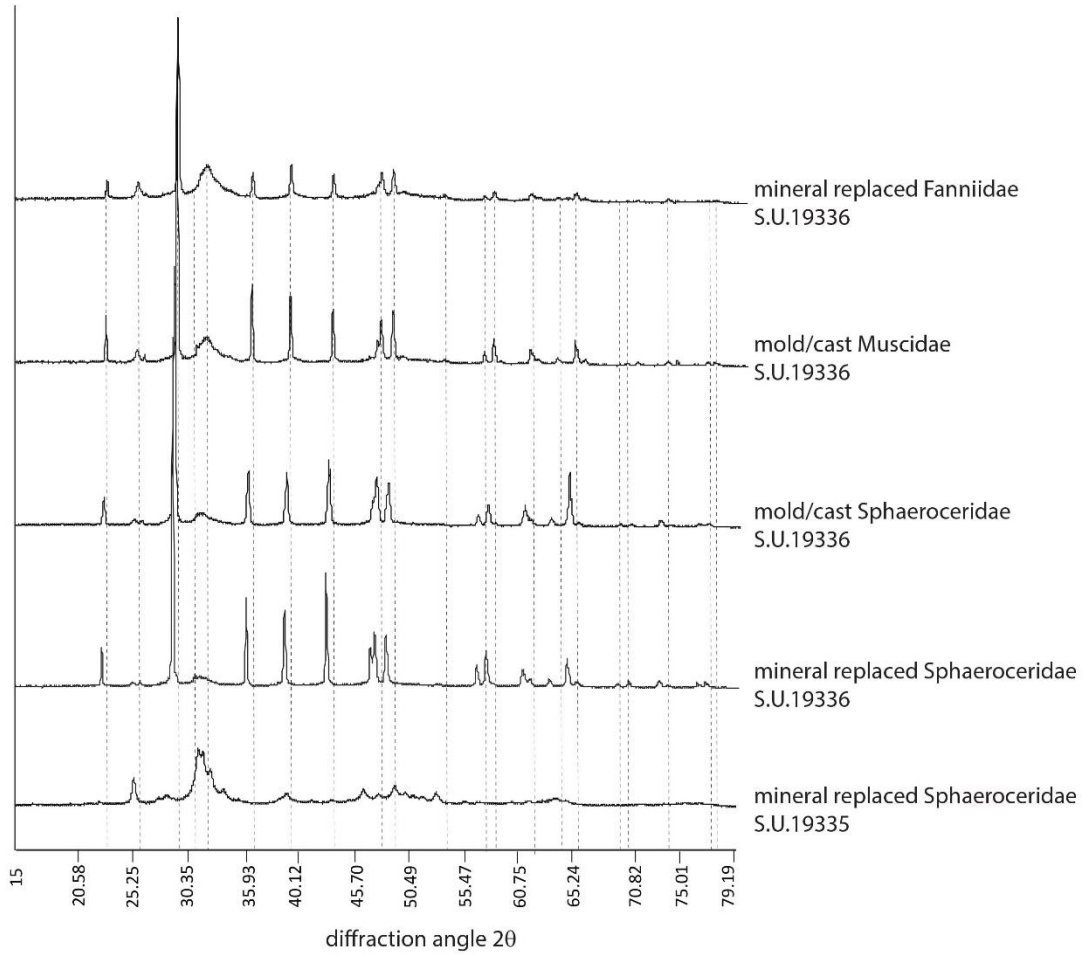


Fig. 4.20 Powder XRD spectra. XRD spectra of specimens collected from S.U.19336 show an overlapping pattern. Some of the peaks are shared with the specimens collected from S.U.19335 whose profile results more amorphous. Dashed lines help in the visualisation of the shifted signal detected intra spectra and enlighten the overlapping positions of 2θ values.

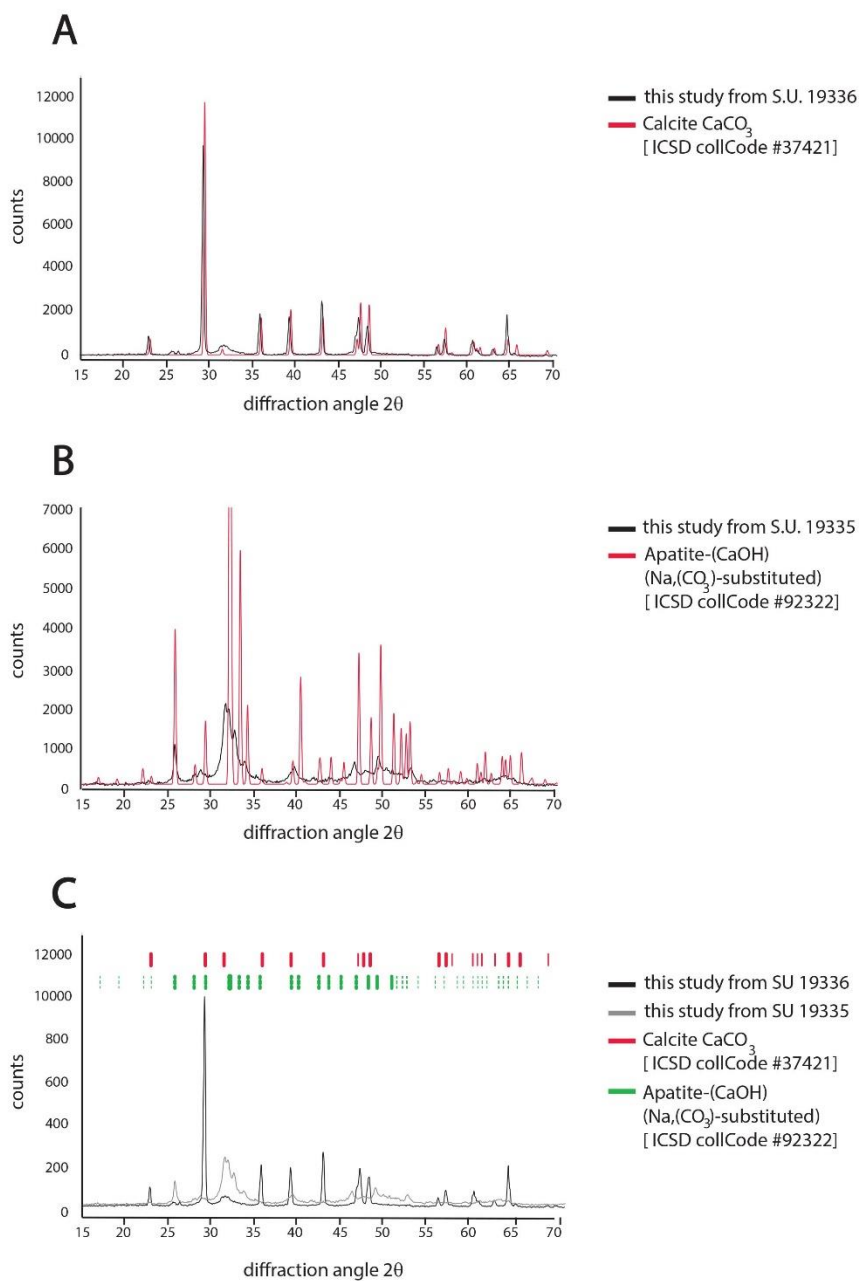


Fig. 4.21 ICSD-experimental XRD data comparison. The comparison of the XRD profile of the CaCO_3 -ICSD #37421 (calcite)(A), and of the apatite-(CaOH)($\text{Na},(\text{CO}_3)$ -substituted)-ICSD #92322 (B) showed a compatibility with the XRD profile obtained from this study.

DNA analysis

DNA was successfully extracted from 50 mg of Sphaeroceridae puparia using all the tested methods (Tab. 4.4); the maximum yield was obtained when Gilbert's digestion buffer combined to QiAamp Investigator Kit was applied.

Tab. 4.4. Qubit® 3.0 Fluorometer DNA quantification extracted from Sphaeroceridae puparia. Concentration values are expressed in ng/μl ± standard deviation (s.dv) calculated on triplicate reactions.

method	[DNA] (ng/μl)	
	entire puparia	fragmented puparia
1. DNEasy power Soil Kit	0.28 ± 0.03	1.25 ± 0.17
2. Gilbert's digestion buffer + QiAamp Investigator Kit	8.83 ± 3.02	7.27 ± 2.51
3. Campos digestion buffer + QIAquick DNA purification kit	3.75 ± 0.23	3.91 ± 0.48
4. prewash step in NaClO 0.5% + method 3	0.72 ± 0.17	1.00 ± 0.37

No significant difference was observed between entire or fragmented samples (χ^2 p-value= 0.57); on the contrary, a significant difference was observed depending on the used kit (χ^2 p-value= 0.039 (fragmented batch), χ^2 p-value= 0.0358 (non-fragmented batch)).

Bioanalyzer traces showed similar distribution curves per each of DNA samples; on average, the size of total DNA is shifted towards the upper marker limit (10,380 bp) in the electropherograms (Fig. 4.22). The intensity of the fluorescence is coherent with the quantification results described above. In all the cases the maximum size of the DNA molecules was over the upper limit, with the maximum peak placed between 2 Kb and 4 Kb. The lower limit of the detected fragments ranges from 40 bp to 800 bp with a highest level of fragmentation observed for DNA samples extracted using the Gilbert's digestion buffer combined to the QiAamp Investigator Kit (Qiagen, Hilden, Germany) (Gilbert et al., 2007) (Fig. 4.22A), and using the Campos' digestion buffer combined to QIAquick DNA purification kit (Campos and Gilbert, 2012) (Fig. 4.22C). No differences related to the applied method was observed, as well as no difference was detected between fragmented or entire puparia.

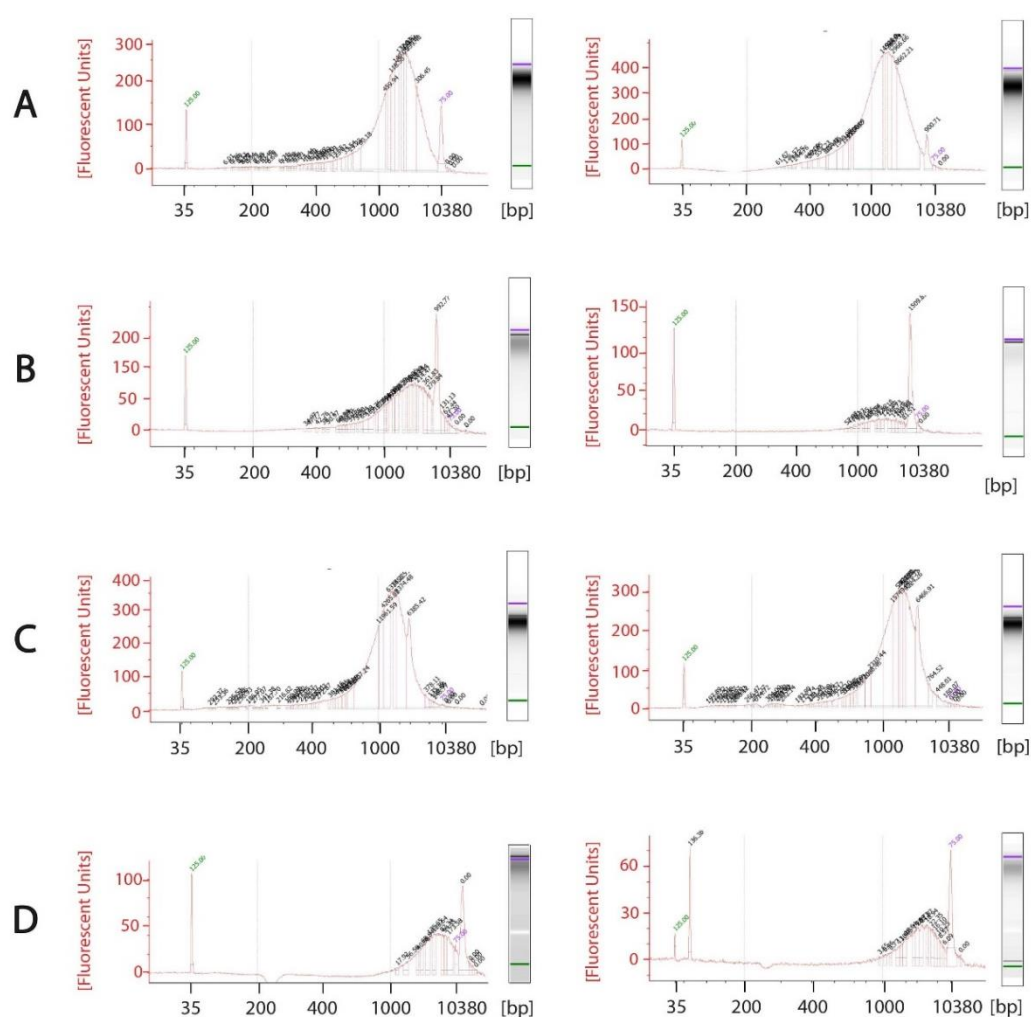


Fig. 4.22. Bioanalyzer traces of total DNA extracted from *Sphaeroceridae* puparia. The electropherogram and the relative gel-like image are shown as example per each of the DNA extraction methods (A-D) applied on fragmented (left column) or entire (right column) *Sphaeroceridae* puparia. Letters A-D refer to numbers 1-4 as per Tab. 4.4.

The amplification of the mini-barcode regions using Op111, Op211, Op311 primers failed in all the cases. On the contrary, both the bacterial 16S rRNA and/or the eukaryotic 18S rRNA targets were successfully amplified except when DNA extracted with method 4 as per Tab. 4.4 was used as template. Amplicons showed the expected sized, ~500 bp and ~150 bp respectively (Appendix A, Supplementary Figure A1), but were not sequenced as it fell out the purposes of the work.

4.1.2 Discussions

Entomological investigations performed on Via Satta (Sassari) archaeological deposits are key to demonstrate how insects can contribute to the interpretation of the site, not only through species identification but also through their state of preservation. The interpretation of the results is given outlining these two aspects.

The entomofauna of Via Satta well as a key to interpret its usage

Fly species (Tab. 4.1) identified in the medieval well in Sassari are commonly found in association to decomposing matter in anthropic unhygienic environments and conditions, and thus were given the classification of “cesspits indicator taxa”; this definition describes taxa which reliably testify the occurrence of certain events, activities or ecological conditions, in accordance to the definition given by Kenward (1997). Despite the lack of conserved morphological features of Fanniidae puparia, the traces of truncated dorso-lateral processes (Fig. 4.1) indicate the remains belong to *Fannia* genus. This datum is corroborated by the medical and hygienic importance of the widely distributed species of *Fannia*. *Fannia canicularis* Linnaeus 1761 and *Fannia scalaris* (Fabricius, 1794) have been found on a variety of decaying organic materials. The latter is commonly known as “latrine fly” as it is often recorded inhabiting cesspools, latrines, and dunghills, as in the case of the Roman well in the Sherwood Forest (Buckland et al., 2016), or in the 16th century cesspit in York (McCobb et al., 2004). *Fannia scalaris* larvae uses their air filled spikes on their body to float on the surface of cess and waste (Skidmore, 1999, Smith, 1973). The presence of *F. scalaris* which is regularly found in association to livestock (Domínguez and Pont, 2014) can also be explained by the recovery of archaeozoological remains such as bones of *Sus scrofa domesticus* Erxleben 1777, *Bos taurus* Linnaeus 1758, *Capra hircus* Linnaeus 1758 (Wilkins, personal communications). On the contrary, the identification of Muscidae at species level was possible due to the fact the cuticle of puparium was still present and the posterior spiracles still perfectly preserved. *Musca domestica*, *S. calcitrans*, and *M. prolapsa/stabulans* are eusynanthropic species (from the ancient Greek συν + ἄνθρωπος= with humans), thus able to live strictly associated to humans and breed on livestock. In particular, *M. domestica* is attracted to human faeces

and table food and *S. calcitrans* is more attracted to animal carcasses, faeces and sewage, thus having a medical and veterinary importance as they can be vehicles of diseases (Smith, 1986, Greenberg, 1971). *Musca domestica* and *S. calcitrans* were also previously found in contexts similar to the Sardinian pit such as the case of a byre in Neolithic Settlement of Weier, Switzerland (Nielsen et al., 2000), in a 5,000-year old byre in Sweden (Göransson, 2002) and in some medieval deposits in York (Buckland, 1974). As far as *Muscina* species concerns, while *M. prolapsa* can only be recovered from decaying animal matter, *M. stabulans* can be found also on vegetable rotten matter, as well as on birds and human excrements (Skidmore, 1985). Considering that the number of specimens of *Muscina* sp. collected is way larger than *S. calcitrans* and even more than *M. domestica*, it is more likely that *M. stabulans* was mainly present within the assemblage. In fact, its larvae are known to heavily prey on those of *M. domestica* being able to drastically reduced the housefly populations (Skidmore, 1985). Another identification problem was faced in regards to the specimens illustrated in Fig. 4.3. The hypothesis of its identification within *Lispe* genus is in agreement with the environment of the pit, as flies belonging to this genus are known to develop in wet mud and shore debris with high organic content (Skidmore, 1985).

The population of Fanniidae and Muscidae was quantitatively overcome by the thousands of Sphaeroceridae which were predominant both in the waterlogged assemblage (S.U. 19336) and in the wet sediment (S.U. 19335). Morphological analysis aimed to identify the specimens at lower taxonomic level was extremely difficult due to several factors, such as *i*) the lack of recent and detailed description of Sphaeroceridae species, *ii*) the state of preservation of the findings, *iii*) the lack of expert taxonomists studying the immature stages of species within this family, and *iv*) the intra-specific variation of puparia morphology. However, *T. zosteræ* was identified with a certain level of confidence within the assemblage. *Thoracochaeta zosteræ* is a small fly known as “seaweed fly” breeding on decaying seaweed cast up on the shore at the high water mark, usually forming large populations (Belshaw, 1989). It is mainly distributed in the Holarctic region and has rarely been recorded inland. The species was first described by Richard in 1930 but no detailed study was performed on its biology and ecology until 1958, when

Egglishaw wrote his PhD thesis concerning the wrack beds fauna (Egglishaw, 1958). In his work, the first detailed description inclusive of manually drawn figures of *T. zosteræ* immature stages was provided: “*from light to dark-brown in colour with sides compressed dorsoventrally near edge, a clearly defined segmentation of the body, obvious segmental spines, first segment completely introverted*” (Egglishaw, 1958). This description matches with the observations of specimens in this work (Fig. 4.6, Fig. 4.8). Further support about the identification of *T. zosteræ* comes from its records in several archaeological deposits in Europe, with specific regards of England where several works have been published about this small dung fly (Webb et al., 1998, Skidmore, 1999, Nielsen et al., 2000, Tetlow, 2009, Erzinclioglu, 2000, Buckland et al., 2016). In these records, authors point out that *T. zosteræ* requires foul conditions to breed (Belshaw, 1989), a datum which is in line with the description of the Via Satta well used as a dump. Nowadays, this small fly is known to breed on decaying rack beds which are accumulations of detached seaweed deposited on the sea shore. Therefore it has been suggested that *T. zosteræ* exploited a niche similar to its usual ecological habitat with a semi-fluid consistency, enriched in salts and nutrients (Belshaw, 1989). Considering that *T. zosteræ* is a typical sea-shore fly feeding on rotten seaweeds, three possible explanations can support the finding of this species in domestic urban well in the the city of Sassari, far from the sea-shore of about 11 km.

1) The large consumption of fish in Medieval Sardinia is well-established, and it is strictly linked to the Christian traditions. Usually the rich clergy was requested to observe these demands, however also laic people were expected to avoid eating meat during specific times of the year (e.g. Friday and Lent). In conjunction with these periods, the consumption of fish increased. Considering the higher cost of fish compared to the meat, and considering that the 22,4% of the fragments of edible vertebrates found in the well of Via Satta was fish, we can deduce that wealthy people most likely owned a property furnished of the well where the food wastes used to be discarded (Wilkens, personal communication). Additionally, the regulation concerning the selling of the fish dictated by the “*Statuti Sassaresi*” must be considered. The catch was brought to Sassari by the fishmongers from the coast, and had to be sold by the end of the day within a specific day-time regulation. The fish brought in early in the morning had

to be sold midday, and the load brought from 10 am to midday had to be sold by vespers (about 6 pm). Moreover, the fishmongers were not allowed to rest and sit down or to lean and the fish storage in a private house was forbidden (Wilkins, personal communication). In such a strict context designed to guarantee the freshness of the products and the hygienic conditions, we can assume that fish was transported enwrapped in seaweed stacks which the *T. zosteræ* flies came along with. If this hypothesis was confirmed, we should also be aware of the chance that these seaweed wraps were at least partially rotten prior to be thrown into the well in order to attract the flies and provide them the optimal conditions to lay eggs and develop on them. As a paradoxical consequence, the freshness and the good quality of the catch could not be guaranteed, thus representing a huge risk for the fishmongers in regards of the severe law. On the other hand, instead, it can be speculated on the fact that the seaweed was used for other purposes and discarded in the well when still fresh and that the *T. zosteræ* flies population colonised the well upon attraction by decaying seaweed and other organic matter.

- 2) A second explanation need to be searched in the name of the species. Amongst botanists, *Zostera* Linnaeus, 1753 is a well-known genus within the Zosteraceae, a family of aquatic plants living on the seabed not far from the coast or in the salt water of the lagoons. The term “zoster” comes from Latin with the meaning of “belt”, describing the typical strip-shape of the leaves of these plants such as *Zostera noltii* Hornem, 1832 and *Zostera marina* Linnaeus, 1753. Both the species can be found from the arctic waters along the northern Norwegian coasts to the Mediterranean basin (Borum and Greve, 2004). Specifically, the optimal habitat of *Z. marina* is represented by waters and low concentration of salts. A very similar plant which is often confused with the two just mentioned, due to the morphology of the leaves, is *Posidonia oceanica* (L.) Delile, 1813 of the family Posidoniaceae with a distribution limited to the Mediterranean sea (Borum and Greve, 2004). It is worth mentioning that these aquatic plants are currently used as fertilisers for tomatoes crops, for example. Albeit with some

variations⁶, a similar use of these plants in crops fertilisations in medieval Sassari can be hypothesised and therefore justifying the conspicuous colonisation of decaying matter by *T. zosteræ*.

- 3) Lastly, a third explanation can be drawn considering other European records of *T. zosteræ* in similar contexts. The example of a Roman well used as pitfalls in Sherwood forest is the most explicative (Buckland et al., 2016). The record of *T. zosteræ* puparia within the well in the Sherwood forest, which is located almost 113 km far from the closest East coast of England, demonstrates that the species was apparently widespread inland since the Roman times, suggesting that it could find an optimal habitat even far from where the same species is known to live nowadays. This hypothesis is well supported by the fact that during medieval period, the city of Sassari was surrounded by a forest environment which has been progressively replaced by the expansion of the city. Currently, there are no records of *T. zosteræ* in Sardinia, neither according to the Fauna Europaea database (www.fauna-eu.org) nor according to Lorenzo Munari (Natural History Museum, Venice), expert of Sphaeroceridae. The changes of the environmental conditions occurred from the Middle Ages over the centuries, likely due to the anthropic activities, could have brought the lack of suitable ecological conditions for the species and potentially causing its extinction. In addition, the small size of the sampling performed in Sardinia in the modern times did not bring to record the seaweed fly yet. This is an example that corroborates the importance of the environmental archaeoentomological studies in order to derive important information concerning the biodiversity in the past and its changes. If the absence of *T. zosteræ* in Sardinia was confirmed, the case would resume a similar case published by the research FLEA group, concerning the first record of *Phormia regina* Meigen, 1826 from an underground crypt in Castelsardo (Sassari) (Giordani et al., 2018b). As in the case of *T. zosteræ*, *P. regina* is not present nowadays in the Island (www.fauna-eu.org) and

⁶ As well-established, tomatoes crops are originally from South America and were imported to Europe only after 1492 AD. Therefore, their presence in Sassari during Middle Ages would be anachronistic.

its potential extinction can be related to a phenomenon of biological competition with other species.

Certainly, the number of Sphaeroceridae puparia collected (estimated >10,000) reveals that a conspicuous colonisation occurred and the conditions were favoured for these flies in comparison to Fanniidae and Muscidae counting a smaller number of specimens within the whole assemblage (Tab. 4.1). Such a large disparity suggests a competition for the *pabulum* (food source) and it indicates that also the micro-environmental conditions within the well favoured the eggs deposition and the development of Sphaeroceridae.

Overall, the findings of these entomological taxa confirm the usage of the well as a domestic dump and cess-pit where the decaying animal and vegetable wastes created the optimal conditions for multiple events of colonisation by saprophagous flies attracted by the release of volatile organic compounds (VOCs) as by-products of the microbial metabolism (Davis et al., 2013). A recent study from Medellin (Colombia), carried out on insects associated with the composting process of solid urban waste separated at the source, revealed the abundant presence of the same three taxa (Muscidae, Fanniidae, Sphaeroceridae), and other flies confirming their habit in being excellent recyclers of organic matter, which is also well-known in forensic entomology (Morales and Wolff, 2010). Moreover, the entomological data are in agreement with the botanical analysis which, through the identification of a large variety of taxa defined as “latrine wastes indicators”, corroborates the foul status of the medieval well (Bosi and Mazzanti, 2013). Indisputably, by the time that the flies colonised the well, the water stopped to be consumed, thus these taxa well represent bio-markers of the usage of the well. In addition, the warm seasonality of the fruition of the well is confirmed by the entomological data, as the found taxa typically develop between the late spring and the early autumn with a peak of the activity during the summer season (Smith, 1986, Skidmore, 1985).

Understanding the mineralisation phenomenon in relation to the chronological history of the well and its impact on DNA analysis

The recovery of empty puparia suggests that the life cycle had been undertaken *in toto* allowing the adult flies to emerge. However, within the same assemblage several unhatched puparia belonging to all the three main taxa were also found, indicating the immatures did not complete the metamorphosis and failed to emerge as adult flies.

These puparia within the assemblage were preserved over the centuries through the phenomena of waterlogging and mineralisation (Panagiotakopulu, 2004). The waterlogged preservation of “delicate biological remains” (insects and seeds) (Kenward and Hall, 2000) is common in urban archaeological excavations, especially in wells and pits. In fact, water provides the anoxic conditions essential to halt the decaying process promoted by the microbial communities inhabiting the environment, and ensures a stunning preservation of the puparia morphological features necessary to identify the species. This kind of preservation occurred for Muscidae and Sphaeroceridae collected from the S.U.19336 where water was still present at the time of the excavations (Wilkins, personal communications). On the other hand, the replacement of the organic matter by inorganic minerals occurred. In this specific circumstance, the term “preservation” refers to the conservation of the organic remains through mineral fossilisation processes that directly results in retention of information (Purnell et al., 2018). Specimens belonging to all the three taxa were found preserved in a semi or total-fossilised condition (Fig. 4.10). In the first case (semi-mineralised), a phenomenon of inside out mineralisation (infilling) occurred leaving the puparia cuticle intact (mold/cast specimens). In some cases, the shape of the near adult flies was recognisable (Fig. 4.13) or still visible if specimens were observed backlit or through the X-rays scan (Fig. 4.15A). When the mineralisation replaced the whole organic material of the specimens including the puparium itself, the identification was very problematic due to the lack of external features. These two distinct mineralised surfaces were also found by McCobb and co-workers while they investigated some arthropods remains recovered by a 16th century deposit in York (McCobb et al., 2004). Mineralisation of arthropods remains is common in archaeological deposits, especially in urban contexts; the majority of data comes from archaeological excavations

conducted in the United Kingdom bringing to light deposits from Eocene until 17th century (Girling, 1979, McCobb et al., 2004, Smith, 2007, Marshall et al., 2008). In addition, other world records are from France (Huchet, 2014a), Georgia (Messenger et al., 2010), Jamaica (Donovan and Veltkamp, 1994), and Kenya (Leakey, 1952). Although the mineralisation affected mainly organisms within the phylum Arthropoda, also botanical remains such as cereal grains (Marshall et al., 2008), apple seeds (McCobb and Briggs, 2001), and other fruits and seeds (Messenger et al., 2010) were found to be affected by the same phenomenon. So far, the study carried out on Via Satta well represents the first Italian record of mineralised insects fossils. Despite the different latitudes, all these sites share the same nature as cesspits or pitfalls, or they were ancient carboniferous areas which justify the transformations of the findings into mineral fossils. Girling observed that “calcification” phenomenon is due to the organic-rich deposits, pits and drains flushed with hard water (Girling, 1979), suggesting that the environmental conditions play an important role in the taphonomy of the remains.

The chemical investigations, performed following similar studies (McCobb and Briggs, 2001, McCobb et al., 2004, Marshall et al., 2008, Messenger et al., 2010), helped in the interpretation of the studied evidence. Data obtained by the SEM-EDX, FTIR, and powder X-ray overall revealed profiles matching with calcite (calcium carbonate salt) and apatite (calcium phosphate salts) minerals, without highlighting substantial difference taxa-related. Rather, the heterogeneous nature of the sediments and the role played by the environment in crystals nucleation and growth may explain differences in EDX and X-ray profiles of specimens recovered from the wet sediment, S.U. 19335. Although an accurate determination of crystals could not be achieved, literature records (McCobb et al., 2004, Marshall et al., 2008, Messenger et al., 2010) addressed the hypothesis of apatite-preservation, demonstrating that the level of P measured in dipterous puparia studied from several archaeological deposits were significantly higher than in the soil from where they were recovered (Girling, 1979). Similar data are not available for the current study; however, the following considerations may be read in favour of a phosphate-mineral preservations of Diptera from via Satta. It is well known that the calcium carbonate is unstable under low-pH conditions, thus it would rarely be recovered from acidic deposits

(Messenger et al., 2010). McCobb and co-workers (2004) measured the pH of soil solution extracted from sediments collected from a 16th century cesspit, found values within the range 4.95–5.57, and determined a high concentration of calcium phosphate composing mineralised invertebrates. By analogy, *mutatis mutandis*, a similar scenario can be assumed for the Via Satta well. Low-pH values are attributed to the accumulation of by-products of the decay process from plant and animal sources. In fact, CO₂ largely derived by the aerobic microbial metabolism which presumably occurred in initial phases of decay of large volumes of organic waste. Based on the equation $\text{CO}_2 + \text{H}_2\text{O} \leftrightarrow \text{H}_2\text{CO}_3$ (carbonic acid) $\leftrightarrow \text{H}^+ + \text{HCO}_3^-$ (carbonate anion), the formed carbonate ions may combine with other ions to generate carbonate minerals (Allison, 1990). The production of phosphate is also intimately associated with microbial decay process (Marshall et al., 2008). In addition, potential sources of calcium and other cations may be derived from the animal bones and the saturated groundwater. All these elements, related to the interactions of multiple factors such as pH variations, constant presence of water and the natural background geology of the sediments of the well, seem to favour the precipitation of insoluble calcium phosphate complexes within the puparia and the subsequent substitution of the internal soft tissues. This process has been proved to be very rapid (Briggs and Kear, 1993).

Additionally, considering that the phenomenon of inside out mineralisation widely occurred, it is worth evaluating the role of the pupal cage as a selective membrane. It is well-established that chitin is the major component of puparia and that its chemical nature is a determining factor in the *post mortem* survival of fly puparia, and at the same time, it must allow the continuous exchange of gas molecules during the pupation phase, in order to guarantee the survival of the specimen (Vanin and Huchet, 2017). In Via Satta well, likely fly puparia found themselves trapped between a waterlogged anoxic condition and the infilling of the well with soil sediments which resulted in an infiltration of water carrying mineral deposits (permineralisation) into the organic soft tissue through the puparium-selective membrane. This observation can also be extended to other non-animal organisms provided with a semi-permeable coat as the plant seeds, some of which have been found in the same status of preservation of the fly puparia (Fig. 4.23).



Fig. 4.23 *Via Satta* mineralised seeds. (A,C) unknown origin, (B) grapeseed. Scale bar: 1 mm.

The extent of the mineral replacement may correlate with differences in the permeability of the puparium which could be species specific but, above all, with other inter-related factor such as the input of the organic matter in the environment, decay rate, and the hydrogeologic conditions. In regard to the latter, the differences in the preservation of puparia (mold/cast or mineral replaced) undoubtedly reflect the changes in the groundwater level (Wilkins, personal communications), and the finding of thousands of specimens not emerged as adults testifies that an event, likely the infilling of the well, occurred.

The description of mineralisation process as above is also key to justify the failure of DNA characterisation from Sphaeroceridae puparia. In fact, the analyses were carried out on hundreds of waterlogged specimens selected by weight, which, *post facto* included an unknown number of mold/cast mineralised puparia. It is therefore likely that the amplification of the mini-barcode regions failed due to the absence of host DNA, fitting with replacement of soft tissue by inorganic matrices. Consistently, Bioanalyzer traces show the typical pattern of an intact DNA of genomic environmental origin, which was confirmed by the positive amplification of environmental targets. Referring to the definition of “preservation” given by Purnell (Purnell et al., 2018), no genetic information was retained by the Sphaeroceridae specimens molecularly investigated thus proving, expectedly, that the mineralisation as taphonomic process has a destructive impact on DNA survival.

4.2 MINERALISATION OF ENTOMOLOGICAL REMAINS FROM A HUMAN MASS GRAVE IN MACOMER (SARDINIA, ITALY)

4.2.1 Results

Diptera puparia were mainly found nestled in human bones remains as shown in Fig. 4.24, either adhered to mud and soil sediments on the surface, or inside the marrow cavity of bones showing *post mortem* fractures.

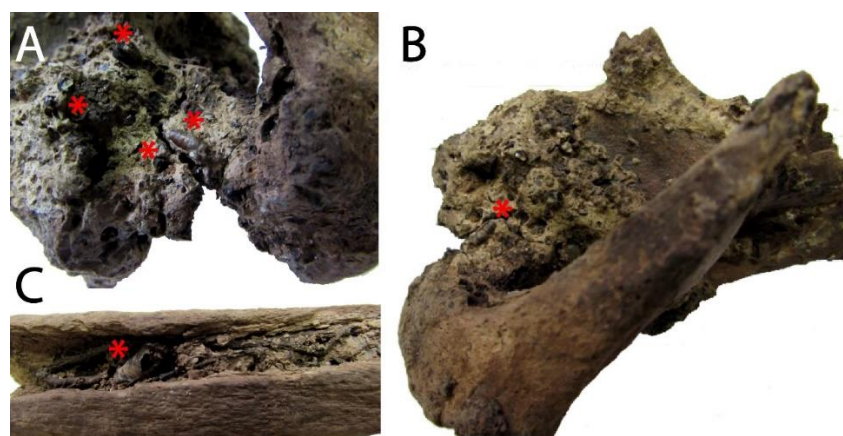


Fig. 4.24 Diptera puparia nested into human bones from the mass grave in Macomer. (A,B) The inorganic mineral matrix covering the surface of the bones can be observed along with the nested Diptera puparia (red*). (C) Some specimens were included within the cavity of the bones.

As per definition given in paragraph 4.1.1, the majority of the findings were identified as fragmented mold/cast mineralised puparia at non definable phases of development (Martín-Vega et al., 2016); the few entire specimens showed the organic cuticle complete or patched, and still attached to the mineral component (Fig. 4.25), as well as the segmentation was still recognisable imprinted on the surface of some specimens (Fig. 4.25A-B, I-L).

Among the best preserved puparia, the observation at higher magnification showed a compact and fibrous structure of mineral casts, as well as the striped pattern of the dorsal side of the puparium (Fig. 4.26A,C). The observation of the assemblage revealed also some specimens near the completion of the metamorphosis cycle, as demonstrated by the presence of a microtrichosity (small hair pattern) preserved on the dorsal surface (Fig. 4.26B). In the majority of the cases, the morphological characters used for species

identification were missing due to the taphonomic transformation of the immatures into mineral fossils.

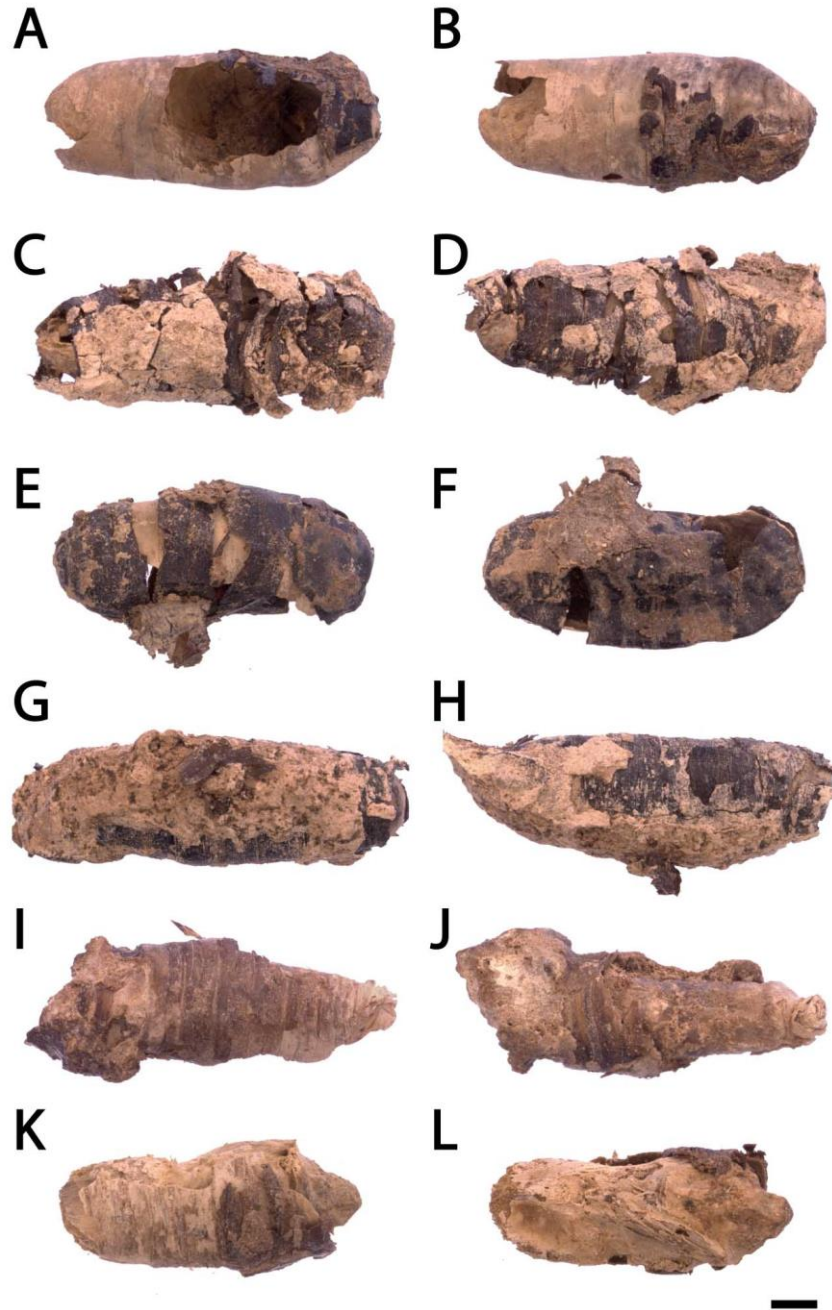


Fig. 4.25 Mold/cast mineralised puparia extracted from human bones. Different level of preservation are shown. The organic cuticle was patched and still attached to the mineral component (A-B, I-L), or complete (C-H). Scale bar: 1 mm.

However, in a few cases the posterior spiracles were preserved with high fidelity and allowed to identify the family Calliphoridae (Fig. 4.26D-F). The size and oval shape of the specimens in Fig. 4.26D, F reminded the ones characteristic of *Lucilia* spp. (Szpila, 2010), as also demonstrated by the comparison with the posterior spiracles of a *Lucilia sericata* (Meigen, 1826) specimens belonging to the private modern and archaeological collection of the FLEA. On the contrary, the smaller size and the rounded shape of the posterior spiracles belonging to specimens in Fig. 4.26E show a close similarity with *Calliphora vicina*. Furthermore, in the latter, the posterior spiracles are located at 45 degrees angle in respect of the anal region, rather than being orthogonal as in *Calliphora vomitoria* (Linnaeus, 1758).

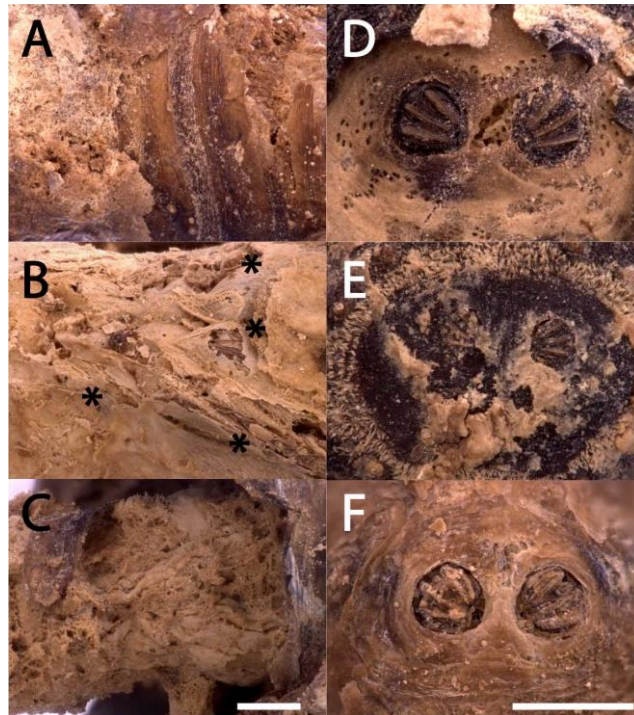


Fig. 4.26 Details of mineralised puparia. (A) Striped pattern of the dorsal side of the puparium, (B,C) compact and fibrous structure of the mineral casts, (B) microtrichosity of the dorsal surface. (D-F) Calliphoridae posterior spiracles. Scale bars: 500 μm .

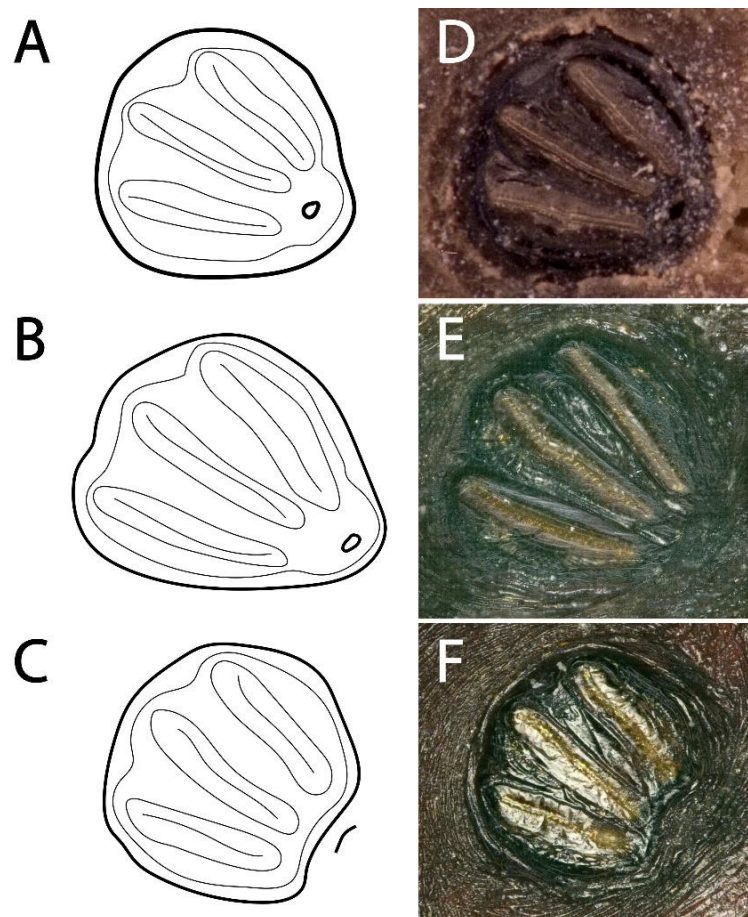


Fig. 4.27 Calliphoridae posterior spiracles comparison. (A,D) Specimens of this study; (B) *Lucilia sericata* hand-drawn illustration; (E) *L. sericata* from FLEA modern private collection, pic. by Dr Giorgia Giordani; (C) *Calliphora vicina* hand-drawn illustration; (F) *C. vicina* from FLEA archaeological collection (Giordani et al., 2018b).

Besides the dipteran remains, two fragments of Coleoptera were found, identified as elytra of the Cleridae beetle belonging to the genus *Necrobia* Olivier, 1795 (Fig. 4.28). Cleridae are small beetles (3–12 mm), also known as ham beetles, and are worldwide distributed even if the majority of the species live in tropical regions with only a few inhabiting colder latitudes (Gerstmeier, 1998). Adults are brightly coloured showing bodies mostly to entirely metallic, between bluish-black to green and orange and are feed on dried animal matters as well as on bones and carcasses. The pattern of the punctuation and the peculiar shape of the distal part of the elytra indicates that the specimens likely belong to *Necrobia rufipes* Degeer, 1775.

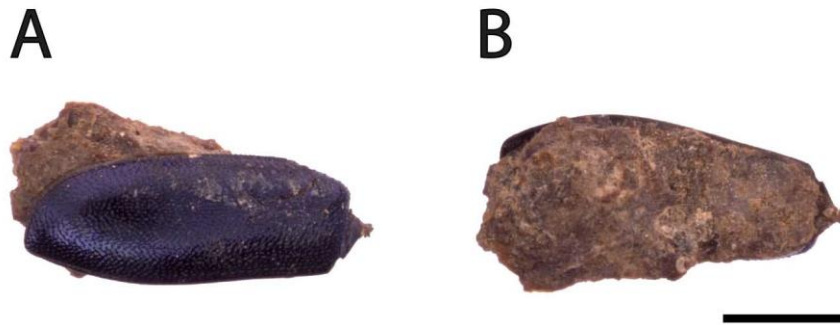


Fig. 4.28 *Necrobia rufipes*, single elytron. (A) Dorsal view, (B) ventral view. Scale bar: 1 mm.

4.2.2 Discussions

The finding of human remains excavated from the mass grave in Macomer (Sardinia) represent a treasure of archaeological importance due to the age of the remains dated to approximately 3,000 years ago, and unique in Sardinia. The still ongoing anthropological studies will provide information about the origin of the human remains, and along with the entomological investigations will help in the reconstitution of the funerary practices. The site offers a great potential from an entomological point of view. The finding of puparia within the cavity of the bones suggests that the identified necrophagous flies are not associated to the decomposition of corpses which those bones belong to, rather they are linked to the decomposition of other bodies placed subsequently. This datum supports the hypothesis of secondary depositions, meaning that the burial site was opened and closed more than once. In addition, the biology of taxa provided further information about the funerary practices, in terms of burial procedure and its seasonality (Dirriegl and Greenberg, 1995, Gilbert and Bass, 1967, Nystrom et al., 2005, Huchet and Greenberg, 2010). The identification of flies within the Calliphoridae family, well known as the first colonisers of a cadaver (Smith, 1986), indicates that corpses were left exposed long enough to allow the flies to lay eggs and developed on them, as proven by the findings of hatched puparia. At the same time, the absence of fly species belonging to other families suggests that the bodies were buried soon after the colonisation of the blow flies. Based on the observation of posterior spiracles, the survived intact characters of identification, species *C. vicina* and *Lucilia* sp. were identified. This datum provides information of the seasonality of the exposure of the corpses, likely falling between early summer and early autumn as confirmed by the seasonal distribution of these species (Hwang and Turner, 2005, Vanin et al., 2008, Prado e Castro et al., 2011, Prado e Castro et al., 2012). However, this might be in contrast with the finding of the single specimen of *N. rufipes* (Coleoptera: Cleridae); *Necrobia rufipes* is known to be of forensic important as it can be found in association to human bodies during the late stages of the decomposition and can be used for the estimation of the mPMI (Turchetto et al., 2001, Bugelli et al., 2015). This species feeds on exposed dried human/animal remains and can be predators of fly larvae (Byrd and Castner, 2001, Gennard, 2007) and it is rarely found on cadavers buried at depths

greater than 30 cm (Pastula and Merritt, 2013). Unfortunately, the information about the depth at which the human bones were found was not communicate by the archaeologists in charge of Macomer excavation, however we are reasonably led to speculate that the burial of corpses in mass graves exceeds 30 cm by far. Therefore, likely the finding of a few fragments of *N. rufipes* is not strictly related to the decomposition of the remains, rather it can be interpreted as a contamination taxon and its presence can be explained by multiple subsequent depositions of the remains (Huchet, 1996).

On the other hand, the state of preservation of the puparia is a key factor to better describe the taphonomy of the grave, and it is worth to be discussed in relation to data of Via Satta well as by the evaluations of the contexts allows to describe a similar scenario and to draw a similar interpretation of the taphonomic process involved in the preservation of the entomological remains. The decaying context of the burials in Macomer along with the constant presence of saturated groundwater created the conditions to favour the permineralisation of the Diptera remains, guaranteeing their high fidelity preservation mainly as mold/cast or mineral replaced, rather than normally preserved (Fig. 4.26, Fig. 4.27). In this context, mineralogical analysis could not be performed in order to preserve the integrity of the archaeological collection and the limited number of available specimens prevented to apply destructive analytical techniques such as powder XRD and FTIR. However, they would have certainly added useful information about the nature of the crystals and on the reconstitution of the micro-environment of the grave. However, we are led to speculate about the inorganic phosphate composition of Macomer findings due to taphonomic transformation of the bones. The dark colouration and scattered bluish spots on bones surface (as per personal communication by Rodriguez (Universitat Autònoma de Barcelona)) are typical of the vivianite (McGowan and Prangnell, 2006, Rothe et al., 2016). Named after the English mineralogist John Henry Vivian (1785-1855) who first found the mineral in its crystalline form in Cornwell (England), vivianite is a hydrated iron phosphate mineral with the formula $\text{Fe}_3(\text{PO}_4)_2 \cdot 8\text{H}_2\text{O}$ (McGowan and Prangnell, 2006). Vivianite is colourless prior the exposure to the air which triggers a change colour into bluish/greenish which become progressively darker due to a process of oxidation (Teodorowich, 1961). This mineral is worldwide distributed both in aquatic

and terrestrial systems such as waterlogged soils, wastewater sludges, and archaeological settings often in association to human and animal remains and waste deposits in close proximity to a source of iron (McGowan and Prangnell, 2006, Mann et al., 1998, Owsley and Compton, 1997). Specifically, the formation of the mineral in archaeological records shows constantly the combination of waterlogged anoxic soils, presence of a phosphate source such as human and animal bones/tissue, and the presence of iron source. Macomer grave satisfies all these requirements, with iron likely deriving from the soil or due to the presence of iron objects included in the burial (McGowan and Prangnell, 2006). In addition, the activity of the microbial communities inhabiting the soils and carrying on the decomposition of the organic matter seems to have an important role in the formation of the vivianite, with particular regards to iron and sulphate reducing bacteria. The release of solutes such as phosphate compounds and Fe^{2+} into the soil along with adsorption-desorption and other mechanisms, causes the fixation of P into iron and calcium phosphates salts such as vivianite and apatite (Rothe et al., 2016). The presence of iron-phosphate minerals in Macomer findings so far remains only a hypothesis which would require further research.

Overall, the formation of the crystal assemblages involved various micro-environmental conditions including several biotic factors, such as *post mortem* and environmental microbial communities (Benbow et al., 2015), and abiotic factors, such as temperature, pH, humidity, and hydrogeological balance. All these elements can differently combine, thus creating specific conditions which are difficult to investigate and reconstruct. However, the importance of considering all the elements contributing to the taphonomy of a specific context in order to reconstruct past events, such as depositional events of human remains based on insects investigations, has been herein demonstrated.

4.3 CONCLUSIONS

This work provides an innovative contribution to environmental archaeology research belonging to Italian heritage. Results of archaeoentomological investigations conducted on archaeological material excavated from two Sardinian sites have been presented as the first record in the island, as well as the first record of mineralised samples at national level. The analysis of Diptera remains were key to interpret archeological sites and potential ecological changes, not only based on the biology of the identified species but also based on their state of preservation.

The canonical morphological identification allowed to reconstruct how a medieval urban well was used, and *post mortem* events of a group of individuals buried in a grave of Roman origin. On the other hand, a deep understanding on how taphonomic processes such as mineralisation are involved in the preservation of the remains also contributed to further support archaeological hypothesis, pointing out that a constant inter-disciplinary approach is key in archaeoentomology research.

Additionally, a piece of information has been added to the molecular archaeology field, outlining how taphonomic processes undertaken by insects remains can be detrimental to genetic analysis.

5

MORPHOLOGICAL DESCRIPTIONS AND DNA BARCODING OF DIPTERA OF FORENSIC INTEREST

5.1 *PHYSIPHORA ALCEAE* (PREYSSLER, 1791) (ULIDIIDAE): MORPHOLOGICAL DESCRIPTIONS, DNA BARCODING AND PHYLOGENETIC ANALYSIS

5.1.1 Results

Morphological descriptions

Adults of *Physiphora alceae* (Preyssler, 1791) (Ulidiinae) can be identified by the colour of their legs, wing shape and microtrichose pattern on the frons. Legs are black with the foreleg showing a creamy-yellow metatarsus (Fig. 5.1).

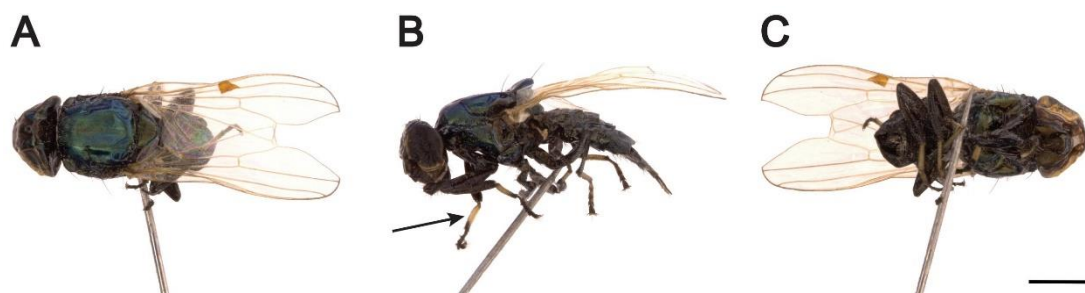


Fig. 5.1 *Physiphora alceae* adult. (A) dorsal, (B) lateral, (C) ventral view. The black arrow indicates the foreleg with the creamy-yellow metatarsus. Scale bar: 1 mm. Photos by Dr Giorgia Giordani.

Wings are totally hyaline with the cell r_{4+5} almost closed similar to *Physiphora longicornis* (Hendel, 1909) (Chen and Kameneva, 2007) (Fig. 5.2A). Two narrow microtrichose patches on each side of the frons represent a further typical morphological character of the species (Fig. 5.2B). A more detailed description was provided by Kamaneva and Korneyev (2010).

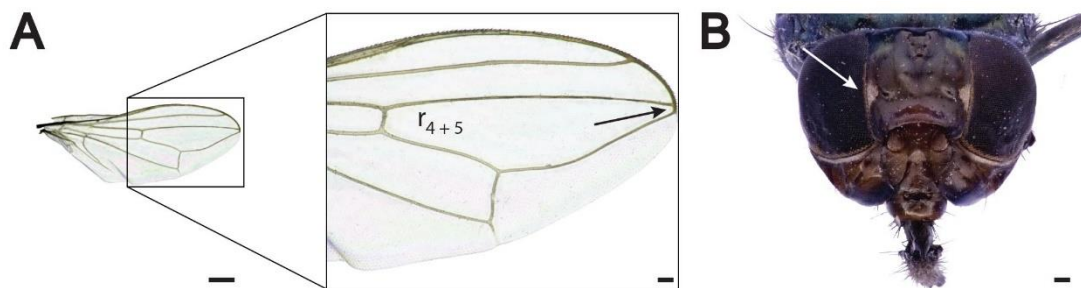


Fig. 5.2 *Physiphora alceae* adult details. (A) Wing showing the r_{4+5} cell almost closed and (B) frontal view head. The white arrow shows the typical narrow white microtrichose patches. Scale bar: (A) 500 μ m, (B) 100 μ m. Photos by Dr Giorgia Giordani.

III instar larva. The body length of third instar larvae is 8.2 ± 0.3 mm (N=3) (Fig. 5.3). Anterior spiracle with short flattened stalk bearing 13–15 nodular branches ranged fan-wise with a slight median introflection (Fig. 5.3A). The posterior spiracles not protruding from the spiracular disc are very close to another and show an ovoid-like shape with a thin, dark-brown and close peritreme (difficult to be seen in the diaphanised specimens) (Fig. 5.3C). The spiracular scar is not included in the peritreme and is located in the dorsal side of each spiracle. The three respiratory slits have an arcuate radial arrangement and converge towards the spiracular scar. Slits one and two are specular and slightly curving one towards the other at the lower extremity (Fig. 5.3C,D).

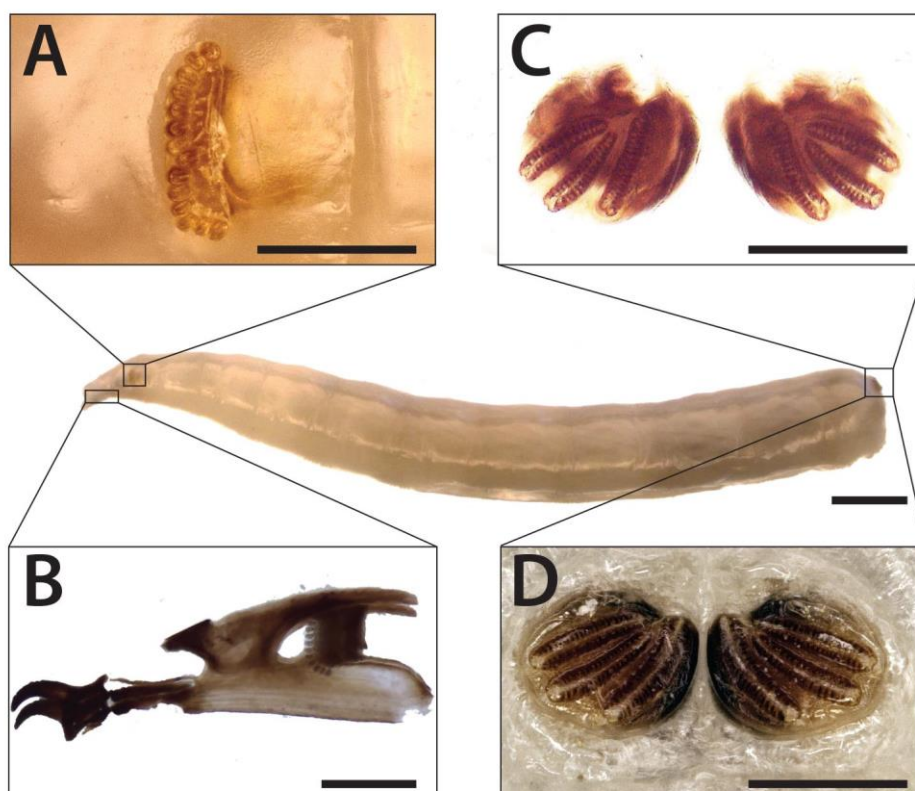


Fig. 5.3 *Physiphora alcaeae* III instar larva morphology. (A) anterior spiracle, (B) cephaloskeleton (C,D) posterior spiracles. Anatomic details have been observed on III instar specimens stored in EtOH 70%. (A, D) and after diaphanisation of soft tissue in NaOH solution (C, B). Scale bars: 1 mm (full length larva), (B) 200 μ m (B), 100 μ m (A,C,D).

The cephalopharyngeal skeleton varies from light to dark brown in colour and measures 0.85 mm x 0.28 mm (maximum length and maximum width respectively) (Fig. 5.3B, Fig. 5.4). The mandible is well sclerotised, has two sharply hooked teeth and a sharp robust

dental sclerite. The basal part of the mandible has a robust process postero-dorsally oriented. The parastomal bar and hypopharyngeal sclerite are elongated and slender. Dorsal cornu of the tentoropharyngeal sclerite is arched, slender, large 1/3 of the ventral cornu, without window. The dorsal (anterior) bridge is robust and well sclerotised. Ventral part of the ventral cornu straight (Fig. 5.4).

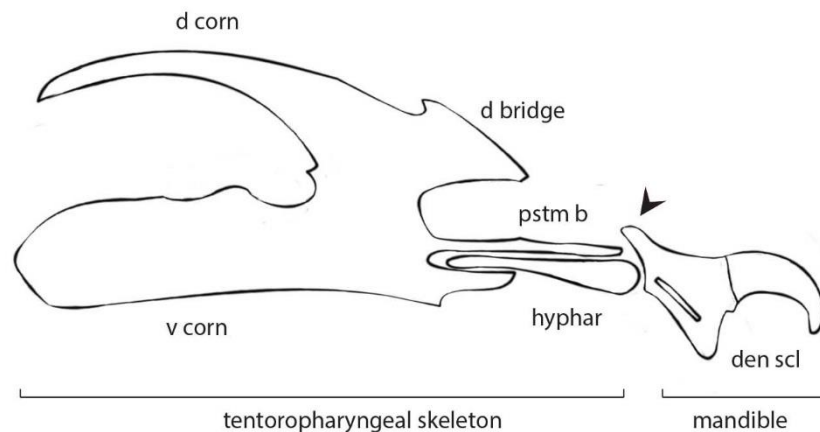


Fig. 5.4 *Physiphora alceae* cephalopharyngeal skeleton morphology of III instar larva. Mandible is composed of dental sclerite (den scl) and its basal part shows a robust process postero-dorsally oriented (black arrow). The hypopharyngeal sclerite (hyphar) links the mandible to the tentoropharyngeal skeleton composed of parastomal bar (pstm b), dorsal bridge (d bridge), dorsal cornu (d corn) and ventral cornu (v corn).

Puparium. Ochre in colour, it measures 4-5 mm in length (Fig. 5.5A-C). The anterior extremity of the puparium seen from a lateral view shows a tapered shape (Fig. 5.5C). Posterior spiracles are very close (Fig. 5.5D). The same characters observed for the III instar larva are also well conserved in the puparium morphology: oval-rounded posterior spiracles, spiracle scar in the dorsal side and excluded by the peritreme which is complete, thick and varies from dark-brown to black in colour, radial oriented respiratory slits (Fig. 5.5D). The anterior spiracles are composed of twelve yellowish finger-like lobes. The intersegmental spines of ventral welt of the seventh abdominal segment are distributed in six ordinate and continuous rows except for the third where spines are grouped by five or six (Fig. 5.5E). The majority of the spines extend forward towards the anal plate but some others are back oriented. In the two rows closest to the anal division spines are large, generally with single rounded tip while finer, shorter and sharp tipped spines form the remaining rows (Fig. 5.5F).

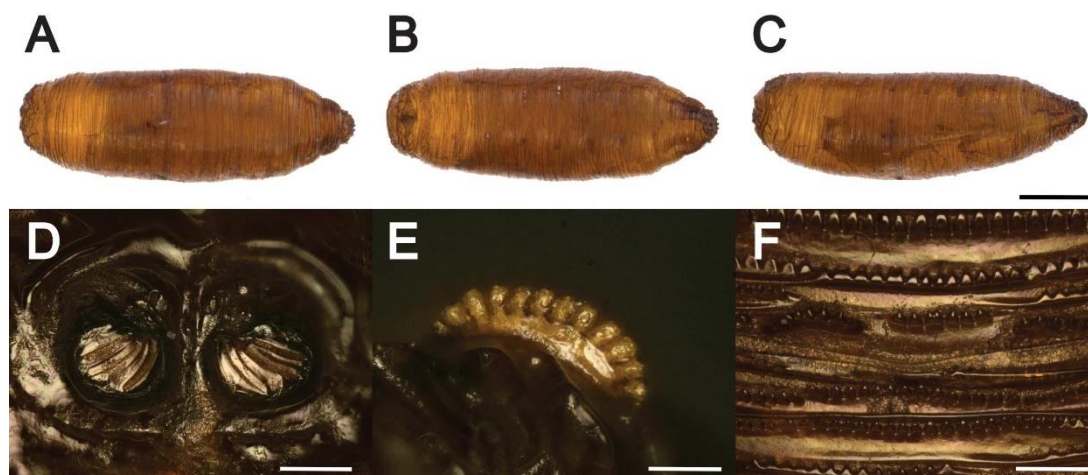


Fig. 5.5 *Physiphora alceae* puparium. (A) dorsal, (B) ventral, (C) lateral view, (D) posterior spiracles, (E) anterior spiracles, (F) ventral spines of abdominal segment 7th. Scale bars: 1 mm (A,B,C), 100 μ m (D,E), 50 μ m (F). Photos by Dr Giorgia Giordani.

Molecular analysis and phylogenetic reconstruction of Ulidiidae

The morphological identification was confirmed by the sequencing of the COI barcoding target and the nucleotides sequences generated have been uploaded on the public dataset [GenBank access numbers: MH686505, MH686506]. The ClustalW alignment produced a dataset of 61 sequences of equal length (520 nucleotide positions) and counting 307 constant sites and 205 informative sites. The GTR+F+I+G4 was selected as the best substitution model, showing the highest w-AIC_c (+0.9647) and the lowest BIC (131107.8044) and used to build the Maximum Likelihood tree with a Log-likelihood of -6098.9844 (Fig. 5.6). The distinction between the two subfamilies Ulidiinae and Otitinae is well supported by the molecular phylogenesis (BS: 98). The node between the groups *Timia-Ulidia* and *Physiphora* is weakly supported by a BS of 48, and both of them are monophyletic. In the first group, no further separation was observed in regards to superior taxonomic levels (genus, species). Within the subfamily Otitinae, the monophyly of the genera is generally well supported while no further well supported clusters distinction can be argued. Additionally, the genus *Homalocephala* shows an unresolved position. In fact, sequences of species within this genus cluster both in the Ulidiinae (*H.*

apicalis) and in the Otitinae (*H. albitarsis* and *H. angustata*) subfamilies, thus showing that the taxonomic resolution of this genus remains unresolved (Fig. 5.6).

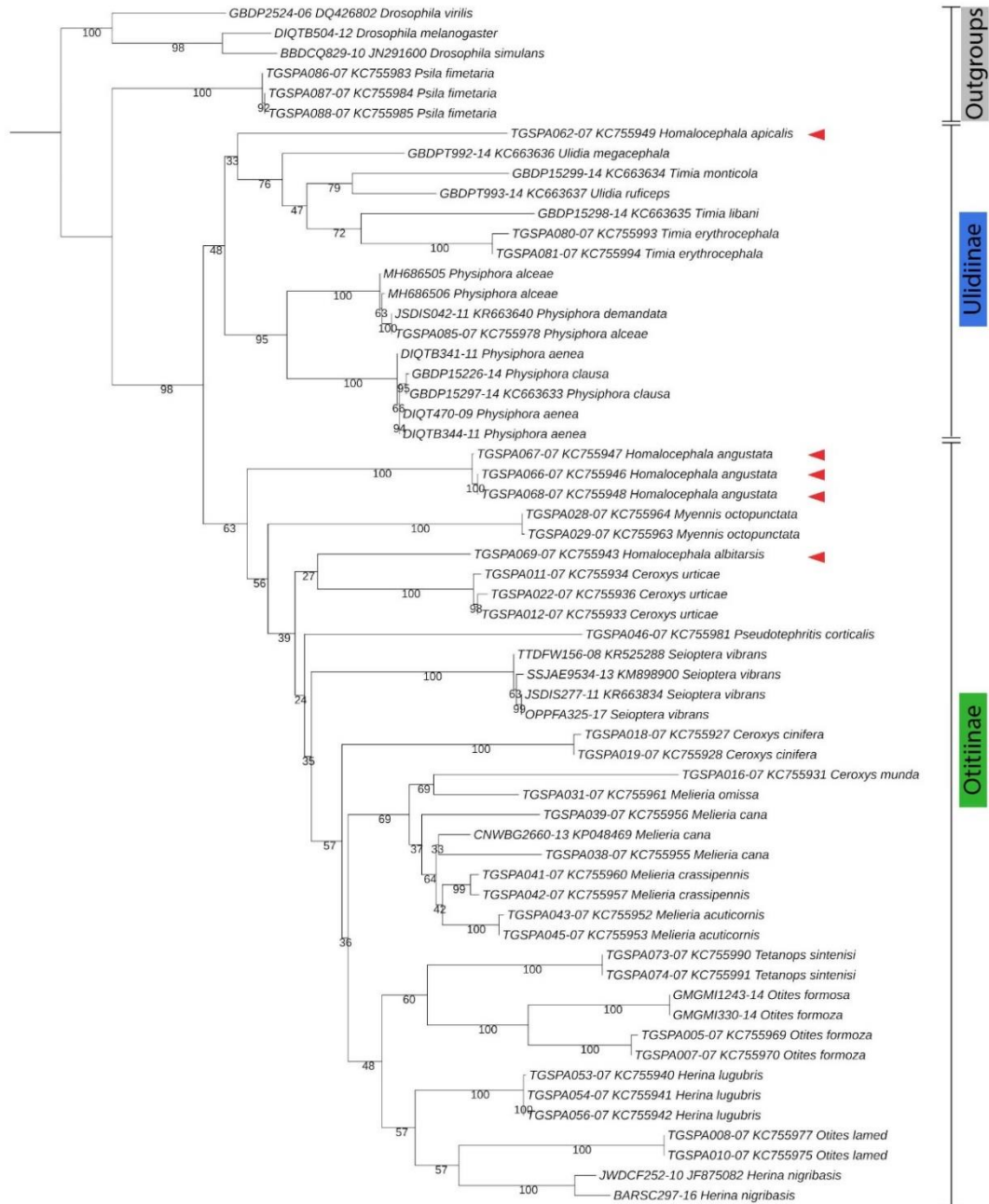


Fig. 5.6 Maximum Likelihood phylogenetic tree. The phylogenetic tree was derived by the alignment of 61 mtCOI barcoding sequences of equal length (520 bp). The displayed topology was obtained upon the selection of the best substitution model (Log-likelihood = -6098.9844). The evolutionary distance between Ulidiinae and Otitinae is strongly supported (BS=98). Red arrows point out to the *Homalocephala* sp.

5.1.2 Discussions

In forensic entomology, the correct, unequivocal identification of the species is the essential step to accomplish the several tasks requested by the legal authorities (Amendt et al., 2004b, Amendt et al., 2007, Amendt et al., 2011). The morphological approach is highly encouraged by taxonomist who dedicate to develop descriptions and/or identification keys to facilitate the work of non-experts (McAlpine et al., 1981, Skidmore, 1985, Smith, 1986, McAlpine et al., 1987, Domínguez and Pont, 2014). However, the available information don't fully cover all the species of forensic interest, and for poorly studied species which are occasionally recovered from forensic contexts, there is still a lack of information. The family Ulidiidae has been receiving more and more attention in forensic entomology as, according to recent studies, species within this family have been found in association to animal carcasses (Sawaby et al., 2018, Al-Mesbah et al., 2012, Baz et al., 2015). Specifically, in the last 10 years, several records described *P. alceae* from animal carcasses used for experimental purposes. The present record of the species from a forensic case in Norther Italy seems to be the first case ever related to a human cadaver and strengthens the hypothesis that Ulidiidae might play a role in forenisc investigations. A complete description of the adults was provided by Galinskaya (Galinskaya et al., 2014) but nothing has been published yet about the immatures, which, indeed are the most frequently collected specimens on crime scenes or during the medico-legal inspections. The Italian case offered the opportunity to accurately describe the morphology of the third instar larva and the puparium, which were so far unknown. The presence of adult specimens found in the assemblage was key to corroborate the morphological identification of the immatures, as in accordance to the European guidelines which recommend, whether possible, to rear the immatures to facilitate the analysis (Amendt et al. 2007). The certainty of the morphological identification allowed to deposit DNA barcoding sequences on GenBank enriching the scarce molecular data available for *P. alceae*. The molecular results were further corroborated through the phylogenetic approach, mainly referring to the work of Galinskaya et al. (2014) who exhaustively outlined the DNA barcoding of Palearctic Ulidiidae and made a comparison with the morphological data of the family. In contrast to their dataset, a smaller dataset of COI

sequences (61) was used, but it was specifically composed of sequences of equal length in order to provide sufficient information for the phylogenetic reconstruction. In addition, unlike the above-mentioned authors, testing different substitutions models fell out of the purposes of the presented work. Our results strongly support the monophyly of the groups Ulidiinae and Otitinae (BS 98, Fig. 5.6). and the observations related to the species separation and to the genus *Homalocephala* are in line with previous results. So far, the taxonomic resolution of this genus has not been well defined yet (Galinskaya et al., 2014) due to the high similarity of its morphological features shared between both Ulidiinae and Otitinae species. In addition, the phylogenesis based on the barcoding target seems not to resolve this strong debate among taxonomists, suggesting that other DNA targets should be tested to evaluate any improvement.

5.2 COMPARATIVE STUDY OF “SKIPPER FLIES” (DIPTERA: PIOPHILIDAE) OF FORENSIC INTEREST: DESIGN OF A DICHOTOMY KEY FOR THE IDENTIFICATION OF PUPARIA AND DNA BARCODING

5.2.1 Results

Pictorial archive and comparative study of puparia morphology

The description of the full puparium (Fig. 5.7), ventral creeping welts (Fig. 5.8) anterior spiracles (Fig. 5.9), anal region with ventral anal tubercles (Fig. 5.10), and posterior spiracles (Fig. 5.11) is provided per each species, and the inter-taxa differences are underlined.

***Centrophlebomyia furcata* (Fabricius, 1794)**

First described by Freidberg (Freidberg, 1981), the full puparium is opaque, pale brown, anteriorly tapered and posteriorly truncated. It is considerably longer and wider than the other Piophilidae described in this study. The length is about 6.84 ± 0.16 mm (N = 3) (Fig. 5.7A). The ventral creeping welts are arranged in 4 equally distant rows and in group of 4-7. The spines are equally oriented towards the posterior end, thick, round-tipped, and of the same size (Fig. 5.8A). Anterior spiracles counting 12 respiratory lobes and papillae slightly introflexed in the central part (Fig. 5.9A). The anal segment is rough and bears a pair of divergent not elongated ventral anal tubercles of equal length (Fig. 5.10A), similar to *P. xanthosoma* (Fig. 5.10E) and *L. varipes* (Fig. 5.10G). Posterior spiracles with three respiratory slits radially arranged and no visible sensilla.

***Piophila megastigmata* McAlpine, 1978**

Bright ochre in colour, the length of the full puparium measures 3.63 ± 1.21 mm (N = 11) (Fig. 5.7B). Slightly larger at the anterior end, the puparium is narrow and truncated at the posterior end as in *L. varipes* (Fig. 5.7C). The ventral creeping welts are arranged in 3 rows with the first two closer than the third one. All the spines are equally oriented towards the posterior end of the puparium and have a finger-like shape, but are bigger

and thicker in the central row, medium in the superior row⁷, and smaller in the inferior⁸ row (Fig. 5.8B). Anterior spiracles have a bilobed fan-shape structure similar to *S. nigriceps* (Fig. 5.9D), *P. xanthosoma* (Fig. 5.9E), *P. nigrimana* (Fig. 5.9F), and *L. varipes* (Fig. 5.9G) and with 12 respiratory lobes (Fig. 5.9B), keeping the same morphology as in the third instar larva (Panos et al., 2013). Short, convergent, and truncated ventral anal tubercles (Fig. 5.10B). Posterior spiracles with three respiratory slits radially arranged and four sensilla disposed alternately, with the medians slightly smaller (Fig. 5.11B).

***Piophilila casei* (Linnaeus, 1758)**

First described by Simmons (Simmons, 1927), the puparium is light brown in colour and the studied specimens showed a full length of 4.40 ± 1.53 mm (N = 16) and of 3.07 ± 0.68 mm (N = 12) when opened (Fig. 5.7C). It is often confused with *P. nigrimana*, but the latter is shorter (Fig. 5.7F) (Martín-Vega et al., 2012). Puparium is truncated at posterior end, and it shows well-marked ventral welts arranged in 3 rows as in *P. megastigmata* but with spines different in shape. The spines in the superior row are big, thick, arranged in groups of 4–6 and sharpened, while the spines in the third row are remarkably smaller, arranged without interruption and with a botton-like shape (Fig. 5.8C). Anterior spiracles have a bilobed finger-like shape, truncated rather than tapered and numbering till 9 respiratory lobes (Fig. 5.9C). Despite the bilobed shape, the border between the two lobes is not well defined as in other species. The puparium shows a pair of elongated ventral anal tubercles which are almost perpendicular to the anal division (Fig. 5.10C). Posterior spiracles with three respiratory slits radially arranged and four rounded sensilla disposed alternately (Fig. 5.11C).

***Stearibia nigriceps* (Meigen, 1826)**

The colour of the puparium is bright yellowish and the size is similar to *P. casei* and *P. xanthosoma*. Posterior end not truncated and ventral welts well visible (Fig. 5.7D), arranged in 2 rows (Fig. 5.8D) similarly to *P. xanthosoma* and *L. varipes* (Fig. 5.8E,G) but

⁷ Closer to the posterior end of the puparium, thus the first row from the top in Fig. 5.8

⁸ Closer to the anterior end of the puparium, thus the first row from the bottom in Fig. 5.8

showing sharpened tips rather than pointed or drops-like. Anterior spiracles have a bilobed fan-like structure, with 12 elongated finger-like respiratory lobes (Fig. 5.9D), similar to *L. varipes* (Fig. 5.9G). The anal region is rather rough and show a pair of slightly elongated, curved, pointed and convergent ventral anal tubercles (Fig. 5.10D), similar to *L. varipes* (Fig. 5.10G). Posterior spiracles show three respiratory slits radially arranged with only the two median rounded sensilla visible in the examined specimen (Fig. 5.11D).

***Prochyliza xanthosoma* Walker, 1849**

Light brown in colour, the full length puparium measures 3.90 ± 0.22 mm (N = 10), it is not truncated at the posterior end and shows well defined ventral creeping welts (Fig. 5.7E) arranged in 2 rows and equally oriented toward the posterior end (Fig. 5.8E). The spines in the superior row are slightly larger than the other row, but all with rounded-tips (Fig. 5.8E). Anterior spiracles have a bilobed fan-like shape with 12 respiratory lobes as the previous species but appearing more compressed (Fig. 5.9E). Anal division very rough and bearing a pair of elongated, pointed, and positioned outwards at 45 degrees ventral anal tubercles (Fig. 5.10E). Posterior spiracles very similar to *P. megastigmata* (Fig. 5.11B), *P. nigrimana* (Fig. 5.11F), and *P. flavipes* (Fig. 5.11I) showing three respiratory slits radially arranged with four pointed trichoid sensilla disposed alternately (Fig. 5.11E).

***Prochyliza nigrimana* (Meigen, 1826)**

Light brown in colour, the length of the full puparium measures 3.72 ± 0.12 mm (N = 10), while the open puparium measures 1.65 ± 0.11 mm (N = 5) in the studied specimens (Fig. 5.7F). Truncated at the posterior end, it shows a defined pattern of the ventral spines arranged in 3 rows, similarly to *P. megastigmata* and *P. casei* (Fig. 5.8B,F). However, unlike *P. casei*, the spines are arranged with no interruptions in all the three rows and have drops-like pointed tips (Fig. 5.8F). The anterior spiracles have a fan-shape with 10-11 respiratory lobes (Fig. 5.9F) arranged very similar to *Piophila* species (Fig. 5.9B,C,D). The ventral anal tubercles are not elongated (Fig. 5.10F). As in the other species, the three slits of the posterior spiracles are radially oriented and as in *P. megastigmata* there are four trichoid sensilla disposed in between them (Fig. 5.11F).

***Liopiophila varipes* (Meigen, 1830)**

Previously described by Martín-Vega (Martín-Vega et al., 2014), the barrel-shaped puparium show a light ochre colouration, and it measures 3.52 ± 0.90 mm (N = 13) in its full length, and 2.65 ± 0.16 mm (N = 7) when open (Fig. 5.7G). The ventral creeping welts are arranged in 2 rows with spines not showing defined tips but a more button-like shape and slightly larger in one of the two rows (Fig. 5.8G). The anterior end is compressed, and as in *P. casei* and *P. nigrimana* the posterior end is truncated, but *L. varipes* shows poorly marked ventral spines (Fig. 5.10G). The anterior spiracles have a fan-shaped structure with 9–11 finger-like respiratory lobes as in *S. nigriceps* (Fig. 5.9G). Anal division is slightly rough, and the ventral anal tubercles are not elongated (Fig. 5.10G). In the posterior spiracles, four trichoid round-shape sensilla are alternately disposed between the three radially oriented respiratory slits (Fig. 5.11G).

***Parapiophila vulgaris* (Fallen, 1820)**

Bright ochre in colour, the puparium has a barrel shape but, in contrast to the other species here described, it is wider and its length is very similar to *P. xanthosoma* (Fig. 5.7H). None of the end are compressed or truncated and the ventral creeping welts are well marked and visible (Fig. 5.10H). The sharpened spines are arranged in 6 rows equally oriented toward the posterior end except for the second row which also shows smaller spines (Fig. 5.8H). The spines in the first row are the largest and rather distant one to another compared to the spines in the other rows. Spines in the last three rows are arranged in groups of 3–5 (Fig. 5.8H). The anterior spiracles are arranged in one hand-like structure, rather than bilobed, and count five respiratory lobes (Fig. 5.9H). The posterior end is very rough and the anal division shows a pair of elongated ventral anal tubercles (Fig. 5.10H). The three slits of the posterior spiracles are arranged similarly to the other species and show four trichoid button-like sensilla in between them (Fig. 5.11H).

***Parapiophila flavipes* (Zetterstedt, 1847)**

Previously described by Martín-Vega (Martín-Vega, 2017), the puparium is bright ochre in colour, and has a barrel shape resembling *P. vulgaris* but shorter as the full length

puparium measure 3.01 ± 0.18 mm (N = 10) in the studied specimens (Fig. 5.7I). As *P. vulgaris* also shows a well-marked ventral welt (Fig. 5.10I) but the arrangement and the morphology of the spines are remarkably different. In *P. flavipes*, the spines are arranged in 6–8 rows and are equally oriented towards the posterior end except for one of the central rows which also show smaller spines (Fig. 5.8I). Differently to the Martín-Vega description (2017), in the analysed specimens the first two rows show thicker spines. All the spines are drop-shaped and are separated one from another with a distance which is equal to the size of the spines themselves (Fig. 5.8I). Anterior spiracles are mono-lobed, and hand-like, counting 3–4 respiratory lobes (Fig. 5.9I). The anal division is rather rough and bears ventral anal tubercles not elongated (Fig. 5.10I). Posterior spiracles not much different from the other Piophilidae species, with three respiratory slits radially arranged and spaced out by four sharpened trichoid sensilla as in *P. megastigamata* (Fig. 5.11I).

***Protopiophila litigata* Bonduriansky, 1995**

With a pale opaque light brown colour, the puparium of *P. litigata* is the smallest in size among the Piophilidae here presented, with a full length measuring 2.82 ± 0.82 mm (N = 10). It shows a cylindrical shape which is narrower at the posterior end (Bonduriansky, 1995) (Fig. 5.7J). The ventral creeping welts are difficult to see using the stereomicroscope only. The SEM provided a better resolution showing an arrangement in 2 rows like *P. xanthosoma*, *P. nigrimana*, and *L. varipes* but, unlike them, the rows are arranged closer and the spines are smaller with truncated tips. In addition, the spines of the first row are thinner (Fig. 5.8J). Ventral anal tubercles are not easily distinguishable in the anal division (Fig. 5.10J). Anterior spiracles fan-shaped arranged in a compact structure showing 6–7 respiratory lobes (Fig. 5.9J). Posterior spiracles similar to *P. vulgaris* with four button-like sensilla disposed between the three respiratory slits radially oriented (Fig. 5.11J).

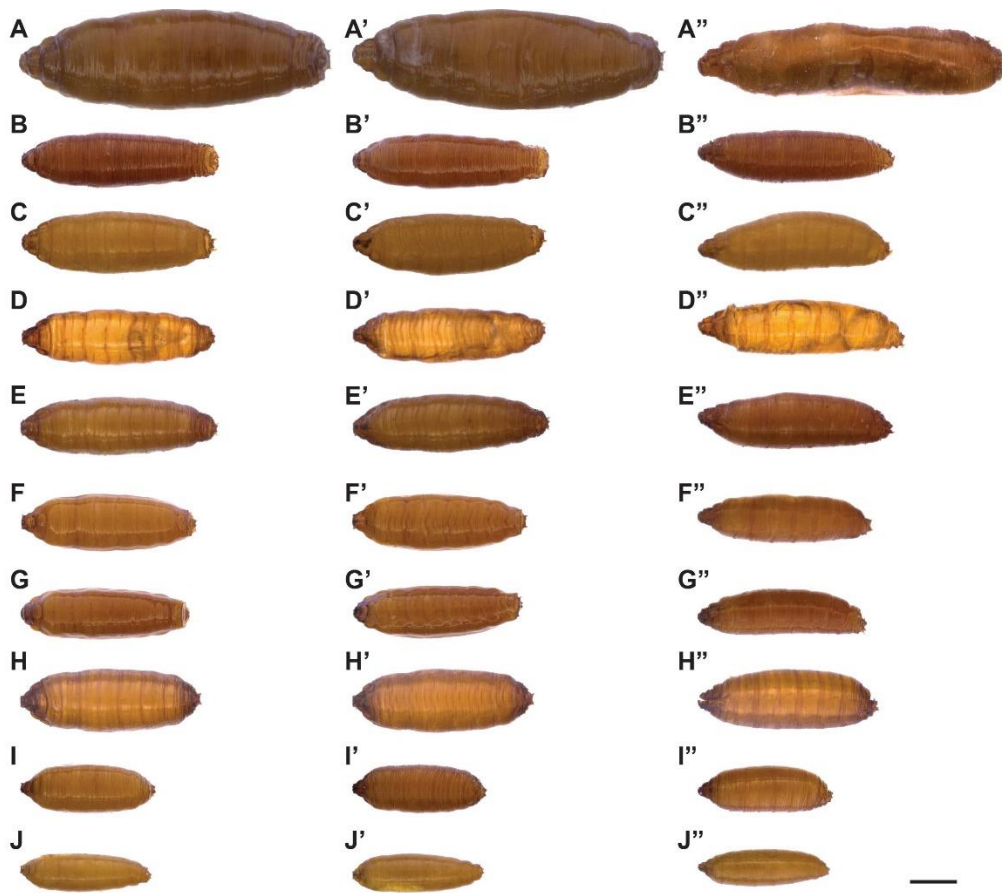


Fig. 5.7 Comparison of ten Piophilidae full puparia. Dorsal, ventral (‘), and lateral (‘’) view of full puparia. (A) *Centrophlebomyia furcata*, (B) *Piophila megastigmata*, (C) *Piophila casei*, (D) *Stearibia nigriceps*, (E) *Prochyliza xanthosoma*, (F) *Prochyliza nigrimana*, (G) *Liopiophila varipes*, (H) *Parapiophila vulgaris*, (I) *Parapiophila flavipes*, (J) *Protopiophila litigata*. Scale bar: 500 μm . Pictures by Dr Giorgia Giordani.

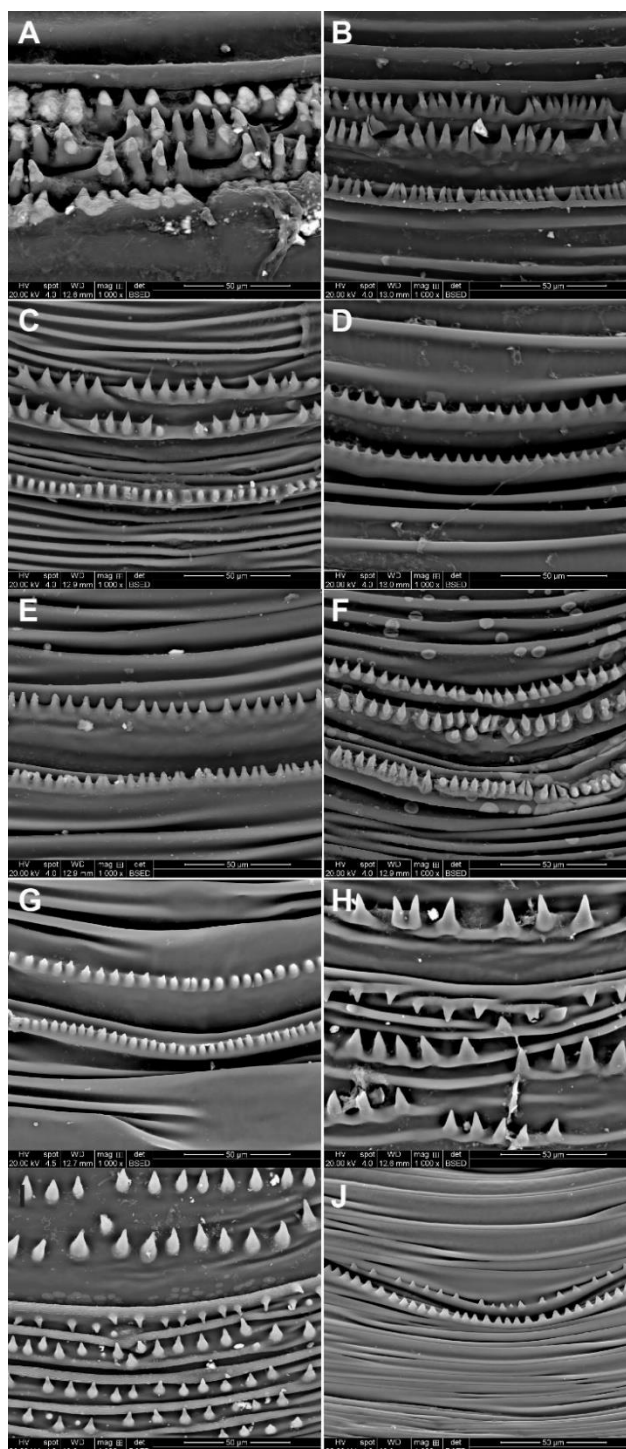


Fig. 5.8 Piophilidae ventral creeping welts SEM view. In each picture, the number of rows is counted from the top to the bottom and follow the posterior-anterior orientation. Nomenclature follows Fig. 5.7. (A) *Centrophlebomyia furcata*, (B) *Piophila megastigmata*, (C) *Piophila casei*, (D) *Stearibia nigriceps*, (E) *Prochyliza xanthosoma*, (F) *Prochyliza nigrimana*, (G) *Liopiophila varipes*, (H) *Parapiophila vulgaris*, (I) *Parapiophila flavipes*, (J) *Protopiophila litigata*. Scale bar: 50 µm. Pictures by Dr Giorgia Giordani.

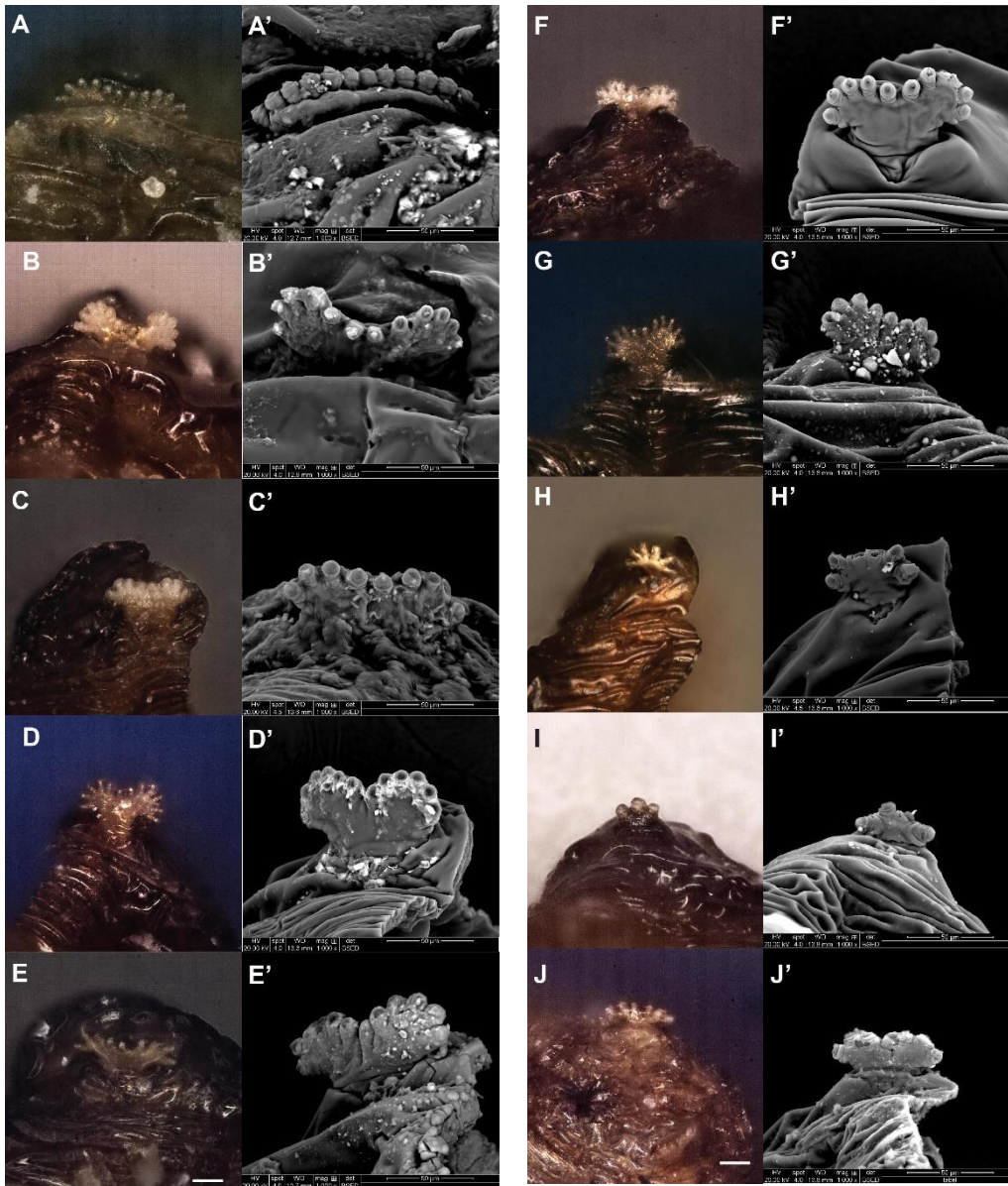


Fig. 5.9 Piophilidae anterior spiracles. Keyence digital microscope (left) and SEM images (right) of the anterior spiracles. Nomenclature follows Fig. 5.7. (A) *Centrophlebomyia furcata*, (B) *Piophila megastigmata*, (C) *Piophila casei*, (D) *Stearibia nigriceps*, (E) *Prochyliza xanthosoma*, (F) *Prochyliza nigrimana*, (G) *Liopiophila varipes*, (H) *Parapiophila vulgaris*, (I) *Parapiophila flavipes*, (J) *Protopiophila litigata*. Scale bars: 50 µm. Pictures by Dr Giorgia Giordani.

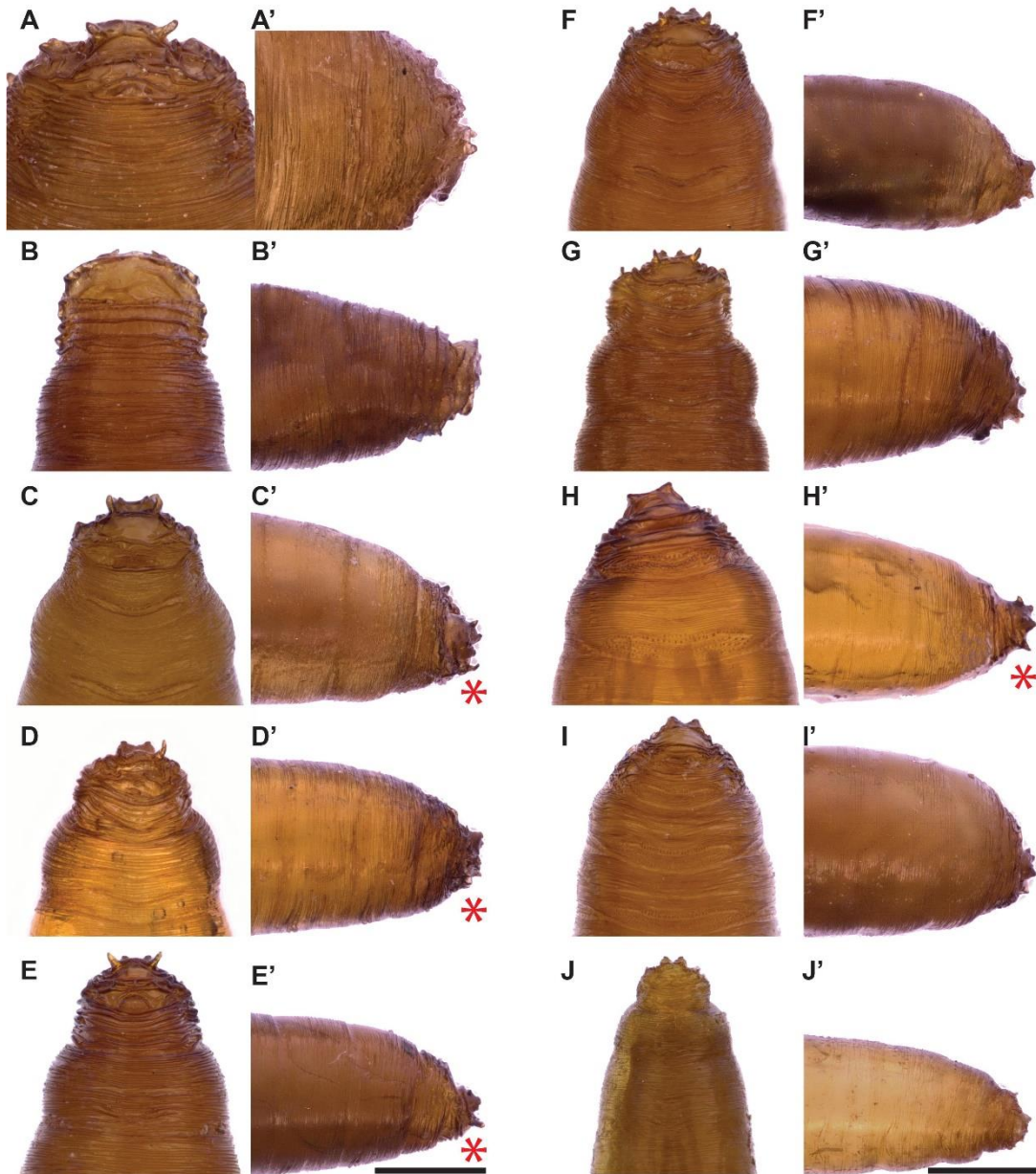


Fig. 5.10 Anal region of Piophilidae puparia. Ventral (left) and lateral (right) view of the anal division showing the extension of the ventral anal tubercles (red*) elongated in (C,D,E,H). Nomenclature follows Fig. 5.7. (A) *Centrophlebomyia furcata*, (B) *Piophila megastigmata*, (C) *Piophila casei*, (D) *Stearibia nigriceps*, (E) *Prochyliza xanthosoma*, (F) *Prochyliza nigrimana*, (G) *Liopiophila varipes*, (H) *Parapiophila vulgaris*, (I) *Parapiophila flavipes*, (J) *Protopiophila litigata*. Scale bar: 200 μ m. Pictures by Dr Giorgia Giordani.

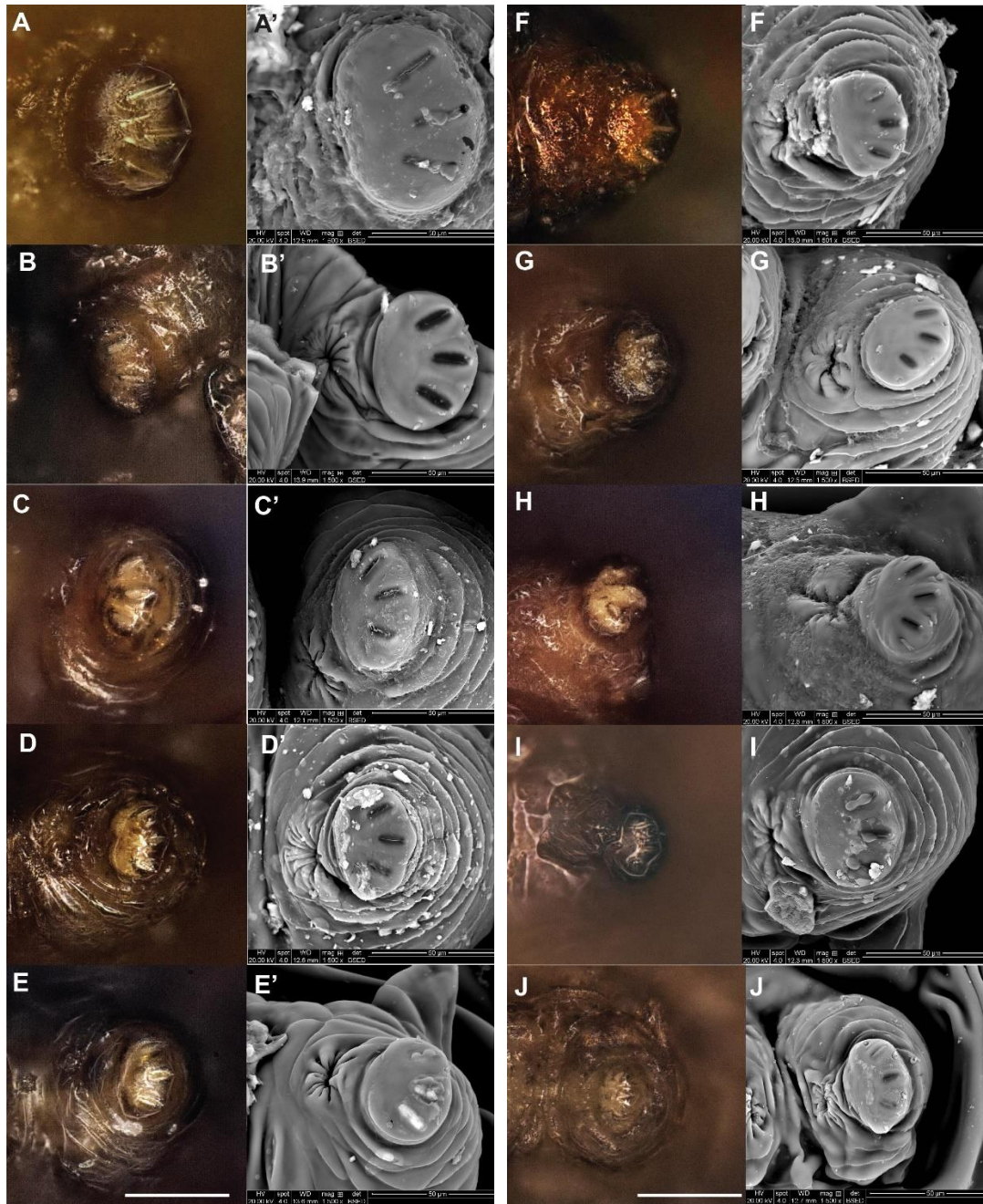


Fig. 5.11 Posterior spiracles of *Piophilidae* puparia. Keyence digital microscope and SEM images of the anterior spiracles. Nomenclature follows Fig. 5.7. (A) *Centrophlebomyia furcata*, (B) *Piophila megastigmata*, (C) *Piophila casei*, (D) *Stearibia nigriceps*, (E) *Prochyliza xanthosoma*, (F) *Prochyliza nigrimana*, (G) *Liopiophila varipes*, (H) *Parapiophila vulgaris*, (I) *Parapiophila flavipes*, (J) *Protopiophila litigata*. Scale bars: 50 μ m. Pictures by Dr Giorgia Giordani.

Overall, the morphological characters of the analysed Piophilidae puparia can be summarised as reported in Tab. 5.1. which represents the last update on the topic after the most recently data published by Martín-Vega (2017). On the basis of that, a dichotomy key for the identification of Piophilidae puparia has been drafted as illustrated in the next paragraph.

Tab. 5.1 Summary of morphological characters of Piophilidae puparia in this study.

species	figures label	no. of rows of spines in the vcw	ant.spiracles - no. of lobes	ventral anal tubercles	post. spiracles sensilla
<i>Centrophlebomyia furcata</i>	A	4	belt shape -12	not elongated, divergent	n/a
<i>Piophila megastigmata</i>	B	3	bilobed fan shaped - 12	not elongated, convergent	with the two median smaller
<i>Piophila casei</i>	C	3	bilobed finger like - 9	elongated, perpendicular	rounded
<i>Stearibia nigriceps</i>	D	2	bilobed finger like - 9	slightly elongated, convergent and sharpened	not confirmed
<i>Prochyliza xanthosoma</i>	E	2	bilobed - 12	elongated, divergent, pointed	pointed
<i>Prochyliza nigrimana</i>	F	3	bilobed fan shaped - 10/11	not elongated	
<i>Liopiophila varipes</i>	G	2	bilobed finger like - 9/11	not elongated	rounded
<i>Parapiophila vulgaris</i>	H	6	monolobed hand like-5	elongated	button-like
<i>Parapiophila flavipes</i>	I	7	monolobed hand like-3/4	not elongated	with the two median smaller
<i>Protopiophila litigata</i>	J	2	monolobed hand like-6/7	not elongated	button-like

Chapter 5

Key for the identification of puparia of Piophilidae of forensic interest

- 1) - anterior spiracles counting less than six respiratory lobes2
- anterior spiracles counting six or more respiratory lobes.....3
- 2) -spines of the ventral creeping welts arranged in 6 rows, with sharpened tips (Fig. 5.8 C,H), not equally oriented in all the rows (Fig. 5.8 H), grouped in 3-5 in the last four rows; ventral anal tubercles elongated (Fig. 5.10 C,E,H).....*Parapiophila vulgaris*
-spines of the ventral creeping welts arranged in 7 rows, drop-shaped (Fig. 5.8I), equally oriented towards the posterior end, spines in the first two rows bigger (Fig. 5.8I); ventral anal tubercles not elongated (Fig. 5.10 A,B,F,G,I,J).....*Parapiophila flavipes*
- 3) -anterior spiracles monolobed hand-like with 6/7 respiratory lobes (Fig. 5.9J), ventral creeping welts spines arranged in 2 rows, very small and with truncated tips (Fig. 5.8J); ventral anal tubercles not elongated (Fig. 5.10 A,B,F,G,I,J)*Protopiophila litigata*
-anterior spiracles bilobed fan-shaped and finger-like counting 9-12 respiratory lobes (Fig. 5.9B-F).....4
- 4) - spines of the ventral creeping welts arranged in 2 rows (Fig. 5.8D,E,G).....5
- spines of the ventral creeping welts arranged in 3 or more rows (Fig. 5.8A-C,F).....7
- 5) -ventral anal tubercles not elongated, ventral creeping spines slightly prominent with not sharpened tips (Fig. 5.8G); anterior spiracles bilobed finger-like with 9/11 respiratory lobes (Fig. 5.9G).....*Liopiophila varipes*
- ventral anal tubercles elongated.....6
- 6) - ventral anal tubercles elongated (Fig. 5.10 C,E,H), sharpened and divergent; posterior end not truncated (Fig. 5.7D,E,H,I); anterior spiracles bilobed fan-shaped with 12 respiratory lobes (Fig. 5.9E).....*Prochyliza xanthosoma*

- ventral anal tubercles slightly elongated (Fig. 5.10D); posterior end not truncated (Fig. 5.7C,F,G); anterior spiracles bilobed finger-like with 9 respiratory lobes (Fig. 5.9D);*Stearibia nigriceps*
- 7) - spines arranged in 3 rows.....8
 - spines with similar size arranged in 4 close rows (Fig. 6.14A); ventral anal tubercles not elongated (Fig. 6.16 A,B,F,G,I,J); anterior spiracles belt-shape with 12 lobes (Fig. 6.15A); full puparium ~7 mm.....*Centrophlebomyia furcata*
- 8) - third row of spines showing truncated tips (Fig. 6.14C); ventral anal tubercles elongated and orthogonal to the anal division (Fig. 6.16 C); posterior end truncated (Fig. 6.13C,F,G);*Piophila casei*
 - third row of spines showing sharpened or drop-like tips (Fig. 6.14B,F), ventral creeping welt prominent, and ventral anal tubercles not elongated (Fig. 5.10 A,B,F,G,I,J).....9
- 9) - third row of spines with sharpened tips (Fig. 6.14B) posterior end truncated (Fig. 6.13C,F,G); anterior spiracles bilobed finger-like with 10/11 respiratory lobes (Fig. 6.15F).....*Prochyliza nigrimana*
 - third row of spines with drops-like tips (Fig. 6.14F) posterior end truncated (Fig. 5.7C,F,G); anterior spiracles bilobed fan shaped with 12 respiratory lobes (Fig. 5.9B);*Piophila megastigmata*

DNA barcoding and phylogenetic reconstruction

The total DNA was successfully extracted from all the specimens as reported in Tab. 5.2.

Tab. 5.2 Qubit® 3.0 Fluorometer DNA quantification extracted from Piophilidae pupae. Concentration values are expressed in ng/μl ± standard deviation (s.dv) calculated on triplicate reads on Qubit.

species	[DNA] (ng/μl)
<i>P. casei</i>	3.61 ± 0.18
<i>P. litigata</i>	3.60 ± 0.30
<i>P. xanthosoma</i>	4.88 ± 0.16
<i>C. furcata</i>	10.50 ± 0.30
<i>P. megastigmata</i>	2.18 ± 0.17
<i>P. nigrimana</i>	3.09 ± 0.26
<i>P. flavipes</i>	6.66 ± 0.38
<i>L. varipes</i>	1.38 ± 0.12
<i>P. atrifrons</i>	19.03 ± 0.09
<i>S. nigriceps</i>	9.51 ± 0.06

The sequencing of the DNA mtCOI barcoding provided good quality nucleotide sequences of the expected size within the range of 618–653 bp (Appendix B, Supplementary Table B3). Morphological identification of the species was confirmed by molecular analysis in all the cases providing a BLAST maximum identification value ranging between 91% and 100% and an E-value equal to 0. In the case of *P. vulgaris* adult specimens the same BLAST score was obtained identifying the species as *Piophila nigriceps*/*Parapiophila* sp., and *P. nigriceps*/*Allopiophila vulgaris*. In the case of *Parapiophila atrifrons*, the GenBank database identified a match at genus level only (Tab. 5.3).

Tab. 5.3 BLAST species identification. *=the same score was obtained for the listed species.

morphological ID	source	size bp	BLAST query cover	BLAST E-value	BLAST max ID value	morphological ID confirmed
<i>C. furcata</i>	pupa	642	75%	0.00E+00	99%	✓
<i>P. megastiganta</i>	pupa	651	74%	0.00E+00	100%	✓
<i>P. casei</i>	pupa	625	77%	0.00E+00	99%	✓
<i>S. nigriceps</i>	L-II	652	99%	0.00E+00	98%	✓
<i>S. nigriceps</i>	adult	618	96%	0.00E+00	99%	✓
<i>P. xanthosoma</i>	pupa	643	99%	0.00E+00	99%	✓
<i>P. nigrimana</i>	pupa	647	74%	0.00E+00	99%	✓
<i>L. varipes</i>	pupa	647	98%	0.00E+00	91%	✓
<i>P. vulgaris</i>	adult	641	99%	0.00E+00	99%	<i>P. nigriceps</i> / <i>Parapiophila</i> sp.*
<i>P. vulgaris</i>	adult	630	97%	0.00E+00	99%	<i>P. nigriceps</i> / <i>A. vulgaris</i> *
<i>P. flavipes</i>	pupa	653	84%	0.00E+00	99%	✓
<i>P. litigata</i>	pupa	644	99%	0.00E+00	99%	✓
<i>P. atrifrons</i>	pupa	638	99%	0.00E+00	99%	genus level only

The alignment produced a block of 106 sequences counting 439 nucleotide positions, of which 275 (62.64%) constant. The GTR+F+I+G was selected as the best nucleotide substitution model based on the BIC (-8732.6) and on the AIC_c (-8250.69) values. The resulting Maximum Likelihood consensus tree with a log Likelihood value equal to -3745.76 is shown in Fig. 5.12. In order to allow an easier reading of the tree, a schematic representation of it is showed along with the taxonomy (Fig. 5.13). Results show that the molecular phylogenetic relationships among Piophilidae species does not follow their morphological classification, at least *in toto*. The genus *Centrophlebomyia* (Tyreophorina) forms an independent cluster branching outside the rest of the tree. A bootstrap value of 75 supports a clear separation between the groups Neottiophilinae-Mycetaulini-*Parapiophila* genus (Piophilina) and Piophilina-*Thyreophora* genus (Thyreophorina) which are monophyletic, with a BS value of 56 and 43, respectively. Within the first groups, the subgroups Neottiophilinae-Mycetaulini are clearly separated from the *Parapiophila/Allopiophila* genus (Piophilina) (BS 95) despite two canadian sequences of *P.*

flavipes cluster along with *Allopiophila luteata* (Mycetaulini). The internal nodes indicate a good resolution at species level showing BS values within the range 90–100. On the other hand, the genus *Protopiophila* forms a separate cluster in respect of the other Piophilina genera (BS 43) and the species *P. latipes* and *P. litigata* are well separated (BS 96). The sub-groups *Lasiopiophila-Prochyliza* and *Piophila* are separated but with a low bootstrap support (BS 27). In addition, a group of sequences of *Parapiophila vulgaris* from Germany (GenBank JN257XXX) and Romania is included in the same cluster of *Thyreophora* sp. Overall, the species are well resolved except for a few cases as highlighted in yellow in Fig. 5.12.

The pairwise distance matrix among all the *Allopiophila/Parapiophila vulgaris*, fully reported in Appendix A, Supplementary Table A5, shows values below 3%, between the European and Canadian group of sequences; values within the range of 13.9–15.6% results between German and the other European *P. vulgaris* sequences; in contrast, the pairwise distance between sequences belonging to the European group is in the range of 0.2–1.4%.

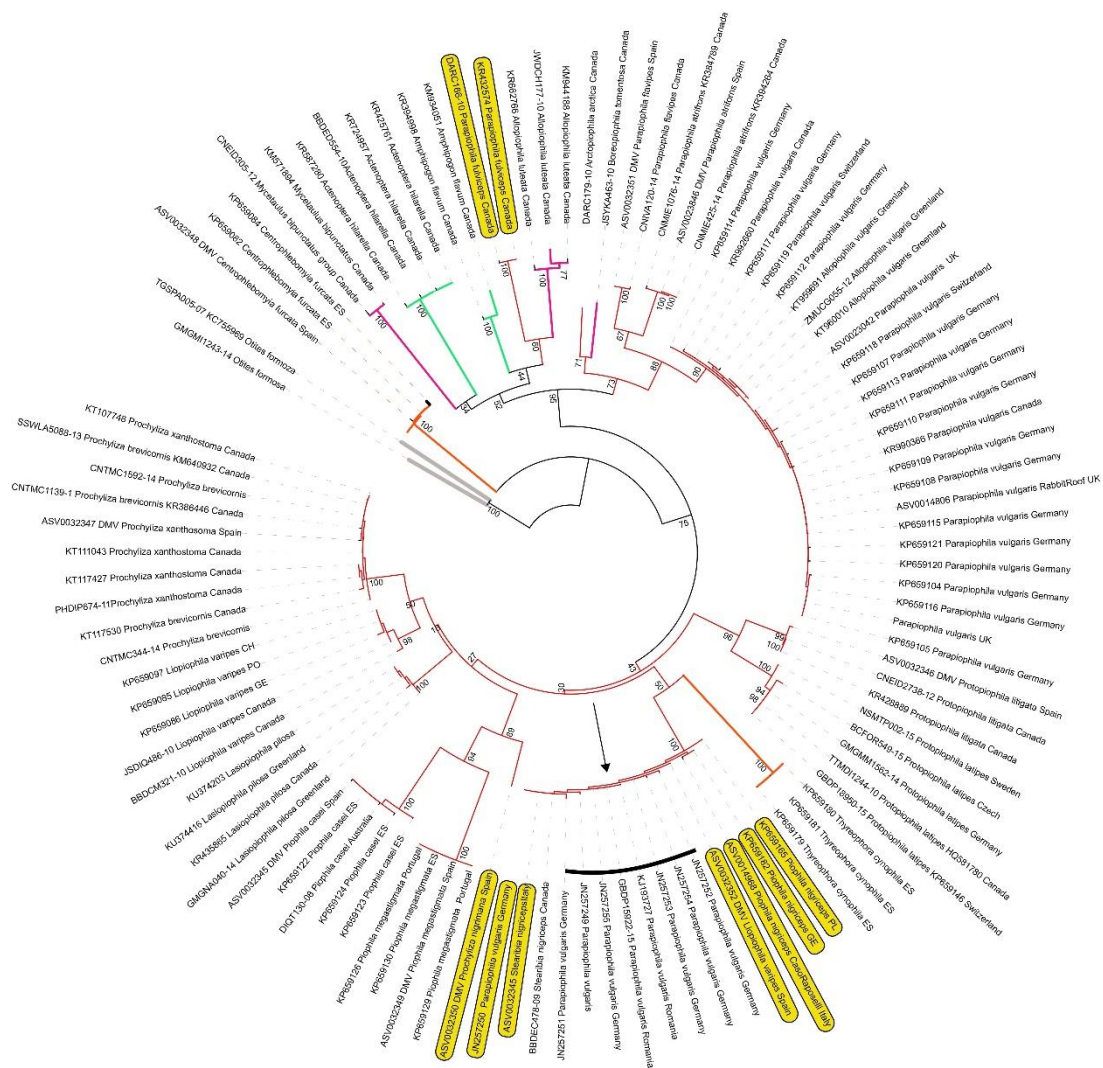


Fig. 5.12 Maximum Likelihood consensus tree. Log Likelihood= -3745.76. The colours of the branches are clarified in Fig. 5.13. Yellow boxes= species out of the expected clusters. Black arrow and line= German *Parapiophila vulgaris* sequences out of the expected clusters.

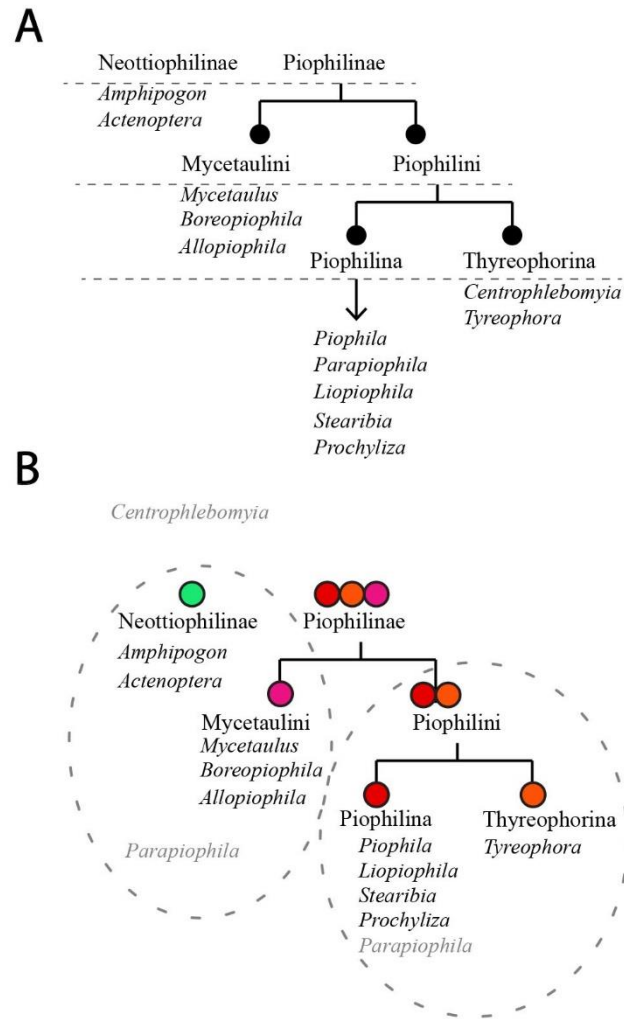


Fig. 5.13 Taxonomic and molecular phylogenetic resolutions of Piophilidae. (A) summary of the Piophilidae taxonomy listing genera used in the phylogenetic analysis of this study; (B) schematic representation of the mtCOI barcoding phylogenetic reconstruction of the Maximum Likelihood tree showed in Fig. 5.12. Grey dashed lines= two main clusters (BS 75). The controversial resolution of the genera *Centrophlebomyia* and *Parapiophila* is also underlined in grey.

5.2.2 Discussions

Due to the important role played by Piophilidae in forensic entomology, accurate descriptions are essential to conduct morphological identification avoiding to face misidentification issues that can have severe consequences in a forensic trial (Rochefort et al., 2015). This family of flies is well known to have a complex taxonomy, not completely resolved yet, and which has been recently reviewed by Martín-Vega (Martín-Vega, 2011) on the original bases provided by McAlpine (1977).

The comparative study herein conducted was aimed at describing the diagnostic characters of puparia of ten species of Piophilidae of forensic interest. Descriptions were available prior to this study for some of the species including *C. furcata* (Freidberg, 1981), *P. casei* (Simmons, 1927), *P. nigrimana* (Martín-Vega et al., 2012), *L. varipes* (Martín-Vega et al., 2014), *P. flavipes* (Martín-Vega, 2017), and *P. litigata* (Bonduriansky, 1995). However, with the exception of the most recent literature, these descriptions were limited to a few characters only, inconsistently among authors, and many of the available illustrations were of poor quality. The comparative study of this work allowed to identify the anatomic features that best differentiate the studied species: the full puparium view (Fig. 5.7) shows the high degree of similarity shared by some of the species, in shape and size. With the exception of *C. furcata*, the largest species (6.84 ± 0.16 mm) (Fig. 5.7A), and *P. litigata*, the smallest (2.82 ± 0.82 mm) (Fig. 5.7J), the other eight are very similar in size. In addition, posterior end can also deceive, as in the case of the closely related species such as *P. casei* and *P. nigrimana* (Fig. 5.7C,F respectively) that are often confused (Martín-Vega et al., 2012). The anterior spiracles instead are quite diverse and useful to discriminate the species (Fig. 5.9), at least at genus level (e.g. *Parapiophila* and *Protopiophila* can be easily distinguished from the genera *Piophila* and *Prochilyza*). However, the anterior end of puparia cannot be found if the adult emerged, unlike the posterior end. In contrast to other necrophagous flies such as Calliphoridae (Szpila, 2010) and Muscidae (Skidmore, 1985, Grzywacz et al., 2015, Grzywacz et al., 2017a, Giordani et al., 2018a), the posterior spiracles of Piophilidae are not so informative to discriminate different species (Fig. 5.11). On the contrary, the anal tubercles borne by the anal division, usually presented as a double pair, one ventral and one dorsal, represent a typical character of

identification for the family Piophilidae (Martín-Vega et al., 2012). The spines of the ventral creeping welts are certainly the most diverse morphological feature among the analysed species and allow to univocally identify them considering the number or rows, the morphology of the tips, the continuous or interrupted pattern, and the orientation towards the posterior or anterior end of the puparium.

Putting together all these observations, which were also compared with the few data available in literature (Freidberg, 1981, Martín-Vega, 2011, Martín-Vega et al., 2012, Panos et al., 2013, Martín-Vega et al., 2014) (Tab. 5.1), a preliminary dichotomy key for the identification of puparia of Piophilidae has been drafted. Certainly, a lot of work has to be done in order to corroborate the data obtained from this study, and the analysis of a higher number of specimens is also desirable and recommended in order to strengthen the observation and overcome the encountered issues related to intra-population variability of the anatomical characters. In fact, in some cases the fundamental characters have been derived only from a few specimens, mainly due to the difficulty in finding a good number of intact and entire close puparia, either in real forensic cases or during field-experiments. Nonetheless, this work represents the beginning of the right direction to solve the still “pending issue” (Martín-Vega, 2017) of the lack of description of puparia of Piophilidae of forensic important, with the final goal to provide a significant support to forensic investigations.

As far as genetic analysis concerns, 9 species out of 11 were correctly identified (82%) using mtCOI target, while a mismatch has been observed in the case of *P. vulgaris* and *P. atrifrons*; the latter case can be explained by the fact that currently there are no COI sequences assigned to *P. atrifrons* in GenBank. This is also a clear example of lack of information related to poorly studied species that can lead to misidentification mistakes. Overall, the pool of the barcoding sequences available for Piophilidae on public database is rather scarce, counting 502 records in GenBank and 685 records in BOLD system. As far as the European records concern, the first Piophilidae barcoding sequences were generated from a few specimens collected from pig carcasses in Germany (Boheme et al., 2011) which were used to run phylogenetic analysis in this study (GenBank accession number JN2572XX). The first systematic barcode database of European Piophilidae of

forensic interest has been recently created (Zajac et al., 2016). The 37% of sequences in the final data set used in this study were derived from there (GenBank accession number KP659XXX). Considering that this is the first work of phylogenetic reconstruction involving Piophilidae species of forensic and non-forensic interest, mainly distributed in Europe but also in Canada and Greenland, it was not possible compare the generated data with others. However, the unexpected topology showing the cluster Neottiophilinae-Mycetaulini (Piophilinae) can find a logical explanation in biogeographical effect. The inclusion of two non-European sequences of *P. flavipes* (Canada origin) show how species with a wide geographic distribution often contain a considerable amount of genetic variability (Zajac et al., 2016).

Additionally, as far as *Parapiophila* McAlpine, 1977 concerns, a few aspects are worthy to be pointed out. This genus is the more controversial of the family of Piophilidae, numbering at least 15 described species (Martín-Vega, 2011), and nine undescribed species according to McAlpine (1977). Based on Ozerov's morphological classification (Ozerov, 2004), *Parapiophila* is synonymous of *Allopiophila* Hendel which may explain the interchangeable use of the two genera also in public DNA records. The clustering of *Allopiophila* sequences with *Parapiophila* sequences in this study (Fig. 5.12) and the intra-specific divergence below 1.64% (Appendix A, Supplementary Table A5) support the evidence Ozerov's statement (2004). The best-known species within this genus is *P. vulgaris* which also has been found on carrion succession. The following considerations clarify the independent cluster formed by *P. vulgaris* sequences from Germany and Romania, out of the main cluster including other European sequences of the same species. The pairwise distance was calculated to verify the hypothesis that a misidentification occurred as recommended by Amendt (2004a). The intraspecific divergence mean of *Allopiophila/Parapiophila vulgaris* sequences is 7% which is over the 3% threshold of discrimination between two species as established by Hebert (2003a) when mtCOI barcoding region is considered. Additionally, the intra-specific variation (13.9% -15.6%) was by far higher than the inter-specific variation (e.g. 0.69%-1.89%). Since European and Canadian sequences showed very low intra-specific variation % values, we are led to exclude that the geographic factor can be the cause of a such high intra-specific difference

between the German and the other European sequences. Rather, it is reasonable thinking that a misidentification occurred at morphological level: in fact, the lowest pairwise distance values (in the range 0.69%–1.89%) were calculated between the “presumed” *Parapiophila vulgaris* German sequences and three others belonging to *Piophila* genus. Furthermore, the fact that *P. vulgaris* sequences have been identified by the authors, as by their declaration, without consulting any specialist (Boheme et al., 2011), can support this hypothesis. What here reported demonstrates the importance of accurately identify the specimens from which DNA sequences are intended to be derived and be uploaded on public data base: inaccuracy in this context, ultimately, may cause a misinterpretation of the phylogenetic analysis which, instead, should be serve as support tool to the whole process of identification.

5.3 CONCLUSIONS

The identification of flies of forensic interest requires the maximum level of accuracy: whether initiated at morphological level, it might require to be confirmed through genetic analysis and supported by molecular phylogenesis. In order to guarantee a reliable applicability of this workflow in forensic entomology, accurate tools of identification must be available to researchers and a continuous research in taxonomy is needed to compensate the lack of information especially related to the immatures. Overall, the work here presented provides new knowledge about the anatomy of immatures stages of *P. alceae* (Ulidiidae), mitigating the still large lack of morphological information of “secondary taxa” that might be encountered in forensic contexts; additionally, a key update about the morphological descriptions of puparia belonging to ten species of Piophilidae of forensic interest has been provided, along with the draft of the first dichotomy key of identification.

These outcomes contribute to reduce the lack of morphological information for two important taxa of forensic interest and provide forensic entomologists an essential guide for the identification of poorly studied and complex taxonomic group of flies frequently misidentified. In addition, they outline the need to critically interpret DNA analysis when using DNA databases and phylogenetic approach, and reveal that an integrated taxonomy-DNA based approach can be the key for accurate analysis whether a continuous research will be undertaken to generate new data.

6 FINAL CONCLUSIONS

The research presented in this thesis provides a comprehensive approach of analysis of Diptera remains recovered from archaeological and forensic contexts. In conclusion, in light to the pre-set objectives, the following outcomes have been achieved.

A deeper understanding of what molecular analysis of modern Diptera puparia involve has been provided; the applied protocol led to efficiently isolate and purify total DNA from the internal *exuviae* of the specimens, ultimately showing that genotyping can be used as a tool to identify flies remains retrieved from forensic contexts.

The unknown hovering around ancient DNA analysis of archaeological empty puparia has been unlocked and the topic deeply explored, providing the first contribution to molecular archaeology field applied to archaeoentomological investigations; however, further research is still needed to validate genotyping as alternative tool of identification of archaeological records. Additionally, as far as environmental archaeology research concerns, the analysis of puparia remains recovered from archaeological Italian heritage innovatively contributed to reveal the great potential of archaeoentomological studies in the reconstitution of human practices; investigations on taphonomic processes involved in the preservation of the findings were key to infer additional information and provide more accurate interpretations.

New morphological data of the immatures of species of forensic interest have been generated compensating the lack of essential information which is needed during forensic entomology investigations, to avoid misidentification issues of poorly studied species; certainly, further research in taxonomy will be beneficial to continuously improve the applicability of morphological studies, as well as to strengthen the applicability of molecular analysis.

REFERENCES

- AL-MESBAH, H., MOFFATT, C., EL-AZAZY, O. M. E. & MAJEED, Q. A. H. 2012. The decomposition of rabbit carcasses and associated necrophagous Diptera in Kuwait. *Forensic Science International*, 217, 27-31.
- ALLISON, P. A. 1990. Carbonate nodules and plattenkalks. In: BRIGGS, D. E. G. & CROWTHER, P. R. (eds.) *Palaeobiology: a synthesis* Oxford: Blackwell Science.
- ALTSCHUL, S. F., GISH, W., MILLER, W., MYERS, E. W. & LIPMAN, D. J. 1990. Basic local alignment search tool. *Journal of Molecular Biology*, 215, 403-410.
- AMENDT, J., CAMPOBASSO, C. P., GAUDRY, E., REITER, C., LEBLANC, H. N. & HALL, M. J. 2007. Best practice in forensic entomology—standards and guidelines. *International Journal of Legal Medicine*, 121, 90-104.
- AMENDT, J., KRETTEK, R. & ZEHNER, R. 2004a. Forensic entomology. *Naturwissenschaften*, 91, 51-65.
- AMENDT, J., KRETTEK, R., ZEHNER, R. & BRATZKE, H. 2004b. Practice of forensic entomology—usability of insect fragments in the estimation of the time of death. *Arch Kriminol*, 214, 11-8.
- AMENDT, J., RICHARDS, C. S., CAMPOBASSO, C. P., ZEHNER, R. & HALL, M. J. 2011. Forensic entomology: Applications and limitations. *Forensic Science, Medicine, and Pathology*, 7, 379-92.
- ASHWORTH, A. C., BUCKLAND, P. C. & SADLER, J. P. 1997. *Studies in Quaternary Entomology: An inordinate fondness for insects*, Chichester, John Wiley & Sons.
- AUSTIN, J. J., ROSS, A. J., SMITH, A. B., FORTEY, R. A. & THOMAS, R. H. 1997a. Problems of reproducibility—does geologically ancient DNA survive in amber-preserved insects? *Proceedings of the Royal Society of London B*, 264, 467-474.
- AUSTIN, J. J., SMITH, A. B. & THOMAS, R. H. 1997b. Paleontology in a molecular world: The search for authentic ancient DNA. *Tree*, 12, 303-306.
- BACKWELL, L. R., PARKINSON, A. H., ROBERTS, E. M., D'ERRICO, F. & HUCHET, J. B. 2012. Criteria for identifying bone modification by termites in the fossil record. *Palaeogeography, Palaeoclimatology, Palaeoecology*, 337-338, 72-87.
- BAILEY, G. 2007. Time perspectives, palimpsests and the archaeology of time. *Journal of Anthropological Archaeology*, 26, 198-223.
- BAIN, A. 2004. Irritating intimates: The archaeoentomology of lice, fleas, and bedbugs. *Northeast Historical Archaeology*, 33, 81-89.
- BALL, S. 2015. Introduction to the families of British Diptera. Part 1: Naming of the parts and glossary. Dipterist Forum. <http://www.dipteristsforum.org.uk>.

- BAREK, H., SUGUMARAN, M., ITO, S. & WAKAMATSU, K. 2017. Insect cuticular melanins are distinctly different from those of mammalian epidermal melanins. *Pigment Cell and Melanoma Research*, 31, 384-392.
- BAZ, A., BOTÍAS, C., MARTÍN-VEGA, D., CIFRIÁN, B. & DÍAZ-ARANDA, L. M. 2015. Preliminary data on carrion insects in urban (indoor and outdoor) and periurban environments in central Spain. *Forensic Science International*, 248, 41-47.
- BELSHAW, R. 1989. A note on the recovery of *Thoracochaeta zosteræ* (Haliday) (Diptera: Sphaeroceridae) from archaeological deposits. *Circaea*, 6, 39-41.
- BENBOW, M. E., TOMBERLIN, J. K. & TARONE, A. M. 2015. *Carrion ecology, evolution, and their applications*, Boca raton, Florida, CRC Press.
- BENELLI, G., CANALE, A., RASPI, A. & FORNACIARI, G. 2014. The death scenario of an Italian Renaissance princess can shed light on a zoological dilemma: Did the black soldier fly reach Europe with Columbus? *Journal of Archaeological Science*, 49, 203-205.
- BOHART, G. E. & GRESSITT, J. L. 1951. *Filth-inhabiting flies of Guam* Honolulu, Hawaii, Bernice P. Bishop Museum
- BOHEME, P., AMENDT, J. & ZEHNER, R. 2011. The use of COI barcodes for molecular identification of forensically important fly species in Germany. *Parasitology Research*, 110, 2325-2332.
- BONDURIANSKY, R. 1995. A new nearctic species of *Protopiophila* Duda (Diptera: Piophilidae), with notes on its behaviour and comparison with *P. latipes* (Meigen). *The Canadian Entomologist*, 127, 859-863.
- BONDURIANSKY, R. 2002. Leaping behaviour and responses to moisture and sound in larvae of piophilid carrion flies. *The Canadian Entomologist* 134, 647-656.
- BORTOLINI, S., GIORDANI, G., TUCCIA, F., MAISTRELLO, L. & VANIN, S. 2018. Do longer sequences improve the accuracy of identification of forensically important Calliphoridae species? *PeerJ*, 6, e5962.
- BORUM, J. & GREVE, T. 2004. The four European seagrass species. In: BORUM, J., DUARTE, C. M., KRAUSE-JENSEN, D. & GREVE, T. M. (eds.) *European Seagrasses: An Introduction to Monitoring and Management, EU Project Monitoring and Managing of European Seagrasses*.
- BOSI, G. & MAZZANTI, M. B. 2013. Informazioni etnobotaniche dai reperti carpologici del pozzo: risultati di un saggio preliminare. In: ROVINA, R. & FIORI, M. (eds.) *Sassari-Archeologia Urbana*. Ghezzano (PI): Felici Editore.
- BRENNER, J. C. 2004. *Forensic Science: An illustrated dictionary*, New York, CRC Press.
- BRIGGS, D. E. G. & KEAR, A. J. 1993. Fossilisation of the soft tissue in the laboratory. *Science*, 259, 1439-1442.

- BUCKLAND, P. C. 1974. Archaeology and environment in York. *Journal of Archaeological Science*, 1, 303-316.
- BUCKLAND, P. C., BUCKLAND, P. I. & PANAGIOTAKOPULU, E. 2016. Caught in a trap: Landscape and climate implications of the insect fauna from a Roman well in Sherwood Forest. *Archaeological and Anthropological Sciences*, 10, 125-140.
- BUCKLAND, P. I., BUCKLAND, P. C. & OLSSON, F. 2014. Paleoentomology: Insects and other arthropods in environmental archaeology. In: SMITH, C. (ed.) *Encyclopedia of Global Archaeology*. New York, NY: Springer.
- BUGELLI, V., FORNI, D., BASSI, L. A., DI PAOLO, M., MARRA, D., LENZI, S., TONI, C., GIUSIANI, M., DOMENICI, R., GHERARDI, M. & VANIN, S. 2015. Forensic entomology and the estimation of the minimum time since death in indoor cases. *Journal of Forensic Sciences*, 60, 525-31.
- BYRD, J. H. & CASTNER, J. L. 2001. *Forensic Entomology the Utility of Arthropods in Legal Investigations*, Boca Raton, CRC Press.
- CAMPOBASSO, C. P., DI VELLA, G. & INTRONA, F. 2001. Factors affecting decomposition and Diptera colonization. *Forensic Science International*, 120, 18-27.
- CAMPOBASSO, C. P., LINVILLE, J. G., WELLS, J. D. & INTRONA, F. 2005. Forensic genetic analysis of insect gut contents. *The American Journal of Forensic Medicine and Pathology*, 26, 161-165.
- CAMPOS, P. F. & GILBERT, T. M. 2012. DNA extraction from keratin and chitin. In: SHAPIRO, B. & HOFREITER, M. (eds.) *Ancient DNA. Methods and Protocols*. Berlin: Springer.
- CANO, R. J., POINAR, H. N., PIENIAZEK, J. J., ACRA, A. & POINAR, G. O. 1993. Amplification and sequencing of DNA from a 120-135 million year old weevil. *Nature*, 363, 536-538.
- CANO, R. J., POINAR, H. N. & POINAR, G. O. 1992. Isolation and partial characterisation of DNA from the bee *Proplebeia dominicana* (Apidae: Hymenoptera) in 25-40 million year-old amber. *Medical Science Research*, 20, 249-251.
- CARTER, D. O., YELLOWLEES, D. & TIBBETT, M. 2007. Cadaver decomposition in terrestrial ecosystems. *Naturwissenschaften*, 94, 12-24.
- CHAPCO, W. & LITZENBERGER, G. 2004. A DNA investigation into the mysterious disappearance of the Rocky Mountain grasshopper, mega-pest of the 1800s. *Molecular Phylogenetics and Evolution*, 30, 810-814.
- CHE MAN, Y. B., SYAHARIZA, Z. A. & ROHMAN, A. 2010. Fourier Transform Infrared spectroscopy: Development, techniques, and application in the analyses of fats and oils In: RESS, O. J. (ed.) *Fourier Transform infrared spectroscopy*. New York, USA: Nova Science Publishers.

- CHEN, X. L. & KAMENEVA, E. P. 2007. A review of *Physiphora* Fallén (Diptera: Ulidiidae) from China. *Zootaxa*, 1398, 15-28.
- CLARY, D. O. & WOLSTENHOLME, D. R. 1985. The mitochondrial DNA molecule of *Drosophila yakuba*: Nucleotide sequence, gene organization and genetic code. *Journal of Molecular Evolution*, 22, 252-271.
- DAVIS, T. S., CRIPPEN, T. L., HOFSTETTER, R. W. & TOMBERLIN, J. K. 2013. Microbial volatile emissions as insect semiochemicals. *Journal of Chemical Ecology*, 39, 840-859.
- DESALLE, R., DESALLE, G. J., WHEELER, W. C. & GRIMALDI, D. 1992. DNA sequences from a fossil termite in Oligo-Miocene amber and their phylogenetic implications. *Science*, 257, 1933-1936.
- DI LUISE, E., MAGNI, P., STAITI, N., SPITALERI, S. & ROMANO, C. 2008. Genotyping of human nuclear DNA recovered from the gut of fly larvae. *Forensic Science International: Genetics*, 1, 591-592.
- DIRRIGL, F. J. & GREENBERG, B. 1995. The utility of insect remains to assessing human burials: A connecticut case study. *Archaeology of Eastern North America*, 23, 1-7.
- DISNEY, R. H. L. 1994. *Scuttle flies: The Phoridae*, London, Chapman & Hall.
- DOMÍNGUEZ, M. C. & PONT, A. C. 2014. Fanniidae (Insecta: Diptera). *Fauna of New Zealand*, 71, 1-91.
- DONOVAN, S. K. & VELTKAMP, C. 1994. Unusual preservation of late Quaternary millipedes from Jamaica. *Lethaia*, 27, 355-362.
- EBEJER, M. J. 2012. Piophilidae (Diptera) from Gibraltar and the puparium of *Piophila megastigmata* McAlpine. *Dipterists Digest*, 19, 65-71.
- EBEJER, M. J. 2015. The picture-winged flies and related families (Diptera, Tephritoidea) of the Maltese Islands. *Bulletin of the Entomological Society of Malta*, 7, 73-91.
- EGGLISHAW, H. J. 1958. *The fauna of wrack beds*. PhD Thesis, Newcastle University.
- ELIAS, S. 2014. Environmental interpretation of fossil insect assemblages from MIS 5 at Ziegler Reservoir, Snowmass Village, Colorado. *Quaternary Research*, 82, 592-603.
- ERZINCLIOGLU, Z. 2000. *Maggots, murder and men: Memories and reflections of a forensic entomologist*, Colchester, Essex, Harley Books.
- FABOZZI, F. J., FOCARDI, S. M., SVETLOZAR, T. R. & ARSHANAPALLI, B. G. 2014. Model Selection Criterion: AIC and BIC - Appendix E. In: FABOZZI, F. J., FOCARDI, S. M., SVETLOZAR, T. R. & ARSHANAPALLI, B. G. (eds.) *The basics of financial econometrics: Tools, concepts, and asset management applications*. Hoboken, NJ, USA: John Wiley & Sons.

- FELSENSTEIN, J. 1981. Evolutionary trees from DNA sequences: A maximum likelihood approach. *Journal of molecular evolution*, 17, 368-376.
- FODDAI, D. & MINELLI, A. 1994. Fossil arthropods from a full-glacial site in Northeastern Italy. *Quaternary Research*, 41, 336-342.
- FOLMER, O., BLACK, M., HOEH, W., LUTZ, R. & VRIJENHOEK, R. 1994. DNA primers for amplification of mitochondrial Cytochrome C oxidase subunit I from diverse metazoan invertebrates. *Molecular Marine Biology and Biotechnology* 3, 294-9.
- FORBES, V., BRITTON, K. & KNECHT, R. 2015. Preliminary archaeoentomological analyses of permafrost-preserved cultural layers from the pre-contact Yup'ik Eskimo site of Nunalleq, Alaska: Implications, potential and methodological considerations. *Environmental Archaeology*, 20, 158-167.
- FORBES, V., DUSSAULT, F. & BAIN, A. 2013. Contributions of ectoparasite studies in archaeology with two examples from the North Atlantic region. *International Journal of Paleopathology*, 3, 158-164.
- FORNACIARI, G., GIUFFRÀ, V., MARINOZZI, S., PICCHI, M. S. & MASETTI, M. 2009. "Royal" pediculosis in Renaissance Italy: Lice in the mummy of the King of Naples Ferdinand II of Aragon (1467-1496). *Memórias do Instituto Oswaldo Cruz*, 104, 671-672.
- FREIDBERG, A. 1981. Taxonomy, natural history and immature stages of the bone-skipper, *Centrophlebomyia furcata* (Fabricius) (Diptera: Piophilidae, Thyreophorina). *Entomologica Scandinavica*, 12, 320-326.
- FULTON, T. L. & STILLER, M. 2012. PCR amplification, cloning, and sequencing of ancient DNA. *Methods in Molecular Biology*, 840, 111-119.
- GALINSKAYA, T. V., SUVOROV, A., OKUN, M. V. & SHATALKIN, A. I. 2014. DNA barcoding of Palaearctic Ulidiidae (Diptera: Tephritoidea): Morphology, DNA evolution, and Markov codon models. *Zoological Studies*, 53, 51-68.
- GENNARD, D. 2007. *Forensic Entomology: An introduction*, Chichester, Wiley.
- GERSTMEIER, R. 1998. *Checkered beetles illustrated key to the Cleridae and Thanerocleridae of the Western Palaearctic* Weikersheim, Margraf Verlag.
- GIANGASPERO, A. 1997. *Le mosche di interesse veterinario. Muscidae. Guida alla conoscenza e al riconoscimento*, Bologna, Edagricole Ed. Calderini.
- GIANTSIS, I. A., CHASKOPOULOU, A. & BON, M. C. 2015. Mild-Vectolysis: A nondestructive DNA extraction method for vouchering sand flies and mosquitoes. *Journal of Medical Entomology* 53, 692-695.
- GILARRIORTUA, M., SALONA-BORDAS, M. I., CAINE, L. M., PINHEIRO, F. & DE PANCORBO, M. M. 2015. Mitochondrial and nuclear DNA approaches for reliable identification of *Lucilia* (Diptera, Calliphoridae) species of forensic interest from Southern Europe. *Forensic Science International*, 257, 393-7.

- GILARRIORTUA, M., SALONA BORDAS, M. I., CAINE, L. M., PINHEIRO, F. & DE PANCORBO, M. M. 2013. Cytochrome b as a useful tool for the identification of blowflies of forensic interest (Diptera, Calliphoridae). *Forensic Science International*, 228, 132-6.
- GILARRIORTUA, M., SALONA BORDAS, M. I., KOHNEMANN, S., PFEIFFER, H. & DE PANCORBO, M. M. 2014. Molecular differentiation of central European blowfly species (Diptera, Calliphoridae) using mitochondrial and nuclear genetic markers. *Forensic Science International*, 242, 274-82.
- GILBERT, B. M. & BASS, W. M. 1967. Seasonal dating of burials from the presence of fly pupae. *American Antiquity*, 32, 534-535.
- GILBERT, M. T., MOORE, W., MELCHIOR, L. & WOROBEY, M. 2007. DNA extraction from dry museum beetles without conferring external morphological damage. *PLoS One*, 2, e272.
- GIORDANI, G., GRZYWACZ, A. & VANIN, S. 2018a. Characterization and identification of puparia of *Hydrotaea* Robineau-Desvoidy, 1830 (Diptera: Muscidae) from forensic and archaeological contexts. *Journal of Medical Entomology*, 56, 45-54.
- GIORDANI, G., TUCCIA, F., FLORIS, I. & VANIN, S. 2018b. First record of *Phormia regina* (Meigen, 1826) (Diptera: Calliphoridae) from mummies at the Sant'Antonio Abate Cathedral of Castelsardo, Sardinia, Italy. *PeerJ*, 6, e4176.
- GIORDANI, G., TUCCIA, F., ZOPPIS, S., VECCHIOTTI, C. & VANIN, S. 2018c. Record of *Leptometopa latipes* (Diptera: Milichiidae) from a human cadaver in the Mediterranean area. *Forensic Sciences Research*, 4, 341-347.
- GIRALDO, H. P. A., URIBE, S. S. I. & LOPEZ, R. A. 2011. Analysis of mitochondrial DNA sequences (Cytb and ND1) in *Lucilia eximia* (Diptera: Calliphoridae). *Revista Colombiana de Entomologia*, 37, 273-278.
- GIRLING, M. A. 1979. Calcium carbonate-replaced arthropods from archaeological deposits. *Journal of Archaeological Sciences*, 6, 309-320.
- GIROUX, M., PAPE, T. & WHEELER, T. A. 2010. Towards a phylogeny of the flesh flies (Diptera: Sarcophagidae): Morphology and phylogenetic implications of the acrophallus in the subfamily Sarcophaginae. *Zoological Journal of the Linnean Society*, 158, 740-778.
- GLOCKE, I. & MEYER, M. 2017. Extending the spectrum of DNA sequences retrieved from ancient bones and teeth. *Genome Research*, 27, 1230-1236.
- GÖRANSSON, H. 2002. Alvastra pile dwelling – a 5000-year-old byre? In: VIKLUND, K. (ed.) *Nordic Archaeobotany – NAG 2000 in Umeå*. VMC KBC Umeå universitet.
- GREENBERG, B. 1971. *Flies and disease: Ecology, classification, and biotic associations*, New Jersey, Princeton University Press.

- GRUPPIONI, G., LABATE, D., MERCURI, L., MILANI, V., TRAVERSARI, M. & VERNIA, B. 2010. Gli scavi della Chiesa di San Paolo di Roccapelago nell'Appennino modenese. La cripta con i corpi mummificati naturalmente. *Pagani e Cristiani. Forme e attestazioni di religiosità del mondo antico in Emilia, IX*. Firenze: All'Insegna del Giglio.
- GRZYWACZ, A., HALL, M. J. & PAPE, T. 2015. Morphology successfully separates third instar larvae of *Muscina*. *Medical and Veterinary Entomology*, 29, 314-29.
- GRZYWACZ, A., HALL, M. J., PAPE, T. & SZPILA, K. 2017a. Muscidae (Diptera) of forensic importance—an identification key to third instar larvae of the Western Palaearctic region and a catalogue of the muscid carrion community. *International Journal of Legal Medicine*, 131, 855-866.
- GRZYWACZ, A., WYBORSKA, D. & PIWCZYŃSKI, M. 2017b. DNA barcoding allows identification of European Fanniidae (Diptera) of forensic interest. *Forensic Science International*, 278, 106-114.
- GULLAN, P. J. & CRANSTON, P. S. 2014. *The insects: An outline of entomology*, Hoboken, John Wiley & Sons.
- GUO, Y., ZHA, L., YAN, W., LI, P., CAI, J. & WU, L. 2014. Identification of forensically important sarcophagid flies (Diptera: Sarcophagidae) in China based on COI and Period gene. *International Journal of Legal Medicine*, 128, 221-228.
- GUTIERREZ, Y. 1990. *Diagnostic pathology of parasitic infections with clinical correlations*, Philadelphia, USA, Lea & Febinger.
- HAGELBERG, E., HOFREITER, M. & KEYSER, C. 2014. Ancient DNA: The first three decades. *Philosophical Transactions of the Royal Society B*, 370.
- HALL, M. & MARTIN-VEGA, D. 2019. Visualization of insect metamorphosis. *Philosophical Transactions of the Royal Society B*, 374.
- HALL, M., WHITAKER, A. & RICHARDS, C. 2012. Forensic entomology. In: MARQUEZ-GRANT, N. & ROBERTS, J. (eds.) *Forensic ecology handbook: From crime scene to court*. First ed. Hoboken, NJ, USA: John Wiley & Sons.
- HALL, T. A. 1999. BioEdit: A user-friendly biological sequence alignment editor and analysis program for Windows 95/98/NT. *Nucleic Acids Symposium Series*, 41, 95-98.
- HAMMER, Ø., HARPER, D. A. T. & RYAN, P. D. 2001. PAST: Paleontological Statistics Software Package for education and data analysis. *Palaeontologia Electronica* 4, 9.
- HANDT, O., HOSS, M. & KRINGS, P., S. 1994 Ancient DNA: Methodological challenges. *Experientia*, 50, 524-529.
- HEBERT, P. D., CYWINSKA, A., BALL, S. L. & DEWAARD, J. R. 2003. Biological identifications through DNA barcodes. *Proceedings of the Royal Society B: Biological Sciences*, 270, 313-21.

- HEINTZMAN, P. D., ELIAS, S. A., MOORE, K., PASZKIEWICZ, K. & BARNES, I. 2013. Characterizing DNA preservation in degraded specimens of *Amara alpina* (Carabidae: Coleoptera). *Molecular Ecology Research*, 14, 606-615.
- HEO, C. C., LATIF, B., KURAHASHI, H., HAYASHI, T., NAZNI, W. A. & OMAR, B. 2015. Coprophilic dipteran community associated with horse dung in Malaysia. *Halteres*, 6, 33-50.
- HERMANEK, P., RATHORE, J. S., ALOISI, V. & CARMIGNATO, S. 2018. Principles of X-ray computed tomography. In: CARMIGNATO, S., DEWULF, W. & LEACH, R. (eds.) *Industrial X-Ray computed tomography*. Cham: Springer.
- HEYN, P., STENZEL, U., BRIGGS, A. W., KIRCHER, M., HOFREITER, M. & MEYE, M. 2010. Road blocks on paleogenomes - polymerase extension profiling reveals the frequency of blocking lesions in ancient DNA. *Nucleic Acids Research*, 38, e161.
- HOANG, D. T., CHERNOMOR, O., VON HAESLER, A., MINH, B. Q. & VINH, L. S. 2018. UFBoot2: Improving the ultrafast bootstrap approximation. *Molecular Biology and Evolution*, 35, 518-522.
- HOFREITER, H., SERRE, D., POINAR, H. N., KUCH, M. & PÄÄBO, S. 2001. Ancient DNA. *Nature Reviews: Genetics*, 2, 353-359.
- HUCHET, J. B. 1996. L'Archéontomologie funéraire: une approche originale dans l'interprétation des sépultures. *Bulletins et Mémoires de la Société d'anthropologie de Paris*, 3-4, 299-311.
- HUCHET, J. B. 2010. Archaeontomological study of the insects remains found within the mummy of Namenkhet Amon, San Lazzaro Armenian Monastery, (Venice/Italy). *Advances in Egyptology*, 1, 59-80.
- HUCHET, J. B. 2014a. Étude archéontomologique In: PÉCHART, S. & ARNAUD, M. (eds.) 22, Rue Lecoindre, REIMS, Marne, Champagne-Ardenne. Service Archéologique de Reims Métropole.
- HUCHET, J. B. 2014b. Insect remains and their traces: Relevant fossil witnesses in the reconstruction of past funerary practices. *Anthropologie (Brno)*, 52, 329-346.
- HUCHET, J. B., DEVERLY, D., GUTIERREZ, B. & CHAUCHAT, C. 2011. Taphonomic evidence of a human skeleton gnawed by termites in a Moche-civilisation grave at Huaca de la Luna, Peru. *International Journal of Osteoarchaeology*, 21, 92-102.
- HUCHET, J. B. & GREENBERG, B. 2010. Flies, Mochicas and burial practices: A case study from Huaca de la Luna, Peru. *Journal of Archaeological Science*, 37, 2846-2856.
- HUCHET, J. B., LE MORT, F., RABINOVICH, R., BLAU, S., COQUEUGNIOT, H. & ARENSBURG, B. 2013a. Identification of dermestid pupal chambers on Southern Levant human bones: Inference for reconstruction of Middle Bronze Age mortuary practices. *Journal of Archaeological Science*, 40, 3793-3803.

- HUCHET, J. B., PEREIRA, G., GOMY, Y., PHILIPS, T. K., ALATORRE-BRACAMONTES, C. E., VÁSQUEZ-BOLAÑOS, M. & MANSILLA, J. 2013b. Archaeoentomological study of a pre-Columbian funerary bundle (mortuary cave of Candelaria, Coahuila, Mexico). *Annales de la Société entomologique de France (N.S.)*, 49, 277-290.
- HURST, R. O. 1956. The degradation of desoxyribonucleic acid during alkaline hydrolysis. *Canadian Journal of Biochemistry and Physiology*, 34, 265-269.
- HWANG, C. & TURNER, B. D. 2005. Spatial and temporal variability of necrophagous Diptera from urban to rural areas. *Medical and Veterinary Entomology*, 19, 379-391.
- JORDAENS, K., SONET, G., RICHET, R., DUPONT, E., BRAET, Y. & DESMYTER, S. 2013. Identification of forensically important *Sarcophaga* species (Diptera: Sarcophagidae) using the mitochondrial COI gene. *International Journal of Legal Medicine*, 127, 491-504.
- KALYAANAMOORTHY, S., MINH, B. Q., WONG, T. K. F., VON HAESLER, A. & JERMIIN, L. S. 2017. ModelFinder: Fast model selection for accurate phylogenetic estimates. *Nature Methods*, 14, 587-589.
- KAMENEVA, E. P. & KORNEYEV, V. A. 2010a. Order Diptera, family Ulidiidae. *Arthropod Fauna of the UAE*, 3, 616-634.
- KAMENEVA, E. P. & KORNEYEV, V. A. 2010b. Order Diptera, family Ulidiidae. *Arthropod fauna of the UAE*, 3, 616-634
- KEMP, B. M., MONROE, C. & SMITH, D. G. 2006. Repeat silica extraction: a simple technique for the removal of PCR inhibitors from DNA extracts. *Journal of Archaeological Science*, 33, 1680-1689.
- KENWARD, H. 2009. Northern regional review of environmental archaeology: Invertebrates in archaeology in the North of England: Environmental studies report. *English Heritage Research Department unpublished report series*. Swindon, UK.
- KENWARD, H. & HALL, A. 1997. Enhancing bioarchaeological interpretation using indicator groups: Stable manure as a paradigm. *Journal of Archaeological Science*, 24, 663-673.
- KENWARD, H. & HALL, A. 2000. Decay of delicate organic remains in shallow urban deposits: Are we at a watershed? *Antiquity*, 74, 519-525.
- KING, G. A. 2012. Isotopes as paleoeconomic indicators: New applications in archaeoentomology. *Journal of Archaeological Science*, 39, 511-520.
- KING, G. A. 2014. Exaptation and synanthropic insects: A diachronic interplay between biology and culture. *Environmental Archaeology*, 19, 12-22.

- KING, G. A., GILBERT, M. T., WILLERSLEV, E., COLLINS, M. J. & KENWARD, H. 2009. Recovery of DNA from archaeological insect remains: First results, problems and potential. *Journal of Archaeological Science*, 36, 1179-1183.
- KUMAR, S., STECHER, G. & TAMURA, K. 2016. MEGA7: Molecular Evolutionary Genetics Analysis version 7.0 for bigger datasets. *Molecular Biology and Evolution*, 33, 1870-1874.
- LABATE, D., MERCURI, L., MILANI, V., TRAVERSARI, M. & VERNIA, B. 2011. Notizie preliminari delle indagini archeologiche nella chiesa di San Paolo di Roccapelago nell'Appennino modenese. *La Rocca a Pelago fra identità del passato e vocazioni del presente. Le vicende storiche del complesso architettonico di Roccapelago Roccapelago (Modena)*.
- LAMBKIN, C. L., SINCLAIR, B. J., PAPE, T., COURTNEY, G. W., SKEVINGTON, J. H., MEIER, R., YEATES, D. K., BLAGODEROV, V. & WIEGMANN, B. M. 2012. The phylogenetic relationships among infraorders and superfamilies of Diptera based on morphological evidence. *Systematic Entomology*, 38, 164-179.
- LEAKEY, L. S. B. 1952. Lower Miocene invertebrates from Kenya. *Nature*, 169, 1020-1021.
- MALGORN, Y. & COQUOZ, R. 1999. DNA typing for identification of some species of Calliphoridae: An interest in forensic entomology. *Forensic Science International*, 102, 111-119.
- MANN, R. W., FEATHER, M. E., TUMOSA, C. S., HOLLAND, T. D. & SCHNEIDER, K. N. 1998. A blue encrustation found on skeletal remains of Americans missing in action in Vietnam. *Forensic Science International*, 97, 79-86.
- MARSHALL, L. J., ALMOND, M. J., COOK, S. R., PANTOS, M., TOBIN, M. J. & THOMAS, L. A. 2008. Mineralised organic remains from cesspits at the Roman town of Silchester: Processes and preservation. *Spectrochimica Acta Part A: Molecular and Biomolecular Spectroscopy*, 71, 854-61.
- MARSHALL, S., ROHÁČEK, J., DONG, H. & BUCK, M. 2011. The state of Sphaeroceridae (Diptera: Acalypratae): A world catalog update covering the years 2000-2010, with new generic synonymy, new combinations, and new distributions. *Acta Entomologica Musei Nationalis Pragae*, 51, 217-298.
- MARSHALL, S. A. 2012. *Flies: The natural history & diversity of Diptera*, Richmond Hill, Firefly Books.
- MARTÍN-VEGA, D. 2011. Skipping clues: Forensic importance of the family Piophilidae (Diptera). *Forensic Science International*, 212, 1-5.
- MARTÍN-VEGA, D. 2017. Description of the puparium of *Parapiophila flavipes* (Zetterstedt, 1847) (Diptera, Piophilidae) from specimens in the collection of the Natural History Museum, London. *Boletín de la Asociación Española de Entomología*, 41, 239-245.

- MARTÍN-VEGA, D. & BAZ, A. 2013. Sarcosaprophagous Diptera assemblages in natural habitats in central Spain: Spatial and seasonal changes in composition. *Medical and Veterinary Entomology*, 27, 64-76.
- MARTÍN-VEGA, D., BAZ, A. & DIAZ-ARANDA, L. M. 2012. The immature stages of the necrophagous fly, *Prochyliza nigrimana*: Comparison with *Piophilidae casei* and mediolegal considerations (Diptera: Piophilidae). *Parasitology Reserach*, 111, 1127-1135.
- MARTÍN-VEGA, D., DÍAZ-ARANDA, L. M. & BAZ, A. 2014. The immature stages of the necrophagous fly *Liopiophila varipes* and considerations on the genus *Liopiophila* (Diptera: Piophilidae). *Deutsche Entomologische Zeitschrift*, 61, 37-42.
- MARTÍN-VEGA, D., HALL, M. J. R. & SIMONSEN, T. J. 2016. Resolving confusion in the use of concepts and terminology in intrapuparial development studies of cyclorrhaphous Diptera. *Journal of Medical Entomology*, 53, 1249-1251.
- MARTÍN-VEGA, D., GÓMEZ-GÓMEZ, A., BAZ, A. & DÍAZ-ARANDA, L. M. 2011. New piophilid in town: The first Palaearctic record of *Piophila megastigmata* and its coexistence with *Piophila casei* in central Spain. *Medical and Veterinary Entomology*, 25, 64-69.
- MASUTTI, L. & ZANGHERI, S. 2001. *Entomologia generale e applicata*, Padova, Italy, CEDAM- Case editrice Dott. Antonio Milani.
- MAZZANTI, M., ALESSANDRINI, F., TAGLIABRACCI, A., WELLS, J. D. & CAMPOBASSO, C. P. 2010. DNA degradation and genetic analysis of empty puparia: Genetic identification limits in forensic entomology. 195, 99-102.
- MAZZARELLO, V., CHESSA, D., DELACONI, P., MARONGIU, P., KELVIN, D. J., KELVIN, N., CAMPUS, F., DEMURTAS, F. M., SANNA, S., POMPONI, V., SERRA, R., BANDIERA, P., MONTELLA, A. & RUBINO, S. 2014. Bioarchaeological analysis of Castelsardo's mummies. *Italian Journal of Anatomy and Embriology*, 119.
- MAZZETTE, R., COLLEO, M. M., RIU, G., PIRAS, G., PIRAS, F., ADDIS, M., PES, M., PIRISI, A., MELONI, D., MUREDDU, A., SPADA, S., FIORI, M., COINU, M. & LENTINI, A. 2010. Produzione di "casu marzu" in condizioni controllate: valutazione dell'effetto della colonizzazione da *Piophila casei* sulle caratteristiche microbiologiche e chimiche dei formaggi. *Italian Journal of Food Safety* 7, 45-54.
- MCALPINE, J. F. 1977. A revised classification of the Piophilidae, including "Neottiophilidae" and "Thyreophoridae" (Diptera: Schizophora). *The Memoirs of the Entomological Society of Canada*, 109, 1-66.
- MCALPINE, J. F., PETERSO, B. V., SHEWELL, G. E., TESKEY, H. J., VOCKEROTH, J. R. & WOOD, D. M. 1981. *Manual of Nearctic Diptera Vol. 1*, Ottawa, Ontario, Biosystematics Research Institute

- MCALPINE, J. F., PETERSON, B. V., SHEWELL, G. E., TESKEY, H. J., VOCKEROTH, J. R. & WOOD, D. M. 1987. *Manual of Nearctic Diptera Vol. 2*, Ottawa, Ontario, Biosystematics Research Institute
- MCCOBB, L. M. E. & BRIGGS, D. E. G. 2001. Preservation of fossil seeds from a 10th century AD cess pit at Coppergate, York. *Journal of Archaeological Science*, 28, 929-940.
- MCCOBB, M. L. E., BRIGGS, D. E. G., HALL, A. R. & KENWARD, H. K. 2004. The preservation of invertebrates in 16th century cesspits at St. Saviourgate, York. *Archaeometry*, 46, 157-169.
- MCDONAGH, L. M. & STEVENS, J. R. 2011. The molecular systematics of blowflies and screw worm flies (Diptera: Calliphoridae) using 28S rRNA, COX1 and EF-1 α : Insights into the evolution of dipteran parasitism. *Parasitology*, 138, 1760-1777.
- MCGOWAN, G. & PRANGNELL, J. 2006. The significance of vivianite in archaeological settings. *Geoarchaeology: An International Journal*, 21, 93-111.
- MCGREGOR, D. P., FORSTER, S., STEVEN, J., ADAIR, J., LEARY, S. E. C., LESLIE, D. L., HARRIS, W. J. & TITBALL, R. W. 1996. Simultaneous detection of microorganisms in soil suspension based on PCR amplification of bacterial 16S rRNA fragments. *BioTechniques*, 21, 463-471
- MÉGNIN, J.-P. 1894. *La Faune des Cadavres: Application de l'Entomologie à la Médecine Légale*, Paris, G. Masson.
- MEIKLEJOHN, K. A., WALLMAN, J. F. & DOWTON, M. 2013. DNA barcoding identifies all immature life stages of forensically important flesh fly (Diptera: Sarcophagidae). *Journal of Forensic Sciences*, 58, 184-187.
- MESSAGER, E., BADOU, A., FRÖHLICH, F., DENIAUX, B., LORDKIPANIDZE, D. & VOINCHET, P. 2010. Fruit and seed biomineralization and its effect on preservation. *Archaeological and Anthropological Sciences*, 2, 25-34.
- MIOKOVIC, B., ZIVKOVIC, J. & KOZACINSKI, L. 1997. Autochthonous Croatian 'rotten' cheese. *Veterinarski Arhiv*, 67, 25-32.
- MORALES, G. E. & WOLFF, M. 2010. Insects associated with the composting process of solid urban waste separated at the source. *Revista Brasileira de Entomologia*, 54, 645-653.
- MORROW, J. J., BALDWIN, D. A., HIGLEY, L., PIOMBINO-MASCALI, D. & REINHARD, K. J. 2015. Curatorial implications of *Ophyra capensis* (Order Diptera, Family Muscidae) puparia recovered from the body of the Blessed Antonio Patrizi, Monticiano, Italy (Middle Ages). *Journal of Forensic and Legal Medicine*, 36, 81-3.
- MORROW, J. J., MYHRA, A., PIOMBINO-MASCALI, D., LIPPI, D., ROE, A., HIGLEY, L. & REINHARD, K. J. 2016. Archaeoentomological and

- archaeological investigations of embalming jar contents from the San Lorenzo Basilica in Florence, Italy. *Journal of Archaeological Science: Reports*, 10, 166-171.
- NIELSEN, O. B., MAHLER, V. & RASMUSSEN, P. 2000. An arthropod assemblage and the ecological conditions in a byre at the Neolithic settlement of Weier, Switzerland. *Journal of Archaeological Science*, 27, 209-218.
- NORTON, R. A., BONAMO, P. M., GRIERSON, J. D. & W.A., S. 1988. Oribatid mite fossils from a terrestrial Devonian deposit near Gilboa, New York. *Journal of Paleontology*, 62, 259-269.
- NYSTROM, K. C., GOFF, A. & GOFF, M. L. 2005. Mortuary behaviour reconstruction through palaeoentomology: A case study from Chachapoya, Perú. *International Journal of Osteoarchaeology*, 15, 175-185.
- OKELY, E. F. 1974. Descriptions of the puparia of twenty-three British species of Sphaeroceridae (Diptera Acalypterae). *Transactions of the Royal Entomological Society of London*, 126, 41-56.
- OWSLEY, D. & COMPTON, B. 1997. Preservation in late 19th century in coffin burials. In: HAGLUND, W. & SORG, M. (eds.) *Forensic taphonomy: The postmortem fate of human remains*. Boca Raton, Florida: CRC Press.
- OZEROV, A. 2004. On the classification of the family Piophilidae (Diptera). *Zoologicheskii zhurnal*, 83, 600-608.
- PAABO, S., HIGUCHI, R. G. & WILSON, A. C. 1989. Ancient DNA and the Polymerase Chain Reaction. The emerging field of molecular archaeology. *The Journal of Biological Chemistry*, 264, 9709-9712.
- PANAGIOTAKOPULU, E. 2001. New records for ancient pests: Archaeoentomology in Egypt. *Journal of Archaeological Science*, 28, 1235-1246.
- PANAGIOTAKOPULU, E. 2003. Insect remains from the collections in the Egyptian Museum of Turin. *Archaeometry*, 45, 355-362.
- PANAGIOTAKOPULU, E. 2004. Dipterous remains and archaeological interpretation. *Journal of Archaeological Science*, 31, 1675-1684.
- PANAGIOTAKOPULU, E. & BUCHAN, A. L. 2015. Present and Norse Greenlandic hayfields – Insect assemblages and human impact in southern Greenland. *The Holocene*, 25, 921-931.
- PANAGIOTAKOPULU, E., SKIDMORE, P. & BUCKLAND, P. 2007. Fossil insect evidence for the end of the Western Settlement in Norse Greenland. *Naturwissenschaften*, 94, 300-306.
- PANOS, A., ARNALDOS, M. I., GARCIA, M. D. & UBERO-PASCAL, N. 2013. Ultrastructure of preimaginal stages of *Piophilidae* *megastigamata* McAlpine, 1978 (Diptera, Piophilidae): A fly of forensic importance. *Parasitology Research*, 112, 3771-3788.

- PAPE, T. 1996. Catalogue of the Sarcophagidae of the world (Insecta: Diptera). *Memoirs on Entomology, International*. Logan: American Entomological Institute.
- PASTULA, E. C. & MERRITT, R. W. 2013. Insect arrival pattern and succession on buried carrion in Michigan. *Journal of Medical Entomology*, 50, 432-439.
- PAYNE, J. A. 1965. A summer carrion study of the baby pig *Sus scrofa* Linnaeus. *Ecology*, 46, 592-602.
- PECHAL, J. L., CRIPPEN, T. L., TARONE, A. M., LEWIS, A. J., TOMBERLIN, J. K. & BENBOW, M. E. 2013. Microbial community functional change during vertebrate carrion decomposition. *PLoS ONE*, 8, e79035.
- PEDERSEN, M. W., OVERBALLE-PETERSEN, S., ERMINI, L., SARKISSIAN, C. D., HAILE, J., HELLSTROM, M., SPENS, J., THOMSEN, P. F., BOHMANN, K., CAPPELLINI, E., SCHNELL, I. B., WALES, N. A., CAROE, C., CAMPOS, P. F., SCHMIDT, A. M., GILBERT, M. T., HANSEN, A. J., ORLANDO, L. & WILLERSLEV, E. 2015. Ancient and modern environmental DNA. *Philosophical Transactions of the Royal Society B: Biological Sciences*, 370, 20130383.
- PITKIN, B. R. 1988. *Lesser dung flies (Diptera, Sphaeroceridae)*. London, Royal Entomological Society of London.
- PITTONI, E. 2009. Necropoli of Pill'e Matta Quartucciu (Cagliari, Sardinia): Wild bee and solitary wasp activity and bone diagenetic factors. *International Journal of Osteoarchaeology*, 19, 386-396.
- POINAR, G. O. 1994. The range of life in amber: Significance and implications in DNA studies. *Experientia*, 50, 536-542.
- POINAR, H. N., HOSS, M., BADA, J. L. & PAABO, S. 1996. Aminoacid racemization and the preservation of ancient DNA. *Science*, 272, 864-866.
- PONEL, P. 1993. Les Coléoptères du Quaternaire : leur rôle dans la reconstruction des paléoclimats et des paléoécosystèmes. *Bulletin d'Écologie*, 24, 5-16.
- PONEL, P., MATTARNE, V., COULTHARD, N. & YVENIC, J. H. 2000. La Tène and Gallo-Roman natural environments and human impact at the Touffréville rural settlement, reconstructed from Coleoptera and plant macroremains (Calvados, France). *Journal of Archaeological Science*, 27, 1055-1072.
- PONEL, P. & RICHOUX, P. 1997. Difficultés d'interprétation des assemblages de coleoptères fossiles quaternaires em milieu d'altitude. *Geobios*, 21, 213-219.
- PRADELLI, J., ROSSETTI, C., TUCCIA, F., GIORDANI, G., LICATA, M., BIRKHOFF, J. M., VERZELETTI, A. & VANIN, S. 2019. Environmental necrophagous fauna selection in a funerary hypogeal context: The putridarium of the Franciscan monastery of Azzio (Northern Italy). *Journal of Archaeological Science: Reports*, 24, 683-692.
- PRADO E CASTRO, C., SERRANO, A., MARTINS DA SILVA, P. & GARCÍA, M. 2012. Carrion flies of forensic interest: A study of seasonal community

- composition and succession in Lisbon, Portugal. *Medical and Veterinary Entomology*, 26, 417-431.
- PRADO E CASTRO, C., SOUSA, J. P., ARNALDOS, M. I., GASPAR, J. & GARCIA, M. D. 2011. Blowflies (Diptera: Calliphoridae) activity in sun exposed and shaded carrion in Portugal. *Annales de la Société Entomologique de France*, 47, 128-139.
- PURNELL, M. A., DONOGHUE, P. J. C., GABBOTT, S. E., MCNAMARA, M. E., MURDOCK, D. J. E. & SANSOM, R. S. 2018. Experimental analysis of soft-tissue fossilization: Opening the black box. *Palaeontology*, 61, 1-7.
- RAOULT, D., DUTOUR, O., HOUHAMDI, L., JANKAUSKAS, R., FOURNIER, P. E., ARDAGNA, Y., DRANCOURT, M., SIGNOLI, M., LA, V. D., MACIA, Y. & ABOUDHARAM, G. 2006. Evidence for louse-transmitted diseases in soldiers of Napoleon's Grand Army in Vilnius. *The Journal of Infectious Diseases*, 193, 112-20.
- RATNASINGHAM, S. & HEBERT, P. D. N. 2007. BOLD: The Barcode of Life Data System (www.barcodinglife.org). *Molecular Ecology Notes*, 7, 355-364.
- REISS, R. A. 2006. Ancient DNA from ice age insects: Proceed with caution. *Quaternary Science Reviews*, 25, 1877-1893.
- ROCHEFORT, S., GIROUX, M., SAVAGE, J. & WHEELER, T. A. 2015. Key to forensically important Piophilidae (Diptera) in the Nearctic Region. *Canadian Journal of Arthropod Identification*, 27, 1-37.
- ROCHEFORT, S. & WHEELER, T. A. 2015. Diversity of Piophilidae (Diptera) in northern Canada and description of a new Holarctic species of *Parapiophila* McAlpine. *Zootaxa*, 3925, 229-240.
- ROGERS, S. O. & BENDICH, A. J. 1985. Extraction of DNA from milligram amounts of fresh, herbarium and mummified plant tissues. *Plant Molecular Biology*, 5, 69-76.
- ROTHER, M., KLEEBERG, A. & HUPFER, M. 2016. The occurrence, identification and environmental relevance of vivianite in waterlogged soils and aquatic sediments. *Earth-Science Reviews*, 158, 51-64.
- ROVINA, D. & FIORI, M. 2010. Sassari sottosopra. Dieci anni di archeologia urbana. Guida della Mostra. Sassari, Palazzo della Frumentaria, 18 dicembre 2009 – 31 marzo 2010.
- RUMIZA, A. R., KHAIRUL, O., ZUHA, R. M. & HEO, C. C. 2010. An observation on the decomposition process of gasoline-ingested monkey carcasses in a secondary forest in Malaysia. *Tropical Biomedicine*, 27, 373-383.
- SACCHI, E. & PETTI, F. M. 2008. Insect pupation chambers from Pleistocene paleosols of Santo Stefano Island (pontine Archipelago, Central Italy). *Studi Trentini di Scienze Naturali Acta Geologica*, 83, 205-210.

- SALEH, M. S. M. & EL SIBAE, M. M. 1993. Urino-genital myiasis due to *Piophilha casei*. *Journal of the Egyptian Society of Parasitology*, 23, 737-739.
- SALTINI, A. 1984. *Storia delle scienze agrarie*, Bologna, Edagricole.
- SARPONG, D., ODURO-KWARTENG, S., GYASI, S. F., BUAMAH, R., DONKOR, E., AWUAH, E. & BAAH, M. K. 2019. Biodegradation by composting of municipal organic solid waste into organic fertilizer using the black soldier fly (*Hermetia illucens*) (Diptera: Stratiomyidae) larvae. *International Journal of Recycling of Organic Waste in Agriculture*, 8, 45-54.
- SAWABY, R. F., HAMOULY, H. E. & ABO-EL ELA, R. H. 2018. Diagnosis and keys of the main dipterous families and species collected from rabbit and guinea pig carcasses in Cairo, Egypt. *The Journal of Basic and Applied Zoology*, 79.
- SETTI, L., FRANCA, E., PULVIRENTI, A., GIGLIANO, S., ZACCARDELLI, M., PANE, C., CARADONIA, F., BORTOLINI, S., MAISTRELLO, L. & RONGA, D. 2019. Use of black soldier fly (*Hermetia illucens* (L.), Diptera: Stratiomyidae) larvae processing residue in peat-based growing media. *Waste Management*, 95, 278-288.
- SIMMONS, P. 1927. The cheese skipper as a pest in cured meats. *Bulletin of the U. S. Department of Agriculture*, 1453, 1-55.
- SKIDMORE, P. 1985. *The Biology of the Muscidae of the World*, Dordrecht, Springer Netherlands.
- SKIDMORE, P. 1996. *A dipterological perspective on the Holocene history of the North Atlantic Area. Appendix One-Puparia of British Sphaeroceridae*. PhD, University of Sheffield.
- SKIDMORE, P. 1999. The Diptera. In: CONNOR, A. & BUCKLEY, R. (eds.) *Roman and Medieval occupation in Causeway Lane, Leicester*. Leicester: Leicester University Press.
- SMITH, B. C. 2011. *Fundamentals of Fourier Transform infrared spectroscopy*, Boca Raton, Florida, CRC Press.
- SMITH, C. I., CHAMBERLAIN, A. T., RILEY, M. S., STRINGER, C. & COLLINS, M. J. 2003. The thermal history of human fossils and the likelihood of successful DNA amplification. *Journal of Human Evolution*, 45, 203-217.
- SMITH, D. 2017. Locating where archaeological sites occur in intertidal sequences: The use of archaeoentomological data as a proxy for tidal regime. *Journal of Archaeological Science*, 82, 1-16.
- SMITH, D. N. 2007. Southampton French Quarter SOU 1382. Specialist report download E9: Mineralised and waterlogged fly pupae, and other insects and arthropods. Oxford: Oxford Archaeology South.
- SMITH, K. G. V. 1973. *Insects and Other Arthropods of Medical Importance*, London British Museum (Natural History).

- SMITH, K. G. V. 1986. *A Manual of Forensic Entomology*, Ithaca, Cornell University Press.
- SOARES, S., AMARAL, J. S., OLIVEIRA, M. B. P. P. & MAFRA, I. 2013. A SYBR Green real-time PCR assay to detect and quantify pork meat in processed poultry meat products. *Meat Science*, 94, 115–120.
- SUGUMARAN, M. 2002. Comparative biochemistry of eumelanogenesis and the protective roles of phenoloxidase and melanin in insects. *Pigment Cell Research*, 15, 2–9.
- SUGUMARAN, M. 2009. Complexities of cuticular pigmentation in insects. *Pigment Cell and Melanoma Research* 22, 523–525.
- SUKONTASON, K. L., SUKONTASON, K., PIANGJAI, S., CHOOCHOTE, W., VOGTSBERGER, R., C. & OLSON, J. K. 2001. Scanning electron microscopy of the third-instar *Piophilidae casei* (Diptera: Piophilidae), a fly species of forensic importance. *Journal of Medical Entomology*, 38, 756–759.
- SZPILA, K. 2010. Key for the identification of third instars of European blowflies (Diptera: Calliphoridae) of forensic importance. In: AMENDT, J., GOFF, M. L., CAMPOBASSO, P. C. & GRASSBERGER, M. (eds.) *Current Concepts in Forensic Entomology*. Dordrecht: Springer Netherlands.
- SZPILA, K. 2012. Key for identification of European and Mediterranean blowflies (Diptera, Calliphoridae) of medical and veterinary importance – adult flies. In: GENNARD, D. (ed.) *Forensic entomology, an introduction*. Second ed. Hoboken, NJ, USA: Willey-Blackwell.
- SZPILA, K., RICHET, R. & PAPE, T. 2015. Third instar larvae of flesh flies (Diptera: Sarcophagidae) of forensic importance—critical review of characters and key for European species. *Parasitology Research*, 114, 2279–89.
- TAUTZ, D., ARCTANDER, P., MINELLI, A., THOMAS, R. H. & VOLGER, A. P. 2003. A plea for DNA taxonomy. *TRENDS in Ecology Evolution*, 18, 70–74.
- TENORIO, J. A. 1968. Taxonomic and biological studies of Hawaiian Sphaeroceridae (Diptera). *Proceedings, Hawaiian Entomological Society*, 20.
- TEODOROWICH, G. 1961. *Authigenic minerals in sedimentary rocks*, New York, Consultants Bureau Enterprises
- TETLOW, E. 2009. Insects. Southampton French Quarter 1382. *Specialist Report Download E7*. Oxford.
- TIN, M. M., ECONOMO, E. P. & MIKHEYEV, A. S. 2014. Sequencing degraded DNA from non-destructively sampled museum specimens for RAD-tagging and low-coverage shotgun phylogenetics. *PLoS One*, 9, e96793.
- TRAVERSARI, M., MINGHETTI, C., MILANI, V., SHAW, C. N., GRUPPIONI, G. & FRELAT, M. A. 2014. Gli inumati parzialmente mummificati di Roccapelago-Modena (sec. XVIII): ricostruzione delle attività occupazionali di una comunità

- dell' Appennino attraverso l'analisi degli indicatori da sovraccarico biomeccanico con ausilio di modelli virtuali 3D delle ossa. *Annali dell' Università di Ferrara*, 10, 147-154.
- TUCCIA, F., GIORDANI, G. & VANIN, S. 2016a. A combined protocol for identification of maggots of forensic interest. *Science & Justice*, 56, 264-8.
- TUCCIA, F., GIORDANI, G. & VANIN, S. 2016b. A general review of the most common COI primers for Calliphoridae identification in forensic entomology. *Forensic Science International. Genetics*, 24, e9-e11.
- TURCHETTO, M., LAFISCA, S. & COSTANTINI, G. 2001. Postmortem interval (PMI) determined by study sarcophagous biocenoses: Three cases from the province of Venice (Italy). *Forensic Science International*, 120, 28-31.
- VANIN, S. 2012. Archeoentomologia funeraria: risultati e prospettive dallo studio delle mummie di Roccapelago. *Roccapelago e le sue mummie: studio integrato della vita di una piccola comunità dell'Appennino tra XVI e XVIII secolo*. Modena: Academy Editions.
- VANIN, S., BUBACCO, L. & BELTRAMINI, M. 2008. Seasonal variation of trehalose and glycerol concentrations in winter snow-active insects. *Cryo Letters*, 29, 485-91.
- VANIN, S. & HUCHET, J. B. 2017. Forensic entomology and funerary archaeoentomology. In: SCHOTSMANS, E. M., MÁRQUEZ-GRANT, N. & FORBES, S. L. (eds.) *Taphonomy of human remains: Forensic analysis of the dead and the depositional environment*. Manhattan: Wiley.
- VANIN, S., ZANOTTI, E., GIBELLI, D., TABORELLI, A., ANDREOLA, S. & CATTANEO, C. 2013. Decomposition and entomological colonization of charred bodies - a pilot study. *Croatian Medical Journal*, 54, 387-93.
- WEBB, S. C., HEDGES, R. E. M. & ROBINSON, M. 1998. The seaweed fly *Thoracochaeta zosterae* (Hal.) (Diptera: Sphaeroceridae) in inland archaeological contexts: D13c and d15n solves the puzzle. *Journal of Archaeological Science*, 25, 1253-1257.
- WELLS, J. & STEVENS, J. 2008. Application of DNA-based methods in forensic entomology. *Annual Review of Entomology*, 53, 103-20.
- WELLS, J. D., INTRONA, F., DI VELLA, G., CAMPOBASSO, C. P., HAYES, J. & SPERLING, F. A. 2001. Human and insect mitochondrial DNA analysis from maggots. *Journal of Forensic Science*, 46, 685-687.
- WELTON, J. E. 2003. *SEM Petrology Atlas*, Tulsa, Oklahoma, USA, The American Association of Petroleum Geologists.
- WILKENS, B. 2016. La città come ambiente naturale: il caso di Sassari medievale e moderna. *Sardinia, Corsica et Baleares Antiquae: International Journal*, 16, 127-132.

- WILSON, I. G. 1997. Inhibition and facilitation of nucleic acid amplification. *Applied and Environmental Microbiology*, 63, 3741-3751.
- YANG, D. Y. & WATT, K. 2005. Contamination controls when preparing archaeological remains for ancient DNA analysis. *Journal of Archaeological Science*, 32, 331-336.
- YEATES, D. K., WIEGMANN, B. M., COURTNEY, G. W., MEIER, R., LAMBKIN, C. & PAPE, T. 2007. Phylogeny and systematics of Diptera: Two decades of progress and prospects. *Zootaxa*, 1668, 565-590.
- YUSSEFF-VANEGAS, S. Z. & AGNARSSON, I. 2017. DNA-barcoding of forensically important blow flies (Diptera: Calliphoridae) in the Caribbean Region. *PeerJ*, 5, e3516.
- ZAJAC, B. K., MARTÍN-VEGA, D., FEDDERN, N., FREMDT, H., E CASTRO, C. P., SZPILA, K., RECKEL, F., SCHÜTT, S., VERHOFF, M. A., AMENDT, J. & ZEHNER, R. 2016. Molecular identification and phylogenetic analysis of the forensically important family Piophilidae (Diptera) from different European locations. *Forensic Science International*, 259, 77-84.
- ZEHNER, R., AMENDT, J., SCHÜTT, S., SAUER, J., KRETTEK, R. & POVOLNÝ, D. 2004. Genetic identification of forensically important flesh flies (Diptera: Sarcophagidae). *International Journal of Legal Medicine*, 118, 245-247.
- ZHOU, W., APKARIAN, R., WANG, Z. L. & JOY, D. 2006. Fundamentals of Scanning Electron Microscopy (SEM). In: ZHOU, W. & WANG, Z. L. (eds.) *Scanning Microscopy for Nanotechnology*. Springer: New York.
- ZUSKA, J. & LAŠTOVKA, P. 1969. Species-composition of the dipterous fauna in various types of food-processing plants in Czechoslovakia. *Acta Entomologica Bohemoslovaca*, 66, 201-221.

Appendix A

Supplementary Table A1. Diptera Ulidiidae mtCOI barcoding sequences dataset. Sequences are listed per species, BOLD/GenBank accession number, and geographical origin. * = domestic sequences from this study.

Subfamily	Species	BOLD	GenBank	origin
Ulidiinae	<i>Physiphora alceae</i> *		MH686505*	Northern Italy
	<i>Physiphora alceae</i> *		MH686506*	Northern Italy
	<i>Physiphora aenea</i>	DIQT470-09		Australia
	<i>Physiphora aenea</i>	DIQTB341-11		Australia
	<i>Physiphora aenea</i>	DIQTB344-11		Australia
	<i>Physiphora clausa</i>	GBDP15226-14	AB907177	India
	<i>Physiphora clausa</i>	GBDP15297-14	KC663633	Russia
	<i>Physiphora alceae</i>	TGSPA085-07	KC755978	Russia
	<i>Physiphora demandata</i>	JSDIS042-11	KR663640	Canada
	<i>Ulidia megacephala</i>	GBDPT992-14	KC663636	Russia
	<i>Ulidia ruficeps</i>	GBDPT993-14	KC663637	Russia
	<i>Timia monticola</i>	GBDP15299-14	KC663634	Russia
	<i>Timia erythrocephala</i>	TGSPA80-07	KC755993	Russia
	<i>Timia erythrocephala</i>	TGSPA81-07	KC755994	Russia
	<i>Timia libani</i>	GBDP15298-14	KC663635	Russia
	<i>Homalocephala angustata</i>	TGSPA066-07	KC755946	Russia
	<i>Homalocephala angustata</i>	TGSPA067-07	KC755947	Russia
	<i>Homalocephala angustata</i>	TGSPA068-07	KC755948	Russia
	<i>Homalocephala apicalis</i>	TGSPA062-07	KC755949	Russia
	<i>Homalocephala albitarsis</i>	TGSPA069-07	KC755943	Russia
Otitinae	<i>Ceroxys urticae</i>	TGSPA011-07	KC755934	Russia
	<i>Ceroxys urticae</i>	TGSPA012-07	KC755933	Russia
	<i>Ceroxys urticae</i>	TGSPA022-07	KC755936	Russia
	<i>Ceroxys munda</i>	TGSPA016-07	KC755931	Moldova
	<i>Ceroxys cinifera</i>	TGSPA018-07	KC755927	Kyrgyzstan
	<i>Ceroxys cinifera</i>	TGSPA019-07	KC755928	Kyrgyzstan
	<i>Otites lamed</i>	TGSPA008-07	KC755977	Ukraine
	<i>Otites lamed</i>	TGSPA010-07	KC755975	Ukraine
	<i>Otites formosa</i>	GMGMI330-14		Germany
	<i>Otites formosa</i>	GMGMI1243-14		Germany
	<i>Otites formosa</i>	TGSPA007-07	KC755970	Russia
	Subfamily	Species	BOLD	GenBank

Otitinae				
	<i>Otites formosa</i>	TGSPA005-07	KC755969	Russia
	<i>Herina nigribiasis</i>	BARSC297-16		Canada
	<i>Herina nigribiasis</i>	JEDCF252-10	JF875082	Canada
	<i>Herina lugubris</i>	TGSPA053-07	KC755940	Russia
	<i>Herina lugubris</i>	TGSPA054-07	KC755941	Russia
	<i>Herina lugubris</i>	TGSPA056-07	KC755942	Russia
	<i>Melieria crassipennis</i>	TGSPA041-07	KC755960	Russia
	<i>Melieria crassipennis</i>	TGSPA042-07	KC755957	Russia
	<i>Melieria cana</i>	CNWBG2660-13	KP048469	Canada
	<i>Melieria cana</i>	TGSPA038-07	KC755955	Kyrgyzstan
	<i>Melieria cana</i>	TGSPA039-07	KC755956	Russia
	<i>Melieria omissa</i>	TGSPA031-07	KC755961	Turkmenistan
	<i>Melieria acuticornis</i>	TGSPA043-07	KC755952	Russia
	<i>Melieria acuticornis</i>	TGSPA045-07	KC755953	Russia
	<i>Myennis octopuntata</i>	TGSPA028-07	KC755964	Russia
	<i>Myennis octopuntata</i>	TGSPA029-07	KC755963	Russia
	<i>Pseudotephritis corticalis</i>	TGSPA046-07	KC755981	Russia
	<i>Seioptera vibrans</i>	JSDIS277-11	KR663834	Canada
	<i>Seioptera vibrans</i>	OPPFA325-17		Canada
	<i>Seioptera vibrans</i>	SSJAE9534-13	KM898900	Canada
	<i>Seioptera vibrans</i>	TTDFW156-08	KR525288	Canada
	<i>Tetanops sintenisi</i>	TGSPA073-07	KC755990	Russia
	<i>Tetanops sintenisi</i>	TGSPA074-07	KC755991	Russia

Continues from Supplementary Table A1

Outgroup	<i>Drosophila melanogaster</i>	DIQTB504-12		Australia
	<i>Drosophila simulans</i>	BBDCQ829-10	JN291600	Canada
	<i>Drosophila virilis</i>	GBDP2524-06	DQ426802	United Kingdom
	<i>Psila fimentaria</i>	TGSPA086-07	KC755983	Russia
	<i>Psila fimentaria</i>	TGSPA087-07	KC755984	Russia
	<i>Psila fimentaria</i>	TGSPA088-07	KC755985	Russia
	<i>Psila fimentaria</i>	TGSPA089-07	KC755982	Russia

Supplementary Table A2. Diptera Piophilidae mtCOI barcoding sequences dataset. Sequences are listed per species, BOLD/GenBank accession number, and geographical origin

Species	BOLD	GenBank	origin
<i>Piophila nigriceps</i>	BBDEC478-09		Canada
		KP659182	Germany
		KP659165	Poland
<i>Piophila casei</i>	DIQT130-08		Australia
		KP659122	Spain
		KP659123	Spain
		KP659124	Spain
<i>Piophila megastigmata</i>		KP659130	Spain
		KP659129	Portugal
		KP659126	Portugal
<i>Parapiophila atrifrons</i>	CNMIE1076-14	KR384789	Canada
	CNMIE425-14	KR394264	Canada
<i>Parapiophila vulgaris</i>	GBDP15922-15		Romania
		KJ193727	Romania
		KR992660	Canada
		KR990366	Canada
		JN257255	Germany
		JN257254	Germany
		JN257253	Germany
		JN257252	Germany
		JN257251	Germany
		JN25725	Germany
		JN257249	Germany
		KP659121	Germany
		KP659119	
		KP659118	
		KP659117	Germany
		KP659116	Germany
		KP659115	Germany
		KP659114	Germany
		KP659113	Germany
		KP659112	Germany
KP659111	Germany		
KP659110	Germany		
KP659109	Germany		
KP659108	Germany		
KP659107	Germany		
KP659105	Germany		

Continues from Supplementary Table A2.

Species	BOLD	GenBank	origin
<i>Parapiophila vulgaris</i>		KP659104	Germany
	GBDP15922-15		Romania
		KJ193727	Romania
<i>Parapiophila flavipes</i>	DARC166-10		Canada
		KR432574	Canada
	CNIVA120-14		Canada
<i>Liopiophila varipes</i>	BBDCM321-10		Canada
	JSDIQ486-10		Canada
		KP659085	Portugal
		KP659086	Germany
		KP659097	Switzerland
<i>Protopiophila litigata</i>	CNEID2738-12		Canada
		KR428889	Canada
<i>Protopiophila latipes</i>	NSMTP002-15		Sweden
	BCFOR549-15		Czech Republic
	TTMDI1244-10	HQ581780	Canada
	GMGMM1562-14	KP659142	Germany
	GBDP18950-15	KP659146	Switzerland
<i>Allopiophila luteata</i>	JWDCH177-10		Canada
		KM944188	Canada
		KR662766	Canada
<i>Allopiophila vulgaris</i>	ZMUCG055-12		Greenland
		KT959691	Greenland
		KT960010	Greenland
		KT959975	Greenland
<i>Prochyliza xanthosoma</i>	PHDIP674-11		Canada
		KT117427	Canada
		KT107748	Canada
		KT111043	Canada
<i>Prochyliza brevicornis</i>	CNTMC1139-1	KR386446	Canada
	SSWLA5088-13	KM640932	Canada
	CNTMC344-14	KR399597	Canada
	CNTMC1592-14	KR395288	Canada
		KT117530	Canada
<i>Lasiopiophila piolsa</i>	GMGNA040-14		Greenland
		KR435865	Canada
		KU374416	Greenland
		KU374203	Greenland
<i>Centrophlebomyia furcata</i>		KP659082	Spain

Continues from Supplementary Table A2.

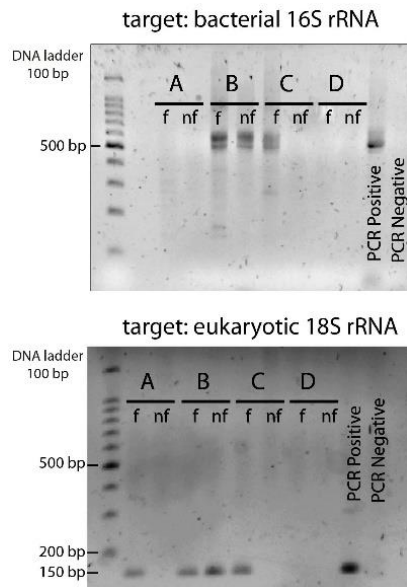
Species	BOLD	GenBank	origin
<i>Centrophlebomyia furcata</i>		KP659084	Spain
<i>Mycetaulus bipunctatus</i>	CNEID305-12		Canada
		KM571894	Canada
<i>Amphipogon flavum</i>		KR394998	Canada
		KM934051	Canada
<i>Arctopiophila arctica</i>	DARC179-10		Canada
<i>Boreopiophila tomentosa</i>	JSYKA463-10		Canada
<i>Actenoptera hilarella</i>	BBDED554-10		Canada
		KR724957	Canada
		KR425761	Canada
		KR587280	Canada
<i>Thyreophora cynophila</i>		KP659181	Spain
		KP659180	Spain
		KP659179	Spain
<i>Otites formoza</i>	GMGMI330-14		Germany
	TGSPA005-07	KC755969	Russia

Supplementary Table A3. Absorbance ratios of Roccapelago DNA extracts measured on non-purified (ROSE buffer lysis suspensions) and purified (1st and 2nd strategy) eluates.

number of puparia	raw DNA eluates		purified DNA eluates		purified DNA eluates	
	ROSE buffer		1 st strategy		2 nd strategy	
	260/280	260/230	260/280	260/230	260/280	260/230
CTRL 1	1.73	1.83	1.99	0.06	1.49	0.5
CTRL 2	1.48	0.36	1.95	1.02	1.75	0.78
CTRL 3	1.53	1.21	2.47	0.87	1.82	0.62
CTRL 5	1.43	0.37	1.94	0.75	1.69	0.59
CTRL 8	1.29	0.28	1.18	2.7	1.23	0.52
Roccapelago 1	1.53	4.75	1.27	3.56	1.47	0.62
Roccapelago 2	1.32	2.69	1.52	0.45	1.4	0.5
Roccapelago 3	1.29	0.32	1.62	-0.01	1.65	0.39
Roccapelago 5	1.25	0.31	1.91	0.69	1.49	0.36
Roccapelago 8	1.56	1.4	1.17	1.04	1.79	1.13

Supplementary Table A4. Absorbance ratios of Castelsardo DNA extracts measured on non-purified (ROSE buffer lysis suspensions) and purified eluates. 1st step= OneStep PCR removal kit (ZymoResearch); 2nd step= ReliaPrep DNA purification and concentration system (Promega); A,B,C= replicates.

number of puparia	raw DNA eluates		purified DNA eluates		purified DNA eluates	
	ROSE buffer		1 st step		2 nd step	
	260/280	260/230	260/280	260/230	260/280	260/230
CTRL A	1.90	0.43	1.82	0.69	1.88	1.08
CTRL B	1.81	5.53	1.83	3.23	1.92	1.14
CTRL C	1.88	2.31	1.91	1.57	1.92	1.06
CSHyd A	1.55	6.59	1.69	0.09	2.07	0.08
CSHyd B	1.57	8.44	1.74	0.21	2.03	0.13
CSHyd C	1.50	5.58	1.61	0.44	2.72	0.04



Supplementary Figure A1. Environmental targets PCR results. Bacterial 16S rRNA (above) and eukaryotic 18S rRNA (below) were successfully amplified when the DNA extracted from Sphaeroceridae puparia was used as template using methods A-D as described in Fig. 4.22: Gilbert's digestion buffer and the QiAamp Investigator Kit (Qiagen) (A), DNEasy power Soil Kit (Qiagen) (B), Campos digestion buffer+ QIAquick DNA purification kit (C), pre-wash in NaClO 0.5% + Campos digestion buffer+ QIAquick DNA purification kit (D). f= fragmented puparia, nf= non-fragmented puparia. DNA ladder: 100 bp.

Supplementary Table A5. Pairwise sequence distances between *Allopiophila/Parapiophila vulgaris* sequences. Red= “presumed” *P. vulgaris* German and Romanian sequences showing a pairwise distance within the range 13.9–15.6% in comparison to the other European and Canadian sequences. Green= intra-specific divergence of the wrongly identified species. Black= pairwise distance values under the threshold between *P. vulgaris* correctly identified species from Europe and extra-Europe.

	1	2	3	4	5	6	7	8	9	10	11	12	13	14
1 ASV0023042 <i>P. vulgaris</i> (this study)														
2 ASV0014806 <i>P. vulgaris</i> (this study)	0.46%													
3 ZMUCG055-12 <i>A. vulgaris</i> (Greenland)	0.69%	0.69%												
4 JN257255 <i>P. vulgaris</i> (Germany) (Boehme et al. 2012)	13.87%	14.55%	13.90%											
5 JN257254 <i>P. vulgaris</i> (Germany) (Boehme et al. 2012)	14.55%	14.55%	13.90%	0.46%										
6 JN257253 <i>P. vulgaris</i> (Germany) (Boehme et al. 2012)	14.21%	14.21%	13.56%	0.23%	0.23%									
7 JN257252 <i>P. vulgaris</i> (Germany) (Boehme et al. 2012)	14.55%	14.55%	13.90%	0.46%	0.46%	0.23%								
8 JN257251 <i>P. vulgaris</i> (Germany) (Boehme et al. 2012)	13.87%	14.55%	13.90%	0.93%	1.41%	1.17%	1.41%							
9 JN257250 <i>P. vulgaris</i> (Germany) (Boehme et al. 2012)	13.87%	14.55%	13.90%	0.46%	0.93%	0.69%	0.93%	0.46%						
10 JN257249 <i>P. vulgaris</i> (Germany) (Boehme et al. 2012)	14.55%	15.25%	14.58%	0.46%	0.93%	0.69%	0.93%	0.93%	0.46%					
11 GBDP15922-15 <i>P. vulgaris</i> (Romania)	13.87%	14.55%	13.90%	0.00%	0.46%	0.23%	0.46%	0.93%	0.46%	0.46%				
12 KT959691_A <i>P. vulgaris</i> (Greenland)	0.69%	0.69%	0.00%	13.90%	13.90%	13.56%	13.90%	13.90%	13.90%	14.58%	13.90%			
13 KJ193727 <i>P. vulgaris</i> (Romania)	13.87%	14.55%	13.90%	0.00%	0.46%	0.23%	0.46%	0.93%	0.46%	0.46%	0.00%	13.90%		
14 KT960010 <i>A. vulgaris</i> (Greenland)	0.69%	0.69%	0.00%	13.90%	13.90%	13.56%	13.90%	13.90%	13.90%	14.58%	13.90%	0.00%	13.90%	
15 KR992660 <i>P. vulgaris</i> (Canada)	0.46%	0.46%	0.69%	14.53%	14.53%	14.19%	14.53%	14.53%	14.53%	15.22%	14.53%	0.69%	14.53%	0.69%
16 KR990366 <i>P. vulgaris</i> (Canada)	0.46%	0.00%	0.69%	14.55%	14.55%	14.21%	14.55%	14.55%	14.55%	15.25%	14.55%	0.69%	14.55%	0.69%
17 KP659121 <i>P. vulgaris</i> (Germany) (Zajac et al. 2016)	0.69%	0.23%	0.92%	14.87%	14.87%	14.53%	14.87%	14.87%	14.87%	15.57%	14.87%	0.92%	14.87%	0.92%
18 KP659120 <i>P. vulgaris</i> (Germany) (Zajac et al. 2016)	0.69%	0.23%	0.92%	14.90%	14.90%	14.55%	14.90%	14.21%	14.21%	14.90%	14.90%	0.92%	14.90%	0.92%
19 KP659119 <i>P. vulgaris</i> (Switzerland) (Zajac et al. 2016)	0.69%	0.69%	0.46%	13.87%	13.87%	13.54%	13.87%	13.87%	13.87%	14.55%	13.87%	0.46%	13.87%	0.46%
20 KP659118 <i>P. vulgaris</i> (Switzerland) (Zajac et al. 2016)	0.23%	0.23%	0.92%	14.21%	14.90%	14.55%	14.90%	14.21%	14.21%	14.90%	14.21%	0.92%	14.21%	0.92%
21 KP659117 <i>P. vulgaris</i> (Germany) (Zajac et al. 2016)	0.23%	0.23%	0.46%	14.21%	14.21%	13.87%	14.21%	14.21%	14.21%	14.90%	14.21%	0.46%	14.21%	0.46%
22 KP659116 <i>P. vulgaris</i> (Germany) (Zajac et al. 2016)	0.69%	0.23%	0.92%	14.55%	14.55%	14.21%	14.55%	14.55%	14.55%	15.25%	14.55%	0.92%	14.55%	0.92%
23 KP659115 <i>P. vulgaris</i> (Germany) (Zajac et al. 2016)	0.46%	0.00%	0.69%	14.55%	14.55%	14.21%	14.55%	14.55%	14.55%	15.25%	14.55%	0.69%	14.55%	0.69%
24 KP659114 <i>P. vulgaris</i> (Germany) (Zajac et al. 2016)	0.46%	0.46%	0.69%	13.87%	13.87%	13.54%	13.87%	13.87%	13.87%	14.55%	13.87%	0.69%	13.87%	0.69%
25 KP659113 <i>P. vulgaris</i> (Germany) (Zajac et al. 2016)	0.69%	0.23%	0.92%	14.90%	14.90%	14.55%	14.90%	14.90%	14.90%	15.60%	14.90%	0.92%	14.90%	0.92%
26 KP659112 <i>P. vulgaris</i> (Germany) (Zajac et al. 2016)	0.93%	0.93%	0.69%	13.87%	13.87%	13.54%	13.87%	13.87%	13.87%	14.55%	13.87%	0.69%	13.87%	0.69%
27 KP659111 <i>P. vulgaris</i> (Germany) (Zajac et al. 2016)	0.69%	0.23%	0.92%	14.90%	14.90%	14.55%	14.90%	14.90%	14.90%	15.60%	14.90%	0.92%	14.90%	0.92%
28 KP659110 <i>P. vulgaris</i> (Germany) (Zajac et al. 2016)	0.69%	0.23%	0.92%	14.87%	14.87%	14.53%	14.87%	14.87%	14.87%	15.57%	14.87%	0.92%	14.87%	0.92%
29 KP659109 <i>P. vulgaris</i> (Germany) (Zajac et al. 2016)	0.46%	0.00%	0.69%	14.55%	14.55%	14.21%	14.55%	14.55%	14.55%	15.25%	14.55%	0.69%	14.55%	0.69%
30 KP659108 <i>P. vulgaris</i> (Germany) (Zajac et al. 2016)	0.46%	0.00%	0.69%	14.55%	14.55%	14.21%	14.55%	14.55%	14.55%	15.25%	14.55%	0.69%	14.55%	0.69%
31 KP659107 <i>P. vulgaris</i> (Germany) (Zajac et al. 2016)	0.93%	0.93%	1.64%	14.55%	15.25%	14.90%	15.25%	14.55%	14.55%	15.25%	14.55%	1.64%	14.55%	1.64%
32 KP659105 <i>P. vulgaris</i> (Germany) (Zajac et al. 2016)	0.69%	0.23%	0.92%	14.55%	14.55%	14.21%	14.55%	14.55%	14.55%	15.25%	14.55%	0.92%	14.55%	0.92%
33 KP659104 <i>P. vulgaris</i> (Germany) (Zajac et al. 2016)	0.92%	0.46%	1.16%	14.87%	14.87%	14.53%	14.87%	14.87%	14.87%	15.57%	14.87%	1.16%	14.87%	1.16%

Continues from Supplementary Table A5

	15	16	17	18	19	20	21	22	23	24	25	26	27	28	29	30	31	32	33	
1	ASV0023042 <i>P. vulgaris</i> (this study)																			
2	ASV0014806 <i>P. vulgaris</i> (this study)																			
3	ZMUCG055-12 <i>A. vulgaris</i> (Greenland)																			
4	JN257255 <i>P. vulgaris</i> (Germany) (Boehme et al. 2012)																			
5	JN257254 <i>P. vulgaris</i> (Germany) (Boehme et al. 2012)																			
6	JN257253 <i>P. vulgaris</i> (Germany) (Boehme et al. 2012)																			
7	JN257252 <i>P. vulgaris</i> (Germany) (Boehme et al. 2012)																			
8	JN257251 <i>P. vulgaris</i> (Germany) (Boehme et al. 2012)																			
9	JN257250 <i>P. vulgaris</i> (Germany) (Boehme et al. 2012)																			
10	JN257249 <i>P. vulgaris</i> (Germany) (Boehme et al. 2012)																			
11	GBDP15922-15 <i>P. vulgaris</i> (Romania)																			
12	KT959691_ <i>A. vulgaris</i> _Greenland																			
13	KJ193727 <i>P. vulgaris</i> (Romania)																			
14	KT960010 <i>A. vulgaris</i> (Greenland)																			
15		0.69%																		
16			0.46%																	
17		0.92%	0.69%	0.23%																
18		0.92%	0.69%	0.23%	0.46%															
19		0.46%	0.69%	0.69%	0.92%	0.93%														
20		0.92%	0.69%	0.23%	0.46%	0.46%	0.93%													
21		0.46%	0.23%	0.23%	0.46%	0.46%	0.46%	0.46%												
22		0.92%	0.69%	0.23%	0.46%	0.46%	0.93%	0.46%	0.46%											
23		0.69%	0.46%	0.00%	0.23%	0.23%	0.69%	0.23%	0.23%	0.23%										
24		0.69%	0.46%	0.46%	0.69%	0.69%	0.69%	0.69%	0.23%	0.69%	0.46%									
25		0.92%	0.69%	0.23%	0.46%	0.46%	0.93%	0.46%	0.46%	0.46%	0.23%	0.69%								
26		0.69%	0.92%	0.93%	1.16%	1.17%	0.23%	1.17%	0.69%	1.17%	0.93%	0.93%	1.17%							
27		0.92%	0.69%	0.23%	0.46%	0.46%	0.93%	0.46%	0.46%	0.46%	0.23%	0.69%	0.46%	1.17%						
28		0.92%	0.69%	0.23%	0.46%	0.46%	0.92%	0.46%	0.46%	0.46%	0.23%	0.69%	0.46%	1.16%	0.46%					
29		0.69%	0.46%	0.00%	0.23%	0.23%	0.69%	0.23%	0.23%	0.23%	0.00%	0.46%	0.23%	0.93%	0.23%	0.23%				
30		0.69%	0.46%	0.00%	0.23%	0.23%	0.69%	0.23%	0.23%	0.23%	0.00%	0.46%	0.23%	0.93%	0.23%	0.23%	0.00%			
31		1.64%	1.40%	0.93%	1.16%	1.17%	1.65%	0.69%	1.17%	1.17%	0.93%	1.41%	1.17%	1.89%	1.17%	1.16%	0.93%	0.93%		
32		0.92%	0.69%	0.23%	0.46%	0.46%	0.93%	0.46%	0.46%	0.00%	0.23%	0.69%	0.46%	1.17%	0.46%	0.46%	0.23%	0.23%	1.17%	
33		1.16%	0.92%	0.46%	0.69%	0.69%	1.16%	0.69%	0.69%	0.23%	0.46%	0.92%	0.69%	1.40%	0.69%	0.69%	0.46%	0.46%	1.40%	0.23%

Appendix B

Supplementary Table B1. mtCOI sequences of *T.molitor* and *C.vicina*, modern specimens. Letters follow Fig. 3.5

>A_Tmolitor
CCTCACTAAGACTATTAATCCGTGCAGAATTAGGAAACCCCGGCTCTCTAATTGGAGACGACCAAATCTAC
AACGTAATTGTTACAGCACATGCTTTTATCATAATTTTTTTCATAGTAATACCAATCATAATTGGAGGATT
CGGAAATTGATTAGTACCTCTAATACTAGGTGCTCCTGACATAGCATTCCCACGAATAAACAACATAAGAT
TCTGATTGCTACCCCTTCACTAAGACTATTATTAATAAGAAGAATTGTAGAAAACGGGGCGGGAACCGGT
TGAACAGTTTATCCACCCTTATCCTCTAATATCGCCCATGGAGGAGCATCTGTCGATTTAGCAATTTTCAG
GCTACATCTAGCAGGGATTTCTGCAATCCTGGGGCCGTAAATTTTATTACAACAGTAATCAACATACGAC
CACAGGGCATAACGTTTCGATCGAATACCGTTATTCGTGTGAGCAGTAGTAATTACCGCAGTACTATTATTA
TTATCCTTGCCAGTATTAGCAGGAGCCATTACCATATTACTTACAGATCGAAACATTAATACATCCTTCTT
TGACCAGCTGGAGGAGGGGACCCAATCTTATACCAACACCTATTCTGATTCTTTGGAC

>B_Tmolitor
CATTTTCGGAGCATGCCTGCAAATAGTGGTACTACTAAGACTATTAATCCGTGCAGAATTAGGAAACC
CCGGCTCTTTAATTGGAGACGACCAAATCTACAACGTAATTGTTACAGCCCACGCTTTTGTAATAATTTTT
TTTATAGTAATGCCAATCATAATTGGAGGTTTCGGAAACTGATTAGTACCTCTAATACTAGGTGCTCCTGA
CATAGCATTCCCACGAATAAACAACATAAGATTCTGATTGCTACCCCTTCACTAAGACTATTATTAATAA
GAAGAATTGTAGAAAACGGGGCGGGAACCGGTTGAACAGTTTATCCCACCTTTATCTTCTAATATTGCCCA
TGGAGGAGCTTCTGTCGATTTAGCAATTTTCAGGCTACATCTAGCAGGGATTTCTGCAATCCTGGGGCCG
TAAATTTTATTACAACAGTAATCAACATACGACCAATAGGAATAAACCTAGACCGAATACCGTTATTTCGTA
TGAGCAGTAGATGAGCAGTATTAATTACTGCAGTCTATTGCTATTATCTTTGCCCGTATTAGCAGGAGCC
ATTACCAGCTGGAGGAGGGGACCCAATCTTATACCAACA

>C_Tmolitor
AGACTATTAATCCGTGCAGAATTAGGAAACCCCGGCTCTCTAATTGAATATTAATTCGATCAGAACGTAAT
TGTTACAGATCATTGATTTATCATAATTTTATTTACAACGTAATTGTTACAGATTGGAGGATTGTAATAAT
TATTAGTACCTCTATGCCAATCATAATTGGAGGAAGCATTCCCACGAATAAACCTCTAATACTAGGTGCTC
CTGACATAGCATTCCCACGAATAAACAACATAAGATTCTGTAGAAAACGGCCTTCACTAAGACTGTTACTA
ATAAGAAGAATTGTAGAAAAATATCGCCCATCCGGTAGCATCTGTCGATCGCCTTTATCCTCTAATATCGC
TAGCAGGGATTTCTGCAATCCTGGGGCCGTAAATTTTATTACAACAGTAATCAACATACAATTC TAGGAC
ATAACGTTTCGATCGAATACAATCATTAAATATACGACCACAGGTATACGCAGTACTCAAATACCATTATTT
GTATGAGCAGTATTAATTACTGCCGTACTAATCTATTATCTTTGCCCGTATTAGCAGGAGCCATTACAAG
CTGGAGGAGGATCGAAACTTCAATACATCCTTTTTTGACCCACTTTGGGGAGGAGACCCAATCCTATA

>D_Tmolitor
TACTTCATTTTTGGAGCGTGATCCGGAATAGGTCCGAACCTCACTAAGACTATTAAATTCGAGCCGAATTG
GAAACCCCGGATCTCTAATTGGAGACGACCAAATCTACAACGTAATTGTTACAGCACATGCTTTTATCATA
ATTTTTTTTCATAGTAATACCAATCATAATTGGAGGATTCGGAAATTGATTAGTACCCTAATACTAGGTGC
TCCTGACATAGCATTCCCTCGGATAAACCATATAAGTTTCTGACTTTTACCTCCTGCACTAAGACTATTAT
TAATAAGAAGAATTGTAGAAAACGGGGCAGGAACCGGTTGGACAGTTTATCCGCTTTATCCTCTAATATC
GCCCATGGGGAGCATCTGTCGATTTAGCAATTTTCACTTTACACTTTGCAGGAATTTCTCCATTTTAGG
AGCTGTAATTTTATTACAACAGTAATCAACATACGATCAATAGGAATAAACCTAGACCAAATACCATTAT
TTGTATTTCGATGAGCAGTAGTAATTACCGCAGTACTATTATTTATCCTTGCCAGTATTAGCAGGAGCC
ATTACCATATTATTAACAGATCGAAACTTCATACCAACACCTATTCTGCCAGCAGG

>E_Cvicina
GATCCCCTAGTGGCCCTGCAAATAGTGGTACTTAAAGATTCTATTTCGAGCCGAATTGGACCCTGGAAC
TAAATGGAGATGACCAATTTATAATGAATTGTTACATCTCATGCTTTTATTATAATTTTTTTTATAGTAAT
ACCAATTATAATTGGAGGATTTGAAATTTGATTAGTCCCTTTAATATTAGGAGCTCCAGAAATAGCCTTCC
CTCGGATAAACCATATAAGTTTCTGACTTTTACCTCCTGCATTAACCTTTACTATTAGTAAGTAGTATAGTA
GAAAACGGAGCTGGAACAGGATGAACTGTTTACCACCTTTATCTTCTAATATTGCCCATGGAGGAGCTTC
TGTTGATTTAGCTATTTTTTCTTTACACTTTGCAGGAATTTCTCCATTTTAGGAGCTGTAAATTTTATTA
CTCCAGTTATTAATATACGATC

>F_ Cvicina
TACGGCGCCTGAGATTAGTTGGACTATCATTAAAGAAATTCTAATTCGAGCCGAACCTAGGGCATCCTGGAGCA
TTAATTGGAGATGACCAAATTTATAATGTAATTGTTACAGCTCATGCTTTTTTATAATTTTTTTTATAGTA
ATACCAATTATAATTGGAGGATTTGGAATTGATTAGTCCCTTTAATATTAGGAGCTCCAGATATAGCCTTC
CCCCAAAAAAAAAAAAAAAAAGTTTCTGACTTTTACCCCGGCTTAACTTTACAATTGAAAAGAAGAAAAGC
AAAAACCGACCGGGAACAGGAGAACTGTTTACCCCCCTTTATCTTCAAAAATCGCCCATGGAGAACCTT
CGGTTGATTTACCAATTTTTCTTTACTTTTACCGGGAATTCCTTCATTTTTTAGGACCGGAAAATTTTATT
ACAACGGTTATTTAAAATACAACCAACAGGAATTACTTTCAACCAAAAACCTTTATTGGTTGGATCTGAAGA
ATTTACGCTTTTATTACCTTTTATCCTTTACCATTTTTACCGGGGGCTATTACTATATAATTAACAAATC
GAAATCTTATATACTTCAATCTTTGACCCACCAGGAGGAGACCCAATCTTGTACCAACATTATATTTT
GATCTTTGGGACAC

>G_ Cvicina
AGTTGTCGTCGACATGCAGCCACAAAAATGATGAATTAGATTTCCCATCTGTTGACAATATAGTAATAGC
ACCAGCTAATACTGAGTAAAGATAATCAAAGTTATAAAGCTGTAATTACTACAGATCAAACAAAATATGGT
ATTCGGTTCGAATGTAATTCCTGTTGATCGTATATTAATAACTGTAGGCCTAAAATTTACAGCTCCTTAAAT
TGAAGAAATTCCTGCTAAGTGTAAAGAAAAAATAGCTAAATCAACAGAAGCTCCTCCATGAGCGATATTAG
AAGATAAAGGTGGGTAAACAGTTCATCCTGTTCCAGCTCCGTTTTCTACTATACTACTACTAATAGTAAA
GTTAATGCAGGAGGGTCAAGTCAAAAATTTATTTGTTTATCCGAGGGAAGGCTATATCTGGAGCTTCTAA
TATTAAGGGACTAATCAATTACCAAATCCTCCAATTATAATTTGGTATTACTATAAAAAAATTTATAATA
AAGCATGAGCTGTACCAATTACATTATAAATTTGGTCATATCCAATTAATGAACCTGGATGTCCTAGTTCG
GCTCGACTTAGAATTTCTTAATGAAAGTTCCAATTATTTCCCGATCAAGCTCCAAAAATAAGTATAAAGT
ACCAATATCTTTAT

>J_ Cvicina
GGGATAATTGGAACCTTCATTAAGAATTCTAATTTGAGCCGAACCTGGACATCCTGGAGCATTAAATTGGAGA
TGACCAAATTTATAATGTAATTGTTACAGCTCATGCTTTTTATTATAATTTTTTTTATAGTAATACCAATTA
ATATTGGAGGATTTGGCTATTGATTAGTCCCTTTAATATTAGGAGCTCCAGATATAGCCTTCCCTCGGATA
ACAATATAAGTTTCTGACTTTTACCTCCTGCATTAACCTTACTATTAGTAAGTAGTATAGTAGAAAAACGG
AGCTGGAACAGGATGAACGTTTACCCACCTTTATCTTCTAATATCGCTCATGGAGGAGCTTCTGTTTGTT
TGGCTATTTTTTCTTTACACTTAGCAGGAATTTCTTCAATTTTAGGAGCTGTAAATTTTATTACTACAGTT
ATTAATATACGATCAACAGGAATTACATTCGACCGAATACCATTATTTGTTTGATCTGTAGTAATTACAGC
TTTATTACTTTTATTATCTTTATAAGTATTAGCAGGTGCTATTACTATATTATTAACAGATCGAAATCTTA
ATACATCATTCTTTGACCCAGCAGGAGGAGACCCAATCTTGTACCAACATTTGTTTGATTCTTTGGAC
ACCCG

>K_ Cvicina
GGGATAATTGGAACCTTCATTAAGAATTCTAATTCGAGCCGAACCTAGGACATCCTGGAGCATTAAATTGGAGA
TGACCAAATTTATAATGTAATTGTTACAGCTCATGCTTTTTATTATAATTTTTTTTATAGTAATACCAATTA
TAATTGGAGGATTTGGTAATTGATTAGTCCCTTTAATATTAGGAGCTCCAGATATAGCCTTCCCTCGGATA
ACAATATAAGTTTCTGACTTTTACCTCCTGCATTAACCTTACTATTAGTAAGTAGTATAGTAGAAAAACGG
AGCTGGAACAGGATGAACGTTTACCCACCTTTATCTTCTAATATCGCTCATGGAGGAGCTTCTGTTGATT
TAGCTATTTTTTCTTTACACTTAGCAGGAATTTCTTCAATTTTAGGAGCTGTAAATTTTATTACTACAGTT
ATTAATATACGATCAACAGGAATTACATTCGACCGAATACCATTATTTGTTTGATCTGTAGTAATTACAGC
TTTATTACTTTTATTATCTTTACCAGTATTAGCAGGTGCTATTACTATATTATTAACAGATCGAAATCTTA
ATACATCATTCTTTGACCCAGCAGGAGGAGACCCAATCTTGTACCAACATTTATTTGATTCTTTGGAC
CACCTGGAA

>L_ Cvicina
AAAAAGGATAAATGGAACCTTCATTAAGAATTCTAATTCGAGCCGAACCTAGGACATCCTGGAGCATTAAATTG
GAGATGACCAAATTTATAATGTAATTGTTACAGCTCATGCTTTTTATTATAATTTTTTTTATAGTAATACCA
ATTATAATTGGAGGATTTGGTAATTGATTAGTCCCTTTAATATTAGGAGCTCCAGATATAGCCTTCCCTCG
GATAAACAATATAAGTTTCTGACTTTTACCTCCTGCATTAACCTTACTATTAGTAAGTAGTATAGTAGAAA
ACGGAGCTGGAACAGGATGAACGTTTACCCACCTTTATCTTCTAATATCGCTCATGGAGGAGCTTCTGTT
GATTTAGCTATTTTTTCTTTACACTTAGCAGGAATTTCTTCAATTTTAGGAGCTGTAAATTTTATTACTAC
AGTTATTAATATACGATCAACAGGAATTACATTCGACCGAATACCATTATTTGTTTGATCTGTAGTAATTA
CAGCTTTATTACTTTTATTATCTTTACCAGTATTAGCAGGTGCTATTACTATATTATTAACAGATCGAAAT
CTTAATACATCATTCTTTGACCCAGCAGGAGGAGACCCAATCTTGTACCAACATTTATTTGATTCTTT
TGGACACACGG

Supplementary Table B2. mtCOI short barcoding sequences (Op311 primers) of *C.vicina*, Roccapelago archaeological samples. 2,3,5: number of puparia used as template for DNA isolation.

Archaeological Standard Protocol	
>2_fw_CATATTAGATGATAAATGGTGGATAAACAGTTCATCCTGTTCCAGCTCCGTTTTCT ACTATACTACTTACTAATAGTAAAGTTAATGCAGGAGGTAAAAGTCAAAAACCTATATATTAT TTATTCGAGAA	136 bp
>2_rv_ATTAGTAAGTAGTATAGTAGAAAACGGAGCTGGAACATGGTATGAACTGTTTATC CACCATTTATCATTCTAATATTGCACATGGAGGAGCTTCTGTTGATTTAGCTATTTTTTCT CTTCACTTAGCTGGAATAAT	127 bp
>3_fw_TATTAGATGATAAAGGTGGATAAACAGTTCATCCATGTTCCAGCTCCGTTTTCTA CTATACTACTTACTAATAGTAAAGTTAATGCAGGAGGTAAAAGTCAAAAACCTATATATTAT TATTCGAGAA	159 bp
>3_rv_GTCTAACCTCTGATAGTCTCTTGCTATTAGTAAGTAGTATAGTAGAAAACGGAG CTGGAACATGGTATGAACTGTTTTATCCACCTTTATCTTCTAATATTGCACATGGAGGAGCT TCTGTTGATTTAGCTATTTTTTCTCTACACTTAGCAGGAATAA	126 bp
>5_fw_CGTAAGCTTCTGATAGTATCTTTCTATTAGTAAGTAGAATAGTAGAAAACGGAGC TGGAACATGGTATGAACTGTTTTATCCACCTTTATCTTCTAATATTGCACATGGAGGAGCTT CTGTTGATTTAGCTATTTTTTCTCTCACTTAGCTGGAATAA	158 bp
>5_rv_GGCCTTCCTCCGATTGCGTCGAGCAGTAGTCATATTAGATGATAAAGGTGGATA AACAGTTCATCCATGTTCCAGCTCCGTTTTCTACTATACTATCTTACTAATAGTAAAGTTA ATGCAGGAGGTAAAATCAAAAACCTATATATTATTTATTCGAGA	160 bp
Phusion Blood HotStart High-Fidelity	
>2_fw_TATTAGTTAGTAGTATAGTAGAAAATCGGAGCTGGAACATGGTATGAACTGTTTA TCCACCATTTATCATTCCCTAATATTGCACATGGAGGAGCTTCTGTTGATTTAGCTATTTTT TCTCTTCACTTAGCTGGAATCTAA	140 bp
>2_rv_GTGCATATTAGAAGATAAAGGTGGATAAACAGTTCATCCATGTTCCAGCTCCGTT TTCTACTATACTACTTACTAATAGTAAAGTTAATGCAGGAGGTAAAAGTCAAAAACCTATA TTATTTATTTCGAGAGATA	134 bp
>3_fw_TTTCTATTAGTTAGTAGTATAGTAGAAAACGGAGCTGGAACATGGTATGAACTGT TTATCCTCCTTTTATCTTCTAATATTGCTCATGGAGGAGCTTCTGTTGATTTAGCTATTTTT TCTCTACACTTAGCTGGAATGAA	139 bp
>3_rv_CAGAGTGCATATTAGAAGATAAAGGTAGGATAAACATGTTTCATCCATGTTACCAG CTCCGTTTTCTACTATACTACTTACTAATAATAAAGTTAATGCAGGAGGTAAAAGTCAAAA ACTTATATTATTTATTCGAGAATAA	141 bp
>5_fw_ATTAGTAAGTAGTATAGTAGAAAACGGAGCTGGAACATGGTATGAACTGTTTATCCA CCTTTATCTTCTAATATTGCACATGGAGGAGCTTCTGTTGATTTAGCTATTTTTTCTCTAC ACTTAGCAGGAATATA	132 bp
>5_rv_GTTTTACGTGCATATTAGAAGATAAAGGTGGATAAACAGTTCATCCAGTTCAGC TCCGTTTTCTACTATACTACTTACTAATAGTAAAGTTAATGCAGGAGGTAAAAGTCAAAA CTTATATTATTTATTCGAGAGATA	140 bp
>8_fw_ATACTAGTAAGTAGTATAGTAGAAAATGGAGCTGGAACAGGATGAACTGTTTACC CTCCTTTATCATCTAATATTGCTCATGGAGGAGCTTCTGTTGATCTAGCTATTTTTTCTCT ACACTTAGCAGGAATAA	133 bp
>8_rv_CGTGAGCATATTAGATGATAAAGGAGGTAAAACAGTTCATCCTGTTCCAGCTCCA TTTTCTACTATACTACTTACTAGTAGTAATGTTAATGCAGGAGGTAAAAGTCAAAAACCTA TATTATTTATTCGAGAAA	134 bp

Supplementary Table B3 mtCOI barcoding sequences of Piophilidae.

>ASV0032345_DMV_Piophila casei_Spain
ATTATTTTAATTCGAGCCAAATTAGGACACCCTGGAGCTTTAATTGGCGATGATCAAATTTATAATGTAATTGT
TACAGCTCATGCATTTGTAATAATTTCTTTATAGTAATACCTATTATAATCGGGGATTTGGAAATGACTTG
TCCCTTTAATATTAGGAGCCCCGATATAGCTTTCCACGAATAAATAATATAAGTTTCTGAATATTACCTCCT
TCTCTAACTCTATTGTTAGTAAGAAGTATAGTAGAAAATGGGGCTGGAACAGGTTGAACTGTTTATCCACCTCT
TTCATCCGTTATTGCCCATGGAGGTGCTTCAGTAGACTTAGCTATTTTTCTCTTCATTTAGCAGGAATTTTCAT
CAATTTTAGGGGCAGTAAATTTTATTACTACTGTAATTAATATACGATCAACCGGAATTACTTTTGATCGAATA
CCTTTATTTGTATGATCCGTTGTAATTACAGCCCTTTATTATTACTTTTATTACCGGTATTAGCAGGAGCTAT
TACAATATTATTAACAGATCGAAATTTAAACACTTCATTCTTTGACCCTGCCGGAGGGGGAGACCAATTCCTT
ATCAACATCTATTTTGATTCTTTGGACATCACG

>ASV0032346_DMV_Protopiophila litigata_Spain
GGAGCTTGAGCGGTATAGTAGGAACTTCCTTAAGTATTTTAATTCGAACTGAATTAGGACACCCTGGAGCTTT
GATTGGAGATGATCAAATTTATAATGTAATTGTTACAGCCCATGCTTTTGTAAATAATTTCTTTATAGTAATAC
CTATTATAATTGGGGGATTCGAAATTTGATTAGTCCCTTTATATATTAGGAGCCCCTGATATAGCTTTCCACGA
ATAAATAATATAAGTTTTTGAATATTACCTCCATCTTAACCCTATTATTGGTTAGTAGTATAGTAGAAAACGG
GGCCGGACAGGTTGAACTGTTTACCCCTCTATCTTCTGTAATTGCACATGGAGGGGCATCTGTTGATTTAG
CTATTTTTTCCCTTCATTTGGCCGATTTCTTCCATTTTAGGGGCAGTAAATTTTATTACTACCGTTATTAAT
ATACGATCAACAGGAATTACTTTTCGACCGAATACCTTTATTTGTTGATCAGTTGTAATTACAGCTCTTTTATT
ACTTTTGTCTTTACCCGTACTTGCAGGAGCAATTACTATATTATTAACAGATCGAAATCTAAATACTTCATTCT
TTGACCCAGCGGGAGGAGACCAATTTTATACCAACATTTATTTTGTTT

>ASV0032347_DMV_Prochyliza xanthosoma_Spain
GAGCTTGAGCTGGATAGTAGGGACTTCTCTTAGTATTTTAATTCGAGCCGAATTAGGACACCCTGGAGCTTTAA
TTGGTGATGACCAAATTTATAATGTAATTGTTACAGCACATGCCCTTTGTAATAATTTTTTTTATAGTTATACCA
ATTATAATTGGAGGATTTGGAAATTTGATTAGTCCCTTTAATATTAGGAGCTCCTGATATAGCTTTCCCTCGAAT
AAATAATATAAGTTTTTGAATACTTCCACCTCTTTAACCTTACTATTAGTAAGAAGTATAGTAGAAAACGGAG
CTGGGACAGGTTGAACTGTTTACCCTCCTCTATCATCTGTAATTGCTCATGGAGGTGCTTCTGTTGATTTAGCT
ATTTTTTCTTTACACCTAGCTGGGATTTCTTCAATTTTAGGGGCTGTTAATTTTATTAACACTGTAATTAATAT
ACGATCAACAGGAATCACTTTTGGACCGAATACCTTTATTTGTTGATCCGTTGTAATTACAGCTCTTTTATTAC
TTTTATCCCTTCCAGTATTAGCCGGAGCAATTACTATATTATTAACGATCGAAATTTAAATACTTCATTTTTT
GACCCAGCTGGAGGAGGAGACCAATTTCTTTTACCAACATTTATTTTGTTT

>ASV0032348_DMV_Centrophlebomyia furcata_Spain
TCTAGAGCTGGATAGTAGGAACCTCATTAAGAATTTAATTCGAGCAGAATTAGGACACCCAGGAGCTTTAATT
GGAGACGACCAAATTTATAATGTAATCGTTACTGCTCATGCATTTGTAATAATTTTTTTTATAGTTATACCTAT
TATAATCGGAGGATTCGGGAATTGACTAGTACCCTTATACTAGGAGCTCCTGATATAGCTTTCCCCCGAATAA
ATAATATGAGATTTTGAATATTACCCCTTCTCTAACGCTTCTGTTAGTAAGCAGTATAGTAGAAAATGGAGCC
GGAACAGGATGAACAGTTTACCCTCCTTTATCATCTGTAATTGCCACGGAGGAGCTTCTGTAGATTTAGCTAT
TTTTTCTTTTACACTTAGCAGGAATTTCTTCAATTTTAGGAGCAGTAAATTTTATTACTACTGTAATTAATATAC
GATCAACAGGAATTACTTTTGGACCGAATACCTTTATTTGTTGATCAGTAGTAATCACAGCACTTTTATTACTT
TTATCTTTACCTGTATTAGCAGGAGCTATTACAATATTACTAACAGATCGAAATTTAAATACATCTTTTTCGA
CCCTGCGGGAGGAGGAGACCAATTTCTTTTACCAACATTTGTTCTGATCTT

>ASV0032349_DMV_Piophila megastigmata_Spain
TTGGTGCTTGAGCTGGATAGTAGGAACCTCTCTTAGTATTCTAATTCGGGCCGAATTAGGACACCCTGGAGCTT
TAATTGGTGATGATCAGATTTATAATGTAATTGTTACAGCACACGCATTTGTAATAATTTTCTTTTATAGTAATA
CCTATTATAATTGGAGGATTTGGAAATTTGATTAGTCCCTTTATATTAGGAGCCCCTGATATAGCTTTCCCCG
AATAAATAATATAAGTTTTTGAATATTACCCCTTCTTAACTCTACTATTAGTGAGATCTATAGTAGAAAACG
GGCCCGAACAGGTTGAACTGTTTATCCCTCTTTCATCTGTCTGCTCATGGAGGTGCATCAGTAGATTTA
GCTATCTTTTCCCTTCATTTAGCAGGATTTTCATCAATTTTAGGGGCTGTAATTTTATTACGACTGTTATTA
TATACGATCAACTGGTATTACCTTTGATCGAATACCTTTATTTGTTTGTGATCTGTTGTAATTACAGCTTTATTAT
TGTTATTATCTCTTCTGTATTAGCCGGAGCAATTAACATATTATTAACAGATCGAAATTTAAATACTTCATTC
TTCGACCCAGCTGGAGGAGGAGACCAATTTCTCTATCAACATTTATTTTGATTCTTTGG

Continues from Supplementary Table B3

>ASV0032350_DMV_Prochyliza nigrimana_Spain
TGCTTGAGCTGGATAGTGGGAACCTCTCTTAGTATTTTAATTCGAGCCGAATTAGGACACCCCGGGCTTTAAT
TGGAGACGATCAAATTTATAATGTAATTGTAACAGCACACGCATTTGTTATAATTTCTTTATAGTAATACCTA
TTATAATCGGAGGATTTGGAAATTGACTAGTCCCTTTAATATTAGGAGCTCCTGATATAGCTTTCCCACGAATA
AATAATATAAGTTTCTGGATATTACCCCTTCTTTAACTTTACTATTAGTAAGAAGTATAGTAGAAAATGGAGC
TGGAACAGGTTGAACTGTTTACCCTCCTCTTTCATCTGTTATTGCTCATGGAGGTGCCTCAGTAGACTTAGCTA
TTTTCTCTTTACATTTGGCTGGAATTTCTTCAATTTAGGGGCGGTAAATTTTATTACAACGTAAATTAATATG
CGATCAACTGGAATTACTTTTGACCGAATACCTTTATTTGTTTGATCGGTTGTAATTACTGCACCTTTATTGCT
TTTATCTTTACCCTGTATTAGCAGGAGCAATTACTATATTACTAACAGATCGAAATTTAAATACTTCATTTTTTG
ACCCGTGCTGGAGGAGGTGATCCAATTCTTTATCAACATTTATTTTGATTTTTTTGG

>ASV0032351_DMV_Parapiophila flavipes_Spain
CTTGAGCAGGATAGTAGGTACTTCCCTAAGTATTTTAATCCGAGCAGAGTTAGGACACCCAGGAGCTTTAATTG
GTGATGATCAAATTTATAATGTAATTGTCACTGCCATGCTTTTGTGATAATTTTTTTTATAGTAATACCAATT
ATAATTGGAGGATTCGGAATTTGATTAGTTCCTTTAATACTAGGAGCTCCTGATATAGCGTTTCCACGAATAAA
TAATATAAGTTTTTGAATACTACCTCCTTCCCTTACACTTTTATTAGTAAGTAGTATAGTAGAAAACGGAGCTG
GTACAGGTTGAACAGTTTACCCTCCCCTTTCTTCTGTTATTGCTCACGGAGGGCTTCTGTTGACTTAGCTATT
TTCTCTCTTCAATTTAGCAGGAATTTCCCTCAATTTCTAGGAGCTGTAAATTTTATCACAACGTAAATTAATATACG
ATCTACAGGTATACCTTTCGACCGAATACCTTTATTTGTTTGATCTGTTGTAATTACAGCTTTATTACTTCTAT
TATCCCTACCAGTTTTAGCGGGAGCTATTACTATATTACTAACAGACCGAAATTTAAATACTTCATTTTTTGAC
CCGGCAGGAGGAGGAGACCCATTCTTTACCAACACTTATTTTGTTTTTTTTGGACACCCG

>ASV0032352_DMV_Liopiophila varipes_Spain
GCTAGAGCAGGAATAGTAGGAACCTCTCTTAGTATTTTAATTCGAGCCGAATTAGGACACCCCGGAGCTTTAAT
TGGAGATGACCAAATTTATAATGTAATTGTTACAGCTCATGCTTTTGTAAATAATTTTCTTTATAGTAATACCAA
TTATAATTGGGGGATTCGGAATTTGATTGGTTCCTTTAATATTAGGAGCCCTGATATAGCCTTCCCTCGAATA
AATAATATAAGTTTCTGAATACCTCCTCCTCTTTAACTCTTCTATTAGTAAGTAGTATAGTAGAAAATGGAGC
TGGGACAGGTTGAACTGTTTATCCTCCTTTATCTTCTGTAATTGCACATGGAGGAGCTTCTGTAGATTTAGCTA
TTTTCTCTTTACATCTTGCTGGAATTTCTTCAATTTAGGGGCTGTAAATTTTATCAGACTGTAATTAACATA
CGATCTACAGGAATTACATTTGACCGAATACCTTTATTTGTTTGATCAGTTGTAATTACTGCTCTTTTATTACT
ATTGTCACTTCTGTTCTAGCAGGAGCCATTACCATATTATTACAGATCGAAATTTAAATACTTCATTTTTTTG
ACCCGGCGGGAGGAGGAGATCCAATTCTTTACCAACACTTATTTTGTTTTTTTTGG

>ASV0023846_DMV_Parapiophila atriformis_Spain
GAGCAGGAATAGTAGGAACATCCCTAAGTATTTTAATCCGGGCAGAACTAGGACACCCAGGAGCCTAATTGGT
GATGATCAAATTTATAATGTAATTGTCACTGCACATGCTTTTGTAAATAATTTTTTTTATAGTAATACCAATTAT
AATTGGGGGATTCGGTAATTGATTAGTTCCTTTAATACTAGGAGCTCCTGATATAGCTTTCCCACGAATAAATA
ATATAAGTTTTTGAATATTACCCTCCTTCTTCTTACACTTTTATTAGTAAGTAGTATAGTAGAAAACGGGGCTGGT
ACAGGCTGAACAGTTTACCCTCCTTCTTCTTCTGTCATTGCTCACGGTGGGGCTTCTGTTGATTTAGCTATTTT
CTCCCTTCATTTAGCAGGTATCTCCTCTATTTTAGGGGCTGTAAATTTTATTACCCTGTAATTAATATACGAT
CAACAGGTATCACTTTGACCGAATACCTTTATTTGTTTGATCTGTAGTAATTACAGCTTTATTATTACTTTTA
TCTTTACCCTGTTTTAGCCGGAGCTATTACTATATTATTAACAGATCGAAATTTAAATACTTCATTTTTTCGATCC
AGCAGGAGGGGAGACCAATTCTTTACCAACACTTATTTTGTTC

>ASV0032345_Stearibia nigriceps_Caso_RobinoInnocenza_Italy
TAATTCGAGCCGAATTAGGACACCCCGGAGCTTTAATTGGAGATGACCAAATTTATAATGTAATTGTTACAGCT
CATGCTTTTGTAAATAATTTCTTTATAGTAATACCAATTATAATTGGGGGATTCGAAATTTGATTGGTTCCCTTT
AATATTAGGAGCCCTGATATAGCCTTCCCTCGAATAAATAATATAAGTTTCTGAATACTTCCCCCTCTTTAA
CTCTTCTATTAGTAAGTAGTATAGTAGAAAATGGAGCTGGGACAGGTTGAACTGTTTATCCTCCTTTATCTTCT
GTAATTGCACATGGAGGAGCTTCTGTAGATTTAGCTATTTTCTTCTTTACATCTTGCTGGAATTTCTCAATTTT
AGGAGCTGTAAATTTTATCACAACGTAAATTAACATGCGATCTACAGGAATTACATTTGACCGAATACCTTTAT
TTGTTTGATCAGTTGTAATTACTGCTCTTTTATTACTATTGTCACCTTCTGTTCTAGCAGGAGCCATTACCATA
TTATTAACAGATCGAAATTTAAATACTTCATTTTTTGACCCGGCGGGAGGAGGAGATCCAATTCTTTACCAACA
CTTATTTTGTTCCTTTGGACACACCT

Continues from Supplementary Table B3

>ASV0014968_Piophilina nigriceps_CasoRaposelli_Italy
CTTGAGCAGGATAGTAGGAACCTCTCTTAGTATTTTAATTCGAGCCGAATTAGGACACCCCGGAGCTTTAATTG
GAGATGACCAAAATTTATAATGTAATTGTTACAGCTCATGCTTTTGTAAATAATTTCTTTATAGTAATACCAATT
ATAATTGGGGGATTCGAAATGATTGGTTCCCTTAATATTAGGAGCCCCTGATATAGCCTTCCCTCGAATAAA
TAATATAAGTTTCTGAATACCTCCCTCTTTAACTCTTCTATTAGTAAGTAGTATAGTAGAAAAATGGAGCTG
GGACAGGTTGAACTGTTTATCCCTCTTATCTTCTGTAATTGCACATGGAGGAGCTTCTGTAGATTAGCTATT
TTCTCTTTACATCTTGCTGGAATTTCTTCAATTTTAGGGGCTGTAAATTTATCACAACCTGTAATTAACATACG
ATCTACAGGAATTACATTTGACCGAATACCTTTATTTGTTTGATCAGTTGTAATTACTGCTCTTTTATTACTAT
TGTCACTTCCGTCTTAGCAGGAGCCATTACCATATTATTAACAGATCGAAATTTAAATACTTCAATTTTTTGAC
CCGGCGGGAGGAGGAGATCCAATTTCTTTACCAACACTTATTTTGATTCTTTGGACACCAC

>ASV0023042_Parapiophilina vulgaris_RabbitRoof_UK
GCTTGAGCAGGATAGTAGGACTTCCCTAAGTATCTTAATCCGAGCAGAGCTAGGACATCCAGGAGCTTTAATT
GGTGATGATCAAATTTATAATGTAATTGTCACCGCCCATGCTTTTGTGATAATTTTTTTTTATAGTAATACCAAT
TATAATTGGGGGATTTGAAATGATTAGTTCCTTTAATACTAGGAGCTCCTGATATAGCTTTCCACGAATAA
ATAATATAAGTTTTTGAATATTACCCCTTCTCTACGCTACTATTAGTAAGAAGTATAGTAGAAAACGGAGCT
GGTACAGGTTGAACAGTTTACCCTCCTCTTTCTTCTGTTATTGCTCATGGAGGGGCTTCTGTTGATTAGCTAT
TTTTTCCCTTACCTAGCAGGAATCTCTTCAATTTTAGGAGCTGTAAATTTATCACAACCTGTAATTAATATAC
GATCTACAGGATCACTTTTGATCGAATACCTTTATTTGTTTGATCTGTTGTAATTACAGCTTTTATTACTT
TTATCTTACCTGTTCTAGCAGGAGCAATTACAATATTATTAACGATCGAAATTTAAATACTTCAATCTTTGA
CCAGCAGGAGGAGGAGACCAATTTCTTTACCAACATTTATTTTGT

>ASV0014806_Parapiophilina vulgaris_RabbitRoof_UK
ACTTACCTAAGTATCTTAATCCGAGCAGAGCTAGGACATCCAGGAGCTTTAATTGGTGATGATCAAATTTATA
ATGTAATTGTCACCGCCCATGCTTTTGTGATAATTTTTTTTTATAGTAATACCAATTATAATTGGGGGATTTGGA
AATTGATTAGTTCCTTTAATACTAGGAGCTCCTGATATAGCTTTCCACGAATAAATAATATAAGTTTTTGAAT
ATTACCTCCTTCTTACGCTACTATTAGTAAGAAGTATAGTAGAAAACGGAGCTGGTACAGGTTGAACAGTTT
ACCCTCCTCTTCTTCTGTTATTGCTCATGGAGGGCTTCTGTTGATTTAGCTATTTTTTCCCTTACCTAGCA
GGAATCTCTTCAATTTTAGGGGCTGTAAATTTATCACAACCTGTAATTAATATACGATCTACAGGTATCACTTT
TGATCGAATACCTTTATTTGTTTGATCTGTTGTAATTACAGCTTTATTATTACTTTTATCTTACCTGTTCTAG
CAGGAGCAATTACAATATTATTAACAGATCGAAATTTAAATACTTCAATCTTTGACCCAGCAGGAGGAGGAGAC
CCAATTTCTTTACCAACATTTATTTGATTCTTTGGCAC
